Karlsruhe Institute of Technology

Optimisation of the reaction parameters in a batch reactor and a CSTR for the recovery of phenol from hydrothermal biomass liquefaction

zur Erlangung des akademischen Grades eines
DOKTORS DER INGENIEURWISSENSCHAFTEN (Dr.-Ing.)

der Fakultät für Chemieingenieurwesen und Verfahrenstechnik des
Karlsruher Institut für Technologie (KIT)

genehmigte
DISSERTATION

von
Dipl.-Ing. Daniel Forchheim[1,2]
aus Karlsruhe

Referent: Prof.Dr. Michael Türk[1]
Korreferentin: Prof.Dr. Andrea Kruse[2]
Tag der mündlichen Prüfung: 25.03.2014

[1] Institut für Technische Thermodynamik und Kältetechnik
[2] Institut für Katalyseforschung und -technologie

Acknowledgements

An dieser Stelle möchte ich besonders meinen Eltern danken, die mich mein Leben lang unterstützt haben, der Forschung und den Wissenschaften nachzugehen. Ich danke Andrea Kruse und Uschi Hornung, die mir mit vielen Hinweisen und in zahlreichen Gesprächen wichtige fachliche Unterstützung und Vertrauen in meine Arbeit entgegengebracht haben. Ein besonderer Dank gilt James Gasson, dessen Kooperation wesentlich die kreativen Momente dieser Arbeit gefördert hat. Ferner hätte ich die praktischen Experimente nicht ohne die tatkräftige Unterstützung vieler Menschen am IKFT durchführen können. Stellvertretend möchte ich hier Birgit Rolli, Thomas Tietz, Matthias Pagel, Sonja Habicht und Armin Lautenbach nennen. Auch ohne die Zuarbeit vieler Studenten wäre diese Arbeit in den letzten Jahren nicht bis zu diesem Punkt gereift. Herzlich danken möchte ich deshalb David Steinbach, Tatjana Sutter, Jonathan Jeras, Philipp Kempe, Saskia Lamour, Lucile Courtinat, Yichie Chien, Yali Liu, Matthew Schumacher, Stephanie Hauschild und Alvaro Herreras. Sie alle haben maßgeblich zum Gelingen dieser Arbeit beigetragen. Schließlich möchte ich meiner kleinen Familie danken, die mich täglich getragen hat und immer die mentale Stütze war, auch wenn an manchen Punkten Unmut, Demotivation oder Verzweiflung geherrscht haben. Meine Frau Raquel und mein ungeborenes Kind haben mir immer die Kraft gegeben, die ich brauchte, um diese Arbeit bis zum Ende zu führen.

Abstract

The recovery of platform chemicals from biomass gains a growing governmental, economic and public interest. This work deals with the hydrothermal liquefaction of lignin. The focus laid on the discovery of the main reaction pathways within the depolymerisation of the lignin-macromolecules, the discovery of bottleneck reactions and the investigation of reaction mechanisms. In this context also the influence of the solvent as well as the influence of catalysis were studied. This was achieved by intensive literature study and experimental work in both batch and continuous reactor. Simulation of the thermodynamic equilibrium as well as modelling of the formal kinetics of the discovered reactions facilitated the evaluation of experimental results. The aim of this work was to provide tools for the optimization of process parameters and to indicate the direction for further studies regarding the conversion of lignin into phenolics. Thus, the economic feasibility of different process scenarios was studied in order to evaluate the attractiveness of a technical process.

Solvent studies involved the comparison of hydrothermal lignin depolymerisation and lignin solvolysis in ethanol. Lignin depolymerisation was found to be faster in water than in ethanol at moderate temperatures (633 K). Furthermore, the comparison of both solvents, water and ethanol, showed that water leads to a narrower spectrum of phenolic products and a tenfold increase of the catechol yield. This is advantageous in respect to the separation of the phenolic product from solvent and by-products. The simulation of the thermodynamic equilibrium with Aspen Plus V7.2 showed that the major part of any organic input material including 100 % of the solvent ethanol at 633 K would be converted into gaseous components while water showed to be resistant against thermal decomposition. Heterogeneous catalysts showed very positive effects on the hydrodeoxygenation of primary or secondary phenolic products from hydrothermal lignin depolymerisation. The application of Raney-Ni *e.g.* selectively catalyses the conversion of catechol into phenol. Among the phenolic products recovered from the lignin degradation phenol is currently most utilized in the chemical industry. Kinetic modelling aided in the validation of the a priori model of reaction pathways and the discovery of bottleneck reactions within the lignin depolymerisation. It was proven that certain reactions can be predicted by the origin of the lignin, or the utilized solvent. Especially the influence of the chosen reactor was elucidated. Employing a Continuous Stirred Tank Reactor (CSTR) facilitates capping reactions, which leads to reduced yields of solid residue and gaseous products. At the same time it favours the formation of phenolic

products. Elucidating reaction mechanisms contribute to the explanation of these phenomena. The production of phenol from lignin by solvolysis in ethanol or hydrothermal degradation is economically not feasible if the current state of the art is considered. Studies of different scenarios showed that yields of phenol and other phenolics from lignin should be increased from at most 10 % to at least 20 % while the lignin/solvent ratio must increase and the mean residence time must be reduced in order to reduce especially the capital related costs.

Zusammenfassung

Die Gewinnung von Plattformchemikalien aus Biomasse bekommt wachsende Aufmerksamkeit seitens Regierungen, Wirtschaft und Öffentlichkeit. Diese Arbeit beschäftigt sich mit der hydrothermalen Verflüssigung von Lignin. Der Fokus liegt auf der Entdeckung der Hauptreaktionspfade, welche die Depolymerisation der Ligninmoleküle umfasst, vor allem der kritischen Reaktionen sowie der Erforschung der Reaktionsmechanismen. In diesem Zusammenhang werden auch der Einfluss des Lösungsmittels und der Katalyse diskutiert. Dies sollte erreicht werden durch intensive Literaturstudien und Laborexperimente im Batchreaktor und im kontinuierlichen Rührkessel. Die Simulation des thermodynamischen Gleichgewichts sowie das Modellieren der Formalkinetik der postulierten Reaktionspfade zeigten sich als probate Mittel für die Evaluierung der Versuchsergebnisse. Das Ziel der Arbeit war es, Werkzeuge für die Optimierung der Prozessparameter verfügbar zu machen und die Richtung für weiterführende Studien der Ligninverflüssigung aufzuzeigen. Dazu gehörte auch eine Machbarkeitsstudie, welche das wirtschaftliche Potential eines technischen Prozesses zur Gewinnung von Phenolen aus Lignin evaluiert.

Zur Untersuchung des Lösungsmitteleinflusses wurde ein Vergleich zwischen hydrothermaler und solvolytischer Spaltung in Ethanol herangezogen. Die Lignin-Depolymerisation war bei moderaten Temperaturen (633 K) in Wasser schneller als in Ethanol. Ferner zeigte der Vergleich zwischen Wasser und Ethanol, ein engeres Produktspektrum bei hydrothermaler Spaltung von Lignin. Gleichzeitig stiegen die Catechol-Ausbeuten um das Zehnfache. Dies bietet vor allem Vorteile in Bezug auf eine Produkttrennung von Lösungsmittel und Nebenprodukten. Eine Simulation mit Aspen Plus V7.2 zeigte, dass der größte Teil der organischen Komponenten inklusive 100 % des Lösungsmittels Ethanol im thermodynamischen Gleichgewicht bei 633 K in Gas umgewandelt würden. Wasser hingegen ist sehr resistent gegen

thermische Zersetzung. Heterogene Katalysatoren zeigten positive Effekte bezüglich der Hydrodeoxygenierung von primären oder sekundären phenolischen Produkten der hydrothermalen Lignin-Depolymerisation. Der Einsatz von Raney-Ni katalysierte beispielsweise selektiv die Umwandlung von Catechol in Phenol. Unter den phenolischen Produkten, die bei der Ligninzersetzung entstehen, ist Phenol derzeit die gängigste Plattformchemikalie in der chemischen Industrie. Kinetische Studien halfen, die a priori postulierten Modellreaktionen zu validieren und die kritischen "Flaschenhals"-Reaktionen ausfindig zu machen. Es konnte gezeigt werden, dass verschiedene Reaktionen vorhergesagt werden können, wenn beispielsweise die Herkunft des Lignins oder das eingesetzte Lösungsmittel berücksichtigt werden. Besonderen Einfluss hat auch der Einsatz verschiedener Reaktortypen. Ein kontinuierlicher Rührkessel erleichtert die Sättigung von Radikalen, was zu einer reduzierten Ausbeute von festen Rückständen sowie gasförmigen Produkten führt. Gleichzeitig wird die Entstehung von phenolischen Produkten gefördert. Wesentliche Erkenntnisse über die Reaktionsmechanismen trugen zur Erklärung dieser Phänomene bei. Die Phenolgewinnung aus Lignin durch hydrothermale oder solvolytische Spaltung in Ethanol ist unter Berücksichtigung des aktuellen Stands der Technik wirtschaftlich nicht machbar. Die Studie verschiedener Szenarien zeigte, dass die Ausbeuten von phenolischen Produkten von etwa 10 % auf mehr als 20 % steigen sollten, wobei gleichzeitig das Lignin/Lösungsmittel-Verhältnis deutlich steigen und die Verweilzeit im Reaktor deutlich gesenkt werden muss um vor allem die Kapitalkosten für die Anlage zu senken.

Contents

Abstract **i**

Glossaries **ix**
Glossary . . . ix
Acronyms . . . ix
Symbols . . . xi

1 Introduction **1**
1.1 Motivation . . . 1
1.2 Background and state of the art . . . 4
1.2.1 Lignin . . . 4
1.2.2 Chemical reaction mechanisms . . . 7
1.2.3 Solvent . . . 8
1.2.4 Kinetic studies . . . 9
1.2.5 Catalysis . . . 10

2 Materials, methods and analysis **13**
2.1 Materials . . . 13
2.2 Methods . . . 14
2.2.1 Microbatch-autoclaves . . . 14
2.2.2 Continuous stirred tank reactor . . . 15
2.2.3 Delplot analysis . . . 17
2.3 Analysis . . . 17
2.3.1 Gas chromatography (GC) . . . 17
2.3.2 Fourier transformed infra red spectroscopy (FT-IR) . . . 19
2.3.3 Karl-Fischer-titration (KFT) . . . 19
2.3.4 Photometry . . . 20

3 Thermodynamic Studies **21**
3.1 Introduction . . . 21
3.2 Input parameters . . . 22
3.3 Results . . . 23
3.4 Discussion . . . 26

4 Influence of solvent on thermal lignin degradation **29**
4.1 Introduction . . . 29
4.2 Experimental Results . . . 29
4.3 Discussion . . . 34

5 Influence of catalysts on thermal lignin degradation **37**
5.1 Introduction . . . 37
5.2 Screening of heterogeneous catalysts . . . 38
5.3 Raney-Nickel . . . 39
5.4 Discussion . . . 42

6 Kinetic studies of lignin degradation **45**
6.1 Lignin depolymerisation in ethanol in a batch-reactor . . . 46
6.1.1 Main intermediates and products . . . 46
6.1.2 Grouped products . . . 50
6.1.3 Kinetic model development . . . 53
6.1.4 Results from model fit . . . 57
6.1.5 Discussion . . . 59
6.2 Lignin depolymerisation in ethanol in a continuous reactor . . . 62
6.2.1 Experimental . . . 62
6.2.2 Results . . . 63
6.2.3 Discussion . . . 73
6.3 Lignin depolymerisation in water in a batch-reactor . . . 76
6.3.1 Model adaptations . . . 78
6.3.2 Results . . . 79
6.3.3 Discussion . . . 83

7 Feasibility study of lignin liquefaction **93**
7.1 Background Scenario . . . 93
7.2 Process design . . . 94
7.3 Main equipment . . . 96
7.4 Cost estimation . . . 100
7.4.1 Market prices . . . 100
7.4.2 Manufacturing costs . . . 102
7.5 Discussion . . . 105

8 Conclusion **111**

Bibliography **117**

List of Tables **129**

List of Figures **133**

A Materials **139**

B Sample workup **145**
B.1 Analysis overview 145
B.2 Extraction 147

C Modelling **151**
C.1 Optimisation function 151
C.2 Solvolysis in ethanol 153
C.3 Solvolysis in water 156
C.4 Analysis of error 159
C.5 Sensitivity analysis 159
C.6 Flux analysis 160

D Extended studies of catalysts **163**
D.1 Homogeneous catalysts 163
D.2 Catalytic hydrothermal decomposition of catechol 165
D.2.1 Results 165
D.2.2 Discussion 170

E Experimental results **173**
E.1 Tables of experimental results 173
E.2 Energy and mass flow 194

F Cost offers **197**

Glossar

aliphatic
: hydrocarbon molecule in which the carbon atoms are linked in open chains.

aromatic
: hydrocarbon molecule comprised of at least one benzene-ring.

bioenergy
: energy obtained through the conversion of biomass into gaseous, liquid or solid fuels or by *e.g.* combustion of biomass.

biofuel
: fuel derived from organic matter, obtained directly from plants, or indirectly from agricultural, commercial, domestic, and/or industrial wastes, instead of from fossil products.

catechols
: catechol derivations, include methyl and ethyl para-substitutions for catechol.

H/C-ratio
: molar quantity of hydrogen divided by the molar quantity of carbon comprised by an organic substance.

hydrothermal
: description of the treatment of a substance at increased temperatures sufficient to break down the chemical structure of the substance in the presence of an aqueous solvent.

liquefaction
: conversion of solid biomass into substances which are liquid at room temperature or soluble in the solvent employed for the treatment.

methoxyphenols
: guaiacol derivations, include methyl and ethyl para-substitutions for guaiacol and syringol and propyl para-substitutions for syringol.

O/C-ratio
: molar quantity of oxygen divided by the molar quantity of carbon comprised by an organic substance.

phenolic
: phenol-derived substance comprised of a single benzene-ring.

phenols
: phenol derivations, include all methyl and ethyl substitutions for phenol.

pyrolysis
: most authors use the term if the mixture of reactants consists of maximum 50 wt% organic solvent.

solvolysis
: reaction of solutes, that are in this case lignin and lignin derived components, and the solvent, that is ethanol. Water is potentially inert.

solvothermal
: description of the treatment of a substance at increased temperatures sufficient to break down the chemical structure of the substance in the presence of an organic solvent.

Acronyms

AA acetic acid
Al aluminium

BDE bond dissociation enthalpy
BET Brunauer, Emmett, Teller

C carbon
CatOH catechol
Co cobalt
COM total manufacturing costs
Cr chromium
CSTR Continuous Stirred Tank Reactor
CyclohexO cyclohexanone
CyclohexOH cyclohexanol

DME dimethyl-ether
DTG derivative thermogravimetry

EoS equation of state
EtCatOH ethylcatechol
EtGua ethylguaiacol
EtOH ethanol
EtPhe ethylphenol
EU European Union
Exp. experiment
Ext extraction

FA formic acid
Fe iron
FID flame ionisation detector
FT-IR Fourier transformed infra red spectrometry

GC gas chromatography
GLE gas-liquid equilibrium
GPC gel permeation chromatography
Gua guaiacol

H hydrogen
HC hydrocarbon
He helium
HHV higher heating value

ILUC indirect land use change

K potassium
KFT Karl-Fischer-titration

LHV lower heating value
Lig lignin
LLE liquid-liquid equilibrium

MA micro batch autoclave
MeCatOH methylcatechol
MeGua methylguaiacol
MePhe methylphenol
methoxyPhOH methoxyphenols
Mo molybdenum
MS mass spectrometry
MtOE million tons of oil equivalent

N nitrogen
n.a. not available
n.d. not detected
Nb niobium
NCW near critical water
Ni nickel

O oxygen
OLC operating labor costs

P phosphor
P&ID piping and instrumentation diagram
Pd palladium
Phe phenol
PhOH phenols
Pt platinum

Rh rhodium
Ru ruthenium

S sulphur
SCW supercritical water
Si silicon
Syr syringol

Ta tantalum
TBM total bare module costs
TCD thermal conductivity detector

TCI total capital investment
TGA thermogravimetric analysis
Ti titanium
TMC total material costs
TUC total utility costs

UV-Vis photometric spectroscopy

Symbols

A_{Ex} heat transfer area

A_j constant describing the threshold value of k_j approaching infinite temperatures, apparent Arrhenius factor

$C_{i,aq,0}$ concentration of the component i in an aqueous solution before extraction.

$C_{i,org}$ concentration of the component i in the organic phase after extraction.

$\overline{c}_p$ average heat capacity.

$E_{A,j}$ constant considering the temperature dependence of k_j, apparent activation energy

f_a factor considering the dilution of the organic phase after the extraction with ethyl acetate and the internal standard pentacosane ($C_{25}H_{52}$)

f_b factor considering the solubility of solvent and extractant

f_c factor considering the change of the solute concentration due to the different input volumes of aqueous sample and extractant

$f_{d,i}$ factor considering the distribution ratio of the solute i in the solvent and the extractant

g gravitational acceleration

H total dynamic head

$\dot{H}_i$ enthalpy stream of component i

ΔH_R reaction enthalpy

k_j formal kinetic rate coefficient of nonelemental reaction j

L_D depolymerised lignin, lump component summarising all lignin derived organic compounds soluble in the solvent, that is water or ethanol, and not measured by gas chromatography (GC)-analysis

$\vec{k}$ vector containing the formal kinetic rate coefficients of all reactions defined within the model

m reaction mass

$\dot{m}$ mass flow through the continuous reactor

m_i mass of component i in the product mixture

$m_{i,aq,0}$ mass of the component i diluted in an aqueous solution before extraction.

$m_{i,org}$ mass of the component i diluted in the organic phase after extraction.

$m_{Lig,0}$ initial mass of lignin

p reaction pressure

p_{in} initial pressure before entering the pump

p_{out} pressure of the effluent of the pump

$\dot{q}$ heat transfer rate

R ideal gas constant

ρ density

$\overline{\rho}$ mean density of a mixture

r_j reaction

R^2 coefficient of determination

σ standard deviation

t experimental duration

τ residence time in a batch reactor

τ' mean residence time in the continuous reactor

T temperature

$T_{c,W}$ critical temperature of water

ΔT difference of fluid temperature entering and emerging the heat exchanger

$\overline{\Delta T}$ mean overall temperature difference between the two fluid streams exchanging heat

T_{in} temperature of fluid entering the heat exchanger

ΔT_{in} temperature difference between hot fluid emerging the heat exchanger and cold fluid entering the heat exchanger

T_{out} temperature of fluid emerging the heat exchanger

ΔT_{out} temperature difference between hot fluid entering the heat exchanger and cold fluid emerging the heat exchanger

V_{aq} volume of aqueous phase

$\dot{V}$ volumetric flow rate, capacity

V_{org} volume of organic phase

V_R reaction volume

w weighing factor

W work, energy

W_o usable work

x overall conversion

Ξ number of experiments

Δy_i sensitivity

y_i^{calc} yield of the component i calculated by employing the adequate model

y_i yield of the component i

$y_{i,j}$ yield of the component i taking part in the reaction r_j

$y_{i,\xi}^{meas}$ yield of the component i measured in the product of experiment ξ

$\overline{y}_i$ average of the yield of the component i measured in the product of identical experiments

$\overline{y}_i^{meas}$ average of the yield of the component i measured in the product of all experiments carried out at the same temperature

y_i' yield of the component i after modification of k_j

$y_{i,0}$ initial yield, that is the mass of the component i divided by $m_{Lig,0}$

Chapter 1

Introduction

1.1 Motivation

Earth's resources of crude oil are limited [OR11]. An important challenge for scientists and engineers is to develop technologies that are largely independent from fossil crude oils. Biomass is supposed to have a high potential to replace crude oil as a basic input material for the production of many organic chemicals and fuels. Political efforts to increase the market share of biomass derived chemicals and fuels in USA and Europe increase. »The European Union (EU) as a whole has set a mandatory target of 20 % for renewable energy's share of energy consumption by 2020 and a mandatory minimum target of 10 % for biofuels for all member states« [Zak+0]. A study carried out by the European Environment Agency reports that a large biomass production capacity is available in Europe, which could produce 190 million tons of oil equivalent (MtOE) of biomass by 2010 with possible increases up to 300 MtOE by 2030 [EEA06]. However, the study »disregards the effect of competition between bioenergy and food production for domestic food supply.« This »would become more important with the assumed rise of the combined carbon permit and energy prices.« In fact, the study considered that »increased demands on agricultural sector output causes intensification of farm management across the agricultural land area, incentives to transform extensively used grassland, olive groves or dehesas [...], into arable land for growing bioenergy crops« and »an inappropriate bioenergy crop mix, which does not take account of the specific environmental pressures of different crops in the context of the main environmental problems in a particular region« [EEA06]. However, it could still not be proven that these

worrisome effects of increasing biomass production can be limited by the current policy and the agricultural industry. On the contrary, the worldwide agricultural production combined with »intensive export-oriented agriculture has increased under open market operations but has been accompanied by both benefits and adverse consequences depending on circumstances such as exportation of soil nutrients and water, unsustainable soil or water management or exploitative labor conditions in some cases« [Bei+08]. In addition, »people have benefited unevenly from these yield increases across regions« [Bei+08]. Furthermore, the increase in bioenergy in Europe is suspected to foment *e.g.* the grubbing of tropical rainforests. These effects of indirect land use change (ILUC) are still discussed, however, »simulations for EU biofuels consumption above 5.6 % of road transport fuels show that ILUC emissions can rapidly increase and erode the environmental sustainability of biofuels« [ADL10]. The recent effects of common agricultural and renewable energy policy in Germany show that *e.g.* the area utilised for the cultivation of maize has risen of approximately 50 % to 2.3 million hectare in the decade from 2000 to 2010 due to high market prices and subsidies [SR11]. 23 % of this area was dedicated to the generation of bioenergy in 2011 [FNR11; Ehr12]. Maize, however is ranked to highly contribute to soil erosion nutrient, leaching to ground and surface water, pesticide pollution and reduction of farmland biodiversity [EEA06].

Should our society rely on the increasing output of the agricultural industry to satisfy its energy demand? The fields of discussion are large and will not be entirely covered here. In order to establish neither the generation of energy nor the production of chemicals from biomass at the expense of biodiversity or social and environmental pressures, within the present work the use of biomass exclusively from waste is proposed. The potential of waste biomass, though hopefully decreasing in the future, is 100 MtOE per year [EEA06].

Lignin, a major component of lignocellulosic biomass, 15-30 % by weight, 40 % by energy [Zak+0], is one of the most abundant renewable organic materials in the world. Large quantities of lignin are available as waste material produced by the pulp and paper industry (black liquor). Worldwide more than 50 million tons of dry lignin are produced annually, of which more than 98 % are burned to recover its energetic value [Gla09; Pul09]. Less than 2 % are used for synthesis of fuel or chemicals. Upcoming technologies are the gasification of black liquor and adjacent synthesis of dimethyl-ether (DME) or Fischer-Tropsch-synthesis [CKL09]. Chemrec is already running a gasification plant in Piteå (Sweden) [Sch12]. From a chemical perspective, lignin is a readily available source of aromatics and phenolics that are present within the structure [KB08a], which at present is only marginally being

used for production of, *e.g.* vanillin [KT89], environmental-friendly glue [Sch07] and in lead batteries [Kog09]. Aromatic and phenolic compounds are, however, of great interest for use as platform chemicals for, *e.g.* the production of synthetic resins or pharmaceuticals, and could possibly be used as an unresolved mixture for fuel blending purposes, based on the anti oxidative properties of hindered phenolics in turbine fuels [AST87]. Among them phenol is the most demanded chemical substance. In 2004 8.5 Mt/a were produced worldwide [Arp07].

Large research effort was inverted in the study of lignin depolymerisation and the production of fuel or chemicals from lignin. In the middle of the last century Lautsch and Piazolo carried out catalysed hydrogenation of lignin in a basic solution and alcohol [LP43]. The investigation continued. A comprehensive summary was available in 1981 written by Meier and Schweers [MS1]. Towards the end of the last century research efforts concentrated on pyrolysis of lignin without solvent (dry pyrolysis) or in organic solvents [FMG87; MB97; APR01]. Most studies which try to elucidate reaction pathways of hydrothermal lignin degradation were conducted in the last decade [WSG11; YM12]. However, no technical process for the production of phenolics from lignin has been released. This might be due to relatively small yields of phenolics from lignin, usually around 10 to 20 wt% maximum [APR01]. The theoretically possible yield is, depending on the type of lignin, between 30 and 50 %. In order to increase the yield of phenolics, catalytic hydrogenation of the liquid product from lignin pyrolysis was applied [Gut+09; Kar+06]. However, most research efforts focus on model substances and disregard real product mixtures which comprise a large variety of single compounds.

In order to understand how yields of phenolics from thermal-chemical lignin degradation can be increased, it is necessary to elucidate important reactions and their participants which occur within the lignin depolymerisation. The intention is to reveal bottleneck reactions and main reaction products. It is thus also necessary to understand reaction mechanisms and how they are influenced by several parameters like temperature, solvent, catalyst, etc. The present work approaches the answers to these questions by focussed experimental work. Simulation of the thermodynamic equilibrium and modelling of the reaction kinetics are strong numerical instruments for the interpretation of the experimental results.

The aim of lignin depolymerisation is to maximise the yield of valuable phenolic products by optimising reaction parameters. The influence of different solvents and catalysts on the phenolic yield from thermal-chemical lignin degradation are discussed in Chapter 4 and 5. The simulation of the thermodynamic equilibrium is especially interesting for the evaluation of the influence of the residence time in the reactor and temperature on the

product composition (see Chapter 3). For the recovery of valuable phenolic products from lignin, it is crucial to understand the main reaction pathways of lignin degradation and reaction kinetics. Up to now, some research has been undertaken in respect to the kinetics of pyrolytic, solvothermal and hydrothermal lignin depolymerisation [KV08; PK08; Var+97; ZHR11; YM12]. The present work includes the development of a formal kinetic model considering the formation and degradation of the main phenolic products as well as the solid and gaseous byproducts (See Chapter 6). The development of a model of the crucial reaction pathways and the kinetic studies allow a suggestion of these optimised parameters and clear statements about the basic design of an industrial process of lignin depolymerisation. A feasibility study of a technical process for thermal-chemical degradation of lignin in both, water and ethanol, was considered to be essential for the evaluation of future research work concerning the production of phenol from lignin (see Chapter 7).

1.2 Background and state of the art

The following sections provide an overview over the state of knowledge and technology concerning the molecular structure of lignin and the methods of separation from the cellulosic parts of biomass (see Section 1.2.1), reactions occurring within thermal-chemical lignin degradation and their mechanisms (see Section 1.2.2), specific solvents used within this work and their effects on lignin degradation (see Section 1.2.3), kinetic studies (see Section 1.2.4) and the influence of homogeneous and heterogeneous catalysts (see Section 1.2.5).

1.2.1 Lignin

Degradation of lignin is a complex process. Not only a vast spectrum of compounds can be produced from lignin, but lignin itself is a largely varietal polymer. The origin of the biomass largely contributes to the structural-chemical variations encountered in different types of lignin. Different types of lignocellulosic biomass consist of different amounts of lignin, with lignin abundance generally decreasing in the order softwood > hardwood > grass/annual plant. In plant cell walls, lignin fills the spaces between cellulose and hemicellulose, and it acts like a resin forming the matrix where fibrous cellulose is embedded [Zak+0]. Lignin is a three dimensional amorphous polymer consisting of methoxylated phenyl-propane building blocks (see Figure 1.1). Varying amounts of the three characteristic phenyl-propane building blocks, shown in Figure 1.2, allow its classification into different types of lignin and subse-

quently into the three broad categories of plant lignin: softwood, hardwood, and grass or annual plant lignin [Pea67, p 339].

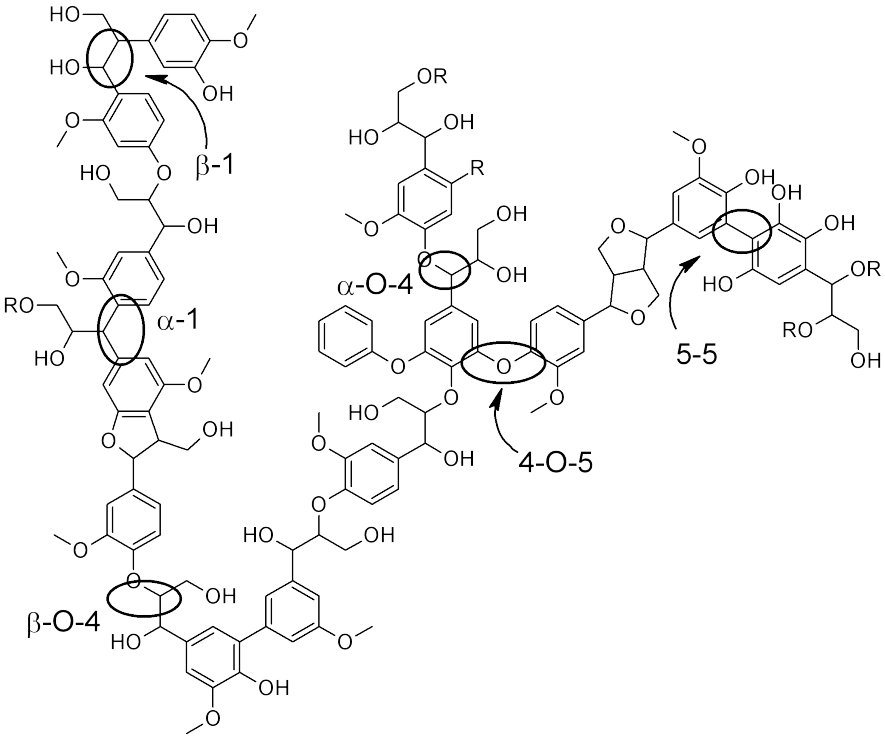

Figure 1.1: Example of lignin structure depicting some of the dominant linkages between the aromatic monomers [WR12].

Table 1.1: BDE of the most predominant linkages (see Figure 1.1.)

Bond	α-O-4	β-O-4	4-O-5	β-1	α-1	5-5
BDE (kJ/mol)	215	290	330	280	360	490

Softwoods are commonly composed of guaiacyl lignin, which is principally made up of coniferyl moieties. Guaiacyl-syringyl lignin contains a combination of sinapyl and coniferyl moieties and is prevalent in hardwoods. Annual plant or grass lignin is mainly composed of *para*-coumaryl units [FN68]. The characteristic variation of these different units can also be observed in the depolymerised products [Dor+99]. The building blocks (aromatic monomers)

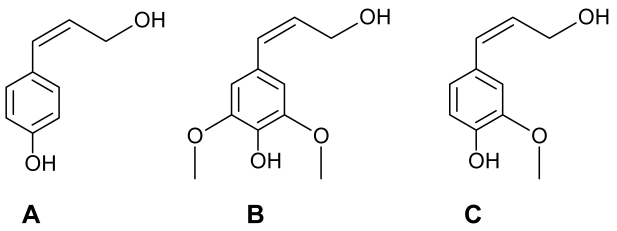

Figure 1.2: The three characteristic aromatic substances which constitute the characteristic monomeric units of lignin: A: *para*-coumaryl alcohol, B: sinapyl alcohol and C: coniferyl alcohol.

are randomly connected through C-C bonds or ether bonds (C-O bonds). The most dominant bonds (80 %) within the lignin structure are ether bonds [RS09]. The distribution of the linkages in the biopolymer structure depends on the type of wood and the part of the plant. The most predominant ether linkages are the β-O-4 and the α-O-4 [WR12]. These and other linkages are depicted in Figure 1.1. The BDE, listed in Table 1.1, reveals that the ether bonds in general are weaker than the C-C bonds. Hence, the cleavage of the ether linkages is the most favourable reaction initiating the depolymerisation of the lignin polymer.

Furthermore, the structure of the lignin separated from the rest of the plant structure (cellulose and hemicellulose) depends on the employed separation method. The separation method can consist in physical treatment, solvent fractionation, chemical or biological treatment [Cos+9]. Alkaline treatment, a chemical treatment, is most commonly employed by the pulp and paper industry. It is a highly efficient separation method, however, involves the incorporation of sulphur which can be problematic for a further chemical treatment especially if heterogeneous catalysts are involved. Various novel developments within the most prominent separation techniques, *i.e.* enzymatic and acid hydrolysis, organosolv pulping and steam explosion have largely contributed to establishing a pathway to a potentially economically valid exploitation of the sugar polymers from lignocellulosic biomass. As a side-effect, they further shape some of the characteristics of the lignin by reacting with functional end-groups in the lignin structure, thus influencing the solubility properties of the isolated polymer.

1.2.2 Chemical reaction mechanisms

By the cleavage of ether bonds, the main linkages between the aromatic rings of the lignin macromolecule, aromatic monomers and oligomers are formed. It is however a challenge to gain a high-value product of homogeneous composition from such a chemically complicated and inhomogeneous component as it is lignin. Hence, it is helpful to understand at least the main chemical mechanisms that are responsible for the most important reactions occurring within lignin depolymerisation.

Formation and degradation of aromatic monomers occur by hydrolysis [TRR11] or radical reaction [DM99]. The most relevant initiation reactions involve the cleavage of the weaker C-O bonds as explained above. If homolytic cleavage and thus radical reaction is assumed, the BDEs are a key value. Faravelli et al. [Far+10] discussed different radical reaction pathways which lead to initial cleavage of ether bonds and the BDEs of some of the bonds which are present in the lignin structure. Hydrolytic reactions involve the heterolytic cleavage of ether bonds, especially β-O-4. Possible hydrolytic reactions occurring within the degradation of lignin were summarised by Lundquist and Lundgren [LL1; Lun6]

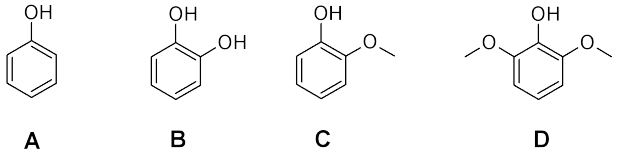

Figure 1.3: Monoaromatic products (phenolics) from lignin depolymerisation: A: phenol, B: catechol, C: guaiacol and D: syringol.

The cleavage of the ether and aryl bonds of the lignin structure yields monoaromatic (phenolic) substances. The most prominent are phenol, catechol, guaiacol and syringol (depicted in Figure 1.3) and alkylated derivatives thereof. The phenolics further decompose by thermal cleavage of the hydroxyl- and methoxyl-group [Run+12; Nim+11a; Nim+11b]. At the temperatures usually applied for liquefaction of lignin (500 - 750 K) the aromatic ring is stable. It decomposes towards higher temperatures [HS2]. The C-O bond of the methoxy-group of guaiacols and syringols is most likely to decompose due to rather low BDE of about 240-250 kJ/mol [Vuo86]. Different pathways of the decomposition of methoxyphenols are comprehensively summarised by Zakzeski et al. [Zak+0].

The recombination of fragments from both radical [McM+04] and hydrolytic [Sai+03] cleavage of lignin ether bonds leads to the build-up of a polymer. This polymer is usually referred to as char. Dorrestijn et al. claimed that char formation can be caused by hydrogen shuttling from the lignin matrix before the actual process temperature is reached, which implies that the structure of lignin under liquefaction conditions is irreversibly changed [Dor+00]. McMillen et al. postulated a repolymerisation of (di-) hydroxybenzene which occurs during liquefaction of coal [McM+04]. Roberts et al. observed polymerisation of monomeric aromates during hydrothermal treatment of lignin and suggest boric acid as an excellent radical scavenging agent [Rob+1]. Some aromatic monomers, such as phenol or cresol, were also found to inhibit the formation of char and reduce the yield of solid residues by scavenging aromatic radicals and thus stopping the repolymerisation reaction [McM+04; Sai+03; Tak+12]. Yokoyama et al. [Yok+98] found that char formation from lignin in aqueous media was promoted by low temperatures, high pressures and long reaction times.

1.2.3 Solvent

Pyrolysis, solvolysis and hydrothermal treatment are the most promising advances to lignin depolymerisation for the purpose of liquefaction and recovery of phenolics [Now+10; KGB09; Moh06]. Lignin depolymerisation and valorisation by hydrodeoxygenation has been widely explored within different pyrolysis and solvolysis approaches. Solvothermal and hydrothermal degradation provide the advantages of mild conditions and a single phase environment due to the miscibility of the organic products in the (supercritical) solvent. M. Kleinert and T. Barth have done intensive research on lignin solvolysis in ethanol using formic acid as hydrogen donor [KB08a; KB08b; Kle+11; KGB09]. Ethanol has a very high solvency for biomass and a low critical temperature which makes it attractive for lignin depolymerisation [Zha+10b]. Further advantages of solvolysis in ethanol over fast pyrolysis are a less oxygenated oil fraction [KB08b] and almost no solid residue (< 5 wt%) [Gel+08; Moh06]. In-situ hydrogen donation is realised by the thermal degradation of formic acid. A very active atomic hydrogen species is produced [Gel+08], which results in a successful deoxygenation and hydrogenation of lignin structures. Various largely demethoxylated phenolic structures comprising a high H/C-ratio and low O/C-ratio [KB08b] were obtained without necessitating any further added catalyst for activation or transfer.

The selection of a solvent for thermal-chemical lignin depolymerisation is one of the key challenges since it has a great impact on the deoxygena-

tion of aromatic intermediates as well as on the formation of char and gas. Liu and Zhang [LZ08] compared water with two organic solvents, that are ethanol and acetone. Increased char yields have to be expected when using water probably due to the higher solubility of oily and tarry products in the organic solvents. However, water shows a narrower product spectrum in respect to phenolic products and a high selectivity in respect to phenol and catechol [WSG08]. This is an advantage especially for the separation of the products, which tends to be less energy and cost intensive at increased concentrations of the target product. The yield of catechol and phenol can be even increased by applying an acidic or a basic environment [TRR11]. Wahyudiono, Sasaki, and Goto [WSG08] pointed out the influence of the water density on the product composition. High water density led to higher phenol and cresol yields between 623 K and 673 K. Further advantages of water are its abundance at rather low prices and its chemical stability at the required temperatures and pressures. In fact in respect to the treatment of black liquor no drying prior to the liquefaction has to be applied, thus energy can be saved.

1.2.4 Kinetic studies

The understanding of the degradation processes and formation of products is an essential step in increasing yields and achieving product requirements. This requires both the elucidation of pathways but also of their kinetics. Kinetic models describing the decomposition of lignin are largely concentrated on global bulk models describing the yields of gas, char and liquids. First attempts describing the degradation were done using a single first order reaction [Nun+85], which were followed by more complex models, involving also multiple competing reactions [Var+97]. A semi-detailed model based on a set of molecular and radical species derived from the main building blocks involved in about 500 elementary or lumped reactions considering the cleavage of different bond-types and repolymerisation reactions was developed by Faravelli et al. [Far+10]. During the last decade the thermal degradation of lignin was studied by various authors applying thermogravimetric analysis [Cho+12; JNB10]. In addition, the kinetics of hydrothermal lignin degradation came in the focus of research. Zhang, Huang, and Ramaswamy calculated formal kinetic parameters of the hydrothermal degradation and the build-up of char in a batch reactor [ZHR11]. Takami et al. applied a Monte-Carlo-Simulation in order to determine the formal rate coefficient of lignin degradation [Tak+12]. The first kinetic model considering the formation and decomposition of phenolics within the lignin degradation in a continuous reactor was reported recently by Yong and Matsumura [YM12].

Experimental studies of the decomposition and charting of network pathways under pyrolysis conditions were reported by Klein and Virk [KV80; JK85; KV08]. They considered the presence of hydrogen and exploited the available intermediate model substances as starting materials, such as syringol, guaiacol and catechol, to try and master the cascade of demethoxylation, deoxygenation, hydrogenation, alkylation, demethylation and methanolisation reactions. The kinetics of the decomposition of both lignin and biomass degradation and different modelling approaches, the latter mainly focusing on global bulk models, have been comprehensively summarised by Miller and Bellan, Prakash and Karunanithi and Brebu and Vasile [MB97; PK08; BV10].

The intention of this work is to establish a model, that considers the main reaction participants and pathways and is able to quantify the amount of phenolic products in dependence of the residence time in the reactor. In addition, bulk products such as char and gas should be quantified respecting the mass balance at every time. A validation of the developed model using literature and employing different reactor systems was conducted. Finally, an adaptation of the model for different solvent systems was discussed.

1.2.5 Catalysis

Both homogeneous and heterogeneous catalysts can influence the reactions occurring during thermal-chemical lignin degradation. While heterogeneous catalysts are more likely to interact with diluted compounds with a relatively low molecular size, such as phenolics, homogeneous catalysts are capable to influence also the cleavage of the ether and alkyl linkages of the lignin molecule [Beh+06]. Toor, Rosendahl, and Rudolf [TRR11] have summarised the effects of homogeneous and heterogeneous catalysts on the hydrothermal liquefaction of biomass in general. According to them alkali salts increase the liquid yield and inhibit the dehydration of the biomass monomers and thus suppress the char formation. Karagöz et al. found that K_2CO_3 also effects the formation of monoaromatic substances and increases the amount of di-hydroxybenzenes (catechols) from hydrothermal liquefaction of sawdust from pine at 553 K [Kar+06]. In addition, alkali salts, especially potassium (K) salts, have a high ability to catalyse the water-gas-shift reaction and thus increase the amount of CO_2 and H_2 at the expense of CO via formate as intermediate. The presence of reactive hydrogen potentially promotes the hydrogenation of organic intermediates [Kru+00; SKR04]. During hydrothermal liquefaction some gasification is crucial since the oxygen is removed under the formation of CO_2. However, extensive gasification will reduce the yield of liquid products [TRR11]. Sergeev and Hartwig claim to have found

a homogeneous nickel carbene catalyst which selectively cleaves aromatic C-O bonds in various aromatic ethers without reduction of aromatic rings or cleavage of aliphatic C-O bonds [SH11].

Heterogeneous catalyst were applied mostly for the gasification of biomass and rarely for direct liquefaction. However, much effort has been spent on the investigation of valorisation of bio-oils by hydrodeoxygenation. The bio-oils are obtained in a first step liquefaction of biomass and in a second step hydrodeoxygenated with the help of a heterogeneous catalyst in a hydrogen donating environment [Wil+09]. Dorrestijn et al. suggest the catalytic hydrogenation in an appropriate hydrogen donating solvent to be the most promising method to produce phenols from lignin [Dor+99]. Catalysts applied for hydrodeoxygenation are heterogeneous catalysts. Wild et al. used ruthenium (Ru) on carbon (C) for valorisation of lignin derived pyrolysis oil [Wil+09]. Other studies show that catalysts based on rhodium (Rh), palladium (Pd) and platinum (Pt) have a high potential to promote hydrodeoxygenation of methoxyphenols in organic solvents [Gut+09] as well as in a gas phase reaction [Zha+11]. The reaction network of catalytic hydrodeoxygenation and the influence of an acid, *e.g.* the support of a metal catalyst, on the oxygen removal were developed by Nimmanwudipong et al. [Nim+11a; Nim+11b; Run+12]. In addition, heterogeneous catalysts comprising nickel (Ni) and molybdenum (Mo) were studied and their effect on the hydrodeoxygenation of bio-oil derived components were proven [LWC11]. Noteworthy in this context is the statement of Rinaldi and Wang saying that the solvent holds the key to control the selectivity of a heterogeneous catalyst in the conversion of lignin into phenols [RW12; WR12]. They reported that Raney-Ni in combination with 2-propanol as solvent and H-donor efficiently catalyses the hydrodeoxygenation of model substrates and bio-oil [WR12]. The influence of heterogeneous catalysts on lignin-derived phenolics and the hydrodeoxygenation of pyrolysis oil in an aqueous phase was studied by Zhao and Lercher [ZL12; ZL2; Zha+1] who suggest the conversion of phenolic components present in bio-oil in an aqueous solvent with Ni or Pd catalysts in combination with an acid, *e.g.* Nafion/SiO_2 [Zha+10a].

The present work focuses on heterogeneous catalysis of the valorisation of phenolics in an aqueous solvent especially with Raney-Ni which showed promising effects on the conversion of catechols into phenols [For+12].

Chapter 2

Materials, methods and analysis

2.1 Materials

For the experimental work two different types of lignin were used which are distinguished by the origin of the wood and the method of separation of cellulose and lignin. The first type of lignin was received from ALM Indiva Pct. Ltd., India, and originates from wheat straw. The separation from the cellulosic parts of the wheat straw was realised in a basic aqueous medium, followed by a precipitation of the cellulose employing a weak acid. The second type of lignin was received from Sekab, Sweden, and originates from spruce which is a softwood. It was treated by enzymatic hydrolysis in order to separate lignin and cellulose. Both types of lignin were dried for at least 16 h at 378 K and ground to a maximum diameter of 0.2 mm. The residual moisture of both types of lignin after drying and storage was 4.5 wt%. The amount of residual cellulose and hemicellulose obtained by analysis and data provided by the producer are listed in Table 2.1 together with the results from CHNS analysis (see Section 2.3.4) yielding the percentage of C, hydrogen (H), nitrogen (N), sulphur (S) and oxygen (O).

Chemicals such as any heterogeneous or homogeneous catalysts, phenolic compounds for analysis and experiments, solvents and gases are listed in Appendix A.

Table 2.1: Characterisation of both lignin types from wheat straw and spruce.

Type/ Origin	Lignin	Cellu-lose[a]	Mois-ture	C	H	O	N	S	Ash
	wt%	wt%	wt%	wt%	wt%	wt%	wt%	wt%	wt%
Wheat straw	>90	<3	4.5	63.8	6.0	27.0	1.5	0.3	1.4
Spruce	40	47	4.5	60.5	6.7	30.1	0.6	0.1	2.0

[a] Including hemicellulose.

2.2 Methods

2.2.1 Microbatch-autoclaves

The most used type of reactors for the experimental work was an in-house custom built micro batch autoclave (MA) of 5 mL or 10 ml inner volume made of stainless steel 1.4571 (see Table A.3). It seals gas-tight up to temperatures of 723 K and pressures of 30 MPa. A simple version of the MA (MA1) permits the loading of the reactor with solids and liquids, however, ventilation and loading with gas is not possible. In order to enable the loading of the MA with gas, the design was modified and gas tubes and valves were attached (gas-input version, MA2). Mechanical drawings of both versions of the MA are to be found in Appendix A. The MAs are easy to handle, can resist high pressures and temperatures and are easy to repair and to replace.

Simple version (MA1)

The MA1 were filled with solvent, lignin and if appropriate a certain amount of catalyst. The remaining volume was flushed with nitrogen gas and thereafter the reactor was screwed tight (metal on metal sealing) in a custom built containment that seals up to pressure of 10 MPa. The MA1 was heated in an oven (HP-5890) at maximum heating rate (approximately 40 K/min). The experiment was started when the desired temperature in the oven was reached. After the determined residence time τ at the temperature T the autoclaves were cooled either by active air cooling of the oven or if more rapid cooling was required in iced water. After cooling the micro-autoclave were again placed in the custom-build containment for ventilation.

Gas-input version (MA2)

The further developed MA2 has one inlet-tube on the side of the bottom part of the autoclave and one outlet-tube connected to the top-part of the MA2 (see Figure A.2). Both tubes can be opened and closed with valves that seal gas-tight up to a pressure of 100 MPa gauge pressure. For safety reasons the reactor had to be ventilated with nitrogen (N_2) at first. After ventilating with N_2 for a time duration of 30 s, the nitrogen-supply was cut and the inlet-tube was connected to a hydrogen bottle. The autoclave was ventilated with hydrogen (H_2), again for 30 s. Afterwards, the outlet-valve was closed and the appropriate pressure of H_2 in the autoclave was adjusted. After pressing H_2, or any other desired gas, into the MA2, the hand-valve was closed and the MA2 was placed in an oven (HP-5890) where it was heated to the desired temperature at maximum heating rate (approximately 40 K/min). After the determined residence time in the oven the MA2 was cooled to room temperature in iced water. For ventilation, the outlet tube of the MA2 was connected to the inlet of a high pressure gas sampling tube that had been ventilated with nitrogen before. The outlet of this gas sampling tube was connected to a gas-meter. Now the hand valve was opened so that the gas inside the reactor would fill the gas sampling tube and afterwards flow into the gas-meter to measure the amount of gas coming out of the MA2.

Sample workup

The volume of gas exiting from the autoclave was measured with a gas flow-meter. A sample of the gas was analysed on a gas chromatograph equipped with a flame ionisation detector (FID) and a thermal conductivity detector (TCD) in order to determine the composition. After ventilation, the reactors were opened and the liquids and solids were removed. The solids were separated from the liquids via filtration and the weight of both phases was determined gravimetrically. For detailed sample work-up of aqueous and organic liquid samples see Appendix B. The analysis of experimental errors is based on replicate experiments and is further explained in Appendix C.4.

2.2.2 Continuous stirred tank reactor

A CSTR was employed for thermal degradation of lignin in order to take advantage from the characteristic properties of this type of reactor, that are the back mixing and a high heating rate [Lev99, p.94ff]. Back mixing enables the interaction of products with unreacted feed. The CSTR has an inner volume of 200 mL, is made of the Ni-based alloy Inconel625 (see

Table A.3) and is heated by incorporated heating cartridges purchased from Watlow (type Firerod). It is designed to bear 923 K and 100 MPa pressure. The stirrer is made of 1.4571 stainless steel. The transmission of the torque between the motor and the shaft of the stirrer is realised by means of a magnet clutch. The magnet coupling has to be maintained below the Curie-temperature (1041 K) to guarantee the magnetic properties of the material and the movement of the stirrer throughout the experiment.

A piping and instrumentation diagram (P&ID) flow scheme of the laboratory plant is shown in Figure A.3. The feeding of the suspension composed of lignin, solvent and co-solvent into the reactor is realised via two screw presses, each with a maximum inner volume of 60 mL. The screw presses were purchased from Swagelok and made of 1.4571 stainless steel. The suspension of ethanol, formic acid and lignin is sucked into the screw press cylinder through a tube on the front end of the cylinder and pressed out through a tube at the lower part of the cylinder of the screw press. In order to avoid plugging by means of sedimentation in the feeding tubes, long and curved tubes in the construction were avoided (length of feeding tubes less than 250 mm, inner diameter: 5.2 mm). The pneumatic valves and the motor of both screw presses are controlled manually and independently from each other which enables a continuous feeding and facilitates a rapid filling of the screw press cylinder while at the same time low flow rates can be realised. Before starting an experiment, the reactor was pressurised and heated to the desired temperature. Throughout the heating period, the reactor was rinsed with ethanol by a third pump.

Upon commencing the experiment, the feed suspension was filled into the reservoir. For mixing purpose the feed was continuously pumped in a circle from the bottom of the feed reservoir to the upper part of the reservoir. The screw press was filled by sucking the feed suspension in from the circulation tubes. After leaving the reactor, the fluid passed a cooler and a depressurising system, consisting of two valves, a pressure measurement system and a proportional and integral controller (see Figure A.3). The product stream then entered a flash separator. In the separator gaseous products were separated from solid and liquid products. The volume of the gas produced was measured using a rotor gas flow meter (Ritter TG1). The latter can optionally be conducted through a gas sample tube. Gas samples can thus be taken at different intervals during the experiment. When the gas flow showed less than 5 % deviation for a minimum of three measurements within 60 min, the stationary state was claimed to be reached. Several liquid samples (including solid particles) were taken throughout the whole experiment by emptying the flash separator via a valve at the bottom of the container. Further work-up procedures were conducted analogue to the work-up described for the batch

reactors (see Appendix B).

2.2.3 Delplot analysis

The Delplot technique bases itself on the analysis of selectivity-conversion plots and can be used for both primary and higher rank products [BKB90]. The basic primary Delplot allows the separation of primary from non-primary reactions for any given reaction order. For a primary Delplot, the yield of a singular ith component (y_i) divided by the overall conversion (x) is plotted over x. Plotting y_i/x^2 over x gives a second rank Delplot, y_i/x^3 over x third rank and so on. The intercept on the y-axis stipulates the rank of the product. If the intercept in a primary rank Delplot of a component is finite, the product is a primary one. If the intercept on the y-axis is zero, then the component is not formed by a primary reaction. The interpretation of intercepts is analogous for higher ranks.

2.3 Analysis

In this section the employed analysis methods are introduced and described. Basic data about the utilised equipment and adjustments are given. Uncertainties of the analytically obtained results and error tolerances were determined by replicate experiments. If error bars are given in any diagram, they are based of the standard deviation σ (see Appendix C.4). 18

2.3.1 Gas chromatography (GC)

GC was employed to quantify the gaseous products and the phenolic products in the liquid product phase. After injection the sample is vaporised in the injection port and carried by a mobile gas phase through a column. Due to the different interaction forces with the surface of the column each constituent of the sample has a characteristic retention time in the column. Thus the separation of the constituents can be achieved. A quantification of the substances emerging from the GC-column was conducted with either a flame ionisation detector FID or a thermal conductivity detector TCD. In the FID the eluent emerging from the GC-column is mixed with hydrogen and air a burned and ionised. The ions are detected by the collector electrodes. The FID facilitates the quantification of substances comprising C. The TCD senses changes in the thermal conductivity of the column effluent and compares it to a reference flow of the carrier gas helium (He).

GC analysis of gaseous samples

Gas phase GC analysis was performed on an Agilent 7890A with a 2 m Molsieve 5A column in series with a 2 m Porapak Q column equipped with a FID front and TCD back detector. The system was controlled by an Agilent laboratory data system. Injections were carried out by manually injecting 100 μL of the ventilated gas from the reactor. Temperature program: Initial temperature 323 K for 22 min, then heating at 20 K/min to 423 K, kept for 15 min. Further heating at 50 K/min to 503 K, kept for 10 min. The injection port was at 523 K, the FID at 503 K and the pressure was kept constantly at 255 kPa. The equipment was calibrated by introducing varying amounts of a standard gas mixture. The system was checked on a weekly basis by introducing the standard gas mixture and recalibrated if necessary. The maximum tolerance of the measured value was 10 vol% in respect to the concentration of each gaseous compound in the standard mixture.

GC-FID analysis of liquid samples

Quantitative GC-FID analysis of liquid products was performed on a HP 5890-II GC equipped with HP auto sampler 5890, a 30 m Rtx-1MS dimethyl-polysiloxan column and FID. The system was controlled by an HP-Chem laboratory data system. Temperature program: Initial temperature 313 K for 6 min, then 5 K/min heating to 453 K, then with a rate of 30 K/min continued heating to 533 K, kept for 5 min. Further heating increase at 30 K/min to a final 573 K and kept for 12 min. The injection port had a temperature of 548 K and the FID was at 603 K. Only organic samples could be analysed on this way. For analysis of an aqueous product an extraction of the phenolic products from the aqueous phase had to be conducted to prepare the sample (see Appendix B.2). The organic liquid samples were diluted in a 1:2 ratio with a prepared standard solution of pentacosane in ethyl acetate (1002 mg/L) as an external standard. injected by the auto-sampler system. Mono-aromatic components were individually calibrated for quantification by running dilution series. The equipment was calibrated by introducing samples with four different determined dilutions of the qualified substances. The system was checked on a weekly basis by introducing a standard mixture with known concentrations of all quantified substances and recalibrated if necessary. The maximum tolerance of the measured value was 10 wt% in respect to the concentration of each substance.

GC-MS analysis of liquid samples

A GC equipped with a mass spectrometry (MS) was used for the first identification and the determination of the retention time of each substance. In a MS the eluent of the GC-column is ionised by impacting them with an electron beam. The ions are separated according to their mass-to-charge ratio in an analyser by electromagnetic fields. Hence, the MS elucidates the chemical structure of the molecule and aids in characterising the substance. Qualitative GC-MS analysis of liquid products was carried out on a Trace Ultra GC coupled with a DSQ II quadrupole MS detector from Thermo Scientific. The samples were diluted in a 1:100 ratio in dichloromethane and were analysed using split injection at 523 K (injector temperature) on a 25 m Ultra 2 silica column ((5 % phenyl)-methylpolysiloxane) from Agilent Technologies. A constant gas flow rate of 1 mL/min and a split ratio of 100 with the following temperature program were applied: Initial temperature 313 K, increased at 6 K/min to 473 K, further increased with 8 K/min to a final 573 K, kept for 5 min. The MS detector was operated in positive ionisation mode at 70 eV with an ion source temperature of 473 K.

2.3.2 Fourier transformed infra red spectroscopy (FT-IR)

Fourier transformed infra red spectrometry (FT-IR) was employed for the analysis of solid samples. It aids in analysing the molecular structure, especially the dominant functional groups of the solid. FT-IR-analysis of the feed material and collected solid residues was performed by preparing and pressing conventional KBr pellets and analysing these on an FT-IR Varian 660-IR in linear transmittance mode. 30 scans were performed after background subtraction and the results averaged. The measurement data was later normalised to compensate for concentration effects.

2.3.3 Karl-Fischer-titration (KFT)

Karl-Fischer-titration (KFT) was used for the determination of the amount of water in selected organic liquid samples. Samples were evaporated in a Metrohm 774 oven processor at 651 K. A volumetric method was performed with the titrant solution Hydranal Composit 5. The end point of the titration was marked with the bipotentiometric method.

2.3.4 Photometry

Photometric spectroscopy (UV-Vis) was applied for the quantification of phenolic compounds in aqueous samples. Applying a standardised test purchased from Hach Lange the sample is mixed with an oxidising agent. All ortho- and meta substituted phenols will form coloured complexes with 4-aminoantipyrine. The absorption of the light of a characteristic wavelength 510 nm is measured in a calibrated photometer. Usually this method is utilised as proof of evidence for the existence of phenolics in a sample. For the quantification of single phenolic compounds, carried out for determining the distribution in water and ethyl acetate (see Appendix B.2), each phenolic substance had to be calibrated individually. The quantification of a phenolic substance from a solution containing different monoaromatic substances is thus not possible.

CHNS analysis

CHNS analysis was applied on the feedstock lignin and on samples from the liquid and solid product phase in order to determine the elemental composition of a sample. The utilised apparatus was a Vario El III by the company Elementar. The percentage of C, H, N and S, which refer to the dry matter excluding the moisture, were directly determined with the Dumas-method. The residual percentage was suggested to be O and ash. The amount of the ash was measured by gravimetric analysis of the residue after heating the sample from 298 K to 1273 K in 4 h and subsequently maintaining the temperature of 1273 K for 2 h

Chapter 3

Thermodynamic Studies

3.1 Introduction

An important question for the evaluation of the experimental results is whether the reactions taking place within the thermal degradation of lignin reach a thermodynamic equilibrium within the predetermined residence time. The lignin which is placed into a batch reactor together with a solvent is isolated from its surroundings, and thus sooner or later thermodynamic equilibrium is reached. The knowledge about the thermodynamic equilibrium provides the possibility to predict the tendencies for the experimental results at increasing residence times and temperatures. The latter has to be treated with care since the reaction rate increases with the temperature and thus the time from the start of the reaction until the state of equilibrium shortens. In addition, the temperature influences the thermodynamic equilibrium itself. Hence, the evaluation of experimental results requires at least a basic knowledge about the involved reactions and the composition in the thermodynamic equilibrium.

The composition of the product mixture after infinite residence time is compared with the experimental results at very long residence times. For the calculation of the composition in the thermodynamic equilibrium the program Aspen Plus V7.2 was employed. Aspen Plus uses different methods for the estimation of the thermodynamic equilibrium. Two of those were chosen for the present work. The group contribution method Unifac (Dortmund) developed by Fredenslund, Jones, and Prausnitz [FJP75] is based on a G^E-model [Pfe04]. The group contribution method describes any complex molecule as a combination of structural groups. This is highly advantageous

when dealing with complex organic material. The excess Gibbs enthalpy as well as activity coefficient and fugacity coefficient were calculated by the model which uses the HYSYS-database included in Aspen Plus containing in excess of 1500 components and over 16000 fitted binaries. It is problematic for the Unifac (Dortmund) model to deal with supercritical components which is done with employing Henry`s law [Asp10]. Unifac (Dortmund) has become very popular due to its large range of applicability and the reliable results predicted for vapour-liquid equilibria as well as for solid-liquid equilibria over a wide temperature range [Gme+02]. Especially char formation may be a challenge for other models, such as the equation of state (EoS) developed by Peng-Robinson, which was developed for gas phase reactions and would thus need further revision if applied for the calculation of the chemical potential of solid reaction components [CF11]. However, for further comparison, the Peng-Robinson-EoS was as well employed to calculate the thermodynamic equilibrium using the minimum search of the Gibbs enthalpy of Aspen Plus since it was especially developed to model thermodynamic equilibrium in the range of the critical point. The literature version of the alpha function and mixing rules were used [PR76; Asp10]. The thermal degradation of lignin in two different solvents that are water an ethanol (EtOH) was evaluated. The product composition in the equilibrium state calculated with both methods, Unifac and Peng-Robinson-EoS were compared. Furthermore the comparison of the data obtained from the Aspen-calculation with experimental data was intended. Few data is available in literature picturing to the liquid-liquid equilibrium (LLE) or the gas-liquid equilibrium (GLE) for mixtures of aromatics in water or ethanol.

3.2 Input parameters

Model substances had to be defined as input material since lignin cannot be sufficiently characterised for the calculation in Aspen due to its inhomogeneous character. Experimental results (experiment (Exp.) 90, 158) thus serve as input parameters for the calculation. Input parameters for the calculation of the thermodynamic equilibrium were chosen according to experimental results at 120 min residence time. After 120 min an entire degradation of the lignin molecule into smaller fractions can be assumed (see Chapter 6). The fraction of depolymerised lignin, which is soluble in ethanol or water, but could not be quantified by GC was described by the chemical compound bisphenol-A. In Table 3.1 all input components considered for the calculation with both methods Unifac and Peng-Robinson-EoS are listed. Table 3.1 includes the initial concentrations of the input components and, whether each

component is to be found in the solid, liquid or gas phase in the equilibrium state. Temperature and pressure for the model calculation were chosen according to the experimental data (T = 633 K, p = 30 MPa). For the calculation of the product composition in the thermodynamic equilibrium additional components are expected; that are propane and propylene in the gas phase, benzene, cyclohexane, cyclohexanone, cyclohexanol and methanol in the liquid phase, anthracene, naphthalene and carbon in the solid phase. For easier comparison with experimental results the initial concentrations are displayed as initial yields $y_{i,0}$. The input mass of lignin corresponds to the sum of all input masses except the input mass of the solvent, that is either water or ethanol.

Table 3.1: Initial yields $y_{i,0}$ for the Aspen-calculation of thermodynamic equilibrium at 633 K, derived from the experimental results at 120 min in water (Exp. 90) and ethanol (Exp. 158, see Appendix E.1).

Compound	Phase	Water	Ethanol
		mg/g_{lignin}	
CO_2	gas	166.81	136.49
CO	gas	1.29	0
CH_4	gas	7.56	15.13
H_2	gas	0.01	0.1
C_2H_6	gas	0	29.66
C_2H_4	gas	0	20.89
C_4H_{10}	gas	0	2.09
H_2O	liquid	7577.62	197.02
Phenol	liquid	1.97	1.39
Catechol	liquid	25.76	1.21
Guaiacol	liquid	3.33	2.7
Ethanol	liquid	0	5982.54
Bisphenol-A	solid	793.27	593.32

3.3 Results

The results of the minimum search of the Gibbs-enthalpy conducted by Aspen employing both the Unifac-method and Peng-Robinson-EoS for the thermal degradation of lignin in water and ethanol are displayed in Table 3.2. Products which, although considered by the model, yielded less than 10^{-4} mg/g_{lignin} were not listed. The results obtained with the Unifac-

method and the Peng-Robinson-EoS are in good agreement to each other. Both methods suggest that in water all participating organic compounds are transformed into gaseous products, mainly CO_2 and CH_4, also smaller amounts of H_2 and CO, but only traces of C_2 to C_4 hydrocarbon gases. On the contrary for the degradation in ethanol both methods suggest high yields of hydrocarbon gases, CH_4 being the most dominant product. The percentage of hydrocarbon gases and CO is more than 100 times higher in ethanol than in water. The yield of CO_2 is three times higher in ethanol than in water. Only the amount of H_2 is higher in water according to the calculations. Furthermore, results shows that at given conditions (633 K and 30 MPa) water is more stable than ethanol. The initial ethanol disappears completely while more than 91 wt% of the initial amount of water is conserved. Phenolic components, that are phenol, catechol and guaiacol are practically absent in the product mixture. Solid carbon was neither calculated for hydrothermal nor for solvothermal degradation in ethanol by none of the two methods. In ethanol significant yields of anthracene and naphthalene in the solid product phase are to be found in the equilibrium state according to the calculations

Table 3.2: Equilibrium yields y_i of thermal lignin degradation in water and ethanol calculated with Unifac and Peng-Robinson-EoS at 633 K and 30 MPa, input concentrations are listed in Table 3.1.

Compound	y_i in water		y_i in ethanol	
	Unifac	Peng-Robinson	Unifac	Peng-Robinson
	mg/g_{lignin}	mg/g_{lignin}	mg/g_{lignin}	mg/g_{lignin}
CO_2	1126.70	1125.84	3328.35	3328.52
CO	0.19	0.20	22.21	21.98
CH_4	521.59	521.90	3339.67	3342.14
H_2	1.08	0.93	0.12	0.12
C_2H_6	0.06	0.07	27.04	26.26
C_2H_4	0.00	0.00	0.01	0.01
C_3H_8	0.00	0.00	1.31	1.24
C_3H_6	0.00	0.00	0.01	0.01
C_4H_{10}	0.00	0.00	0.05	0.05
H_2O	6927.98	6928.69	7.35	7.35
Anthracene	0.00	0.00	228.43	236.04
Naphthalene	0.00	0.00	52.61	61.22

The results obtained by calculation with Aspen were compared with experimental results from thermal degradation of lignin in water (Exp. 148) and ethanol (Exp. 152) at 18 h residence time. Figure 3.1 shows that after

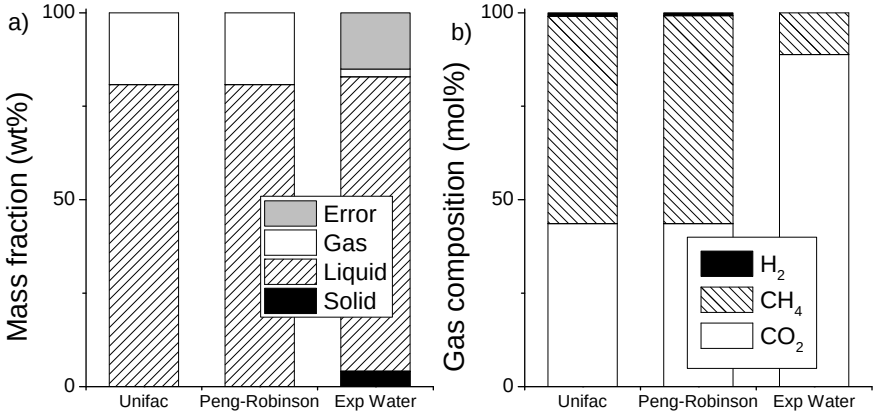

Figure 3.1: Thermodynamic equilibrium calculated by Aspen with Unifac-method and Peng-Robinson-EoS compared with results from Exp. 148 a) mass fraction of of product phases and b) composition of the gas phase; τ = 1080 min; spruce-lignin/water = 132 g/L; T = 633 K.

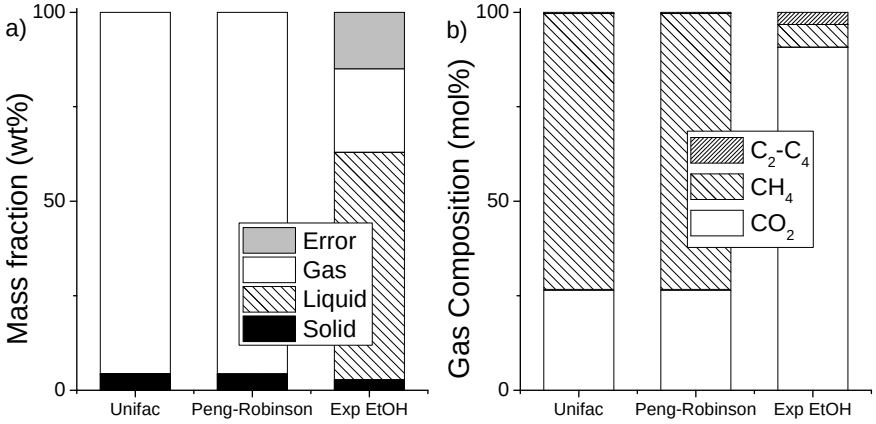

Figure 3.2: Thermodynamic equilibrium calculated by Aspen with Unifac-method and Peng-Robinson-EoS compared with results from Exp. 152 a) mass fraction of of product phases and b) composition of the gas phase; τ = 1080 min; spruce-lignin/ethanol = 132 g/L; T = 633 K.

18 h residence time in water the amount of gas is significantly lower than the calculation results. In addition, the solid residue recovered from the reactor after the experiment was 4.1 wt%. However, calculation results did not show any solid residue. The calculated and the experimentally determined amount of liquid are similar. The gas recovered from the experiment comprises approximately 11 and 89 mol% of methane and CO_2 respectively. H_2 was not detected in the gas phase. In the calculated thermodynamic equilibrium, however, methane makes up more than 50 mol% of the gas and H_2 up to 2 mol%. In fact the experimental results at 18 h do not agree with the calculated values. In respect to the thermal degradation in ethanol similar phenomena were observed. The amount of gas recovered from the experiment at 18 h was very low (22 %) compared to the amount of the calculated gas amount (96 %). The experimentally determined amount of solid residues (2.7 %) is less than the calculated amount of solids (4 %) which comprises exclusively anthracene and naphthalene (see 3.2a). The analysis of the gaseous product of Exp 152 shows similar to the experiment in water approximately 91 mol% of CO_2. The other 9 mol% of the gas are hydrocarbons, mostly methane (6 %). However, according to the calculations, in the equilibrium state methane makes up more than 70 mol% of the gas phase. Only traces of other hydrocarbons and 27 mol% of CO_2 make up the rest of the gaseous product.

3.4 Discussion

The results of the Gibbs-enthalpy minimum search employing the Unifac-model or the Peng-Robinson-EoS shows that at given conditions (633 K, 30 MPa) the major part of the organic input material is gasified. The absence of a liquid phase and the composition of the gaseous phase in the equilibrium state (see Figure 3.2) suggest that ethanol is completely transformed into hydrocarbons and CO_2. The fact that the solvent is entirely or partially consumed by the occurring reactions negatively affects the technical feasibility of the lignin degradation in ethanol since it renders a recirculation and reutilisation of the solvent impossible. The solid product phase resulting from the calculation of the equilibrium state in ethanol makes up 5 wt% of the total product mass and about 30 wt% of the initial lignin mass. It is exclusively composed of aromates, that are anthracene and naphthalene. Hence, the solid phase comprises products from repolymerisation or recombination of aromatic intermediates, *e.g.* phenolics. Phenolics are thus not stable at the determined conditions. They are either gasified or polymerised in ethanol. In water the phenolic products are entirely gasified,

probably since the presence of near critical water (NCW) and supercritical water (SCW) facilitates the degradation of the aromatic ring.

Experimental results show that after 18 h 70 wt% of the initial organic liquid, mainly comprising ethanol, were recovered. This indicates at first that after 18 h the thermodynamic equilibrium is still not reached and secondly suggests a rather slow gasification of ethanol. However, the calculation of the thermodynamic equilibrium and the associated assumptions described here have to be critically evaluated and eventually need improvement. The calculation of the build-up of char is challenging, and can be improved as described by Castello and Fiori [CF11]. The use of model components such as bisphenol-A is a good first approximation, but needs further revision. However, here will always be a source of potential errors due to the heterogeneity of lignin.

Chapter 4

Influence of solvent on thermal lignin degradation

4.1 Introduction

In this chapter the solvothermal depolymerisation of lignin in ethanol and the hydrothermal degradation in water are compared. The main focus lies on the formation and decomposition of selected phenolic components, as well as the formation of char and gas. For this purpose various experiments were carried out utilising different approaches of hydrogen donation, that are elemental hydrogen in combination with a Pd-catalyst and in situ hydrogen formation via degradation of formic acid. All experiments were carried out in 5 ml MA2. For this reactor setup no measurement of the pressure was not applicable. The lignin used for this study was enzymatic hydrolysis lignin from spruce wood. Barth and Kleinert have done intensive research on the lignin solvolysis in ethanol (EtOH) using formic acid as hydrogen donor. They found a large variety of aliphatic and aromatic products comprising few oxygenated components [KB08b], almost no solid residue (< 5 wt%), a high H/C-ratio and a low O/C-ratio [Gel+08; KB08a; Kle+11].

4.2 Experimental Results

Experimental results of the lignin degradation in water and ethanol without hydrogen donor are explored. Experiments were carried out in a MA2 with 5 mL inner volume. The reactors were cooled with iced water after the

reaction. Figure 4.1 shows the results obtained from degradation of spruce lignin in ethanol and H_2O at $T = 633$ K. The development of the solid yield over the residence time is similar for both solvents. After a first decline, the yield of solid product slowly approaches a threshold value. This threshold is slightly higher for experiments in water (approximately 0.34 g/g$_{lignin}$) than in ethanol (approximately 0.27 g/g$_{lignin}$).

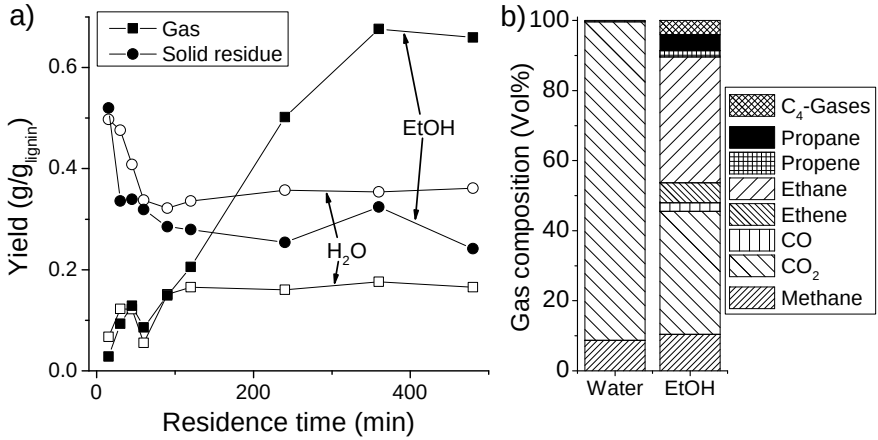

Figure 4.1: Results from thermal degradation of spruce lignin in ethanol (EtOH) or water (H_2O) at $T = 633$ K; spruce-lignin/solvent = 132 g/L; a) yield of gas and solid residue in EtOH (solid symbols, Exp. 153-161) and H_2O (open symbols, Exp. 85-93); b) Gas composition for $\tau = 480$ min

The development of the gas yield over the residence time is similar for both solvents until 100 min residence time. It is increasing with the residence time. The relatively low value at 60 min is considered to be an outlier. However, at residence times longer than 100 min the gas yield of ethanol experiments increases up to almost 0.7 g/g$_{lignin}$ whereas the gas yield of water experiments stays constant at less than 0.2 g/g$_{lignin}$. The GC-analysis of the gas reveals that the gas recovered from water experiments comprises mostly CO_2 (90 vol%) and CH_4 (9 vol%) and only 1 vol% of other hydrocarbon gases. Gas recovered from ethanol experiments on the contrary comprises more than 50 vol% hydrocarbon gases, mainly C_2-gases, that are ethane (37 vol%) and ethene (6 vol%), methane (11 vol%) and also about 9 vol% of C_3-C_4-olefines. Only about 36 vol% of the recovered gas is CO_2.

Figure 4.2 demonstrates the FT-IR-spectra of the solid residue removed from the batch-autoclave after different residence times are compared to the

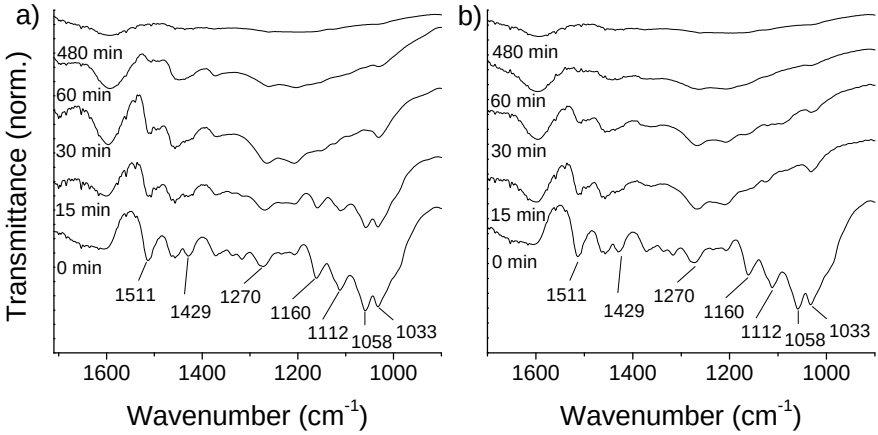

Figure 4.2: FT-IR-analysis of spruce-lignin and the solid residue after 15, 30, 60 and 480 min residence time in a 5mL MA2 with a) ethanol (Exp. 153, 154, 156, 161) and b) H_2O (Exp. 85, 86, 88, 93); lignin/solvent = 132 g/L; T = 633 K

FT-IR-spectrum of spruce-lignin. The solid samples were recovered from the corresponding experiments described above without addition of catalyst or hydrogenation agent. The displayed curve is reduced to the region between 900 and 1700 cm^{-1} since here most of the vibrational bands are visible which are related to the aromatic ring (also compare Table 6.1). The curves are normed and thus only a qualitative comparison is valid. It is clearly visible that most aromatic vibrational bands, *e.g.* at 1511 cm^{-1}, 1429 cm^{-1} and 1058 cm^{-1}, disappear towards residence times above 60 min. Beyond 60 min only minor changes of the spectrum are visible. At increasing residence time all peaks disappear and the curve approximates a horizontal line. The disappearance of the aromatic ring vibrational bands, *e.g.* at 1058 cm^{-1} is visibly faster in water than in ethanol.

Figure 4.3 shows the chromatogram of the liquid products from experiments of lignin solvolysis in ethanol and in water. The hydrogenation was achieved by adding formic acid. The compounds corresponding to the different peaks are listed in Table 4.1. The chromatogram shows the relative abundance of the substances present in the liquid product in case of ethanol experiments. Since the analysis of the aqueous liquid product was not possible in case of water experiments, an extraction of the phenolics into an organic extraction phase, that is ethyl acetate, was carried out (see Appendix B.2).

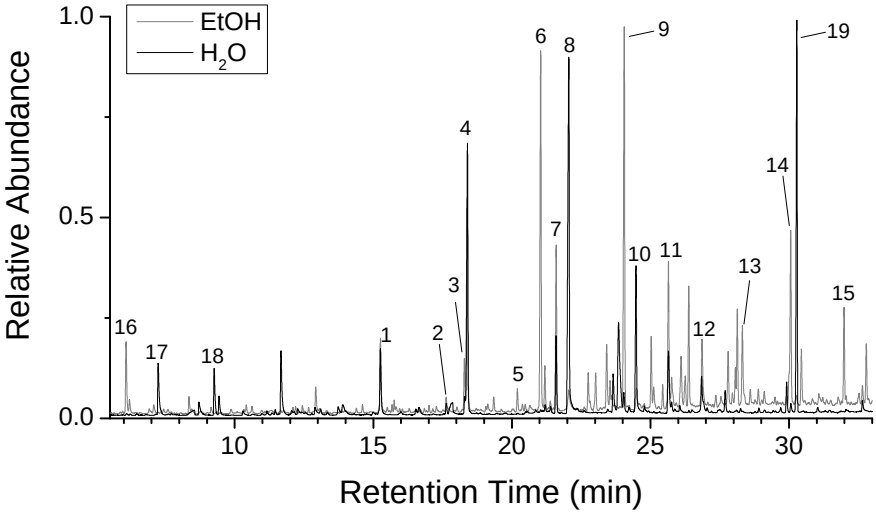

Figure 4.3: GC-FID-chromatogram of liquid product (EtOH, Exp. 143) and organic phase after extraction of aqueous liquid product (H_2O, Exp. 142) after thermal treatment of spruce-lignin; lignin/solvent = 132 g/L; FA/solvent = 107g/L; $T = 633$ K, $\tau = 60$ min

Hence, the chromatogram in Figure 4.3 labelled with »H_2O« shows the analysis of the extraction phase. Due to the specific coefficient ($f_{d,i}$), which indicates the transfer ratio of each phenolic compound from the aqueous to the organic phase, the peak area is influenced by the extraction which has to be considered for the interpretation of the chromatograms. The chromatograms reveal that after the thermal degradation of spruce-lignin in water catechol is the predominant phenolic product. Solvolysis in ethanol on the other hand yields higher amounts of ethyl substituted phenols and methoxyphenols than hydrothermal degradation of lignin. In Figure 4.3 the peak of 4-ethylphenol and 4-ethylguaiacol in the H_2O curve is practically not visible. Furthermore, the peaks of syringol and its alkylated derivatives are clearly more dominant in the liquid sample after solvolysis in ethanol. Among the non phenolic compounds present in the liquid products, cyclopentanone and 2-methylcyclopentanone are more abundant after hydrothermal treatment. Ethanol yields aliphatic compounds such as 1,1-diethoxyethane. Generally, the number of different phenolic compounds in hydrothermal treatment is lower.

Table 4.1: Identified products with corresponding retention time in the GC-FID.

Compound class	#	Name	Molecular formula	Retention time (min)
Methoxyphenols	4	guaiacol	$C_7H_8O_2$	18.36
	7	4-methylguaiacol	$C_8H_{10}O_2$	21.58
	9	4-ethylguaiacol	$C_9H_{12}O_2$	24.03
	11	syringol	$C_8H_{10}O_3$	25.63
	13	4-methylsyringol	$C_9H_{12}O_3$	28.20
	14	4-ethylsyringol	$C_{10}H_{14}O_3$	30.13
	15	4-propylsyringol	$C_{11}H_{16}O_3$	32.06
Catechols	8	catechol	$C_6H_6O_2$	22.05
	10	4-methylcatechol	$C_7H_8O_2$	24.48
	12	4-ethylcatechol	$C_8H_{10}O_2$	26.85
Phenols	1	phenol	C_6H_6O	15.25
	2	2-methylphenol	C_7H_8O	17.61
	3	4-methylphenol	C_7H_8O	18.27
	5	2-ethylphenol	$C_8H_{10}O$	20.18
	6	4-ethylphenol	$C_8H_{10}O$	21.02
Others	16	1,1-diethoxyethane	$C_6H_{14}O$	6.22
	17	cyclopentanone	C_5H_8O	7.47
	18	2-methylcyclopentanone	C_7H_8O	9.47
	19	pentadecane	$C_8H_{10}O$	30.30

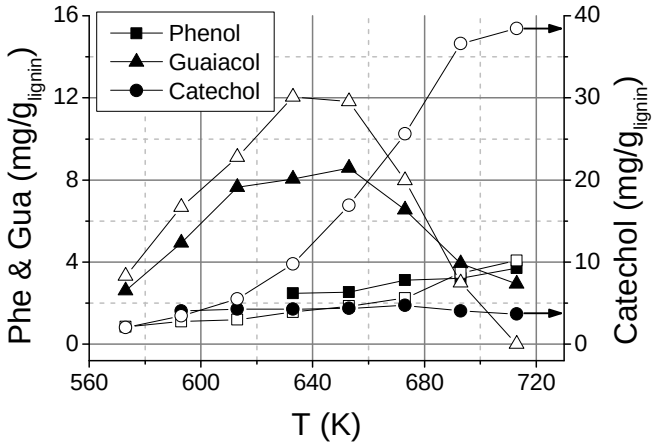

Figure 4.4: Yield of different phenolics from lignin solvolysis in ethanol (solid symbols, Exp 126-133) and H_2O (open symbols, Exp 134-141) at different temperatures; spruce-lignin/solvent = 80 g/L; 8 mg Pd-catalyst; 1 MPa H_2 initial pressure; τ = 60 min

Experiments of thermal degradation of spruce-lignin with elemental hydrogen combined with a Pd-catalyst confirm that in the presence of water the amount of catechols increases significantly. Above 673 K the hydrothermal treatment of spruce-lignin yields up to 38 mg/g$_{lignin}$ catechol. At any tested temperature the yield of catechol after thermal degradation of spruce-lignin in ethanol was at most 5 mg/g$_{lignin}$ (see Figure 4.4). Furthermore, the results of experiments with Pd-catalyst show that the sensitivity of the yields of all contemplated compounds, that are guaiacol, catechol and phenol, in respect to changes of the temperature at 60 min residence time is higher for hydrothermal experiments than for ethanol solvolysis. This becomes especially visible around the critical temperature of water ($T_{c,W}$ = 647 K).

4.3 Discussion

The results presented in this chapter show that water is an effective solvent in respect to the recovery of phenolics from lignin and selective in respect to the yield of catechols. FT-IR-analysis of the solid residue reveals that spruce-lignin degrades faster in water than in ethanol. In respect to the FT-IR-spectrometry of the solid residue, typical aromatic vibrational bands, *e.g.*

at 1058 cm^{-1}, disappear after less than 15 min in water whereas in ethanol these bands are still visible after 30 min (see Figure 4.2). This is probably due to different reaction mechanisms in both solvents. In a hydrothermal environment hydrolysis favours the cleavage of C-O bonds. This is also discussed more detailed in Chapter 6.3. Compared to the solvolysis in ethanol, hydrothermal treatment shows a narrower products spectrum of phenolic products. Especially ethylated phenols and methoxyphenols are hardly detectable in the aqueous liquid product. The abundance of 4-ethylphenol and 4-ethylguaiacol in the presence of ethanol indicates that the solvent itself is involved in alkylation reactions. The formation of 1,1-diethoxyethane as well as butane and propane in ethanol is also explicable by the combination of smaller olefines or ethanol. Hence, the high reactivity of ethanol in comparison to water leads to a broader product spectrum. Lignin degradation in water, which is basically inert at the determined conditions, on the contrary yields relatively high amounts of catechol and its derivatives. This is an advantage in respect to the economical feasibility since a decreased number of substances in the product mixture and an increased selectivity in respect to few phenolic products facilitates the separation of the products from waste and solvent in the process. Cyclopentanone and 2-methylcyclopentanone, which are present in the liquid sample after hydrothermal degradation of lignin, most probably originate from the residue cellulose in the spruce-lignin. Solvolysis in ethanol yields higher amounts of gas, probably due to the gasification of ethanol since increased concentrations of ethane and ethene are observed. The lower amount of char in ethanol can be explained by the increased solubility of organic components, such as aromatic oligomers produced by *e.g.* repolymerisation of phenolic monomers [McM+04], in ethanol at room temperature.

Chapter 5

Influence of catalysts on thermal lignin degradation

5.1 Introduction

In this chapter experimental results concerning the influence of heterogeneous catalysts on lignin degradation are presented. Heterogeneous catalysts have a high potential to promote hydrogenation reactions, *e.g.* the hydrogenation of phenolic intermediates. Homogeneous catalysts, being less limited by transport phenomena, are more likely to interact with the lignin-macromolecule and thus favour the cleavage of the bonds between aromatic monomers [Beh+06]. The focus of the investigation lies on heterogeneous catalysts comprising different metals. The catalysts were selected following the recommendations of other research documentations (see Chapter 1.2.5). Rh, Pt, Pd and Ni already proved to catalyse the hydrodeoxygenation of phenolics. Pd and Ni were also used in hydrothermal conditions [Zha+10a]. cobalt (Co) is a standard hydrogenation catalyst for the hydrodeoxygenation of pyrolysis-oil [Gut+09], however, has not been tested in a hydrothermal environment. All selected heterogeneous catalysts were from typical hydrogenation catalysts of the eighth subgroup of the periodic table of the elements. A screening of the effects of homogeneous catalysts, that are acidic and basic solutions, on lignin degradation can be found in Appendix D.1.

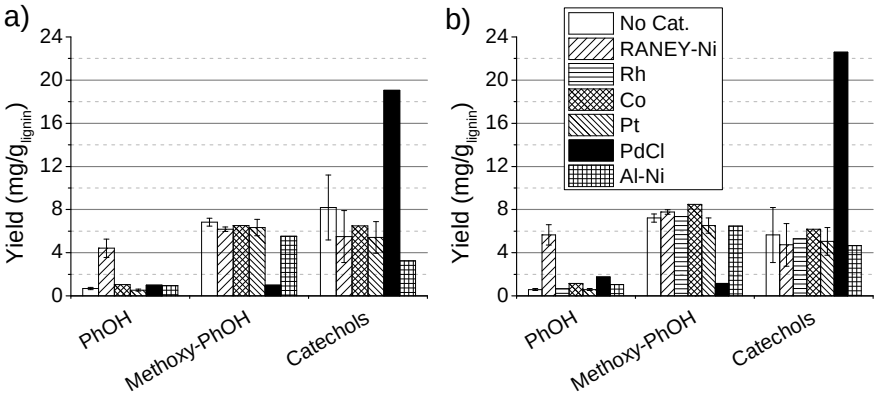

Figure 5.1: Effect of different heterogeneous catalysts on the yield of phenols, methoxyphenols and catechols from hydrothermal lignin degradation (Exp. 8-20 and 27-31), spruce-lignin/water = 133 g/L; T = 633 K; τ = 30 min; 0.10 g/g$_{lignin}$ Raney-Ni, 0.08 g/g$_{lignin}$ Rh on act. C, 0.08 g/g$_{lignin}$ Pt on act. C, 0.07 g/g$_{lignin}$ Co, 0.08 g/g$_{lignin}$ $PdCl_2$, 0.13 g/g$_{lignin}$ Al-Ni; reactor pressurised with a) N_2 (5 MPa initial pressure) and b) H_2 (5 MPa initial pressure).

5.2 Screening of heterogeneous catalysts

It was shown in the past that heterogeneous catalysts have a high potential to promote hydrodeoxygenation of methoxyphenols which are present in bio-oils [16, 17]. Elemental hydrogen is supposed to be absorbed on the surface of the hydrogenation catalyst in order to be transformed into reactive hydrogen radicals. The latter react with the organic lignin fragments, *e.g.* phenolics. It is suggested that in situ produced hydrogen from the lignin degradation takes part in the hydrogenation of phenolics in a similar way.

An important question in this context is whether the addition elemental hydrogen is indispensable for the catalytic hydrogenation of the phenolics or whether the in situ production of hydrogen from lignin degradation is sufficient. In order to answer this question experimental results of catalytic lignin degradation under H_2 atmosphere were compared with results obtained under N_2 atmosphere. The gas, H_2 or N_2, was pressed with an initial pressure of 5 MPa into the 5 mL MA2 which had been loaded with lignin, water and catalyst. Figure 5.1a shows the yields of phenols, methoxyphenols and catechols after hydrothermal catalytic degradation of spruce-lignin under N_2

atmosphere, Figure 5.1b shows the results from experiments with additional H_2. The results show that the influence of additional elemental H_2 is negligible since the yields of all quantified phenolics are similar and within the range of uncertainty. The results of a screening of different heterogeneous catalysts, namely Raney-Ni, rhodium on activated carbon (Rh on act. C), platinum on activated carbon (Pt on act. C), cobalt powder (Co), palladium-chloride ($PdCl_2$) and aluminum-nickel (aluminium (Al)-Ni) is shown in 5.1. The experimental results reveal that among the investigated catalysts Raney-Ni and $PdCl_2$ in the used concentrations have a major influence on the yield of the phenolic products. Phenol, *o*-cresol and *p*-cresol showed similar tendencies and were thus summarised within the (lump)-component phenols (PhOH). In the same way guaiacol and 4-methylguaiacol were summarised within the component methoxyphenols (methoxyPhOH) and catechol and 4-methylcatechol within the component catechols. The thermal degradation of spruce-lignin with Raney-Ni shows a sixfold increase of the yield of phenols from 1 to maximum 6 mg/g_{lignin} compared to experiments without catalyst. The application of $PdCl_2$ on the thermal lignin degradation reduces the yield of methoxyphenols from more than 5 mg/g_{lignin} to less than 2 mg/g_{lignin} and increases the yield of catechols from about 5 mg/g_{lignin} to about 20 mg/g_{lignin}.

5.3 Raney-Nickel

The screening experiments presented in the preceding section show the effect of Raney-Ni on the formation of phenols. The latter are the phenolic products from lignin degradation with the largest variety of applications in the chemical industry. After evaluation of the catalyst screening experiments a more detailed study of the effect of Raney-Ni on the hydrodeoxygenation of intermediate phenolic products seems to be valuable. In a series of experiments, the input mass of Raney-Ni is varied at a constant temperature (633 K) and residence time (30 min). For a better representation of the data the phenolic products were grouped as described in the preceding section. The results are demonstrated in Figure 5.2. They reveal that with increasing input amount of Raney-Ni the yield of methoxyPhOH and catechols decreases and the yield of PhOH increases. At very high input concentrations of Raney-Ni (>250 mg/g_{lignin}) the yield of phenol decreases.

In order to find out more about the reaction mechanisms which lead to an increased yield of phenols, additional experiments with intermediate substances were carried out. Catechol was diluted in water and placed together with 55 mg Raney-Ni into a MA2. The autoclave was pressurised with 1 MPa

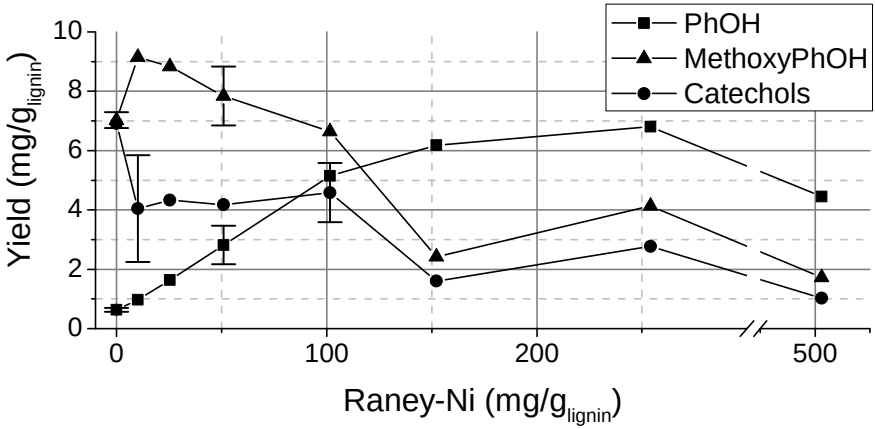

Figure 5.2: Yield of PhOH, methoxyPhOH and catechols at different loadings of Raney-Ni (Exp 10-11 and 21-31); spruce-lignin/water = 133 g/L; T =633 K; τ =30 min.

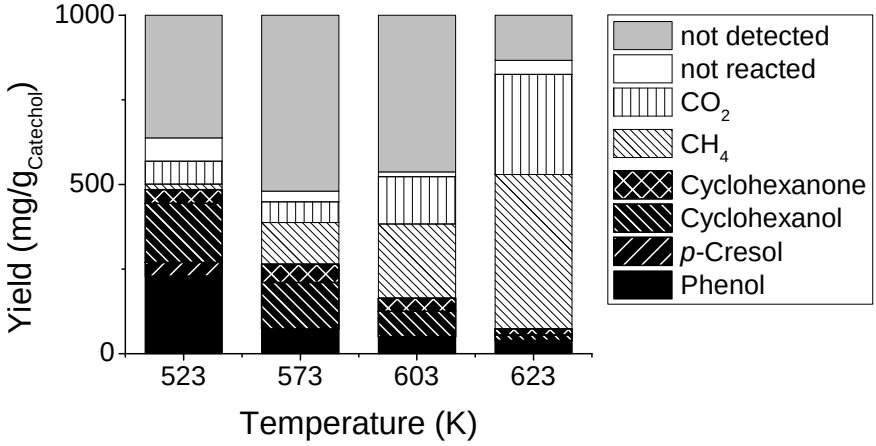

Figure 5.3: Product composition after hydrogenation of 10 g/L catechol in water at different temperatures with 55 mg(dry matter) Raney-Ni (Exp 36-39); 1 MPa initial pressure H_2; τ = 60 min.

H_2 in order to guarantee a hydrogenation of catechol. The in-situ production of H_2 might as well occur but is supposed to be inferior for the thermal decomposition of catechol compared to the thermal degradation of lignin. The mixture of reactants was exposed to different temperatures from 523 K to 623 K with a residence time of 60 min. The results displayed in Figure 5.3 reveal that the highest yield of phenol of 229 $g/g_{catechol}$ is obtained at 523 K. The phenol yield decreases with increasing temperature. However, the yield of gaseous products increases up to 296 $g/g_{catechol}$ CO_2 and 457 $g/g_{catechol}$ CH_4 at 623 K. Other important byproducts are cyclohexanol and cyclohexanone. The influence of temperature and reaction time on the Raney-Ni catalysed reaction from catechol to phenol is described in more detail in Appendix D.2, where furthermore the reaction pathways within catalysed hydrothermal catechol decomposition and their kinetics are discussed.

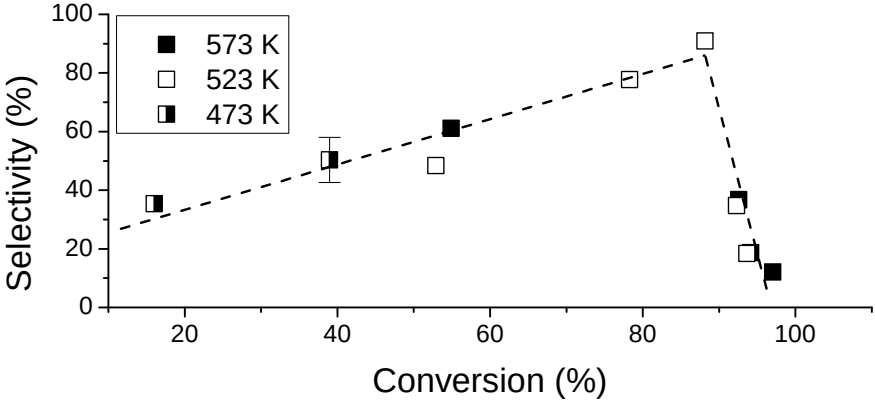

Figure 5.4: Selectivity of phenol over catechol conversion after hydrothermal catechol decomposition catalysed with Raney-Ni (Exp. 103-105, 114-118 and 122-125); input: 5 ml catechol/water-solution (5 g/L); different temperatures and residence times.

Numerous experiments concerning the hydrothermal decomposition of catechol catalysed by Raney-Ni were carried out in 10 mL MA2. It was observed that the selectivity of phenol increases with the catechol conversion and reaches its maximum of about 90 % with the corresponding conversion of catechol of 88 %. At conversions above 90 % the selectivity of phenol rapidly decreases (see Figure 5.4). The graph shows a coefficient of determination R^2 of 0.44 for the linear fit of the selectivity at a conversion lower than 80 % and a R^2 of 0.85 for the linear fit at a conversion higher than

80 %. This tendency is independent from the reaction temperature. Elsewhere the results of analogue experiments with guaiacol are documented [For+12], which show that phenol does not play a major role as product from the Raney-Ni catalysed hydrothermal decomposition of guaiacol. More important products are cyclohexanol and cyclohexanone.

5.4 Discussion

Heterogeneous catalysts proved to be effective on the hydrodeoxygenation of phenolic intermediates even in water. In addition, the in-situ production of hydrogen from hydrothermal lignin degradation is sufficient for the catalytic hydrogenation. $PdCl_2$ was observed to yield high amounts of catechols and low amounts of methoxyphenols from the hydrothermal lignin degradation. It can thus be assumed that it catalyses the reaction from methoxyphenols to catechols (see Figure 5.1). However, this should be proven by an experimental study of the hydrothermal decomposition of methoxyphenols in the presence of $PdCl_2$. The studies of the hydrodeoxygenation of aromatic substances in a hydrothermal environment carried out by Zhao and Lercher showed that Pd catalyses selectively the hydrogenation of the aromatic ring [Zha+1]. Ni on the contrary promotes »hydrogenolysis to cleave the C-O bonds, followed by removal of the oxygen atoms anchored to the aromatic moieties by sequential hydrogenation and dehydration reactions« [ZL12]. These findings agree with the results of experiments with Raney-Ni in the present work. Raney-Ni catalyses selectively the conversion from catechols to phenols, which is analogue to the cleavage of the C-O bond and the removal of an oxygen atom anchored to the aromatic ring. The maximum selectivity of phenol was obtained at 523 K. With increasing temperature and residence time cyclohexanol and cyclohexanone as well as gaseous products, that are CH_4 and CO_2, were observed after the catalytic hydrothermal decomposition of catechol with Raney-Ni. This indicates hydrogenation of the aromatic ring, as observed by Zhao and Lercher, but also gasification of the aromatic substances. Kruse et al. showed that the presence of Raney-Ni favours the gasification of aromatics in NCW and SCW [Kru+00; SKR04]. Probably this is also the reason for decreasing yields of phenol from spruce lignin with increasing input amounts of Raney-Ni beyond 250 mg/g_{lignin}. The yields and selectivities of phenol from catechol were compared with a study carried out by Wahyudiono, Sasaki, and Goto of the hydrothermal decomposition of catechol at temperatures between 643 and 663 K without catalyst [WSG09]. They documented a maximum selectivity of 20 %-25 % in respect to the molar input amount of catechol. The addition of Raney-Ni

increases the phenol selectivities to 90 % at 88 % conversion of catechol at a significantly lower temperature of 523 K. Raney-Ni is thus a powerful catalyst for the hydrothermal conversion from catechol to phenol. The study of the influence of homogeneous catalysts on the hydrothermal lignin degradation (see Appendix D.1) indicates that basic catalysts, that are KOH and NaOH, increase the yield of catechols. HCL decreases the yield of methoxyphenols and increases the yield of catechols. These results agree with the assumption that both acetic and basic catalysts facilitate hydrolysis which favours the cleavage of C-O bonds *e.g.* in the methoxyl-group [TRR11; Zha+1]. The application of homogeneous catalysts is a promising way to increase the yield of phenolics from lignin. However, the results obtained here need to be complemented in order to be sufficient for stating clear tendencies.

Chapter 6

Kinetic studies of lignin degradation

Kinetic models describing the depolymerisation of lignin are limited and are largely concentrated on global lump models describing the yields of gas, char and liquids. This chapter provides systematically obtained experimental data interpreted with a model which considers the kinetics of the crucial pathways (reactions) respecting the overall mass balance at any time. The interpretation of the model and the kinetic data obtained helps understanding the reaction mechanisms and determining bottleneck reactions. The first attempt of modelling the kinetics of lignin degradation was based on data obtained from the thermal degradation of lignin from wheat straw in ethanol and formic acid in a batch-autoclave at 633 K (see Section 6.1). The same model was further employed to describe the experimental data obtained in a CSTR (see Section 6.2). Finally, on the basis of the existing model for ethanol and formic acid, a modified model was developed which was able to describe the hydrothermal degradation of lignin from spruce in a batch-reactor (see Section 6.3). The modelling of lignin degradation in systems which are different in respect to the solvent, water or ethanol, and the reactor, batch reactor or CSTR, and the comparison of the results provide the possibility to a more profound knowledge about the influence of different process parameters on lignin degradation.

6.1 Lignin depolymerisation in ethanol in a batch-reactor

A formal kinetic model describing the main reaction pathways yielding phenolics, char and gas from wheat straw lignin in a hydrogen enriched solvolysis reaction system using ethanol as solvent has been developed. 10 experiments (Exp. 44-53, see Appendix E.1) were conducted using a mixture of 0.33 g lignin, 0.27 g formic acid and 2.5 g ethanol. The reactions were carried out at a constant temperature of 633 K and residence times of 15, 30, 45, 60, 90, 120, 240, 360, 480, and 1180 min. For comparison with the CSTR (see Section 6.2) note that in a Batch reactor the residence time is equal to the experimental duration. For the experiments in a CSTR, however, both terms have to be distinguished. Replicate experiments were performed for 60, 120 and 240 min residence times to assess experimental uncertainty.

6.1.1 Main intermediates and products

Global mass balance

The products comprise three major phases in varying ratios: gas, solid and liquid phase. The recovered amounts of these three phases are dependent on the residence time, and are illustrated in a global mass balance diagram in Figure 6.1.

The decomposition of formic acid at 633 K contributes largely to the initial high gas yields. Extended residence time shows a continued growth in the amount of gas and a reduction of the single liquid phase obtained. Minimum amounts of solid residue in reference to the amount of input lignin are reached at 90 min (1.2 wt%) and 240 min (1.0 wt%). Although pressures in the reactors could not be measured, comparable experiments in a larger batch reactor have shown reaction pressures between 29 MPa and 33 MPa [Gas+10]. Based on the decreased formic acid to ethanol loading ratio, the pressure in the presented experiments is expected to be reduced by 3-6 MPa.

Gas phase

Analysis of the different components comprising the gaseous phase, see Figure 6.2, show that up to 1.9 wt% of CO is produced at low residence times. The yield, however, quickly decreases to be replaced by a rapid increase of CO_2. The high value (1600 mg/g_{lignin}) of the CO_2 yield at 240 min residence time is supposed to be an outlier. Although H_2 is detected, it is only present in minor amounts of some 0.01 wt% and further diminishes with increased

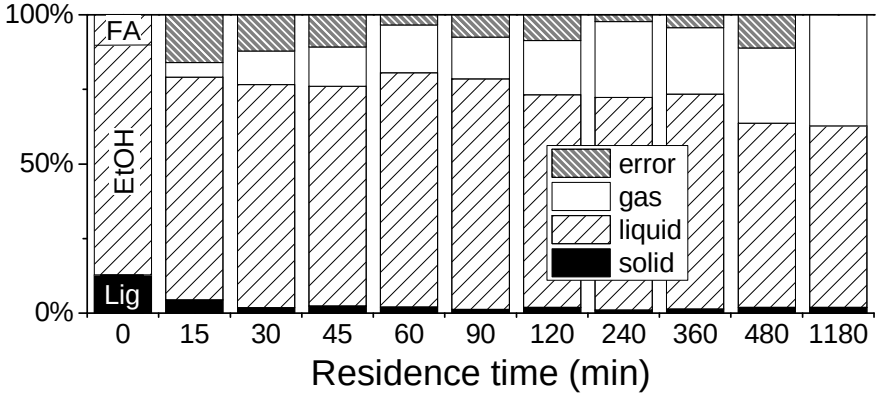

Figure 6.1: Liquid, gas and solid reaction products at varying residence times are compared with the input amounts of Lig, EtOH and FA at reaction time *zero* of the experimental series. All experiments (Exp. 44-53) were conducted at the same loading conditions: 0.33 g Lig, 0.27 g FA, and 2.5 g EtOH; $T = 633$ K.

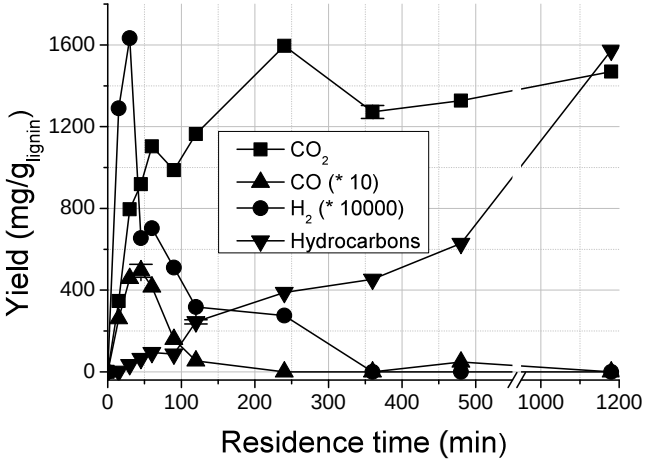

Figure 6.2: Individual yield of the gaseous product components, quantified on GC-FID and GC-TCD. The values for CO and H_2 have been multiplied by a factor of 10, respectively 10000, to enable a better visibility on the given scale; $T = 633$ K.

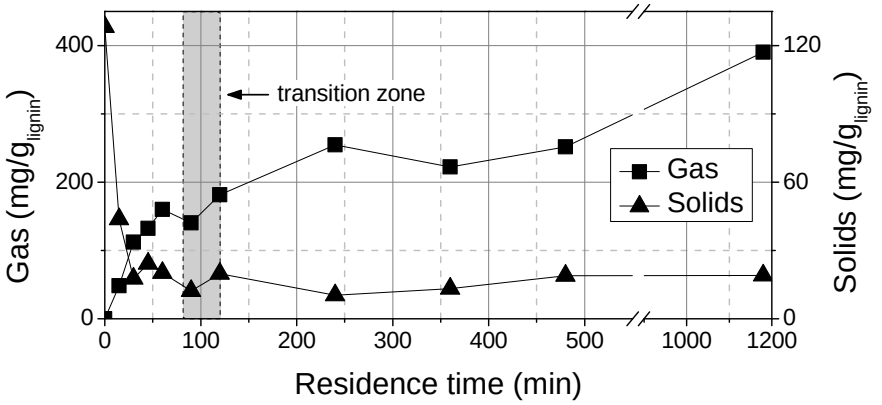

Figure 6.3: Gas and solid residue yields for experiments carried out at varying residence times. A transition zone, indicating the change from largely lignin characteristic solids to char is indicated, utilising the results from FT-IR analysis; $T = 633$ K.

residence time. Degradation of formic acid has been reported to occur via two different pathways, yielding either CO and H_2O or CO_2 and H_2 [YS98]. The alcoholic solvent has been seen to influence the ratio of the two main degradation pathways of formic acid to yield CO_2 and H_2 or CO and H_2O in a roughly 3:2 ratio [Kle+11]. The rapid consumption of H_2 suggests a central function and fast incorporation in the depolymerisation of the polymeric lignin structures. The continued increase in total amount of gaseous products and the formation of hydrocarbon gases (including CH_4, C_2H_6, C_2H_4, C_3H_8, C_3H_6, C_4H_{10}) points towards the importance of gasification and cracking in later phases of the reaction process.

Solid Residue

The solid residue was weighed after the reaction was terminated. Due to repolymerisation reactions causing an increase of solids after an initial decrease, additional analysis of the solids were required to allocate the transition point between a predominantly unreacted lignin-type structure and polyaromatic char (see Figure 6.3). To estimate the degree of depolymerisation and conversion of lignin, as well as the transition to coking, FT-IR spectra of the solid residue and a sample of the input lignin were taken. Figure 6.4 shows the FT-IR spectrum of the unreacted lignin with labeled characteristic absorption bands. The spectrum reflects the predominant aro-

matic ring structures with hydroxyl and C-O moieties. The relatively identical intensities of the absorption bands at 1511 and 1603 cm^{-1} indicate an increased ratio of syringyl relative to guaiacyl moieties in the polymer [FW87, pp 151-154]. The largely abundant *para*-coumaryl moieties do not enable a characteristic band allocation. All allocated origins of bands and their alterations throughout residence time are summarised in Table 6.1.

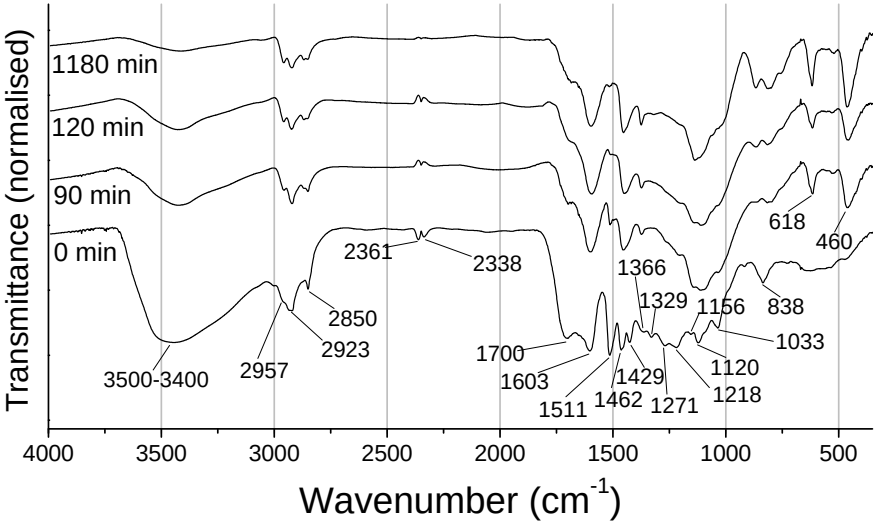

Figure 6.4: FT-IR spectra of unreacted lignin and of the collected solid residues at 90, 120 and 1180 min residence time. The largest alterations take place during the first 120 min and are documented in Table 6.1; $T = 633$ K.

Large alterations can be observed in the FT-IR spectrum of the solid residues within the first 120 min residence time (see Figure 6.4) for four example spectra taken from the lignin and solid residues from the reactors after 90, 120 and 1180 min. The most dominant alteration is the disappearance of hydroxyl functions, which is seen in the decrease of the broad -OH stretching band at 3500-3400 cm^{-1}. Decreasing absorbance of aromatic ring vibrational bands (1511, 1429 cm^{-1}), especially in combination with C=O stretching (1700, 1329, 1271, 1218, 1120, 1033 cm^{-1}) are clearly visible, illustrating the decomposition to monoaromatic units, and their solubility in the oil. These bands play a role in estimating the transition period from a largely lignin-like structure to a polyaromatic char. Roy, Bag, and Sen quantified the content of lignin, using the aromatic ring vibrational band at 1511 cm^{-1} [RBS87]. Analysis of collected FT-IR data, shows the disappearance of this

band between 90 and 120 min.

Liquid Phase

The liquid single-phase recovered was of a dark brownish colour and of a pungent odour. The single phase remained stable, without any precipitation, phase separation or change of chemical composition as observed by GC analysis, also after several weeks of storage at 278 K. For analysis, the crude product was evaluated without further separation, thus retaining the original amount of remaining ethanol and process water. The water content was found to increase from 3.9 wt% at 30 min to 14.7 wt% at 1180 min residence time.

One major focus of the kinetic model are the selected key components. For the monoaromatic compounds quantified in the liquid phase, the maximum error for the single replicates were found be 5.3 wt%, which is considered to be within an acceptable range, furthermore, consistent trends for the development over the residence time of all phenolic products are clearly visible in Figure 6.5.

6.1.2 Grouped products

The focus of the liquid analysis is to evaluate the monomeric phenolics in terms of their yields as a function of residence time. For this, different phenolics were grouped according to their degree and type of oxygenation. Their time-dependent yields are given in Figure 6.5. 4-Ethyl substitution is the dominant substitution for all species. In addition, 2-ethyl and 2- and 4-methyl substituted phenolics were quantified and included in some of the compound classes.

Figure 6.5a shows the methoxylated phenolics which an initial rapid increase until approximately 90 min is followed by a decrease. The by comparison more rapid decrease of syringol supports the previously observed conversion of syringol to guaiacol [Dor+99]. In general, all methoxylated phenolics, including syringol, show a large similarity in their time-dependent yield profile. A B-spline function based on averaged values of the single constituents helps to illustrate the overall trends. The profile suggests the single constituents to be primary products within the analysis focus, and subsequently the rapid decrease in concentration supports their identification as intermediates.

According to several investigations conducted under pyrolysis and hydrolysis conditions [JK85; LK85], catechols are found to be products of the secondary decomposition of methoxylated phenolics. Figure 6.5b shows the

Table 6.1: Characteristic FT-IR absorptions and observed changes between the biomass feed and the solid residue samples

Observed band cm^{-1}	Literature cm^{-1}	Origin[Her71; LI92; LPH97; Ye+12]	Peak characteristics in unreacted lignin	Peak alterations in solid residue
3500-3400	3450-3400	-OH stretching	broad	initial strong decrease
2957, 2923, 2850	2940-2820	-OH stretching in methyl and methylene groups	very weak, intense, weak	strong decrease at 2923 cm^{-1}
2361, 2338			weak	constant decrease
1700	1715-1710	C=O stretching non-conjugated to the aromatic ring		disappears after 30 min
	1675-1660	C=O stretching in conjugated to the aromatic ring		
1603	1605-1600	Aromatic ring vibrations	intense	decreases
1511	1515-1505	Aromatic ring vibrations	intense	disappears after 120 min
1462	1470-1462	C-H deformations (asymmetric)		
1429	1430-1425	Aromatic ring vibrations		disappears after 30 min
1366	1370-1365	C-H deformations (symmetric)	weak	intensifies
1329	1330-1325	Syringyl ring breathing with C-O stretching	weak	disappears after 45 min
1271	1270-1275	Guaiacyl ring breathing with C-O stretching		disappears after 45 min
1218	1220	Syringyl ring breathing	weak	disappears after 60 min
1156	1160	Aromatic C-H in plane deformation, guaiacyl type	weak	
1120	1120	Aromatic C-H in plane deformation, syringyl type	weak	
1033	1030	Aromatic C-H in plane deformation guaiacyl type and C-O deformation of primary alcohol		disappears after 45 min
917			weak	
867				appears at 240 min
838	834	*para*-substituted aromatic group		disappears at 90 min
810				appears at 240 min
618				appears at 90 min
460				appears at 90 min

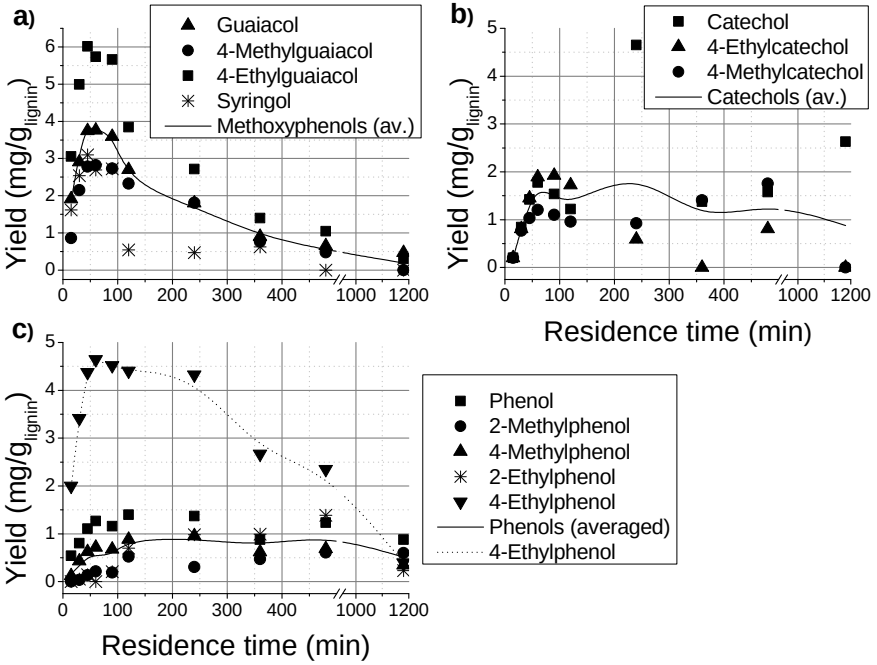

Figure 6.5: Yields of key components for the different phenolic compound classes: a) methoxyphenols, b) catechols and c) phenols over residence time; $T = 633$ K.

different quantified catechols as well as the averaged trend function. A somewhat slower initial increase in comparison to the methoxylated species with lower yields is found, together with a slight decrease at over 90 min residence time. However, the two values for catechol at 240 and 1180 min differ largely from the values for the substituted species, breaking with the generally decreasing yields. These high values were treated as outliers for further analyses.

The dominance of 4-ethyl substituted species is especially noticeable for 4-ethylphenol in Figure 6.5c. Indeed, the rapid yield increase of this compound can be compared more to the increase of the methoxyphenols than to other phenolic constituents. The slow decrease over time however suggests that it is a more stable product within the degradation and reaction pathways of the monomeric units. The other non-methoxylated phenolics show a very slow yield increase, which when averaged, remains at a roughly con-

stant yield value after 240 min residence time. The initial strong increase of 4-ethylphenol suggests a different reaction pathway compared to the rest of the phenols. Demethanisation and deoxygenation reactions link the different compound classes (see Table 4.1). However, the overall yield shows that a large proportion of the components is lost when increasing the residence time. This is due to char-formation or gasification processes.

6.1.3 Kinetic model development

Discerning the rank of key reaction steps

Delplot analysis was performed to confirm the indicative ranks of the phenolic species which had been grouped according to their compound classes as described above. Due to the uncertainty of the compositional transition from lignin to char, the necessary overall conversion rate for Delplot analysis was approximated by summing up all quantified monoaromatic species in the liquid. Full conversion is described by a maximum yield (indifferent as to the different classes involved) for all of these components. This is reached at 60 min residence time, after which the total yield declines, first slightly and then more rapidly.

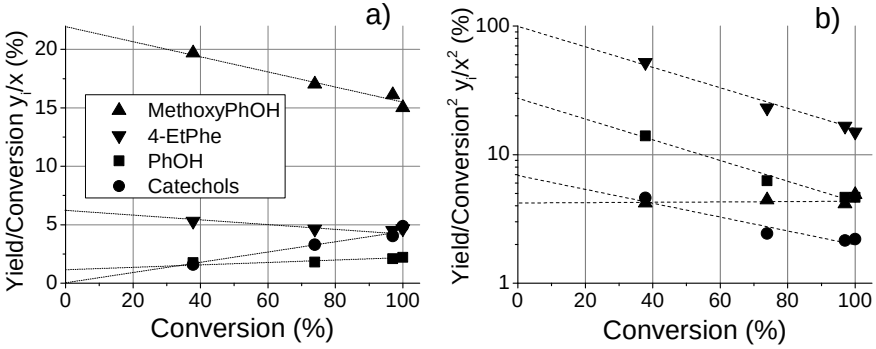

Figure 6.6: Methoxyphenols, phenols, 4-ethylphenol and catechols in dependence from the conversion, a) first rank Delplot, b) second rank Delplot; $T = 633$ K

Figure 6.6a shows the first rank Delplot with the three component lumps and 4-ethylphenol. The intercepts of the extrapolated trend lines towards zero conversion show that the methoxylated phenols and 4-ethylphenol are clearly finite, indicating them to be primary products. Clearly, considering the possible decomposition of syringol to form guaiacol, the latter can also

be a secondary product. However, this reaction pathway was not considered for the present work. The extrapolated intercept of the y-axis, at the value zero, for the catechol lump shows it to be of a higher rank and thus at least a secondary product. The phenol lump intercepts the y-axis slightly under the value of 1. This suggests phenols to be a primary product within the reaction network. Multiple reaction pathways yielding the various products can of course occur in such a complex system, also with varying ranks, requiring further exploration [KHB12]. However, due to the complexity of this model and multitude of unknowns within the reaction pathways, use of the interpretation extensions could not be applied. Competing and parallel reactions must be expected, but the analysis performed here is restricted to identification and description of the major pathways at given reaction conditions, while still recognising that further reactions exist. Reviewing the plots of the primary product 4-ethylphenol suggests multiple pathways of quantitative significance that could potentially also produce other phenols directly from the biomass as primary products. The interpretation for this component is tentative, as the extrapolation based upon four data-points introduces a large degree of uncertainty in the determination of the y-axis intercept. The second rank Delplot in Figure 6.6b shows that all y-axis intersections are now finite, thus categorising catechols as secondary products.

Formulating a model pathway

In terms of the wide product spectra observed in these reactions, a lump-model is expected to be the best approach and the analysis is focused on identifying and describing the significant reaction pathways. Single components which have been quantified in the course of the experimental work were used in the modelling, as well as global lump components. This allows the mapping of the complete pathway from the biomass to specific target compounds, such as phenol. Observations made in the experimental part of this study, as well as literature knowledge, are combined to formulate the model presented in Figure 6.7.

Under given temperature conditions, lignin is seen to depolymerise efficiently and quickly. Solid residue detected after more than two hours residence time is assumed to mainly originate from repolymerisation reactions of phenolic compounds, such as catechols or phenols [McM+04]. Guaiacol has been stipulated as one of the key intermediates that forms phenols and catechols from lignin. The reaction pathway from methoxyphenols to catechols (k_2) yields additional gas which is not further characterised since detailed information about the gas composition are not considered by the formal kinetic model. The amount of the gas produced from these reactions as well

as from the formation of phenol [JK85] (k_4) or char (k_5) and dealkylation reactions (k_8, k_{14}) is however very small relative to the gas which originates from the gasification of formic acid and ethanol (k_{12}, k_{13}).

Alkylation and dealkylation reactions (k_7-k_9, k_{14}) are very dependent on the substituents attached to the aromatic ring [HKB12], and prior studies suggest that alkylation reactions would be largely preferred by guaiacols [Mil+99]. The abundance of 4-methyl and -ethyl substituents observed for guaiacols, which are also present in catechols and phenols, suggests the alkylation to take place either immediately from reactive species during the depolymerisation process, or as a very fast reaction from guaiacol, rendering 4-ethylphenol to be the most abundant of this compound class. Either way, the initial residence time step chosen is not able to describe this reaction, and as the alkylation pattern of the *para-* position is subsequently seen in both catechols and phenols, lumping of the different alkylations is used. 2-Ethyl substitution is however, in significant quantities only found for phenols. Thus, a separate *ortho-* alkylation is proposed for 2-ethylphenol (k_8), to explore the importance of this reaction. Furthermore, since dealkylation of 4-ethylphenol and alkylation of 2-ethylphenol is considered, the consideration of the reverse reactions, that are alkylation of 4-ethylphenol and dealkylation of 2-ethylphenol, is reasonable.

All gaseous and inorganic liquid products, namely CO_2, CO, H_2, H_2O and hydrocarbon gases (HC-gases), such as CH_4, C_2H_4, C_2H_6, C_3H_6, C_3H_8, C_4H_{10} were grouped under the model lump component «gas». Furthermore, L_D (depolymerised lignin) is a lump component containing all components derived from lignin that are not detected or quantified by GC, but however, are soluble in ethanol, *i.e.* can not be categorised as solid residue or gas.

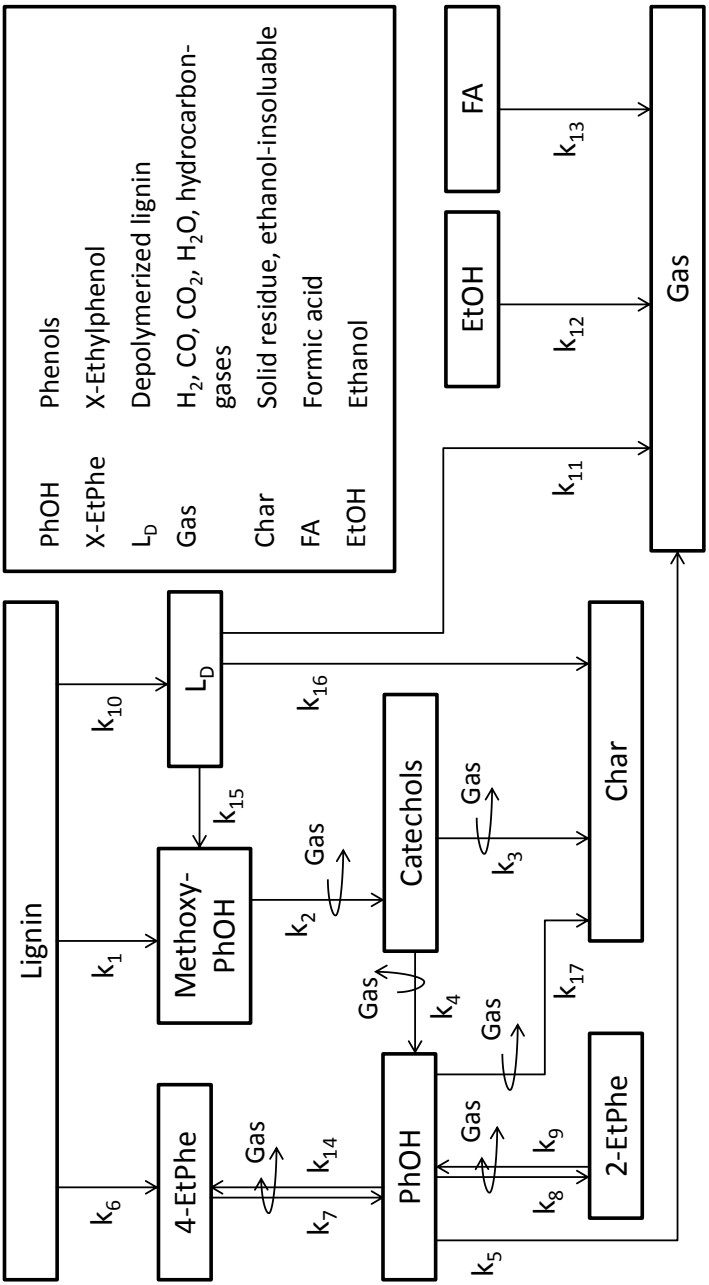

Figure 6.7: Scheme of main reaction participants and pathways of the depolymerisation of wheat straw lignin in ethanol and formic acid; gaseous products of ethanol and formic acid gasification take part in reactions 2-4, 7-9, 14 and 17. This is indicated by curved arrows; $T = 633$ K.

6.1.4 Results from model fit

The formal kinetic rate coefficients of the determined reactions were optimised using the algorithm explained in Appendix C. Different variations of the model shown in Figure 6.7 were considered, including additional reaction pathways, among them the direct conversion of methoxyphenols into phenols. After evaluating the results of the minimum search, the model version presented in Figure 6.7 was concluded to be the most appropriate. The focus was put on an acceptable mathematical fit for phenolic products. For the evaluation of the quality of the model fit the coefficient of determination R^2 and the standard deviation σ were calculated as described in Appendix C.4. The results are shown in Table 6.2. The standard deviation of the experimental results determined by replicate experiments is depicted by the error bars in Figure 6.8 and 6.9. The coefficient of determination R^2 is above 0.5, thus acceptable, for all phenolic products except 2-ethylphenol. The latter component shows a comparably high standard deviation and a low coefficient of determination. The model fit for the yield of gas and and solid residue are also acceptable since the coefficient of determination is high. Not only the development of the phenolics yield could be described (see Figure 6.8), the model also allowed to describe the yields of lumped gaseous products and solid residue (see Figure 6.9). Comparing the three rate coefficients which represent the three primary reactions of lignin degradation (k_1, k_6 and k_{10}) it can be observed that the reaction to L_D (k_{10}) is the fastest. The fit curve for lignin shows that a total conversion of lignin can be assumed after 100 min to 120 min, which is in good agreement to the results obtained from the FT-IR analysis of the solid residue.

Table 6.2: Coefficient of determination R^2 for the model fit and standard deviation σ of calculated and experimental yields (see Appendix C.4).

	Methoxy-PhOH	PhOH	Catechols	4-EtPhe	2-EtPhe	Char	Gas
R^2	0.96	0.59	0.88	0.57	-0.21	0.89	0.88
σ	14	44	20	30	113	56	26

The rate coefficients of the reaction of catechol to phenol (k_4) is very low compared to other coefficients within the model and therefore of minor importance. The same is true for the gasification of phenols (k_5). Ethylation of phenols is the only reaction pathway which is assumed to be reversible as described above. The rate coefficients of ethylation and deethylation are of the same order of magnitude. The ethyl substitution in the *para*- posi-

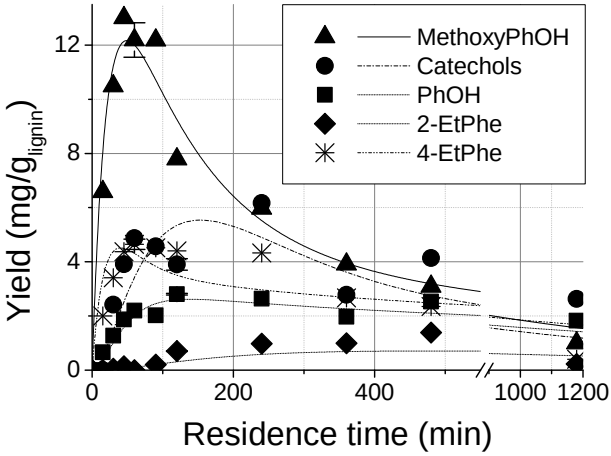

Figure 6.8: The experimental values are compared with the model fit functions for the quantified key phenolic compounds; $T = 633$ K.

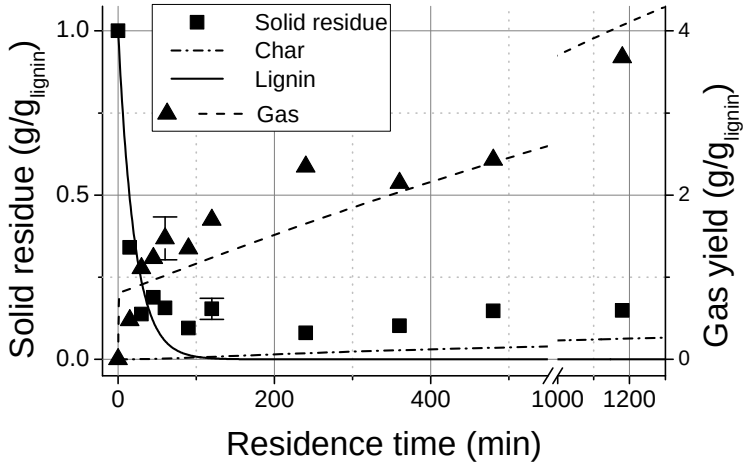

Figure 6.9: Fits of the gas-lump and the solid residue compared with the experimental data. The differentiation between lignin and char in the solid residue was accomplished largely by FT-IR analysis, as illustrated in Figure 6.4; $T = 633$ K.

tion (k_{14}) is slightly faster than deethylation (k_7), whereas the ethylation in ortho-position (k_8) is about three times slower than deethylation (k_9). Char formation from L_D (k_{16}) is of minor importance compared to the gasification of L_D (k_{11}). Char formation from catechol (k_3) on the other hand is faster than from phenol (k_{17}) or from L_D.

Table 6.3: Formal kinetic rate coefficients (k_j) of all 17 reactions defined within the developed model (see Figure 6.7)

k_j	k_1	k_2	k_3	k_4	k_5
(min^{-1})	$7.94{\cdot}10^{-04}$	$8.65{\cdot}10^{-03}$	$1.09{\cdot}10^{-02}$	$2.24{\cdot}10^{-06}$	$5.81{\cdot}10^{-15}$
k_j	k_6	k_7	k_8	k_9	k_{10}
(min^{-1})	$3.61{\cdot}10^{-04}$	$1.79{\cdot}10^{-02}$	$1.92{\cdot}10^{-03}$	$5.71{\cdot}10^{-03}$	$4.68{\cdot}10^{-02}$
k_j	k_{11}	k_{12}	k_{13}	k_{14}	k_{15}
(min^{-1})	$8.32{\cdot}10^{-04}$	$4.99{\cdot}10^{-04}$	$3.56{\cdot}10^{+26}$	$2.04{\cdot}10^{-02}$	$3.56{\cdot}10^{-05}$
k_j	k_{16}	k_{17}			
(min^{-1})	$4.16{\cdot}10^{-05}$	$1.17{\cdot}10^{-03}$			

Within the model, polyaromatic components derived from the biomass (L_D) are assumed to decompose directly into gaseous components (k_{11}), but can also form methoxyphenols (k_{15}) and char (k_{16}). Mathematical fitting showed that the latter route is of minor importance. The fit also confirms that the degradation of formic acid is very fast at given temperatures (k_{13}). The degradation of ethanol (k_{12}) is significantly slower. However, at long residence times it is of importance, if a recovery of the solvent ethanol is considered for a technical process. This is in good agreement to the results obtained from the thermodynamic studies (see Chapter 3).

6.1.5 Discussion

Replicate experiments showed the averaged percentage error for the measured global lump products, that are solid residue and gas, to be 13 wt% and 10 wt% respectively. Standard deviations for these two average values were calculated to be 6 % and 2 % respectively. A possible explanation for this error is found in the determination of the solid residue moisture. Although the solids were weighed before and after drying, it is likely that a certain amount of the volatile moisture attached to the solid residue evaporated during separation of liquids and solids before weighing.

Gas chromatographic analysis of the liquid product gives results for the yield of 12 different kinds of phenolic components, certainly less than the

real number of different phenolic products from lignin depolymerisation, but sufficient to evaluate a simple reaction network as suggested by Jegers and Klein for the pyrolysis of lignin [JK85]. The quality of results is supported by the acceptable fit of the single measurement data points in respect to the calculated yields as shown in Figure 6.10. The better the fit, the closer the data points plot to the diagonal line. The coefficients of determination R^2 is above 0.5, thus acceptable, for all components except 2-ethylphenol. The latter component could hardly be detected in the liquid product. Thus the error analysis is very sensitive to slow changes of the yield or concentration which yields a high standard deviation (113 %) and a low coefficient of determination (-0.21). However, important for the validation of the model is also that the tendency of the development of yield over reaction time can be described as basically different from 4-ethylphenol.

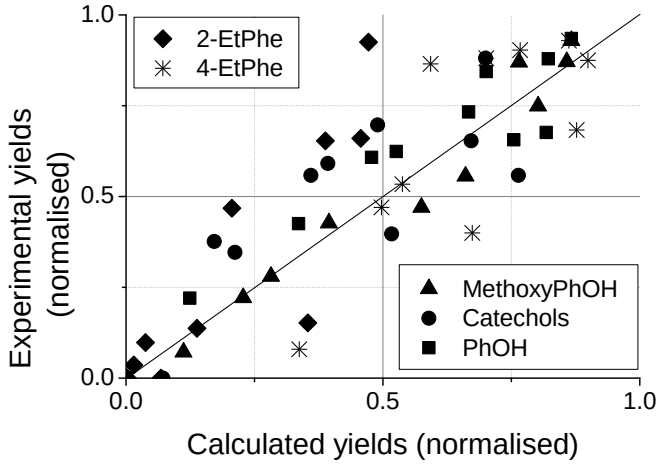

Figure 6.10: Comparison of calculated and experimental data for product yields of all phenolic (lump) components. Normalising factors (mg/g_{lignin}): MethoxyPhOH: 14.0, Catechols: 7.0, PhOH: 3.0, 4-EtPhe: 5.0, 2-EtPhe: 1.5.

Results from the FT-IR analysis of the solid residue as well as results from the fit of the rate coefficients show that approximately 100 min after starting the reaction, most of the lignin structure has disappeared. Solvolytic cleavage of the ether bonds present in the lignin structure, as already postulated for lignin degradation in a mixture solvent of ethanol and water by Yuan et al., is assumed to be the preferred reaction mechanism [Yua+10].

The observed effects of water on guaiacol pyrolysis describes a further parallel pathway based on the solution of the guaiacol molecules, thus preventing these from participating in free-radical reactions in order to form high molecular weight material [LK85]. This reaction pathway is believed to be transferable also to other protic solvent systems as well as lignin. Furthermore, external hydrogen donor sources have been reported to cap the radical moieties with hydrogen, thus reducing the radical concentration, which can be advantageous and suppress repolymerisation reactions [Dor+99]. The reaction coefficient of the degradation of guaiacol (k_2) under pyrolytic conditions at 633 K (*circa.* 0.0084 min^{-1}) obtained by Vuori [Vuo86], is comparable to the value calculated within the fit of this model (0.0087 min^{-1}). The good agreement of one of the calculated rate coefficients with those found in literature for similar reactions shows that the model is not only a mathematical method for the simulation of experimentally determined values, but also sensible in respect to the chemistry of lignin degradation.

4-Ethyl groups are generally the dominant substituents for all species at lower residence times. The occurrence of 4-ethylphenol as a primary product strongly suggests that ethyl group substituents are both a product of alkylation reactions in *ortho-* and *para-* position [HKB12] and depolymerisation. Supported by the Delplot analysis, it can be concluded that 4-ethylphenol is a primary product of lignin degradation. 2-Ethylphenol, however, is a late product and its yield hardly decreases toward very high residence times. It is thus assumed that 4-ethylphenol is formed directly from the lignin structure whereas 2-ethylphenol is formed by ethylation of phenols.

Hydrogen donor solvents have been seen to influence various biomass degradation processes. The high yields of ethyl substituted guaiacols, and indeed also catechols and phenols at lower residence times, may be related to the capping of highly reactive vinyl- (to ethyl-) substituted guaiacol intermediates by these donor solvents [PK84; Ye+12]. This could be part of the reason for the high yield of 4-ethyl substituents for the different phenolic species, which in the work of Ye et al. comprised a total of 30 % (together with 4-vinyl substitutes) of all lignin derived components quantified [Ye+12].

The comparison of polymerisation pathways from catechol (k_3) and phenol (k_{17}) shows that catechols are more prone to repolymerise with k_3 being greater than k_{17}. This agrees with the results obtained by McMillen et al. [McM+04], who found that especially cresols are able to cap the radical induced coupling of hydroxybenzenes under pyrolysis conditions. The low reaction rates for gas formation from phenol (k_5) furthermore supports the suggestion that mono-hydroxyl phenols are stable, contrary to the reactive methoxyphenols and catechols [JK85].

The model fits experimental values well and the derived rate constants

match values found in literature. The number and choice of selected lumps, as well as their interaction pathways, are sufficient to describe the degradation of lignin with a focus on the deoxygenation and ethylation reactions in the production of mono-aromatics under the given reaction conditions. Alteration of temperature in the range of 643 K to 663 K [Kle+11] has been reported to show some systematic variations in the product spectrum. The model is based on to the use of ethanol as solvent medium as a source for ethylation reactions. The general degradation pathways shown in this section are however also found for alternative hydrogen donor systems [For+12]. The necessity of the introduced single 4-ethylphenol component, suggests that adaptations to the model for different types of lignin would be necessary.

6.2 Lignin depolymerisation in ethanol in a continuous reactor

Based on a selected number of experiments in a MA1 and a continuous stirred tank reactor (CSTR) the applicability of the kinetic model developed in Section 6.1 to a different reactor system, that is a CSTR, and to varying reaction temperatures is explored. The applicability of the model to these alternate reaction conditions was tested and the fit quality was evaluated using sensitivity and flux analysis (see Appendix C.5 and C.6). Furthermore, the influence of temperature and the characteristics of a continuous reactor system on both a molecular as well as a global lump level was monitored. This aids in the understanding of the chemical reaction mechanisms and sets a basis for future investigative work.

6.2.1 Experimental

Experiments using comparable loading ratios and identical reaction temperature were performed in both, MA1 (Exp. 56-61) and CSTR (Exp. 62-64, 68; see Appendix E.1). For different experiments in the CSTR the pressure and the mass flow $\dot{m}$ was varied. These two parameters influence the mean residence time in the CSTR (see Table 6.4). Important for the further observations is the density inside the reactor at different reaction conditions. The density is proportional to the total mass of reactants inside the CSTR m.

$$m = \rho \cdot V_R, \qquad V_R = 200\ mL. \tag{6.1}$$

The density ρ is assumed to be constant throughout the experiment and

is estimated employing the density of ethanol at the given pressure and temperature [Baz+07; DP04]. Since the reaction volume V_R is equal to the volume of the reactor, the reaction mass m results to be constant throughout the experiment. Further experiments were conducted in the CSTR varying the temperature in the range between 633 and 673 K. The formic acid to lignin ratio of was 1.1:1 in the batch reactor and 1.2:1 in CSTR. The ethanol to lignin ratio was 9:1 for the batch-experiments and 9.5:1 in the experiments conducted in the CSTR.30

Table 6.4: Experimental conditions, estimated total reaction mass (m) and mass flow ($\dot{m}$) for batch and continuous reactor.

Exp.	Reactor	T	Pressure	(mean) Residence time	m	$\dot{m}$
		K	MPa	min	g	g/h
56/57	MA1	653	-[a]	150	3.9	
58/59	MA1	653	-[a]	60	3.9	
60/61	MA1	653	-[a]	140	3.9	
62	CSTR	653	25	52	62.8	72.8
63	CSTR	653	30	59	72.3	74.1
64	CSTR	653	20	39	50.2	75.6
65	CSTR	633	25	56	69.7	74.6
66	CSTR	673	25	44	56.2	76.3
67	CSTR	653	25	37	62.8	102.5
68	CSTR	653	25	21	62.8	180.4

[a] The design of the MA did not enable the measurement of resulting pressures. Comparable experiments have shown pressures between 29 and 33 MPa [Gas+10]. The pressure in presented experiments is expected to be reduced by 3-6 MPa due to a decreased FA/EtOH loading ratio.

6.2.2 Results

General tendencies

In this section experiments carried out in a MA1 (Exp. 58, 59) and a CSTR (Exp. 63) at 653 K and approximately 60 min (mean) residence time are compared and evaluated. The mass balance diagram in Figure 6.11a compares the mass fraction of the three different output phases with the mass fractions of the input substances, that are ethanol, lignin and formic acid. In case of the batch-experiment (Exp. 58) in MA1 the results after 60 min residence time were considered. In case of the CSTR experiment, the exper-

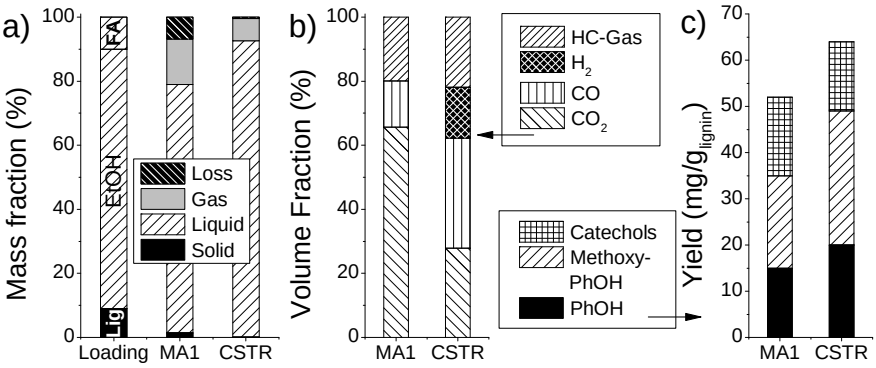

Figure 6.11: Results of lignin degradation in MA1 and CSTR at 653 K and 60 min (mean) residence times (Exp. 58, 63); a) liquid, gas and solid reaction products compared on a wt% basis with the input amounts of lignin from wheat straw Lig, EtOH and FA, b) Composition of the product gas, c) yields of PhOH, methoxyPhOH and catechols.

imental results obtained in the stationary state (see Chapter 2.2.2) of the experiment with the corresponding mean residence time (59 min, Exp. 63) were observed. The diagram reveals that a clear reduction of the relative yields of gas and recovered solids can be achieved by transferring reactions from a batch to a continuous reactor setup. The mass balance shows a mass loss for the batch experiments of < 7 wt% and for the CSTR experiments of < 6 wt%.

The gaseous products comprise a mixture of H_2, CO, CO_2 and hydrocarbons in the C_1 to C_4 range, of which C_2H_6 and C_2H_4 are the largest contributors. A Comparison between batch and continuous operation shows both considerable impact on the quantity of gaseous products as well as on the gas composition (see Figure 6.11b). A considerable decrease of CO_2 by a factor of 2, a 2 to 4 fold increased amount of CO and a large increase of H_2 are observed in continuous operation. Whereas in batch processes, hydrogen is readily consumed [Gas+2], the surplus of H_2 in the CSTR is a product of the continuous feeding, but also continuous tapping of gaseous components from the reactor. In addition, a control experiment was carried out in a MA1 at 653 K and 11 h residence time without biomass (Exp. 55). The input comprised 89 wt% ethanol and 11 wt% formic acid. The product contained 73 wt% liquid and 27 wt% gas and the main gaseous components were CO_2, C_2H_6, C_2H_4, C_4H_{10} that contribute with, respectively, 53 wt%,

13 wt%, 9 wt% and 13 wt% to the gaseous product. Also H_2, CO, CH_4 and C_3-gases were detected. The high amount of C_2-gases demonstrates that the gasification of ethanol also contributes to the elevated gas production (see Chapter 3.

To be able to include not only global lump products, but to also capture the role of typical deoxygenation and demethanisation reactions between monomeric phenolics in the liquid phase, 12 selected, 2- and 4-methyl, respectively -ethyl, substituted as well as non-substituted monomeric key components were quantitatively determined and grouped according to their structural properties, *i.e.* in accordance with their degree and type of oxygenation as described in Section 6.1. The yields for the grouped components per g initial lignin are shown in Figure 6.11c. The yield of each phenolic compound is given in Appendix E.1 (Exp. 58, 63). The total yield percentage of all key compounds lies between 3 and 7 wt% on an initial lignin basis. As only a comparatively small number of key compounds were chosen, the obtained percentage of monomeric compounds in the product is an underestimation of the actual content. For all of the three grouped compound classes of phenolic compounds, that are methoxyphenols, catechols and phenols, a dominance of 4-ethyl substituents is observed. The total yield of phenolics can be increased by about 1 wt% from approximately 5 to more than 6 wt% on an initial lignin basis, if the reaction is transferred from a batch reactor to a CSTR. Especially the yield of phenols and methoxyphenols is increased, the yield of catechol is similar at about 60 min (mean) residence time.

Model fit and comparison

The adapted kinetic model was used to fit the results of the temperature dependent experimental series (Exp. 64-66). The experimental results for the transition phase between non-stationary and stationary state in the CSTR are represented by the shattered data points in Figure 6.12. The continuous curves represent the results from the model fit. The modelling was carried out applying the methods presented in Appendix C. In order to minimise the the difference between calculated and experimental yields, the formal kinetic parameters $E_{A,j}$ and A_j were optimised (Equations C.1 to C.3). For the comparison of experimental and calculated yields of the phenolic products, see Figure 6.16. The coefficient of determination R^2 and the standard deviation σ of the experimental yields from the calculated yields of the phenolic products is listed in Table 6.5. The model fit of the experimental results of 2-ethylphenol was difficult which is discussed in Section 6.1. Besides, also the model fit of 4-ethylphenol and catechols was critical as the low coefficient of determination shows. The resulting formal kinetic rate co-

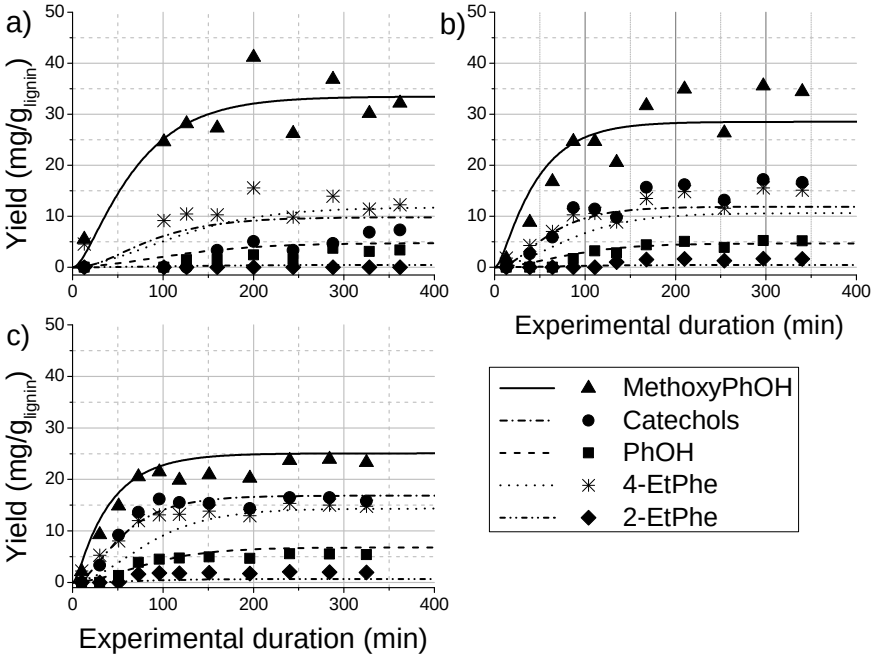

Figure 6.12: Comparison between the CSTR-fit of phenolic lumps and their measured quantities for Exp. 64-66 conducted at a) 633 K, b) 653 K and c) 673 K; mean residence times are between 39 and 56 min (see Table 6.4).

efficients k_j, apparent activation energies $E_{A,j}$ and the Arrhenius factors A_j are listed in Table 6.6. The fits for both CSTR and batch experiments from Section 6.1 were evaluated using flux and sensitivity analysis (see Figure 6.13 and Figure 6.14).

Comparisons between the single formal kinetic rate coefficients are given in the last column in Table 6.6. If the quotient of k_j(CS,633 K)/k_j(MA,633 K) is smaller than 0.02 or greater than 50, the field is left blank since such values simply show a great difference between the CSTR-fit and the MA-fit. Nevertheless, this difference is discussed in Section 6.2.3 and an eventual disagreement is pointed out. These show that the resulting formal kinetic rate coefficients are similar for both fits in respect to most reactions involved in the formation and degradation of phenolics (k_1, k_2, k_5, k_6, k_{10}). The reaction rates of all these reactions increased by transferring them to a CSTR, however, the maximum increase factor was 3.3. Among the reaction rates of

Table 6.5: Coefficient of determination R^2 for the model fit and standard deviation σ of calculated and experimental yields of phenolic products (see Figure 6.12).

	methoxyPhOH	PhOH	catechols	4-EtPhe	2-EtPhe
R^2	0.80	0.62	0.55	0.31	-0.55
σ	18	41	37	30	118

the primary reactions (k_1, k_6 and k_{10}) the increase factors were even smaller, 3.1 for the formation of methoxyphenols from lignin (k_1), 1.3 for the formation of 4-ethylphenols (k_6). Also the fluxes of these reactions were similar for both fits. However, the fluxes for all three reactions (r_1, r_6 and r_{10}) were smaller for the CSTR fit (see Figure 6.13), the flux of r_6 was reduced by a factor of 2.2 from $8.0{\cdot}10^{-4}$ to $3.6{\cdot}10^{-4}$ g/mL. On the contrary the formation of methoxyphenols from L_D as well as the conversion of catechols into phenols, respectively r_{15} and r_4, were more than 30 times faster in the CSTR according to the model fit. The fluxes of both reactions increased of a factor greater than ten to $3.0{\cdot}10^{-3}$ g/mL and $1.1{\cdot}10^{-3}$ g/mL for r_{15} and r_4 respectively. Hence, the sum of the fluxes which lead to a formation of methoxyphenols (r_{15} and r_1) at 60 min (mean) residence time more than doubles if the reaction is transferred from a batch to a continuous reactor. In addition, the flux of the conversion of methoxyphenols into catechols (r_2) also doubles. The flux from lignin to phenol via methoxyphenols and catechols is thus favoured by a continuous reactor according to the results from modelling. The reversible reactions are obviously in equilibrium since the fluxes of these reactions (r_7 and r_{14} as well as r_8 and r_9) are equal (see Figure 6.13). The formal kinetic rate coefficients of the char formation from catechols (k_3), phenols (k_{17}) and L_D (k_{16}) significantly decrease by a factor of more than 10 when the reaction is transferred to a CSTR. Contemplating the flux of the repolymerisation of phenols (r_{16}), which is relatively low ($< 10^{-4}$ g/mL), it is easily visible that this reactions plays a minor role in both reactor systems. On the contrary the fluxes of the char formation from L_D (r_{17}) and the repolymerisation of catechols (r_3) are both reduced from respectively $1.9{\cdot}10^{-4}$ to $1{\cdot}10^{-4}$ g/mL and $1{\cdot}10^{-4}$ to $< 10^{-4}$ g/mL.

Table 6.6: Formal kinetic rate coefficients k_j, apparent activation energies $E_{A,j}$ and Arrhenius factors A_j of the 17 reactions defined in the model (see Figure 6.7) at different temperatures for the CSTR-fit are compared with rate coefficients calculated for the batch-fit at 633 K.

r_j	E_A	$\log(A/A')$[a]	k_j(CS,673 K)[b]	k_j(CS,653 K)[b]	k_j(CS,633 K)[b]	k_j(MA,633 K)[b]	k_j(CS,633 K)/ k_j(MA,633 K)[b]
	kJ/mol	min^{-1}	min^{-1}	min^{-1}	min^{-1}	min^{-1}	
r_1	96	5.30	$7.32 \cdot 10^{-3}$	$4.34 \cdot 10^{-3}$	$2.48 \cdot 10^{-3}$	$7.95 \cdot 10^{-4}$	3.1
r_2	87	5.40	$4.06 \cdot 10^{-2}$	$2.51 \cdot 10^{-2}$	$1.51 \cdot 10^{-2}$	$8.24 \cdot 10^{-3}$	1.8
r_3	(528)	1.61	$<10^{-6}$	$<10^{-6}$	$<10^{-6}$	$2.02 \cdot 10^{+0}$	
r_4	8	-0.88	$3.07 \cdot 10^{-2}$	$2.94 \cdot 10^{-2}$	$2.80 \cdot 10^{-2}$	$7.97 \cdot 10^{-4}$	35
r_5	34	0.72	$1.21 \cdot 10^{-2}$	$1.01 \cdot 10^{-2}$	$8.25 \cdot 10^{-3}$	$2.47 \cdot 10^{-3}$	3.3
r_6	57	1.35	$9.22 \cdot 10^{-4}$	$6.77 \cdot 10^{-4}$	$4.87 \cdot 10^{-4}$	$3.75 \cdot 10^{-4}$	1.3
r_7	14	1.60	$3.40 \cdot 10^{+0}$	$3.16 \cdot 10^{+0}$	$2.92 \cdot 10^{+0}$	$3.27 \cdot 10^{-2}$	
r_8	1	2.72	$4.35 \cdot 10^{+2}$	$4.32 \cdot 10^{+2}$	$4.30 \cdot 10^{+2}$	$8.74 \cdot 10^{-3}$	
r_9	(0)	3.63	$4.29 \cdot 10^{+3}$	$4.29 \cdot 10^{+3}$	$4.29 \cdot 10^{+3}$	$2.71 \cdot 10^{-2}$	
r_{10}	75	5.18	$2.20 \cdot 10^{-1}$	$1.46 \cdot 10^{-1}$	$9.43 \cdot 10^{-2}$	$4.71 \cdot 10^{-2}$	2.0
r_{11}	(0)	-9.28	$<10^{-6}$	$<10^{-6}$	$<10^{-6}$	$1.62 \cdot 10^{-4}$	
r_{12}	188	11.40	$6.43 \cdot 10^{-4}$	$2.30 \cdot 10^{-4}$	$7.70 \cdot 10^{-5}$	$2.69 \cdot 10^{-4}$	0.3
r_{13}	(0)	0.21	$1.56 \cdot 10^{+0}$	$1.55 \cdot 10^{+0}$	$1.55 \cdot 10^{+0}$	$1.09 \cdot 10^{+8}$	
r_{14}	(0)	0.86	$7.22 \cdot 10^{+0}$	$7.22 \cdot 10^{+0}$	$7.22 \cdot 10^{+0}$	$4.20 \cdot 10^{-2}$	
r_{15}	17	-1.67	$1.11 \cdot 10^{-3}$	$1.02 \cdot 10^{-3}$	$9.22 \cdot 10^{-4}$	$3.04 \cdot 10^{-5}$	30
r_{16}	129	6.12	$1.37 \cdot 10^{-4}$	$6.76 \cdot 10^{-5}$	$3.20 \cdot 10^{-5}$	$4.18 \cdot 10^{-4}$	0.1
r_{17}	125	5.79	$1.31 \cdot 10^{-4}$	$6.65 \cdot 10^{-5}$	$3.22 \cdot 10^{-5}$	$5.41 \cdot 10^{-4}$	0.1

[a] A'=1 min^{-1}.

[b] CS : continuous reactor, MA : microbatch-autoclave.

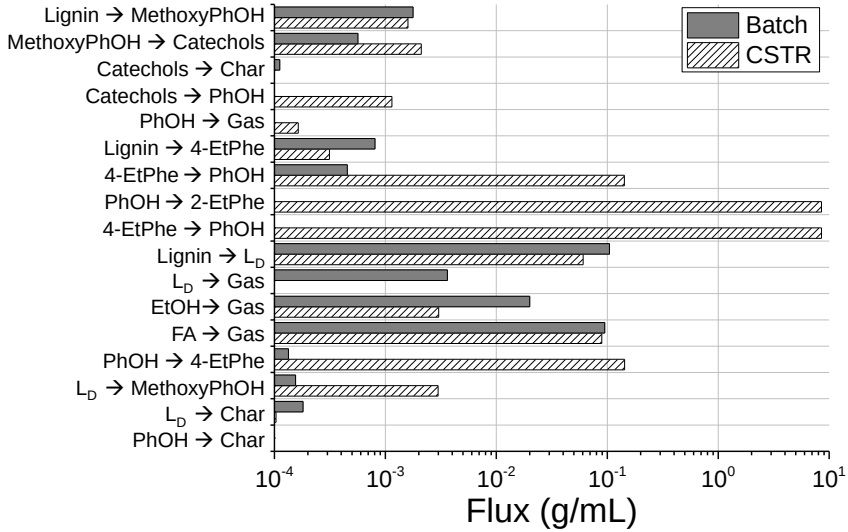

Figure 6.13: Comparison of the fluxes of each reaction defined in the model (see Figure 6.7) calculated for both batch-fit and CSTR-fit at 60 min (mean) residence time τ (τ') and 633 K (see Appendix C.6).

The formal kinetic rate coefficient of the gasification of L_D (k_{11}) decreases by a factor greater than 50, its flux decreases from a relatively high value in a batch reactor ($3.2 \cdot 10^{-3}$ g/mL) to a negligible value ($< 10^{-4}$ g/mL) in a continuous reactor. The flux of the gasification of ethanol decreases from 0.022 g/mL to $3.0 \cdot 10^{-3}$ g/mL if the reaction is transferred from MA to CSTR. The formal rate coefficient for the gasification of phenols is increased by a factor of 3.3. However, the flux in a CSTR of this reaction at 60 min residence time is still negligible. The flux of the gasification of formic acid is similar for both, the CSTR-fit and the batch-fit, although the formal kinetic rate coefficient (k_{13}) calculated by the CSTR-fit and the batch-fit differ from each other by a factor more than 50. The gasification of formic acid (r_{13}) is, if the reversible reactions are not considered, the fastest reaction in both fits.

The sensitivity analysis as explained in Appendix C.5 yields a matrix showing the sensitivity of each defined component to all considered reactions (see Figure 6.14). If none of the components is sensitive to a defined reaction, the formal kinetic rate coefficient can not be optimised mathematically since a modification of the formal kinetic rate coefficient does not show an effect on the yield of any component. Nevertheless the reaction might be essential

for the model since it is the only pathway leading to a certain component. Figure 6.14 shows that all phenolics are sensitive to the primary formation of methoxyphenol (r_1) and its most important competing reaction (r_{10}). However, the sensitivity to r_{10} of all phenolic products is reduced in the CSTR-fit compared to the sensitivity in the batch-fit. Major differences between the batch and the CSTR fit were found in respect to the char yield, which is only sensitive to the formation of char from L_D (r_{16}) in the CSTR-fit and to the char formation from catechol (r_3) as well as to the preceding reactions (r_1, r_2) in the batch-fit. Noteworthy is the increased sensitivity of all phenolics to the formation of methoxyphenols from L_D, which is not existent in the batch fit, however, significant in the CSTR fit. A very similar observation can be made for the sensitivity of catechols, phenols and ethylated phenols to the conversion of catechols into phenols. On the contrary the sensitivity of phenols and ethylated phenols to the formation of 4-ethylphenol from lignin is higher in the batch-fit compared to the CSTR-fit.

Temperature dependence of formal kinetic parameters

When increasing the temperature in the CSTR from 633 to 673 K, decreasing amounts of solids (-1.5 wt% on a global mass scale) and increasing amounts of produced gas (+9.9 wt% on a global mass scale) were recovered (see Appendix E.1). The yields of all phenolic products increased with the temperature except the yield of methoxyphenols, which were found to decrease. This tendency is correctly described by the model fit (see Figure 6.12). Figure 6.15a shows that the initial slope of the curve describing the yield of methoxyphenols is similar for all temperatures. It further reveals that the yield of methoxyphenols is reduced by about 1/3 for 673 K in respect to the maximum yields achieved at 633 K. The yield of catechols is overestimated by the model for 633 K and underestimated for 653 K (see Figure 6.15b). The slope describing the increase of the yield of catechols and phenols during the non-stationary state increases with temperature. Higher yields of both compound classes are found for higher reaction temperatures. Noteworthy is the almost threefold increase of the catechols yield within the contemplated temperature range (633 to 673 K). In addition the catechols yield at 633 K seems to have not reached the stationary state until 360 min experimental duration.

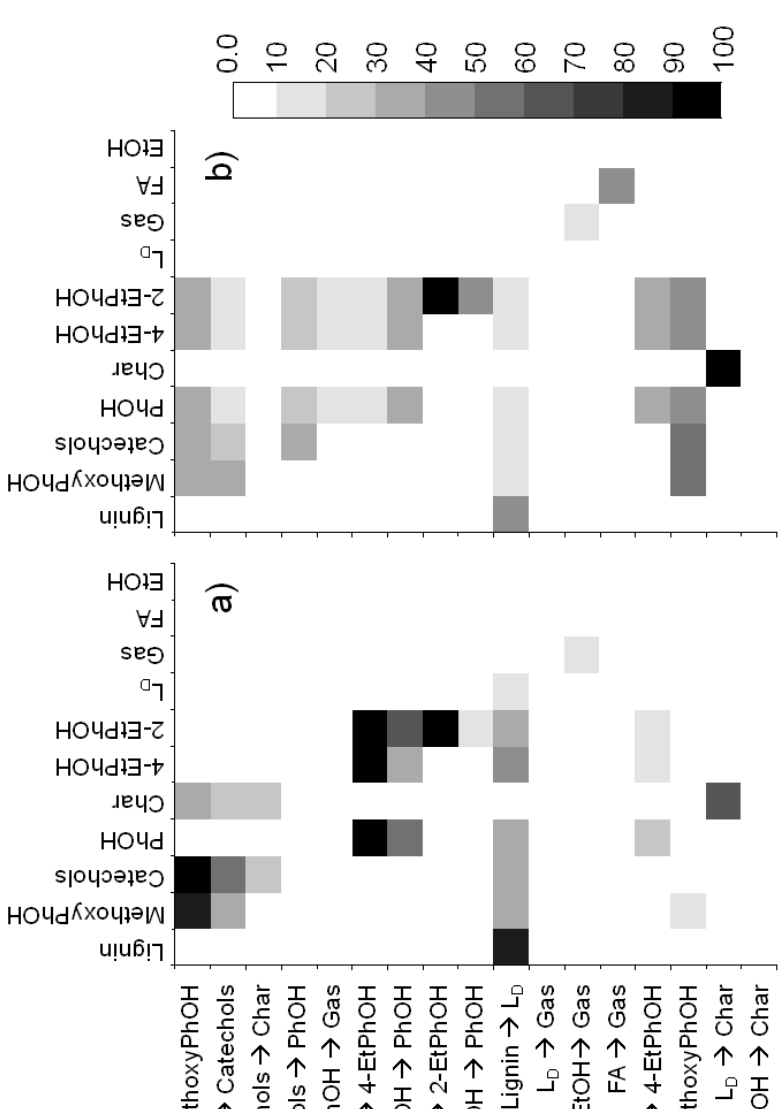

Figure 6.14: Sensitivity on a scale from 0 to 100 % (see Appendix C.5) of the calculated yields at 633 K and 60 min (mean) residence time to a variation of rate coefficients by factor 2 for a) batch-fit and b) CSTR-fit.

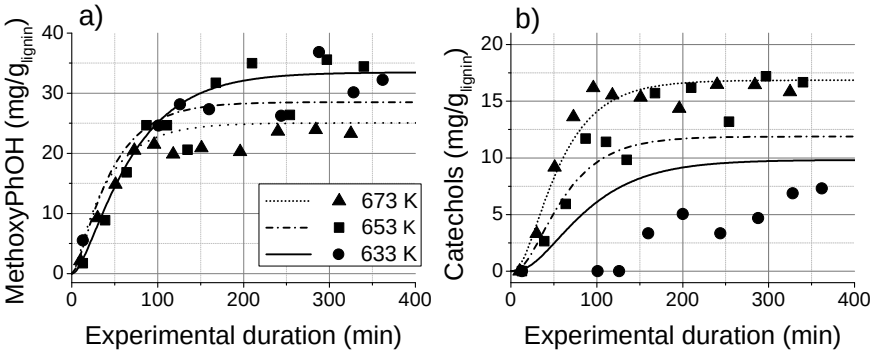

Figure 6.15: Results from the CSTR-fit of the experimental yields at different temperatures and mean residence times (Exp. 64-66) of a) methoxyphenols and b) catechols.

The calculated apparent activation energies listed in Table 6.6 indicate the temperature dependence of each reaction. Alkylation and dealkylation reactions of phenols (reactions r_7-r_9 and r_{14}) as well as the gasification of formic acid and L_D show an apparent activation energy close or equal to zero, *i.e.* a negligible temperature dependence of the formal kinetic rate coefficient. However, these results have no influence on the description of the product yields since these reactions are reversible and in equilibrium as shown above. The reaction with the highest activation energy (r_3) is of minor importance since the formal rate coefficients and fluxes are negligible. Comparing the apparent activation energies of the gasification of ethanol (r_{12}) and formic acid (r_{13}), it can clearly be observed that formic acid is instantaneously gasified at all temperatures, whereas the gasification of ethanol is much more sensitive to temperature changes. Hence, the main reason for the increased gas yield found at higher temperatures next to further cracking reactions [Kle+11], is due to the increased gasification of ethanol. The formation of methoxyphenols (E_{A1}=96 kJ/mol) shows a higher apparent activation energy than the reaction of its decomposition (E_{A2}=87 kJ/mol). The same phenomenon is observed in respect to catechols. The calculated apparent activation energy of the formation of catechols (E_{A2}) is higher than for the conversion of catechol into phenol (E_{A4}=8 kJ/mol) which is the major reaction of catechol decomposition.

6.2.3 Discussion

The CSTR-fit as well as the batch-fit of the formal kinetic rate coefficients show that the developed model shown in Figure 6.7 considers the main reaction pathways of wheat straw lignin degradation in ethanol with formic acid. The optimised formal kinetic parameters approximate the yields of the phenolic products, thus the model is able to describe the general tendencies of the phenolics yield in a CSTR (compare also Figure 6.16). Sensitivity and flux analysis demonstrate the applicability of the model for both reactor systems, batch reactor and CSTR.

Comparison of the results from this work with literature values shows a good general agreement, and thus further confirm the validity of the developed model. Jegers and Klein found slightly varying estimated rate constants for catechol and guaiacol decomposition during Kraft lignin pyrolysis at 673 K, depending on their alkyl substitution. 4-Ethyl substituted catechols and guaiacols were seen to decompose faster than their 4-methyl substituted analogues, which in turn decomposed faster than the non-substituted compounds. Averaged, at 673 K rate constants of 0.029 min^{-1} (0.031 min^{-1} in this work) for catechols and 0.042 min^{-1} (0.041 min^{-1} in this work) for guaiacols were found. Pure guaiacol displayed a decomposition rate constant of 0.038 min^{-1} [KV08] at 673 K, illustrating the non-influence of other species on the decomposition rate.

Various activation energies for lignin degradation have been reported by Brebu and Vasile [BV10]. The most common values for single first order decomposition are found to vary between 54 and 79 kJ/mol between 517 - 582 K, increasing to 81 kJ/mol at higher temperatures up to 1440 K [Ram70; DRS74; Nun+85]. The apparent activation energy describing the primary lignin degradation in this work, that is principally $E_{A,10}$ (= 75 kJ/mol), is within this typical span.

The model correctly describes the increase of yields of catechols and phenols and the decrease of the yield of methoxyphenols at increasing temperatures (see Figure 6.12). However, one phenomenon is observed that was not correctly described by the model. The experimental results at 673 K show that approximately 100 min into the experiment, the yield increase of catechols stagnates (see Figure 6.15 b) and the actual final yield at long experimental durations is seen to be very similar to the yield at 653 K. The model underestimates the catechol yield in the stationary state at 653 K since the slope of the catechol yield during the first 100 min of the experiment at 653 K is lower than at 673 K. In addition, the phenomenon leads to and overestimation of the rate coefficient of the formation of catechol (k_2) at 633 K. The abrupt stagnation of the catechol yield is difficult to describe

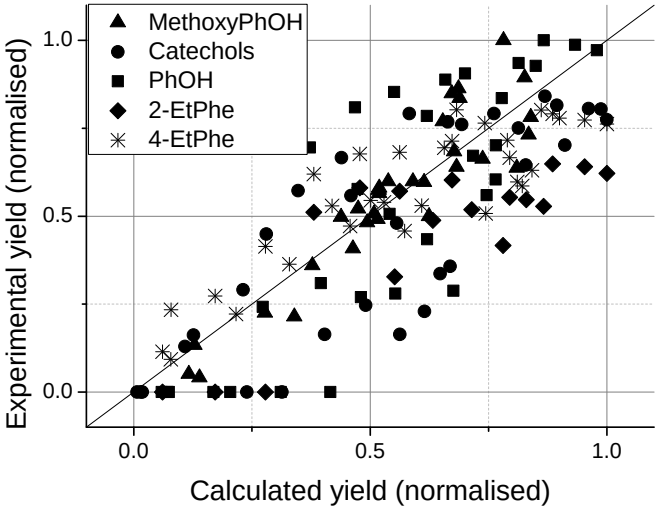

Figure 6.16: Comparison of the normalised calculated and experimental data for product yields of all phenolic (lump) components. The following normalising factors (mg/g_{lignin}) were used for better comparability: MethoxyPhOH: 42.1; Catechols: 20.4; PhOH: 5.6; 4-EtPhe: 19.4; 2-EtPhe: 3.1.

by any formal kinetic model. Neither the consideration of additional intermediates, reactants or reaction pathways which are not considered by the model, nor increased reaction orders were able to improve the fit. A change of the reaction mechanism caused by *e.g.* phase separation in the reactor might be a reason. The effect of the density on the reaction mechanism might also play an important role. In this work, however, only the effect of the density on the residence time was considered. This leads to an underestimation of the yield o 4-ethylphenol at 653 K and thus a rather low coefficient of determination at this temperature while the approximation of the experimental yield of 4-ethylphenol by the model is acceptable at 633 K and 673 K. Further research effort has to be spent on the clarification of these phenomena. The study of ethanolysis and hydrothermal degradation of intermediate phenolic products, that are methoxyphenols, catechols and ethylphenol, are suggested.

Both model fits show that the main fluxes of the reactions r_{10}, r_{12}, r_{13} are in the same order of magnitude, whereas the gasification of ethanol seems

to be favoured in the batch reactor. Small differences can be due to slightly different input concentrations and due to the assumption that all reaction orders are 1. The suppression of the gasification and the formation of char from L_D can be explained by a parallel reaction from the reactive component L_D to a stable, ethanol-soluble component L_D. The latter obviously occurs within lignin depolymerisation but is not crucial for describing the experimental results. A CSTR facilitates reactions of early intermediates and later products, *e.g.* L_D and phenols respectively. This might result in the scavenging of radicals and the suppression of char formation as described in other works [Sai+03; McM+04; Tak+12; Aid+02; Fan+05].

The sensitivity analysis shows a high sensitivity of all phenolic components to the formation of L_D (r_{10}), which is the reaction competing with the primary phenolic products methoxyphenols and 4-ethylphenol. Hence, the key for increasing the phenolic yield is to accelerate the formation of methoxyphenols (r_1) and 4-ethylphenol (r_6) and to suppress the competing parallel reaction (r_{10}). However, the CSTR-fit revealed that another important reaction pathway to yield phenolics is via the reactive intermediates L_D (r_{15}) and that this pathway is favoured in a CSTR. The modelling reveals that in a CSTR the major reaction pathway from lignin to phenol is via methoxyphenols and catechol, whereas in a batch reactor it is via 4-ethylphenol.

The formal kinetic rate coefficients of the primary reaction of lignin depolymerisation (r_1, r_6 and r_{10}) calculated for the CSTR-fit are higher than for the batch-fit (factor 1.3 to 3.1). These are the result of the impact of stirring and the increased heating rate in the CSTR. The temperature dependence of the formation of methoxyphenols and catechols (r_1 and r_2, respectively) is higher than those of the subsequent decomposition reactions (r_2 and r_4, respectively). This implies that increased temperatures lead to an increased yield of catechols and methoxyphenols. However, a temperature increase within the range of 633 - 673 K is not seen to aid in an accumulation of these monomeric units (see Figure 6.15a). This can be explained by a drop of the mean residence time with increasing temperatures due to changing densities.

The calculated apparent activation energies of the alkylation and dealkylation of phenols (E_{A7}-E_{A9} and E_{A14}) are close to zero and thus the formal kinetic rate coefficients of these reactions are not sensitive to temperature changes. Obviously, the only important fact for modelling these reversible reactions in a CSTR is the thermodynamic equilibrium. Fluxes and the temperature dependence of the mentioned reactions are of minor importance. Furthermore, the gasification of formic acid (r_{13}) and L_D (r_{11}) resulted to be insensitive to temperature changes ($E_{A,j}$ close to 0) whereas the tem-

perature sensitivity of the repolymerisation of catechol (E_{A3}) is very high (528 kJ/mol). These values are of minor importance due to an exceptionally high rate coefficient as for the gasification of formic acid (k_{13}) or an exceptionally low rate coefficient as for the repolymerisation of catechol (k_3). The sensitivity analysis shows that none of the reaction participants is sensitive to a change of k_3 or k_{11}. The gasification of ethanol is mainly influenced by residence time and temperature. The flux of this reaction is one of the highest at 60 min residence time. High temperatures and long residence times favour the gasification of ethanol. In the CSTR the flux of ethanol gasification is considerably lower (0.003 g/mL) than in a batch reactor (0.022 g/mL). Thus, the model fit implies a transfer from batch to CSTR to suppress the gasification of ethanol.

The transfer from batch to CSTR showed a suppression of gasification and repolymerisation of reactive intermediates as well as of phenolic products. In addition the gasification of ethanol was reduced. The formation of methoxyphenols from reactive intermediates (L_D) was revealed to be an important reaction pathway, favoured in a CSTR to increase the yield of phenolics.

6.3 Lignin depolymerisation in water in a batch-reactor

Hydrothermal degradation of lignin has become more important in the last years. Some research has been done, especially focusing on the reaction kinetics of the degradation of model compounds [WSG08; WSG09; WSG11]. Zhang, Huang, and Ramaswamy described the lignin degradation in hot compressed water and the build-up of char [ZHR11]. Yong and Matsumura [YM12] studied the reaction kinetics of lignin depolymerisation in SCW in a continuous reactor considering both, global lump components and single phenolic components. In this chapter the question should be answered whether the model shown in Section 6.1 can be adapted in order to describe the hydrothermal depolymerisation of enzymatic hydrolysis lignin from spruce wood (softwood) in a batch-reactor. Experiments (Exp 69-102, see Appendix E.1) were carried out in a 5 mL MA2. The reactants for all experiments were 0.33 g of spruce-lignin and 2.5 g of water. Neither a hydrogen donor nor any homogeneous or heterogeneous catalysts were added. The modelling of the major reaction pathways and the formal kinetics were validated by comparing calculated and experimental yields of phenolics as well as solid and gaseous lump products. In addition, the formal kinetic parameters resulting from an optimisation were compared with values from literature.

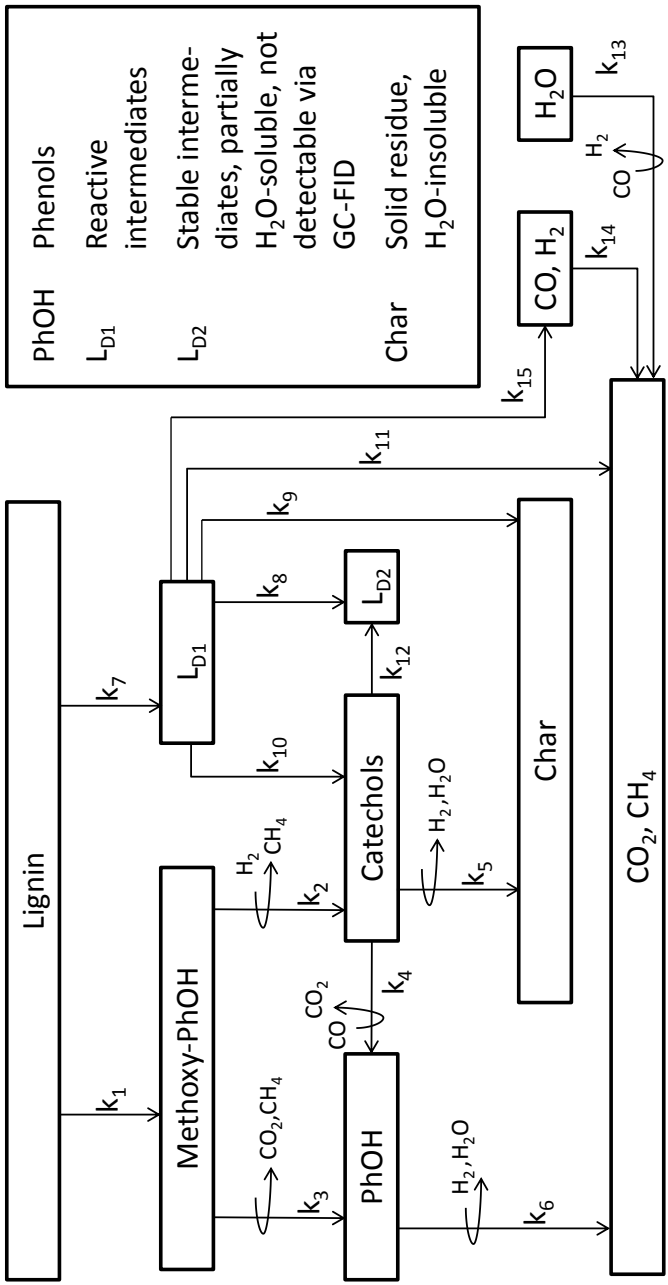

Figure 6.17: Scheme of main reaction participants and pathways of the hydrothermal depolymerisation of spruce-lignin; gaseous components take part in reactions 2-6 and 13. This is indicated by curved arrows.

6.3.1 Model adaptations

The development of the formal kinetic model describing the hydrothermal lignin depolymerisation in a batch reactor is based on the scheme of reaction pathways developed in Section 6.1. However, the model had to be adjusted to the application for the different solvent, *i.e.* water instead of ethanol, and type of lignin. The lignin used here was an enzymatic hydrolysis lignin from spruce (softwood) which is principally made up of coniferyl moieties. It was consequently observed that the most prominent initial products from spruce-lignin were methoxyphenols, while only small amounts of 4-ethylphenol were detected. Lignin from wheat straw, which was used in Section 6.1, on the contrary yields significant amounts of 4-ethylphenol since it contains more *para*-coumaryl units. Hence, for the modelling of the degradation of spruce-lignin a primary formation of 4-ethylphenol did not have to be considered. In addition, hydrothermal degradation of lignin yields high amounts of catechols compared to thermal degradation in ethanol or acetone [LZ08]. It is however impossible to describe such high yields by assuming the formation of catechols exclusively via methoxyphenols. A parallel pathway for the formation of catechol was considered. However, the primary intermediate of this pathway is unknown. It is supposed to be among the lump component named L_D. Yong and Matsumura did not report increased catechol yields, thus did not consider this parallel pathway of catechol formation [YM12]. This is probably due to the low loadings of lignin (0.1 wt%). The lump component L_D comprises all water soluble components that could not be quantified by GC-analysis as well as volatile organic components which were adsorbed on the solid residue and thus did not pass the filter during product separation but were evaporated during the drying of the solid residues. The component L_D could analytically not be quantified, however, its existence is reasonable to be assumed in order to close the mass balance. Previous studies concerning repolymerisation reactions and scavenging of organic radicals [Far+10; Sai+03] led to the assumption that among the lump component L_D reactive components (L_{D1}) and stable components (L_{D2}) can be distinguished.

In addition, the gaseous products were further distinguished into reactive intermediates (CO, H_2) and stable products (CO_2 and CH_4). Gaseous products were assumed to be formed via the gasification of organic components derived from lignin. Furthermore, methanisation and water-gas-shift-reaction were taken into account. These adaptions of the model shown in Figure 6.7 lead to a modified model which is assumed to be able to describe the reactions taking place throughout the hydrothermal depolymerisation of a softwood-lignin. The modified model is shown in Figure 6.17. The mod-

elling of the kinetics of hydrothermal lignin degradation was carried out as described in Appendix C. All reactions were assumed to be of first order. The resulting differential equations are listed in Appendix C.3. Since the formal rate coefficients depend on the temperature, Equations C.1 to C.3 were applied for their optimisation.

6.3.2 Results

The overall experimental results are summarised in Appendix E.1 (Exp. 69-102). The experimental yields of stable gaseous products (CO_2 and CH_4) and solid residue are displayed in Figure 6.18, represented by the individual data points. Results of hydrothermal lignin depolymerisation show a recovery of stable gaseous products of maximum 25 wt% on an initial lignin basis, of which 24 wt% are CO_2. After an initial rapid increase of the yield of CO_2 and CH_4 until approximately 60 min residence time, the yield approximates a finite threshold value. This threshold increases with the temperature. The maximum yield of 15 mg/g_{lignin} CO was measured at 653 K and 30 min residence time (Exp. 95). It was observed to peak at residence times between 30 and 120 min. With increasing temperature the maximum of the peak increased and the peak shifted to shorter residence times (see Appendix E.1, Exp. 69-102). H_2 could not be detected in the gaseous product, however, was assumed to be formed and instantaneously consumed, since several reactions which occur within hydrothermal lignin degradation require the presence of reactive hydrogen, *e.g.* the formation of catechol by demethylation of methoxyphenol [Vuo86] or the hydrolytic scission of one hydroxyl-group of the catechol molecule [WSG09].

After an initial decline until approximately 60 min residence times the yield of solid residue approximates a finite threshold value. This threshold varies marginally with the temperature. Not converted lignin and char could gravimetrically not be distinguished. The measured yield of solid residue was thus compared with the sum of the calculated yields of not converted lignin and char. The interpretation of the FT-IR-spectrum of the solid residue aids in analytically determining the zone of transition from not-reacted lignin to char. Figure 4.2b shows the FT-IR-spectra of spruce-lignin and the solid residue after different residence time in the MA1 at 633 K. Most aromatic vibrational bands, *e.g.* at 1511 cm^{-1} 1429 cm^{-1} and 1058 cm^{-1}, disappear until residence times of 60 min. The interpretation of the FT-IR-spectra is analogous to the lignin degradation in ethanol in Section 6.1.

The yield of solid residue is described by the model assuming a primary decomposition of the lignin followed by the build-up of char. The standard deviation σ of experimental and calculated yields is 18 %. Gaseous products

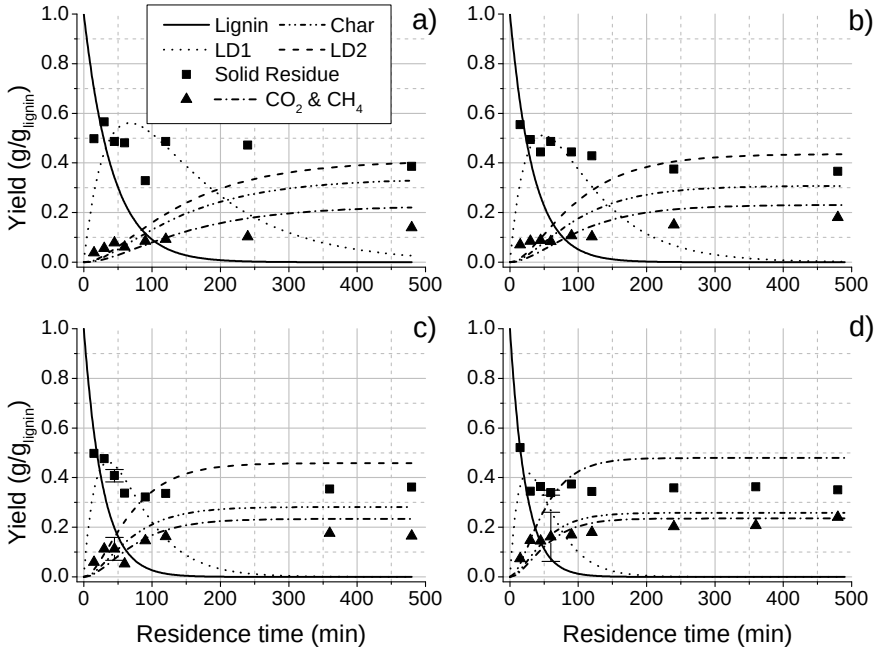

Figure 6.18: Comparison between the model-fit of solid and gaseous lump components and measured quantities of solid residue and stable gaseous compounds (CO_2 and CH_4) for experiments carried out at a) 593 K, b) 613 K, c) 633 K, d) 653 K.

are assumed to be formed via the gasification of L_{D1} and phenols. In addition, CO_2 and CH_4 were assumed to be produced during the decomposition of methoxyphenols and catechols (see Appendix C.3). The water-gas-shift reaction contributes to the conversion of CO into CO_2 due to the excessive amount of water present in the reactor. The yield of the stable gaseous compounds CO_2 and CH_4 is underestimated by the model during the initial increase up to approximately 90 min. When the yield approaches the threshold, it is overestimated at any contemplated temperature. The standard deviation σ of experimental and calculated yields for stable and reactive gaseous compounds is 19 %.

The total yield of phenolic products reached about 3.5 wt% of the initial input mass of lignin (see Figure 6.19). The dominant phenolic products were catechols, that are catechol, 4-methylcatechol and 4-ethylcatechol. The

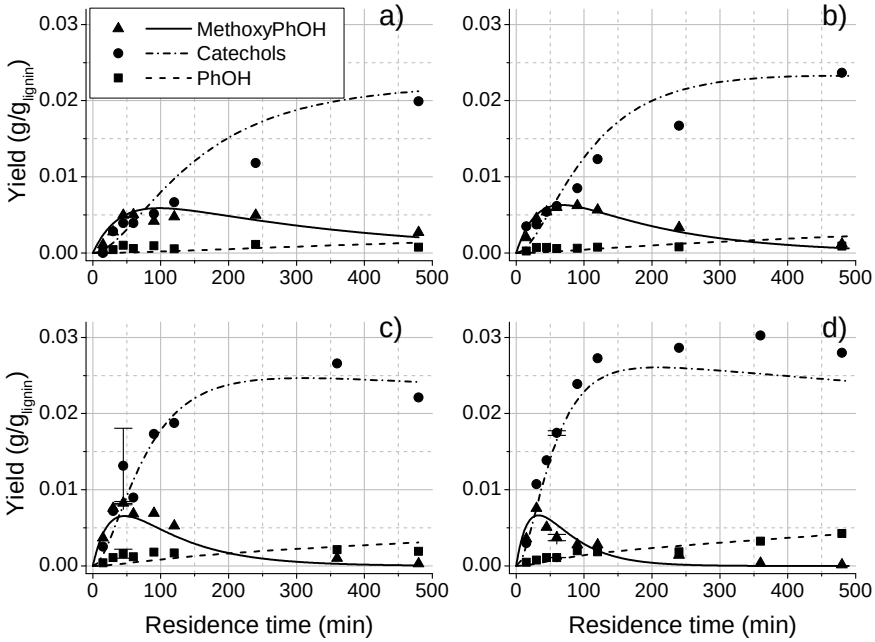

Figure 6.19: Comparison between the model-fit of phenolic lumps and their measured quantities for experiments conducted at a) 593 K, b) 613 K, c) 633 K, d) 653 K; error bars show standard deviation σ obtained from similar reproduced experiments at the corresponding residence time and temperature.

yield of catechols increased with the residence time and the temperature approximated a threshold maximum yield. After an initial rapid increase of the yield of methoxyphenols it decreased with the residence time. The peak of the yield of methoxyphenols shifted from 90 min at 613 K to 30 min at 653 K. The higher the temperature the slimmer is the form of the peak. The yield of phenols increased with the residence time and the temperatures. In addition to the experimental yields (individual data points) the calculated yields are displayed in Figure 6.19 (continuous curves). The formation and degradation of methoxyphenols as well as the high yield of catechol can be described by the model. Furthermore, the increasing yield of phenols can be described by the model. The standard deviation σ of the experimental from the calculated yields of methoxyphenols, catechols and phenols are 12 %, 8 % and 15 % respectively, the R^2 for these phenolics is 0.78, 0.88, 0.10

respectively. While R^2 for methoxyphenols and catechols is acceptable, the approximation of the yield of phenols by the model is much worse especially for low yields of phenols. For relatively high yields of phenols, which were especially obtained at increased temperatures, a better approximation of the model fit could be achieved. For the yields of phenols from the experiments at 653 K $R^2 = 0.83$. Table 6.7 shows all optimised formal kinetic parameters resulting from the search of the minimum difference between the calculated and the measured yields (see Equation C.1). The optimisation considered the formal kinetic rate coefficients of the formation of char (k_5) and L_{D2} (k_{12}) from catechols to be negligible. For all other reaction pathways sensible values of $E_{A,j}$ and A_j were calculated. The dominating primary pathway of lignin degradation is the formation of L_{D1} since the resulting formal rate coefficient k_7 is about 100 times larger than the formal rate coefficient of the formation of methoxyphenols k_1 for all considered temperatures.

Table 6.7: Apparent activation energies $E_{A,j}$, Arrhenius factors A_j and rate coefficients k_j at different temperatures for the 15 reactions defined in the model (see Figure 6.17).

r_j	E_A kJ/mol	log(A/A′)[a] -	k(593 K) min^{-1}	k(613 K) min^{-1}	k(633 K) min^{-1}	k(653 K) min^{-1}
r_1	58	1.4	$1.91{\cdot}10^{-4}$	$2.81{\cdot}10^{-4}$	$4.02{\cdot}10^{-4}$	$5.63{\cdot}10^{-4}$
r_2	101	6.4	$2.64{\cdot}10^{-3}$	$5.16{\cdot}10^{-3}$	$9.68{\cdot}10^{-3}$	$1.75{\cdot}10^{-2}$
r_3	94	5.0	$5.15{\cdot}10^{-4}$	$9.61{\cdot}10^{-4}$	$1.72{\cdot}10^{-3}$	$2.98{\cdot}10^{-3}$
r_4	55	1.0	$1.34{\cdot}10^{-4}$	$1.93{\cdot}10^{-4}$	$2.72{\cdot}10^{-4}$	$3.76{\cdot}10^{-4}$
r_5	3037	3.2	$< 10^{-6}$	$< 10^{-6}$	$< 10^{-6}$	$< 10^{-6}$
r_6	66	1.0	$1.84{\cdot}10^{-5}$	$2.85{\cdot}10^{-5}$	$4.27{\cdot}10^{-5}$	$6.26{\cdot}10^{-5}$
r_7	32	1.2	$2.38{\cdot}10^{-2}$	$2.94{\cdot}10^{-2}$	$3.58{\cdot}10^{-2}$	$4.31{\cdot}10^{-2}$
r_8	81	4.6	$3.52{\cdot}10^{-3}$	$6.01{\cdot}10^{-3}$	$9.90{\cdot}10^{-3}$	$1.58{\cdot}10^{-2}$
r_9	58	2.6	$2.89{\cdot}10^{-3}$	$4.25{\cdot}10^{-3}$	$6.09{\cdot}10^{-3}$	$8.53{\cdot}10^{-3}$
r_{10}	72	2.5	$1.55{\cdot}10^{-4}$	$2.49{\cdot}10^{-4}$	$3.89{\cdot}10^{-4}$	$5.90{\cdot}10^{-4}$
r_{11}	75	3.8	$1.45{\cdot}10^{-3}$	$2.39{\cdot}10^{-3}$	$3.82{\cdot}10^{-3}$	$5.92{\cdot}10^{-3}$
r_{12}	296	5.0	$< 10^{-6}$	$< 10^{-6}$	$< 10^{-6}$	$< 10^{-6}$
r_{13}	48	1.6	$1.92{\cdot}10^{-3}$	$2.65{\cdot}10^{-3}$	$3.58{\cdot}10^{-3}$	$4.75{\cdot}10^{-3}$
r_{14}	42	2.2	$2.71{\cdot}10^{-2}$	$3.59{\cdot}10^{-2}$	$4.68{\cdot}10^{-2}$	$5.99{\cdot}10^{-2}$
r_{15}	69	2.8	$4.75{\cdot}10^{-4}$	$7.52{\cdot}10^{-4}$	$1.16{\cdot}10^{-3}$	$1.73{\cdot}10^{-3}$

[a] $A' = 1 min^{-1}$

6.3.3 Discussion

Comparison of ethanol and water model

For the comparison of the two different models, developed for the degradation of wheat-straw-lignin in ethanol and formic acid on the one hand and for the degradation of spruce-lignin on the other, a flux analysis for 633 K and 131 min residence time was carried out. Figure 6.20 shows that the most prominent primary reaction in both models is the conversion of lignin into L_{D1} (r_7) since its flux is higher than that of the parallel reactions, that is the conversion of lignin into phenolics. The flux of r_7 is approximately 0.11 g/mL for both models. The formal kinetic rate coefficient is $4.7{\cdot}10^{-2}$ and $3.6{\cdot}10^{-2}$ min^{-1} respectively for the ethanol and the water model. Similar observations can be made for the conversion of lignin into methoxyphenols (r_1). Hence, the primary lignin degradation seems to be slightly faster in ethanol. However, it was demonstrated in Chapter 4 that lignin depolymerisation is faster in water if exactly the same conditions and the same type of lignin were chosen. The type of lignin has thus a significant influence on the kinetics of its primary degradation [JNB10].

Major differences between lignin depolymerisation in water on the one hand and ethanol on the other are the increased yield of catechols and solid residue (see Chapter 4). Modelling suggests different reaction pathways for the formation of both catechols and char. While in ethanol catechols are exclusively formed via methoxyphenols, in water the more important pathway is via the lump component L_{D1}. The flux of the conversion of L_{D1} into catechols at 633 K and 131 min is approximately $2.0{\cdot}10^{-3}$ g/mL and thus significantly higher than the flux of the conversion of methoxyphenols into catechols which results to be approximately $5.8{\cdot}10^{-3}$ g/mL. Comparing the formal kinetic rate coefficients of the reaction pathways originating from catechols (k_4, k_5, k_{12}) the fastest reaction is the conversion of catechols into phenols. Its formal kinetic rate coefficient is $2.7{\cdot}10^{-4}$ min^{-1}, whereas the formal kinetic rate coefficients of the reactions describing the repolymerisation of catechols (k_5, k_{12}) are negligible ($<10^{-6}$ min^{-1}). The fluxes of all three reactions are very small ($<10^{-4}$ g/mL). The model suggests thus the repolymerisation of catechols in water to be of almost no importance. This is a contradiction to many previous studies which assume the repolymerisation of monoaromatic compounds to be very important for high yields of char [Sai+03; Tak+12]. Modelling of lignin solvolysis in ethanol also suggests the repolymerisation of catechol to be the more significant reaction causing high yields of char. The flux analysis shows much higher fluxes for this reaction in ethanol than in water (see Figure 6.20). It is indispensable to put more

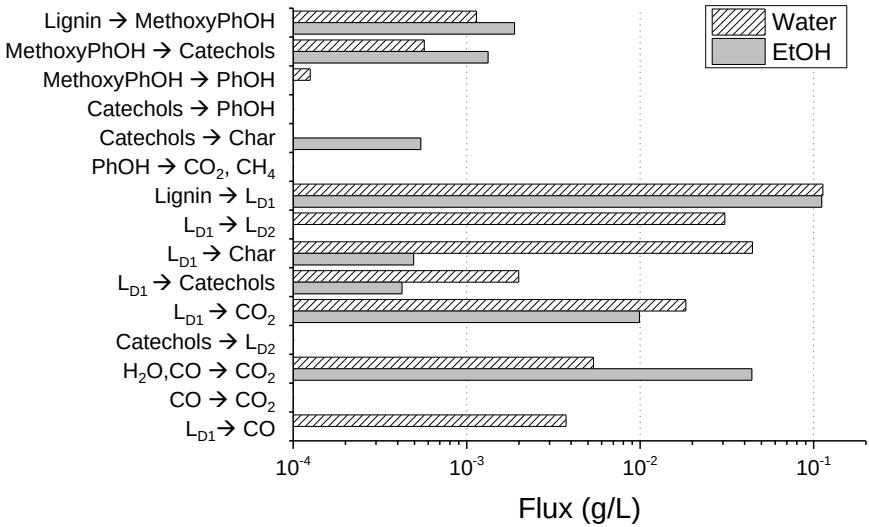

Figure 6.20: Fluxes of main reactions comprised by the developed model of hydrothermal depolymerisation of spruce-lignin (see Figure 6.17), reactions r_1, r_2, r_4, r_5, r_6, r_7, r_9, r_{11} are compared with analogue reactions of lignin solvolysis in ethanol (see Section 6.1); $\tau = 131$ min; $T = 633$ K; lignin/water=132 g/L.

effort into the investigation on the key intermediate component(s) which are crucial for the formation of catechols and char since it assists in the comprehension of the chemical mechanisms. The critical question is whether the inhibition of the repolymerisation of phenolics or the provocation of the cleavage of oligomeric aromates is the main instrument to raise the overall yield of phenolic products.

The formation of gas via L_{D1} is very similar in both solvents since the fluxes are in the same order of magnitude (see Figure 6.20). The water model considers two reactions that contribute to the gasification of L_{D1}, that are the conversion of L_{D1} into stable gases (r_{11}), that are CO_2 and CH_4, and into intermediates (r_{15}), that are CO and H_2. The sum of the fluxes of both reactions can be compared with the flux of the gasification reaction of L_D calculated by the ethanol model which are 0.02 g/L and 0.01 g/L respectively. The conversion of L_D into char and also into gaseous products is suggested to be faster in water than in ethanol. However, it has to be taken into account that the ethanol model deals with a very dominant gas formation reaction

which is the gasification of formic acid. The flux of this reaction is almost 10 times higher than the flux of the gasification of L_D (see Figure 6.13) which makes it more difficult for the model to describe the latter reaction. The modelling of gaseous and solid products is partially successful. Tendencies can be described, like the rapid decrease of solid residue at short residence times due to the depolymerisation of lignin. However, the underestimation of the gas yield at short residence times and the overestimation at long residence times lead to an increased standard deviation of calculated and measured quantities (19 %). Hence, the modelling of gaseous components has to be reviewed and the model has to be refined. A suggestion for future models is to consider the gasification of lignin as a primary reaction. Obviously the formation of CO_2 and CH_4 is more immediate. This is also suggested by Yong and Matsumura [YM12].

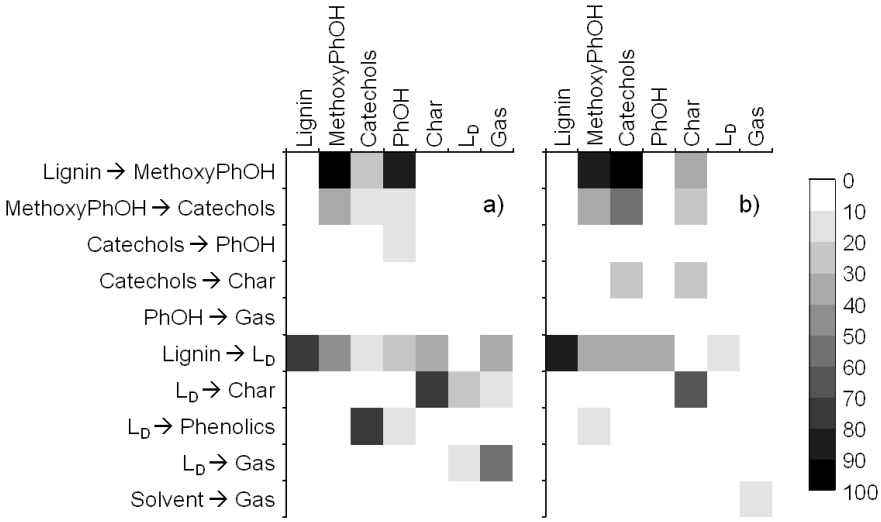

Figure 6.21: Sensitivity matrices considering comparable reactions and intermediates or products of a) the model of hydrothermal degradation of spruce-lignin and b) the solvolysis in ethanol and formic acid of wheat-straw-lignin; $\tau = 131$ min; $T = 633$ K; lignin/solvent=132 g/L.

The sensitivity analysis shows very similar results in respect to the reactions discussed above (see Figure 6.21). The high sensitivity of lignin and the moderate sensitivity of all phenolic products to the primary conversion of lignin into L_{D1} are similar in both solvents. As already shown for the

lignin solvolysis in ethanol, also in water the key of increasing the phenolic yield is to suppress the formation of L_D and increase the reaction rate of the formation of monomeric methoxyphenols. However, hydrothermal lignin degradations shows that promoting the formation of catechols from intermediates (L_{D1}) must also aid in increasing the yield of phenolics. Char shows a higher sensitivity to the formation of L_{D1} in water. On the contrary, in ethanol, it shows a higher sensitivity to the formation of catechols. Gaseous products show a moderate sensitivity to the formation and gasification of L_{D1}, whereas in ethanol the sensitivity to those reactions is negligible. This is in good agreement with the conclusions that are drawn from the flux analysis. The low sensitivity of the gaseous products within the ethanol model to the conversion of L_{D1} into char and gas is certainly due to the dominant gasification of formic acid.

Degradation of lignin

The presented model is validated by comparison with literature values. Table 6.8 shows the apparent kinetic parameters resulting from the kinetic studies of different approaches of thermal lignin degradation, all based on lump-models. Summarised are the most recent works based on pyrolysis, solvolysis and hydrothermal degradation. The kinetic studies of pyrolytic lignin degradation use thermogravimetric analysis (TGA). Some other studies of the last three decades will be additionally discussed in the text. Várhegyi et al. [Var+97] reported lower apparent activation energies for pyrolytic lignin degradation (34-65 kJ/mol) than Cho et al. [Cho+12] (74 kJ/mol) or Jiang, Nowakowski, and Bridgwater [JNB10] (134-172 kJ/mol) since they used wood without separation of the lignin fraction. Várhegyi et al. conclude that the determination of the kinetics of lignin degradation is difficult since the flat lignin derivative thermogravimetry (DTG)-peak is superposed by the more prominent cellulose peak. A study from 1985 by Nunn et al. [Nun+85] reports activation energies very similar to those found by Cho et al. Jiang, Nowakowski, and Bridgwater [JNB10] analysed different types of lignin and found that the activation energy depends on both, the plant species from which the lignin is separated and the separation method. The apparent Arrhenius factor, on the contrary, is less dependent on these two parameters. Jiang, Nowakowski, and Bridgwater additionally considered the reaction order. All other authors considered pseudo-first-order reactions. Studies of the hydrothermal degradation of lignin are mostly based on experiments conducted in batch reactors. Takami et al. [Tak+12] applied a Monte Carlo simulation on the results from gel permeation chromatography (GPC) for the kinetic studies. They found formal kinetic coefficients similar to those

obtained in the water model and the ethanol model [Gas+2]. However, all three studies used different types of lignin. The formal kinetic rate coefficients k(633 K) obtained from the works of Zhang, Huang, and Ramaswamy [ZHR11] and Yong and Matsumura [YM12] are significantly higher than those obtained from other studies of lignin depolymerisation. It is worth to mention that the latter study was carried out in a continuous reactor which might have an influence on the heating rate. However, the apparent activation energy documented by Yong and Matsumura is very similar to the apparent activation energy obtained in this work [YM12].

In general the apparent activation energy obtained for pyrolytic lignin degradation tends to be higher than for depolymerisation in water. The resulting formal kinetic rate coefficients obtained for hydrothermal and solvolytic study of lignin degradation spread over a wide range of values. Hence, the reaction rate of primary lignin degradation potentially depends, apart from the thermal degradation method, on the type of lignin and the separation method, on the type of the solvent and the heating rate. Comparing different kinetic studies of lignin degradation based on lump models, it was found that all discussed parameters showed a relevant impact and cannot be discarded. The formal kinetic rate coefficients calculated in this work are in good agreement with the results from other kinetic studies. The thermal degradation of lignin comprises many reactions and complex mechanisms. Efforts concerning the study of detailed kinetics and mechanisms focus on the characterisation of the most abundant chemical structures in the heterogeneous polymer and the linkages between them [Far+10; WR12]. If differences between pyrolysis, solvolysis and hydrothermal processes need to be considered, phase exchange mechanisms, solubility and evaporation conditions of lignin and its degradation products might also have an influence. Reaction mechanisms which are important for the cleavage of C-O bonds or repolymerisation of lignin fragments, especially the differences of pyrolysis and hydrolysis in respect to these mechanisms, are discussed in the following subsections by means of phenolic model substances.

Table 6.8: Comparison of different kinetic studies of thermal lignin degradation, all based on lump-models; values obtained from this work refer to a lump of the reactions represented by k_1+k_7 in the water model (Figure 6.17) and by k_1+k_6+k_{10} in the ethanol model (Figure 6.7).

Source	Thermal treatment	Lignin, Concentration	T-range K	k(633 K) min^{-1}	E_A kJ/mol	log(A/A')[a]
Water-model (k_1+k_7)	Depolymerisation in NCW, batch	Lignin from spruce by enzymatic hydrolysis, 11.5 wt%	593-653	$3.6 \cdot 10^{-2}$	32	1.2
[ZHR11]	Depolymerisation in NCW, batch	Alkali-lignin from Pine, 10 wt%	573-683	$2.0 \cdot 10^{0}$	n.a.	n.a.
[YM12]	Depolymerisation in SCW, continuous	Alkali-lignin from spruce, 0.1 wt%	663-733	$2.0 \cdot 10^{2}$[b]	34	3.4
[Tak+12]	Depolymerisation in water and *p*-Cresol, batch	Organosolv-lignin, 2.3 wt%	623-693	$3.0 \cdot 10^{-2}$	79	2.9
Ethanol-model (k_1+k_6+k_{10})	Solvolysis in EtOH/FA, batch	Lignin from wheat straw by weak hydrolysis, 9 wt%	633	$4.8 \cdot 10^{-2}$	n.a.	n.a.
[JNB10]	Pyrolysis, TGA	Several types of lignin obtained by different separation methods	773-1073	$6.8 \cdot 10^{-2}$-$2.3 \cdot 10^{-1}$[b]	134-172	10-13
[Cho+12]	Pyrolysis, TGA-MS and pyroprobe (batch)	Organosolv- and enzymatic hydrolysis-lignin from maple	523-673	$6.1 \cdot 10^{-1}$	74	5.9

[a] $A' = 1 min^{-1}$

[b] extrapolated rate coefficient

Decomposition of methoxyphenols

The validation of the present model was thus additionally supported by the comparison of formal kinetic parameters of the decomposition of homogeneous reactions of less complex components occurring within the thermal degradation of lignin. Table 6.9 shows the results of different kinetic studies of the thermal decomposition of methoxyphenols and catechols. Methoxyphenols tend to decompose by the cleavage of the methyl C-O bond. The aromatic ring and the hydroxyl group are more stable [Vuo86]. The formal kinetic rate coefficients at 633 K k(633 K) obtained in the water model is $1.1{\cdot}10^{-2}$ min^{-1} which is in good agreement to other kinetic studies of hydrothermal and solvothermal decomposition of methoxyphenols [For+12; Gas+2; WSG11]. Values of k(633 K) obtained by studies of pyrolytic decomposition of methoxyphenols are lower and range from $2.8{\cdot}10^{-5}$ min^{-1} to $2.1{\cdot}10^{-3}$ min^{-1} [DM99; KV08; Vuo86]. However, the activation energy obtained from pyrolysis is significantly higher than that obtained from hydrothermal lignin degradation in NCW and SCW. Dorrestijn and Mulder [DM99] claimed that guaiacol decomposes via a radical-induced mechanism. They studied the kinetics of guaiacol decomposition at elevated temperatures. The obtained kinetic parameters are in good agreement of those obtained by Vuori [Vuo86] who also studied pyrolytic decomposition of guaiacols at lower temperatures. The latter author reported, that in addition to free radical chain reactions hydrolytic decomposition of guaiacols occurs. He claims that this is due to the presence of water which is formed during the pyrolytic decomposition of guaiacol. Furthermore, Lawson and Klein found that the formal kinetic rate coefficient at 656 K slightly increased if water was present [LK85] which indicates a shift of the dominant reaction mechanism from radical-induced to hydrolytic cleavage. Since water is abundantly present, hydrolysis is assumed to be the dominant mechanism for the hydrothermal decomposition of methoxyphenols [TRR11]. In a previous work was discovered that around the critical point of water a shift of the apparent activation energy of guaiacol decomposition occurs due to a change of the dominant reaction mechanism from hydrolytic to radical-induced decomposition [For+12]. This explains that the apparent activation energy obtained from different studies conducted in NCW or SCW vary in a relatively wide range from 39 to 85 kJ/mol [For+12; WSG11]. The apparent activation energy obtained from studies of thermal decomposition of methoxyphenols in organic solvents or without solvent are significantly higher (> 170 kJ/mol). Due to the lower activation energy hydrolytic cleavage of the C-O bond of methoxyphenols is faster at moderate temperatures (< 673 K).

Decomposition of catechols

Furthermore, kinetic studies carried out in order to determine the formal kinetic rate coefficients of the thermal decomposition of catechol shall be discussed. Catechol decomposes into other phenolic substances, *e.g.* phenol [Nim+11a]. In addition it is potentially responsible for the formation of char by repolymerisation [McM+04]. Wahyudiono, Sasaki, and Goto studied the hydrothermal decomposition of catechol and found higher molecular structures. Their amount increases with residence time and temperature. However, the formation of phenol and other monoaromatic components was dominant [WSG09]. Analogously modelling of the hydrothermal lignin degradation shows, that the polymerisation of catechol is of minor importance since the competing reaction, which is the conversion of catechols into phenols (r_4), is faster (see Table 6.7). The study of lignin degradation kinetics by Yong and Matsumura [YM12] reports a higher formal kinetic rate coefficient for polymerisation than for the conversion into phenol. However, the lumped formal kinetic coefficient comprising conversion into phenols and polymerisation obtained by Yong and Matsumura (3.9 min^{-1}) differs significantly from the values obtained in the water model ($2.9 \cdot 10^{-4}$ min^{-1}) and by Wahyudiono, Sasaki, and Goto $2.4 \cdot 10^{-4}$ min^{-1}.

Table 6.9: Comparison of different kinetic studies of thermal decomposition of methoxyphenols, lump of the reactions represented by k_2+k_3 in the water-model (Figure 6.17) and by k_2 in the ethanol-model (Figure 6.7), and catechols, lump of the reactions represented by k_4+k_5+k_{12} in the water model.

Source	Thermal treatment	Reactant, Concentration	T-range K	k(633 K) min^{-1}	E_A kJ/mol	log(A/A')[a]
Water-model (k_2+k_3)	Solvolysis in NCW, batch	Lignin from spruce by enzymatic hydrolysis, 11.5 wt%	593-653	$1.1 \cdot 10^{-2}$	85	5.0
[WSG11]	Solvolysis in NCW and SCW, batch	Guaiacol, 1.24 wt%	653-673	$1.8 \cdot 10^{-2}$[b]	39	1.5
[For+12]	Catalysed solvolysis in NCW, batch	Lignin from spruce by enzymatic hydrolysis, 9 wt%,	603-633	$1.5 \cdot 10^{-2}$	170	12
Ethanol model (k_2)	Solvolysis in ethanol/formic acid, batch	Lignin from wheat straw by weak hydrolysis, 9 wt%	633	$8.7 \cdot 10^{-3}$	n.a.	n.a.
[Dor+99]	Pyrolysis in N_2 and cumene, continuous	Guaiacol, 6 mol%	688-784	$3.0 \cdot 10^{-5}$[b]	239	15
[Vuo86]	Pyrolysis in tetralin, batch	Guaiacol, 50 mol%	598-648	$2.8 \cdot 10^{-5}$	237	15
[KV08]	Pyrolysis, batch	Guaiacol	523-800	$2.1 \cdot 10^{-3}$	190	13
Water-model (k_4+k_5+k_{12})	Solvolysis in NCW, batch	Lignin from spruce by enzymatic hydrolysis, 11.5 wt%	593-653	$2.9 \cdot 10^{-4}$	55	1
[YM12]	Solvolysis in SCW, continuous	Alkali-lignin from spruce, 0.1 wt%	663-733	$3.9 \cdot 10^{0}$[b]	151	12
[WSG09]	Solvolysis in NCW, batch	Catechol, 1.1 wt%	643-663	$2.4 \cdot 10^{-4}$[b]	51	0.6

[a] $A' = 1 min^{-1}$
[b] extrapolated rate coefficient

Chapter 7

Feasibility study of lignin liquefaction

A preliminary feasibility study is essential for the evaluation of a technical process. Further research should follow a pathway which is economically promising. The intention in this chapter is to compare two approaches of lignin liquefaction, solvolysis in ethanol and hydrothermal degradation, in order to discover which one provides a higher economic potential. The assumption of the parameters essential for a technical realisation of the production of phenolics from lignin leads to a rough estimation of the total manufacturing costs (COM) of phenol. A preliminary design of the technical process including the main apparatus and equipment was carried out in order to estimate the module costs and the total capital investment (TCI) of the plant. For this utility and labor costs had to be estimated. Experimental results from Exp. 66 and 98 were employed to estimate the input amount of lignin and solvent as well as the yields of phenolic, gaseous and solid products.

7.1 Background Scenario

A technical process consists of the following units: pre-treatment, reactor, separation and purification. For this study was assumed that the lignin conversion unit is a part of a larger facility, treating the lignocellulosic biomass as a whole. Hence, the pre-treatment is part of the existing global infrastructure. In the case of solvolysis in ethanol it can be assumed that the plant is integrated in an ethanol-production plant comprising the fermentation of

cellulose for ethanol production and the liquefaction of lignin in ethanol. In order to calculate the streams and fluxes within the process the capacity of the plant has to be defined considering a global biomass treatment plant including both the fermentation of the lignocellulosic raw material and the liquefaction of lignin in ethanol. Humbird et al. [Hum+1] carried out a process design of a fermentation plant with a capacity of 730 kt of corn stover per year. The design of a plant converting softwood into ethanol by Wingren et al. [WGZ03] deals with a capacity of 200 kt of dry input material per year and about 60000 m^3 ethanol per year. Haase [Haa2] carried out a cost estimation for a plant with a capacity of 450 kt of dry wood per year.

The hydrothermal lignin degradation might be integrated into a pulp mill. The dry matter of the residue from the pulp production, so called black liquor, contains up to 50 % lignin. Black liquor is the main waste stream emerging from the pulp process. It is dried and burned in order to recover the energy from the organic material and to recycle the chemicals for the pulp process. The integration of the lignin liquefaction into a pulp process would provide the most convenient feedstock situation since phenolics would be produced from grave to cradle by using an internal waste stream as feedstock [Tow+07]. The energy and cost intensive drying of the black liquor would be eliminated. Furthermore, the char which is produced within the hydrothermal treatment of the lignin could still be used for the generation of heat or electric power. However, the behaviour of the chemicals in a hydrothermal process and their recovery for further usage in the pulp mill has not been studied so far. Thus, and for a better comparison of the hydrothermal process with the ethanol approach, the conditions of the hydrothermal process were chosen to be equal to those of the ethanol process.

For this study, the size of the plant was chosen to be rather small compared to other scenarios mentioned above due to the great amount of solvent in the feed and the relatively long residence time (up to 90 min) in the reactor. For the following calculations the capacity of the plant was assumed to be 8000 t/a of dried biomass. The plant was assumed to run 8000 h/a.

7.2 Process design

For the solvolytic lignin degradation a CSTR was assumed to be the most effective reactor based on the results documented in Chapter 6.2. The input stream consisting of lignin and fresh solvent is first mixed with the recycled solvent and thereafter pressurised by a pump (A). Before entering the reactor (C) it is preheated by the output stream from the reactor in a heat exchanger

(B). The reactor is heated by a thermal oil heater (D). The thermal oil is heated up in a gas-combustion chamber. The advantage of this indirect heating system is that all tubes in the heating-circle are low-pressure tubes. In addition, it ensures the prevention of explosion or ignition in case of a leak in the feeding tube. A direct heating of the feed in a combustion chamber would be too dangerous, especially if it contains ethanol and formic acid. If water is used as solvent, a direct heating of the input stream might be an economically more interesting solution. However, in the case of direct heating the tubes which conduct the input stream through the combustion chamber have to be designed to withstand the high pressures of the fluid.

The output stream is cooled in the first heat exchanger (B) by the input stream. The solid particles, that are char or not reacted lignin, can be separated by *e.g.* a cyclone (E) before the output stream is further cooled in a second heat exchanger (F) by fresh water. After separating the gases in *e.g.* a flash separator (G), the solvent is separated from the product and recycled. The product is further separated into phenol, other phenolics and a fraction consisting of all other organic substances which usually have a tarry or oily texture (H). A detailed design of the separation process was not carried out.

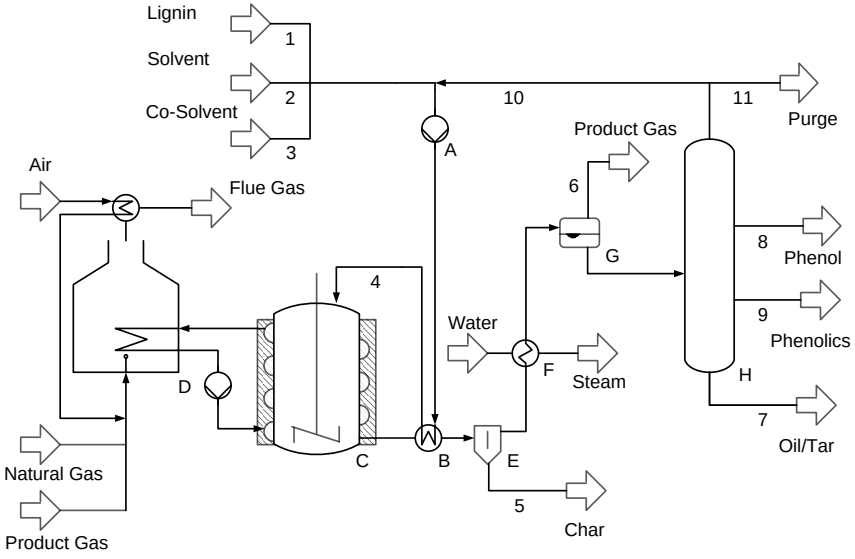

Figure 7.1: Process scheme with main components (labelled with letters) an streams (labelled with numbers).

Table 7.1: Streams defined for the lignin liquefaction process (see Figure 7.1) for both, ethanol and water approach.

Stream	1	2	3	4	5	6
Unit	t/h	t/h	t/h	t/h	t/h	t/h
EtOH	1.00	1.34	1.22	11.70	0.05	1.11
H_2O	1.00	0.50	0.00	8.58	0.34	0.18

Stream	7	8	9	10	11
Unit	t/h	kg/h	kg/h	t/h	t/h
EtOH	2.35	3.00	63.00	8.14	0.04
H_2O	0.44	1.40	31.20	7.08	0.50

7.3 Main equipment

For a preliminary cost estimation the necessary equipment items have to be identified and their costs have to be estimated. Based on the process displayed in Fig. 7.1 the main equipment items are the pump, the heat exchangers, the jacketed stirred reactor, the heater including combustion chamber, chimney, thermal oil and circulation pump. The costs of the equipment necessary for the separation of the products is estimated by a factor. The dimensions of the different apparatus are estimated using the results from the experiments Exp. 66 and 98 for the ethanol and water approach respectively. The price increase for offers collected earlier than 2012 was estimated by the price-index by Kölbel/Schulze [VCI12]. The conversion of the currency was estimated by the Euro-course from September 2012 (1.29 \$/€).

Pump

The selection of the pump for the transfer of the feed suspension is essential for the estimation of its costs. The pumped fluid consists of the liquid solvent and solid lignin particles. The target pressure was 25 MPa and the temperature of the fluid was assumed to be 343 K. For the selection of the pump the volumetric flow rate of the fluid, that is the capacity $\dot{V}$, had to be calculated (see Equation 7.1). Hence, the mean density of the pumped fluid $\overline{\rho}$ was estimated by considering the density of all constituents i of the fluid at 343 K. The density of ethanol, formic acid and water at 343 K are 0.74, 1.16 and 0.98 t/m^3 respectively [VDI06]. The density of lignin was estimated to be 1.4 t/m^3 [Haa2]. The most convenient pump for the given transfer challenge is a plunger pump (displacement pump). The total dynamic head H was calculated employing Equation 7.2 considering the gravitational acceleration

g. The useful work W_o was calculated employing Equation 7.3 considering the pressure difference between the initial pressure p_{in} and the setup pressure in the reactor p_{out}. The influence of valves and accessories or tubes on the pressure causing a loss of head was neglected. The efficiency of the pump was assumed to be 85 %.

$$\dot{V} = \frac{\dot{m}}{\overline{\rho}} = \dot{m} \left(\sum_i \frac{\dot{m}_i \cdot \rho_i}{\dot{m}} \right)^{-1} \tag{7.1}$$

$$H = \frac{p_{in} - p_{out}}{\bar{\rho} \cdot g}, \quad g = 9.81\ m/s^2 \tag{7.2}$$

$$W_o = \dot{V} \cdot (p_{in} - p_{out}) \tag{7.3}$$

All parameters necessary for the estimation of the purchased costs of the plunger pump are listed in Table 7.2. The purchased costs for the pump can be estimated using the data from Peters [PT04, p.518]. According to Peters the purchased costs for the pump range from 6660 € for the water approach to 9030 € for the ethanol approach. However, according to the offer from Schäfer & Urbach for a plunger pump with a capacity of 16.8 m^3/h and 4100 m total dynamic head in 2010 the purchased costs are 108 k€ (see Appendix F), 120 k€ considering the price-index for 2012. For this study the costs were estimated based on the offer from Schäfer & Urbach for both the ethanol and the water approach, which is the more conservative estimation.

Table 7.2: Parameters used for the estimation of the purchased costs of the pump.

Pump (A)	$\overline{\rho}$	$\dot{m}$	$\dot{V}$	H	W_o	W
	kg/m^3	t/h	m^3/h	m	kW	kW
EtOH	844	11.7	13.9	3020	113	133
Water	1027	8.6	8.4	2482	58	68

Reactor

In respect to the investment costs the reactor is commonly the less expensive part of a chemical plant. Separation and purification units form the major part of these costs. The costs of the reactor were estimated by its size. Assuming a capacity 1 t/h dry lignin, the total throughput passing the reactor is 11.7 t/h for solvolysis in ethanol and formic acid and 9.58 t/h for the hydrothermal approach. The density in the reactor was estimated

by the density of the solvent at the determined conditions (T and p) in the reactor. In Table 7.3 the reaction conditions are listed for both ethanol and water approach. The mean residence time τ' was estimated according to the experimental results. The resulting reactor volume V_R was calculated by the mass flow $\dot{m}$ (see Section 7.1), the density according to Bazaev et al. [Baz+07] and the mean residence time. The purchased costs of the jacketed stirred reactor in dependence of the reactor volume were estimated according to Peters [PT04, p.628]. The increased costs for a high-pressure reactor are considered by multiplication of the purchased costs of a none pressurised reactor with the factor 10.6 [PT04, p.556]. The data collected from Peters are dated for the year 2002. The resulting factor for the price increase is 1.28 [VCI12]. The purchased costs of the reactor for the ethanol and the water approach were 1.482 M€ and 1.270 M€ respectively.

Table 7.3: Reaction conditions and resulting reactor volume V_R for both ethanol and water approach.

Approach	T	p	τ'	ρ	$\dot{m}$	V_R
	K	MPa	min	kg/m^3	t/h	m^3
EtOH	673	25	44	280	11.7	30.5
Water	653	25	90	446	8.6	28.8

Heat exchanger

In order to calculate the purchased costs of the two heat exchangers (B and F), the heat transfer area A_{Ex} had to be determined (see Equation 7.4). Both heat exchangers were assumed to be counter current flow heat exchanger with a transfer coefficient k_{sum} of 600 W/(m^2·K) [Wag09]. Heat exchanger (B) was employed to pre-heat the input stream from a temperature below the evaporation temperature of the solvent (T_{in} = 343 K) to a temperature of T_{out} = 453 K and to cool the product stream entering the heat exchanger with a temperature of 673 and 653 K in the ethanol and the water approach, respectively. In the heat exchanger (F) the product stream requires further cooling to a temperature of T_{out} = 343 K by an independent water stream (see Fig. 7.1) which was suggested to be evaporated at atmospheric pressure (0.1 MPa). The steam leaving the heat exchanger (F) should have a temperature of around T_{out} = 453 K in order to be used elsewhere in the plant as a source of thermal energy.

$$A_{Ex} = \frac{\dot{q}}{k_{sum} \cdot \overline{\Delta T}} \tag{7.4}$$

Table 7.4: Data concerning heat exchanger (B and F) for both ethanol and water approach.

Heat-	Cold Stream			Hot Stream					
Exchanger	T_{in}	T_{out}	$\overline{c}_p$	T_{in}	T_{out}	$\overline{c}_p$	$\overline{\Delta T}$	$\dot{q}$	A_{Ex}
	K	K	$\frac{kJ}{kg \cdot K}$	K	K	$\frac{kJ}{kg \cdot K}$	K	MW	m^2
EtOH B	343	453	3.40	673	575	3.80	226	1.22	9.0
EtOH F	298	453	4.18	583	343	3.65	80	2.84	68.1
Water B	343	453	4.19	653	584	6.71	220	1.50	11.4
Water F	298	453	4.18	584	343	4.47	81	3.51	72.5

For the determination of A_{Ex} the rate of heat transfer $\dot{q}$ was calculated by Equation 7.5.

$$\dot{q} = \overline{c}_p \cdot \Delta T \cdot \dot{m} \tag{7.5}$$

The specific heat capacity was estimated by the average heat capacity $\overline{c}_p$ of the solvent for the corresponding temperature difference ΔT. In order to determine ΔT the entering and emerging temperature of one stream, that is either hot or cold stream, had to be defined. These temperatures were partially determined through the reaction parameters of the model experiments and partially through reasonable assumptions (see explanation above and Table 7.4). Furthermore, for the calculation of A_{Ex} the mean overall temperature difference between the two fluids $\overline{\Delta T}$ has to be determined according to Equation 7.6

$$\overline{\Delta T} = \frac{\Delta T_{in} - \Delta T_{out}}{ln\left(\frac{\Delta T_{in}}{\Delta T_{out}}\right)}, \tag{7.6}$$

where the difference between the temperature of the hot fluid emerging the heat exchanger and the cold fluid entering the heat exchanger is ΔT_{in} and the difference between the temperature of the hot fluid entering the heat exchanger and the cold fluid emerging the heat exchanger is ΔT_{out}.

The rate of heat transfer in both heat exchangers (B and F), the input temperatures of cold and hot stream, the mean overall temperature difference as well as the heat transfer area are listed in Table 7.4. After calculation of the heat transfer area A_{Ex} the purchased costs for the heat exchangers could be estimated according to Peters [PT04, p.681]. Considering also the price-index and the dollar-course the purchased costs of the heat exchangers for the ethanol and the water approach are 25 k€ and 37 k€ respectively.

Thermal oil heater

For the estimation of the purchased costs of the thermal oil heater, the rate of heat transferred to the feed was calculated with Equation 7.5 analogously to the transferred heat in a heat exchanger. The initial lower temperature of 453 K is equal to the output temperature of the cold stream of heat exchanger (B). The target temperature is equal to the reaction temperature, which is 673 K and 653 K for the ethanol and water approach respectively. The mean specific heat capacity ($\overline{c}_p$) of the fluid of the feed was determined as shown in Equation 7.1 and resulted to be 3.8 and 5.4 kJ/(kg·K) for the ethanol and the water approach respectively. The resulting rate of heat transfer $\dot{q}$ was 2.72 and 2.57 MW for the ethanol and water approach, respectively. Assuming an efficiency factor of 0.85, the power capacity of the heater was calculated to be at least 3.2 MW and 3.1 MW for the ethanol and water approach, respectively. The basis for the cost estimation of the heater was an offer from HTT for a thermal oil heater from 2010 with a power capacity of 3.4 MW. The offer is supposed to be suitable for a conservative cost estimation. The price-index by Kölbel/Schulze indicated a price increase factor from 2010 to 2012 of 1.06. The resulting purchased costs for both ethanol and water approach is 617 k€.

7.4 Cost estimation

7.4.1 Market prices

For the following calculations data about material and utility prices, prices for labor, etc. have to be provided. The required data is collected from different sources in order to estimate the costs for both the ethanol and the water approach, and is presented in Table 7.5.

The price of lignin was estimated considering the prices of alkali-lignin which is a waste material and thus fits best into the background scenario. The prices for alkali-lignin vary in dependence of the degree of drying [Pul09]. For the ethanol approach dried lignin should be used, for the water approach a lignin containing 50 % moisture or more is also a possible feedstock. Market prices for technical formic acid with 85 % purity were considered for this study although for the experiments formic acid with a higher purity was used. However, prices for bulk amounts of formic acid with a higher purity were not available. The price of 390 €/t for ethanol can be achieved in Brazil, in Europe the price is up to 500 €/t [Haa2]. The price of waste water (purge stream 11) which is produced in large quantities in the water approach was estimated according to Peters who reports prices of process

Table 7.5: Estimated prices for reactants, products and utilities.

Input/Output material	Quality	Bulk Prices	Unit	Source
Alkali-lignin	dried	480	€/t	[EIA11]
Alkali-lignin[a]	50 %	160	€/t	[Pul09]
Formic acid	85 %	800	€/t	[Imh12]
Ethanol	96 %	390	€/t	[Haa2]
Water		1	€/t	[PT04]
Phenol		1600	€/t	Appendix F
Other phenolics		953	€/t	Appendix F
Natural Gas		0.048	€/kWh	[VCI11]
Product-gas EtOH		136	€/t	[VCI11]
Product-gas Water		21	€/t	[VCI11]
Char		107	€/t	[VCI11]
Tar/Oil	12.5 %	49	€/t	[VCI11]
Electricity		0.13	€/kWh	[VCI11]
Steam		0.03	€/kWh	[VCI11]

[a] Lignin contains 50 % water, price refers to dry lignin.

water of maximum 0.46 $/t [PT04, p.898]. Considering a price increase from 2002 to 2012, the price was assumed to be significantly higher (see Table 7.5). The price of phenol was estimated using the price report by ICIS in July 2012. The prices of other phenolics, that are catechols and methoxyphenols, were estimated with the benzene-price which is usually the raw material for the production of these substances.

Both the ethanol and the water approach yield considerable amounts of gas, char and oil. These products can be used for the generation of heat which causes a reduction of the material or the utility costs. The benefit or credit however depends on the heating value of the products. The lower heating value (LHV) of the gaseous products can be determined by calculating the LHV of its constituents. The gaseous products from the ethanol experiment have a LHV of 4.2 kWh/kg, those from the water experiment 0.65 kWh/kg (see Appendix E.2). Assuming a price for natural gas of 0.327 €/kWh [VCI11] the credit which can be achieved for the gaseous products of the ethanol and the water approach were estimated to 136 and 21 €/t respectively. The higher heating value (HHV) of the char was estimated by the results from the elemental analysis and employing the calculation method developed by IGT [Tal81]. The HHV of the solid residue from both the ethanol experiment Exp. 66 and water experiment Exp. 98 are 31 MJ/kg (see Appendix E.2). This value is in the range of the HHV of high bituminous coal which has a HHV above 30 MJ/kg [DIN84]. Thus the price

for char was estimated by the price for coal which is 107 €/t in 2011 [VCI11]. The oil-fraction is comprised of all liquid products excluding the solvent and the phenolic products. The LHV of the oil-fraction can be estimated only for the ethanol experiment since the obtained results for this case allowed to carry out an energy balance (see Appendix E.2). The resulting LHV was 5.3 MJ/kg which is about 12.5 % of the minimum LHV of fuel oil (42 MJ/kg [DIN84]). Thus the credit for the oil-fraction was estimated to be 12.5 % of the fuel oil price in 2011 (see Table 7.5). Although the LHV of the oil fraction obtained from the water experiment could not be determined, the estimation of the credit was assumed to be valid for both the ethanol and the water approach.

7.4.2 Manufacturing costs

For the preliminary cost estimation different cost items were considered, that are the TCI, the total material costs (TMC), total utility costs (TUC) and the operating labor costs (OLC). Based on these cost items the COM of the product (phenol) were estimated. This value serves best to carry out an economic evaluation of the process.

Investment costs (TCI)

The TCI are based on the costs of the main equipment, which were determined in the preceding section. In addition, costs for the separation equipment were estimated in order to determine the total bare module costs (TBM). Costs for additional equipment like tubes, valves, control units, buildings, engineering and construction were estimated by applying empiric factors (see Table 7.6). These factors were taken from Baerns [Bae+06, pp 463-477].

Utility costs (TUC)

Utility costs were calculated on the basis of experimental results. Among all input and output streams (see Table 7.1) the following streams were suggested to be essential for the calculation of the TUC since their utilisation was foreseen for the purpose of energy generation: The output of gaseous (6) and solid (5) products and the output of liquid (7) products (oil/tar) excluding phenol (8) and phenolics (9). The necessary electric and thermal energy is estimated from the energy balance for experiment Exp. 66 (see Appendix E.2) and the required energies for the heater and the pump calculated in Section 7.3. The steam recovered from heat exchanger (F) was

Table 7.6: Total Capital Investment TCI calculated by various factors based on TBM.

Item	Factor	Costs	
		EtOH-approach M€	H_2O-approach M€
Heater		0.617	0.617
Reactor		1.482	1.270
Pump		0.120	0.120
Heat exchanger		0.027	0.040
Separation equipment	0.70	5.241	4.776
TBM	1.00	**7.487**	**6.823**
On-Site Costs			
Equipment installation	0.15	1.123	1.024
Tubes & Valves	0.80	5.989	5.459
Measuring and control engineering	0.35	2.620	2.388
Electrical equipment	0.20	1.497	1.365
Buildings & site preparation	0.65	4.866	4.435
Insulations & fire protection	0.15	1.123	1.024
Off-Site Costs			
Engineering	0.40	2.995	2.729
Unexpected costs	0.20	1.497	1.365
Capital Costs (TCI)	3.90	**29.198**	**26.611**

assumed to be used as energy source elsewhere in the process. A surplus of 50 % of the required energy was considered for the separation equipment. The total utility costs are displayed in Table 7.7.

Operating labor (OLC)

The operating labor costs for a common bio refinery which runs 8000 h/a were analysed by Baerns [Bae+06, pp 463-477]. The operation of the plant requires 2 skilled workers and one supervisor for each of the five shifts. In addition, one technician and one head of unit are required. The total operating labor costs for the entire plant including ethanol production and lignin liquefaction are thus 1.172 M€/a. The lignin production is estimated to require 1/3 of the operating labor of the entire plant which is calculated to 0.391 M€/a (see Tab. 7.8) for both ethanol and water approach.

Table 7.7: Energy demands and utility costs (TUC).

Utilities	EtOH-approach		H_2O-approach	
	Demand MWh/a	Costs M€/a	Demand MWh/a	Costs M€/a
Electricity	912	0.114	912	0.114
Natural gas	27200	1.295	25600	1.219
Separation (overall 50%)		0.726		0.617
Steam	-22745	-0.682	-23840	-0.715
TMC		**1.453**		**1.235**

Table 7.8: Operating Labor Costs (OLC).

	Wages	Annual Costs	Rel. Costs	
			EtOH-approach	H_2O-approach
	k€/a	M€/a	€/kg$_{Phe}$)	€/kg$_{Phe}$)
Skilled workers	64	0.640	26.67	57.14
Supervisor	70	0.350	14.58	31.25
Technician	72	0.072	3.00	6.43
Unit head	110	0.110	4.58	9.82
OLC bio refinery		1.172	48.83	104.64
OLC phenol-production		**0.391**	16.28	34.88

Total manufacturing costs COM

For the determination of the COM the annual capital related costs which comprise depreciation, maintenance, working capital, contingency and fees were assumed to make up 23 % of the TCI. The maintenance and working capital were estimated similar to a fossil fuel refinery and lower than a chemical plant. The depreciation was assumed to be linear and distributed over ten years. The residual value after ten years of the plant was assumed to be equal to the disassembly costs [Bae+06, pp 463-477]. Furthermore, costs for transport, laboratory charges, packaging and distribution as well as waste treatment were considered. The sum of these costs was estimated to be around 2.9 % of the overall manufacturing costs and is listed in Table 7.9 under miscellaneous. The relatively low value is a consequence of the assumption that the plant is part of a larger facility. The resulting manufacturing costs are 909 € and 749 € per kilogram of produced phenol for the ethanol and water approach, respectively. This is several hundred times higher than the actual market price of phenol (1.6 €/kg).

7.5 Discussion

The preliminary cost estimation shows that the COM (see Table 7.9) for phenol from lignin are much higher than the market price of phenol (1.6 €/kg). Both the ethanol and the water approach are thus currently economically not feasible, although the water approach shows lower manufacturing costs at still very low yields of phenol (0.14 wt%). An increase of the yield can reduce the manufacturing costs dramatically. In order to find the bottleneck-parameters which mainly influence the COM, different scenarios were observed. The parameters which were contemplated within this work were:

- the **phenol yield**; depending on the type of the lignin used and the separation method applied on the lignin, the yield of phenolics and especially phenol can be increased to maximum about 30 wt% [APR01]. However, the maximum yield of phenol from waste lignin containing 50 to 70 % of cellulose and impurities will be significantly smaller. 10 to 20 % seem realistic. Thus the influence of the variation of the phenol yield on the COM should be investigated.

- The **lignin/solvent ratio** in the feed. This parameter might be increased to 30 wt%. Black liquor containing 30 wt% dry material is still pumpable since most of the biomass is diluted. The transfer of an ethanol/lignin suspension is assumed to be more challenging if the

Table 7.9: Total Manufacturing Costs COM.

Costs	EtOH-approach		H_2O-approach	
	Annual Costs M€/a	Rel. Costs €/kg$_{Phe}$)	Annual Costs M€/a	Rel. Costs €/kg$_{Phe}$)
Raw Material				
Lignin	3.84	160.00	1.28	114.29
Solvent	4.19	174.59	0.00	0.36
Formic Acid	7.81	325.33	0.00	0.00
Credits				
Phenolics	-0.48	-20.01	-0.24	-21.24
Product Gas	-1.78	-74.24	-0.05	-4.04
Char	-0.03	-1.39	-0.30	-27.03
Oil	-0.92	-38.31	-0.17	-15.52
Sum material	12.62	525.98	0.52	46.82
Utilities	1.45	60.53	1.23	110.24
Operating Labor	0.39	16.28	0.39	34.88
Capital related costs	6.72	279.81	6.12	546.48
Miscellaneous	0.64	26.48	0.25	22.15
COM	21.82	**909.08**	8.52	**748.76**

percentage of solid lignin is increased since the solubility of lignin in ethanol is lower than in basic aqueous media.

- Decreasing the **mean residence times** will reduce the TCI due to a smaller reactor at a constant capacity of the plant. The values employed to calculate the basic case for the water approach were taken from a batch experiment. However, the results presented in Chapter 6.2 showed that in a CSTR the residence time can be reduced significantly due to *e.g.* the elevated heating rate.

- The reduction of the utility costs due to optimisation of the energy fluxes can be achieved by a reduction of the **consumption of natural gas**. A reduction of 25 % (800 kW) seems reasonable, if *e.g.* the reaction enthalpy (9600 kW, see Table E.5) calculated for the ethanol approach can be partially recovered.

- The reduction of the module **costs of the heater** by 30 % if direct heating of the feed is applied. This option is only possible for the water approach due to safety aspects.
- The reduction of the costs of the **separation equipment** from 70 % to 60% of the TBM. Since no detailed estimation of the module costs for separation equipment was carried out, this factor can vary between 40 and 70 % [Bae+06, pp 463-477]. Obviously these costs depend also on the phenol yield and the selectivity for special phenolic products. It was already shown in Chapter 4 that the water approach shows a narrower product spectrum and a high selectivity for catechols. This is supposed to facilitate the separation of the products and thus decrease the module costs.
- The **lignin price** assumed for the basic case is above the costs for the recovery of lignocellulosic biomass [Haa2]. If the lignin is recovered from a waste stream, the prices for lignin can be reduced.

Considering the mentioned parameters three scenarios different to the basic case were suggested (see Table 7.10). The composition of the COM for the basic case of the ethanol approach shows that the material costs are the main contributor to the COM. The reasons thereof are the consumption of formic acid and the gasification of ethanol. On the contrary for the water approach the capital related costs make up the greatest part of the COM (see Figure 7.2). For the design of a plant which deals with high pressures, the TCI are high since reactor, pipes, heater, etc. have to withstand these high pressures. In addition the amount of solvent which circulates in the plant is much higher than the throughput of lignin. This results in big vessels and pipes that are accordingly more expensive. Hence, the COM would shrink significantly if the lignin/solvent ratio was increased to 30 % (Scenario 1). The application of Scenario 1 on the water approach has no influence on the material costs since the yields of phenol, char, gas, etc. were assumed to be constant. However, also the overall capacity of the plant, and the percentage of ethanol which is gasified were assumed to be the same as in the basic case. Thus, in absolute numbers, less formic acid was assumed to be used and less ethanol gasified. This leads to a dramatic decrease of the material costs for the ethanol approach. In Scenario 1 the COM were determined to be lower for the ethanol than for the water approach.

If the mean residence time could be reduced, exclusively the capital related costs would shrink (Scenario 2, Figure 7.2). A mean residence time of 10 min reduces the capital related costs to 59 % and the COM to 71 % of the original costs in the basic case for the water approach. For the ethanol

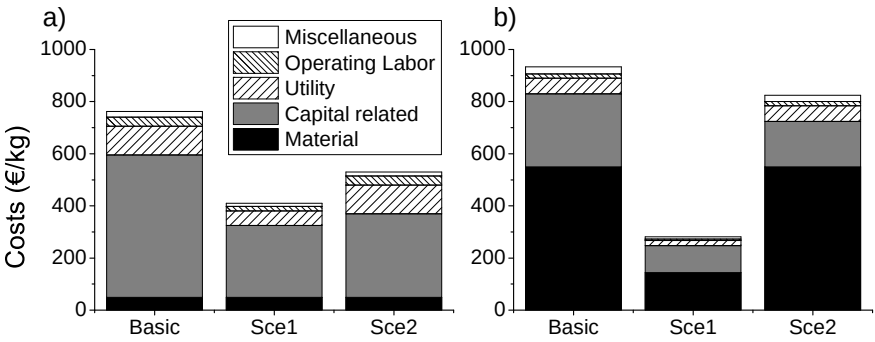

Figure 7.2: COM of phenol from lignin for the basic case and 2 different scenarios (see Table 7.10) for a) the water approach and b) the ethanol approach.

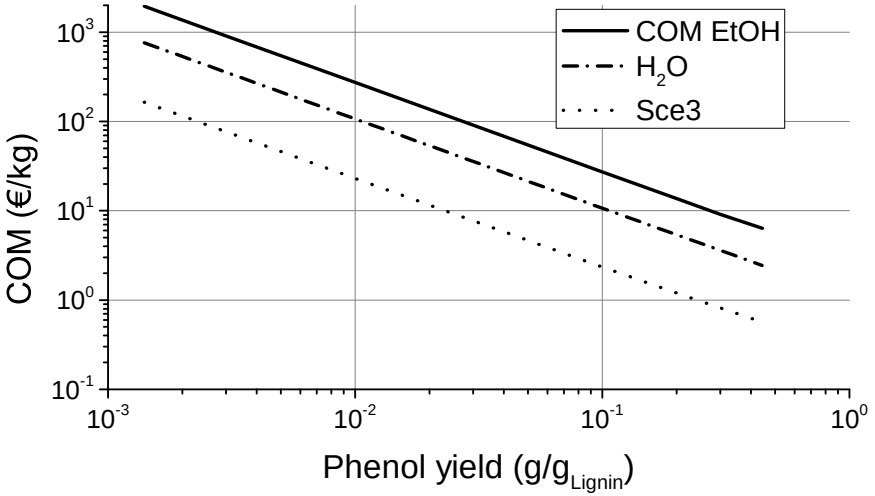

Figure 7.3: COM of phenol from lignin in dependence of the phenol yield for the basic case of both ethanol and water approach; scenario 3 (see Table 7.10) is displayed for the water approach.

Table 7.10: Scenarios of the plant design and cost estimation for solvolytic lignin liquefaction and phenol production

Scenario	Modified parameters		Approach	Affected parameters	
Sce1	Lignin/solvent	30 wt%	EtOH	Input lignin	2.7 t/h
			H_2O	Input lignin	2.0 t/h
Sce2	τ	10 min	EtOH	Reactor Vol.	7.0 m^3
			H_2O	Reactor Vol.	3.2 m^3
Sce3	Lignin/solvent	30 wt%	H_2O	Input lignin	2.0 t/h
	τ	10 min		Reactor Vol.	3.2 m^3
	Natural gas consumption	75 %			
	Heating equipment	70 %			
	Separation equipment	60 %			
	Lignin price	107 €/t			

approach the COM is reduced to 88 % of the original value in the basic case. The greater reduction for the water approach results from the longer mean residence in the basic case compared to the ethanol approach. Furthermore, since the module costs in the basic case of the water approach are lower than in the basic case of the ethanol approach, the reduction of the COM with decreasing residence times is more dramatic for the water approach.

An increased phenol yield reduces the COM most significantly. A yield of 10 % would reduce the COM to 10.70 € and 27.32 € per kilogram phenol for the water and the ethanol approach, respectively (see Figure 7.3). However, this is still too much to make the process economically attractive. And even if the phenol yield could be increased to 30 %, the COM were still above the market price of phenol. Scenario 3 assumes that several parameters can be improved (see Table 7.10). However, even though the residence time could be reduced to 10 min, the module costs for the heater and the separation equipment as well as the consumption of natural gas and the price of lignin would decrease, the phenol yield still has to be increased to 20 % in order to gain a profit from the production of phenol from lignin.

The production of phenol from lignin by solvolysis in water or ethanol is economically not feasible if the current yields and process parameters are considered. The most important parameter influencing the feasibility is the phenol yield. However, even if the phenol yield could be increased to 45 wt%

referring to the input amount of lignin, which seems not very realistic at the current state of research, a process would still not be economically attractive. A reduction of the mean residence time in the reactor, an increase of the lignin/solvent ratio are also key parameters which contribute to the necessary drastic reduction of the capital related costs. In fact this study provides a rough and conservative estimation of the capital related costs. A more detailed knowledge about the equipment costs, especially the separation equipment, might show that these costs can be reduced. The water approach shows better economic opportunities than the ethanol approach since the feedstock situation provides large quantities of cheap feedstock, the solvent is more stable and abundantly available at low prices. Future research should thus focus on black liquor. However, the yield of phenol and other phenolics has to be increased to at least 20 %, the lignin/solvent ratio should be increased significantly (20 to 30 %) and the mean residence time has to be reduced to maximum 10 to 30 min in order to make the process economically attractive.

Chapter 8

Conclusion

This work deals with the thermal depolymerisation of lignin, especially the solvolysis in ethanol and the hydrothermal degradation. The main reaction products were analytically discovered from experimentally obtained product phases. The focus of this work laid on the discovery of the main reaction pathways and the identification of the bottlenecks. Employing the tool of modelling of the formal kinetics of the discovered reactions, the investigation of reaction mechanisms was possible. In addition the influences of the application of different solvents, that are water and ethanol, and different catalysts were investigated. Finally, the economic feasibility of different process scenarios was studied in order to evaluate the attractiveness of a process which aims at the production of phenol from lignin.

Thermodynamic studies of the lignin degradation showed that even at elevated residence times of 18 h in a batch reactor a system comprising lignin and either water or ethanol had not reached thermodynamic equilibrium. Hence, a kinetic modelling of the degradation was decided to be more convenient to model the yields of major products at reasonable residence times. The simulation of the equilibrium with Aspen Plus V7.2 showed that the major part of the organic input material including 100 % of the solvent ethanol at 633 K would be converted into gaseous components. The gasification of ethanol is thus problematic for the solvolysis of lignin in ethanol. Lignin depolymerisation is faster in water than in ethanol at moderate temperatures (633 K). This was proven by the evaluation of FT-IR-analysis of the solid residues at different residence times. However, the reaction rate of lignin degradation does not exclusively depend on the solvent and the temperature. The type of lignin, the separation method, the thermal degradation

method and the heating rate also play an important role [Cho+12; Var+97; JNB10]. Furthermore, the comparison of both solvents, water and ethanol, showed that water leads to a narrower spectrum of phenolic products and a tenfold increase of the catechol yield. This is advantageous in respect to the separation of the phenolic product from solvent and by-products. The gasification of ethanol at temperatures above 633 K is significant at residence times above 120 min in a batch reactor. The gas yield increases to approximately 70 wt% at 8 h residence time on an initial lignin basis. Experimental results from a CSTR showed a threefold increase of C_2-gases, that are ethane and ethene, to over 10 wt% on an initial lignin basis, if the temperature was increased from 633 K to 400 K at less than 1 h mean residence time. These facts show that the gasification of ethanol is critical at temperatures above 633 K and has to be considered for the design of a technical application.

Furthermore, the effects of heterogeneous metal catalysts on the hydrothermal lignin depolymerisation were studied. Heterogeneous catalysts have minor influence on the primary lignin depolymerisation. However, the effects on the consecutive reactions, such as the hydrodeoxygenation of phenolic intermediates are significant. For example, $PdCl_2$ catalyses the conversion of methoxyphenols into catechols. In respect to the hydrothermal lignin degradation, the application of Raney-Ni seems especially interesting since it selectively catalyses the conversion of catechol into phenol since among the phenolic products recovered from the lignin degradation phenol finds currently the most applications in industry. Hence, the kinetics of the formation and decomposition of phenol within the hydrothermal decomposition of catechol catalysed by Raney-Ni was studied in more detail. It was found that the presence of Raney-Ni significantly increases the conversion of catechol to 88 % and the selectivity of phenol to 90 % at moderate temperatures of approximately 523 K. For comparison, the non-catalysed conversion of catechol into phenol yields a maximum selectivity of 34 % at 15 % conversion at 683 K [WSG09]. The catalysis of primary lignin degradation by cleavage of the ether bonds was not observed employing heterogeneous catalysts. However, both, basic and acidic homogeneous catalysts have a high potential to influence the mentioned reaction [Beh+06]. First screening experiments were successful and showed a threefold increase of the yield of catechols in the presence of KOH and NaOH (see Appendix D.1). HCl had an influence also on the yield of methoxyphenols as well as CO and CO_2. In order to intensify the knowledge in this sector, further investigation effort is recommended.

The focus of this work laid on the development of a model containing the

main reaction pathways of the lignin depolymerisation. The formal kinetics defined by this model should be able to describe the phenomena which were observed within the experimental part of this work, especially the product spectrum of phenolic products, but also considering bulk products such as char or gas. The modelling was carried out for thermal degradation of wheat-straw-lignin in ethanol and formic acid as well as for the thermal degradation of spruce-lignin in water. Assumptions based on the study of literature and the observation of experimental results, yielded a series of straightforward reaction pathways. The evaluation of the optimised formal kinetic parameters of the previously defined reactions showed a very good correspondence with values from literature, especially for the hydrodeoxygenation of phenolic intermediates such as methoxyphenols and catechols. In addition, the model is able to describe the yields of phenolic products and the development of the yields over reaction time. The applicability of the ethanol model on both, batch reactor and CSTR, was proven, although the formal kinetic parameters had to be slightly modified. The model was able to describe the basic tendencies of phenolic yields. The resulting apparent kinetic parameters of the formation and decomposition of phenolics agree with values from literature. The modelling reveals the basic differences between the two different solvents, the two different types of lignin and the effect of two different reactors. The degradation of wheat-straw-lignin yields relatively high amounts of the primary product 4-ethylphenol. This is due to the structure of wheat-straw-lignin which comprises an elevated percentage of *para*-coumaryl units. 4-Ethylphenol is derived from *para*-coumaryl alcohol. Ethylation of phenol occurs at higher residence times and contributes less to the formation of ethylphenols. Consequently, the most prominent primary phenolic products from the degradation of spruce-lignin are methoxyphenols since it mainly comprises coniferyl units. The build-up of char is suppressed if the lignin degradation is transferred from a batch-reactor to a CSTR. The coexistence of early and late products of thermal lignin degradation in a CSTR facilitates the scavenging of reactive substances, *e.g.* radicals. This might also be the reason for decreasing gas yields and increasing yields of phenolic products from 5 to over 6 wt% on an initial lignin basis. The repolymerisation of phenolic products, basically catechols, were of minor importance according the model of hydrothermal degradation of spruce-lignin. The formation of char was more likely caused by the combination of reactive lignin-derived intermediates. The modelling shows the bottleneck reactions of thermal lignin degradation which inhibit the formation of larger amounts of phenolics. Especially the primary formation of methoxyphenols is much slower than the degradation into other reactive fragments which further react into char or gas. However, modelling also revealed that a secondary pathway

leads from these lignin derived fragments to the phenolic products. The latter is favoured in a CSTR. Furthermore, it could also be proven that the mechanism of the cleavage of the C-O bonds present in the methoxyl-group is facilitated in water at moderate temperatures of 633 K. Hydrolysis is the dominant mechanism in the presence of water. However, the mechanism changes around the critical point of water (T_c = 646 K). In SCW thus the cleavage of C-O bonds is radical induced.

The modelling of the formal kinetics of thermal lignin degradation is a powerful tool which aids in understanding the reaction bottlenecks and the reaction mechanisms. The models introduced here, however, have to be further refined and amplified in order to describe *e.g.* the composition of the gaseous product and to elucidate the reactions which lead to the increased yield of catechols in water. This requires additional experimental studies. The tools for evaluation and modelling can be find in this work.

The production of phenol from lignin by solvolysis in ethanol or hydrothermal degradation is economically not feasible if the current yields and process parameters as well as the current market prices for the potential products are considered. The most important parameter influencing the feasibility is the phenol yield. However, even if the phenol yield could be increased to 30 wt% referring to the input amount of lignin, which seems to be the maximum at the current state of the art, a process would still not be economically attractive. A reduction of the mean residence time in the reactor and an increase of the lignin/solvent ratio in the feed are also key parameters which contribute to the necessary drastic reduction of the capital related costs. The yield of phenol and other phenolics has to be increased to at least 20 %, the lignin/solvent ratio should be increased significantly (20 to 30 %) and the mean residence time has to be reduced to maximum 10 to 30 min in order to make the process economically attractive. However, the feasibility study provides a rough and rather conservative estimation of the capital related costs.

Hydrothermal lignin degradation shows better economic opportunities than solvolysis in ethanol since the feedstock situation provides large quantities of cheap feedstock, the solvent is more stable and abundantly available at low prices. Future research should thus focus on black liquor. However, the yield of phenol from black liquor will be reduced since it usually contains more than 50 wt% residues, *e.g.* cellulose and hemicellulose.

The present work shows that hydrothermal depolymerisation of lignin has a certain potential for the recovery of phenolic platform chemicals. It has significant advantages over thermal lignin depolymerisation in organic

solvents, *e.g.* ethanol. Furthermore the potential of catalysts in combination with water is considerable. A combination of a homogeneous catalyst favouring the cleavage of C-O bonds and a heterogeneous catalysts for the adjacent valorisation of phenolic products is a promising approach to maximise the yield of valuable phenolics. However, at the current state of research a technical process is not recommended since it is economically not attractive.

Future research effort in respect to the hydrothermal lignin degradation should focus on

- black liquor since it is the most abundantly available waste product containing lignin in an aqueous solution. Furthermore, it provides the possibility to realise a grave to cradle process since the feedstock is a waste material.
- A more intensive investigation of the influence of heterogeneous and homogeneous catalysis is recommended in order to maximise the yield of phenolics.
- In respect to the study of kinetics, the model developed in the present work should be amplified in order to provide a tool covering different feedstocks and a detailed prediction of the formation of gaseous by-products and solid residue. Here the focus should be the lump-component L_D since its constituents play a central role for the lignin degradation.

Bibliography

[ADL10] P. Al-Riffai, B. Dimaranan, and D. Laborde. *Global Trade and Environmental Impact Study of the EU Biofuels Mandate*. Final Draft Report. International Food Policy Institute (IFPRI), Mar. 2010.

[Aid+02] T. M. Aida, T. Sato, G. Sekiguchi, T. Adschiri, and K. Arai. "Extraction of Taiheiyo coal with supercritical water-phenol mixtures". *Fuel* 81.11-12 (2002), pp. 1453–1461.

[APR01] C. Amen-Chen, H. Pakdel, and C. Roy. "Production of monomeric phenols by thermochemical conversion of biomass: a review". *Bioresource Technology* 79.3 (2001), pp. 277–299.

[Arp07] H.-J. Arpe. *Industrielle Organische Chemie: Bedeutende Vor- und Zwischenprodukte*. 6th ed. Wiley-VCH Verlag GmbH & Co. KGaA, 2007. ISBN: 9783527315406.

[Asp10] Aspen. *Aspen Physical Property System Methods*. Aspen Technology, Inc. 200 Wheeler Road Burlington, MA 01803-5501 USA, 2010.

[AST87] ASTM. "Standard Specification for Aviation Turbine Fuels". *Annual Book of ASTM Standards* 1655.82 (Jan. 1987), pp. 835–844.

[Bae+06] M. Baerns, A. Behr, J. Gmehling, H. Hofmann, U. Onken, and A. Renken. *Lehrbuch Technische Chemie*. 1st ed. Wiley-VCH, 2006. ISBN: 3527310002.

[Baz+07] A. Bazaev, I. Abdulagatov, E. Bazaev, and A. Abdurashidova. "PVT Measurements for Pure Ethanol in the Near-Critical and Supercritical Regions". *International Journal of Thermophysics* 28.1 (2007), pp. 194–219.

[Beh+06] F. Behrendt, Y. Neubauer, K. Schulz-Tönnies, B. Wilmes, and N. Zobel. *Direktverflüssigung von Biomasse - Reaktionsmechanismen und Produktverteilungen*. Tech. rep. Bundesanstalt für Landwirtschaft und Ernährung and Technische Universität Berlin, June 2006.

[Bei+08] N. Beintema, D. Bossio, F. Dreyfus, M. Fernandez, A. Gurib-Fakim, H. Hurni, A.-M. Izac, J. Jiggins, G. K.-. Berisavljevic, R. Leakey, W. Ochola, B. Osman-Elasha, C. Plencovich, N. Röling, M. Rosegrant, E. Rosenthal, and L. Smith. *Agriculture at a Crossroads - Summary for Decision Makers of the Global Report*. Tech. rep. International Assessment of Agricultural Knowledge, Science and Technology for Development (IAASTD), Apr. 2008.

[BK08] T. Barth and M. Kleinert. "Motor Fuels From Biomass Pyrolysis". *Chemical Engineering & Technology* 31.5 (2008), pp. 773–781.

[BKB90] N. Bhore, M. Klein, and K. Bischoff. "The Delplot Technique: A New Method for Reaction Pathway Analysis". *Industrial & Engineering Chemistry Research* 29.2 (1990), pp. 313–316.

[BV10] M. Brebu and C. Vasile. "Thermal degradation of lignin - A review". *Cellulose Chemistry & Technology* 44.9 (2010), pp. 353–363.

[CF11] D. Castello and L. Fiori. "Supercritical water gasification of biomass: Thermodynamic constraints". *Bioresource Technology* 102.16 (2011), pp. 7574–7582.

[Cho+12] J. Cho, S. Chu, P. J. Dauenhauer, and G. W. Huber. "Kinetics and reaction chemistry for slow pyrolysis of enzymatic hydrolysis lignin and organosolv extracted lignin derived from maplewood". *Green Chemistry* 14.2 (2012), pp. 428–439.

[CKL09] S. Consonni, R. E. Katofsky, and E. D. Larson. "A gasification-based biorefinery for the pulp and paper industry". *Chemical Engineering Research and Design* 87.9 (2009). Special Issue on Biorefinery Integration, pp. 1293 –1317.

[Cos+9] L. da Costa Sousa, S. P. Chundawat, V. Balan, and B. E. Dale. "'Cradle-to-grave' assessment of existing lignocellulose pretreatment technologies". *Current Opinion in Biotechnology* 20.3 (2009), 339–347.

[DIN84] DIN. *Mineralöle und Brennstoffe 1. Grundnormen, Normen über Eigenschaften und Anforderungen*. Ed. by DIN Deutsches Institut für Normung e. V. 9th ed. Beuth Verlag GmbH, 1984. ISBN: 3410114599.

[DM99] E. Dorrestijn and P. Mulder. "The radical-induced decomposition of 2-methoxyphenol". *Journal of the Chemical Society. Perkin Transactions* 2.4 (1999), pp. 777–780.

[Dor+00] E. Dorrestijn, L. J. Laarhoven, I. W. Arends, and P. Mulder. "The occurrence and reactivity of phenoxyl linkages in lignin and low rank coal". *Journal of Analytical and Applied Pyrolysis* 54.1-2 (2000), pp. 153–192.

[Dor+99] E. Dorrestijn, M. Kranenburg, D. Poinsot, and P. Mulder. "Lignin depolymerization in hydrogen-donor solvents". *Holzforschung* 53 (1999), pp. 611–616.

[DP04] H. Dillon and S. Penoncello. "A Fundamental Equation for Calculation of the Thermodynamic Properties of Ethanol". *International Journal of Thermophysics* 25.2 (2004), pp. 321–335.

[DRS74] D. Domburg, G. Rossinakaya, and V. Sergeeva. "Study of thermal stability of b-ether bonds in lignin and its models". *4^{th} International Conference on Thermal Analysis*. 1974, pp. 211–221.

[EEA06] EEA. *How much bioenergy can Europe produce without harming the environment?* Tech. rep. European Environment Agency (EEA), July 2006.

[Ehr12] C. Ehrenstein. "Wenn der Acker nur noch Strom erzeugt". *Die Welt* 3 (Jan. 2012).

[EIA11] EIA. *Coal Production and Preparation Report*. Tech. rep. U.S. Energy Information Administration, Nov. 2011.

[Fan+05] Z. Fang, T. Sato, R. Smith, H. Inomata, K. Arai, and J. Kozinski. "Reaction chemistry and phase behavior of lignin in high-temperature and supercritical water". *Bioresource Technology* 99 (2005), pp. 3424–3430.

[Far+10] T. Faravelli, A. Frassoldati, G. Migliavacca, and E. Ranzi. "Detailed kinetic modeling of the thermal degradation of lignins". *Biomass and Bioenergy* 34.3 (2010), pp. 290–301.

[FJP75] A. Fredenslund, R. L. Jones, and J. M. Prausnitz. "Group-contribution estimation of activity coefficients in nonideal liquid mixtures". *AIChE Journal* 21.6 (1975), pp. 1086–1099.

[FMG87] O. Faix, D. Meier, and I. Grobe. “Studies on isolated lignins and lignins in woody materials by Pyrolysis - Gas Chromatography - Mass Spectrometry and off-line Pyrolysis - Gas Chromatography with Flame Ionization Detection”. *Journal of Analytical and Applied Pyrolysis* 11 (1987), pp. 403–416.

[FN68] K. Freudenberg and A. Neish. *Constitution and Biosynthesis of Lignin*. 2nd ed. Springer Verlag, 1968. ISBN: 9783540042747.

[FNR11] FNR. *Maisanbau in Deutschland*. Tech. rep. Fachagentur Nachwachsende Rohstoffe e.V. (FNR), Apr. 2011.

[For+12] D. Forchheim, U. Hornung, P. Kempe, A. Kruse, and D. Steinbach. “Influence of RANEY Nickel on the formation of intermediates in the degradation of lignin”. *International Journal of Chemical Engineering* (2012), Article ID 589749.

[FW87] D. Fengel and G. Wegener. *Wood Chemistry Ultrastructure Reactions*. 1st ed. Verlag Kessel, 1987. ISBN: 9783935638395.

[Gas+10] J. Gasson, M. Kleinert, T. Barth, D. Forchheim, E. Sahin, A. Kruse, and I. Eide. “Lignin Solvolysis: Upscaling of the Lignin-to-Liquid Conversion Process towards Technical Applicability”. *Proceedings of the 18th European Biomass Conference*. 2010, pp. 10–13.

[Gas+2] J. R. Gasson, D. Forchheim, T. Sutter, U. Hornung, A. Kruse, and T. Barth. “Modeling the Lignin Degradation Kinetics in an Ethanol/Formic Acid Solvolysis Approach. Part 1. Kinetic Model Development”. *Industrial & Engineering Chemistry Research* 51.32 (Aug. 2012), 10595–10606.

[Gel+08] G. Gellerstedt, J. Li, I. Eide, M. Kleinert, and T. Barth. “Chemical Structures Present in Biofuel Obtained from Lignin”. *Energy & Fuels* 22.6 (2008), pp. 4240–4244.

[Gla09] W. Glasser. “Lignin - Retrospect and Prospect”. *Gülzower Fachgespräche* 31.7 (2009), pp. 42–44.

[Gme+02] J. Gmehling, R. Wittig, J. Lohmann, and R. Joh. “A Modified UNIFAC (Dortmund) Model. 4. Revision and Extension”. *Industrial & Engineering Chemistry Research* 41.6 (2002), pp. 1678–1688.

[Gut+09] A. Gutierrez, R. Kaila, M. Honkela, R. Slioor, and A. Krause. “Hydrodeoxygenation of guaiacol on noble metal catalysts”. *Catalysis Today* 147.3-4 (2009), pp. 239–246.

[Haa2] M. Haase. “Entwicklung eines Energie- und Stoffstrommodells zur ökonomischen und ökologischen Bewertung der Herstellung chemischer Grundstoffe aus Lignocellulose”. PhD thesis. Karlsruhe Institute of Technology, 2012.

[Her71] H. L. Hergert. “Infrared Spectra”. *Lignins: Occurrence, Formation, Structure and Reaction*. Ed. by K. Sarkanen and C. Ludwig. 1st ed. Wiley Interscience, New York, USA, 1971, pp. 268–272.

[HKB12] B. Holmelid, M. Kleinert, and T. Barth. “Reactivity and Reaction Pathways in Thermochemical Treatment of Selected Lignin Model Compounds under Hydrogen Rich Conditions”. *Journal of Analytical & Applied Pyrolysis* 98 (Nov. 2012), pp. 37–44.

[HS2] C. M. Huelsman and P. E. Savage. “Intermediates and kinetics for phenol gasification in supercritical water”. *Physical Chemistry Chemical Physics* 14.8 (2012), pp. 2900–2910.

[Hum+1] D. Humbird, R. Davis, L. T. C. Kinchin, D. Hsu, A. Aden, P. Schoen, J. Lukas, B. Olthof, M. Worley, D. Sexton, and D. Dudgeon. *Process Design and Economics for Biochemical Conversion of Lignocellulosic Biomass to Ethanol: Dilute-Acid Pretreatment and Enzymatic Hydrolysis of Corn Stover*. Tech. rep. National Renewable Energy Laboratory (NREL), Golden, CO., 2011.

[Imh12] Imhoff. *Oral offer from IMHOFF & STAHL GmbH*. Nov. 2012.

[JK85] H. E. Jegers and M. T. Klein. “Primary and secondary lignin pyrolysis reaction pathways”. *Industrial & Engineering Chemistry Process Design and Development* 24 (1985), pp. 173–183.

[JNB10] G. Jiang, D. J. Nowakowski, and A. V. Bridgwater. “A systematic study of the kinetics of lignin pyrolysis”. *Thermochimica Acta* 498 (2010), pp. 61–66.

[Kar+06] S. Karagöz, T. Bhaskar, A. Muto, and Y. Sakata. “Hydrothermal upgrading of biomass: Effect of K_2CO_3 concentration and biomass/water ratio on products distribution”. *Bioresource Technology* 97.1 (Jan. 2006), pp. 90–98.

[KB08a] M. Kleinert and T. Barth. “Phenols from Lignin”. *Chemical Engineering & Technology* 31.5 (2008), pp. 736 –745.

[KB08b] M. Kleinert and T. Barth. “Towards a Lignincellulosic Biorefinery: Direct One-Step Conversion of Lignin to Hydrogen-Enriched Biofuel”. *Energy Fuels* 22 (2008), pp. 1371–1379.

[KGB09] M. Kleinert, J. R. Gasson, and T. Barth. "Optimizing solvolysis conditions for integrated depolymerisation and hydrodeoxygenation of lignin to produce liquid biofuel". *Journal of Analytical and Applied Pyrolysis* 85.1-2 (2009), pp. 108–117.

[KHB12] M. Klein, Z. Hou, and C. Bennett. "Reaction Network Elucidation: Interpreting Delplots for Mixed Generation Products". *Energy Fuels* 26.1 (2012), pp. 52–54.

[Kle+11] M. Kleinert, J. Gasson, I. Eide, A.-M. Hilmen, and T. Barth. "Developing Solvolytic Conversion of Lignin-to-Liquid (LtL) Fuel Components: Optimization of Quality and Process Factors". *Cellulose Chemistry & Technology* 45 (2011), pp. 3–12.

[Kog09] K. Kogure. *Lead Storage Battery*. Patent JP2009129725. 2009.

[Kru+00] A. Kruse, D. Meier, P. Rimbrecht, and M. Schacht. "Gasification of Pyrocatechol in Supercritical Water in the Presence of Potassium Hydroxide". *Industrial & Engineering Chemistry Research* 39.12 (2000), pp. 4842–4848.

[KT89] A. Klemola and J. Touvinen. *Method for the production of vanillin*. Patent US4847422. 1989.

[KV08] M. Klein and P. Virk. "Modeling of Lignin Thermolysis". *Energy Fuels* 22 (2008), pp. 2175–2182.

[KV80] M. Klein and P. Virk. "Model Pathways for Gas Release from Lignites". *Preprints of Papers - American Chemical Society, Division of Fuel Chemistry* 25.4 (1980), pp. 180–190.

[Lag+98] J. Lagarias, J. Reeds, M. Wright, and P. Wright. "Convergence Properties of the Nelder–Mead Simplex Method in Low Dimensions". *SIAM Journal on Optimization* 9.1 (1998), pp. 112–147.

[Lev99] O. Levenspiel. *Chemical Reaction Engineering*. 3rd ed. Wiley-VCH, 1999. ISBN: 9780471254249.

[LI92] S. Lau and R. Ibrahim. "FT-IR Spectroscopic Studies on Lignin from Some Tropical Woods and Rattan". *Pertanika* 14.1 (1992), pp. 75–81.

[LK85] J. Lawson and M. Klein. "Influence of Water on Guaiacol Pyrolysis". *Industrial and Engineering Chemistry, Fundamentals* 24 (1985), pp. 203–208.

[LL1] K. Lundquist and R. Lundgren. "Acid Degradation of Lignin. Part VII. The Cleavage of Ether Bonds." *Acta Chemica Scandinavica* 26 (1971), 2005–2023.

[LP43] W. Lautsch and G. Piazolo. "Über die Hydrierung von Lignin und ligninhaltigen Stoffen mit Wasserstoff abgebenden Mitteln, insbesondere Alkoholen". *Berichte der deutschen chemischen Gesellschaft (A and B Series)* 76.5 (1943), pp. 486–498.

[LPH97] C. E. López Pasquali and H. Herrera. "Pyrolysis of Lignin and IR Analysis of Residues". *Thermochimica Acta* 293 (1997), pp. 39–46.

[Lun6] K. Lundquist. "Low-molecular weight lignin hydrolysis products". *Applied Polymer Symposium* 28 (1976), 1393–1407.

[LWC11] K. Li, R. Wang, and J. Chen. "Hydrodeoxygenation of Anisole over Silica-Supported Ni_2P, MoP, and NiMoP Catalysts". *Energy & Fuels* 25.3 (2011), pp. 854–863.

[LZ08] Z. Liu and S. Zhang. "Effects of various solvents on the liquefaction of biomass to produce fuels and chemical feedstocks". *Energy Conversion and Management* 49.12 (2008), pp. 3498 – 3504.

[MB97] R. Miller and J. Bellan. "A Generalized Biomass Pyrolysis Model Based on Superimposed Cellulose, Hemicellulose and Lignin Kinetics". *Combustion Science & Technology* 126 (1997), pp. 97–137.

[McM+04] D. F. McMillen, R. Malhotra, S.-J. Chang, S. E. Nigenda, and G. A. S. John. "Coupling pathways for dihydroxy aromatics during coal pyrolysis and liquefaction". *Fuel* 83.11-12 (2004), pp. 1455–1467.

[Mil+99] J. Miller, L. Evans, A. Littlewolf, and D. Trudell. "Batch Microreactor Studies of Lignin and Lignin Model Compound Depolymerization by Bases in Alcohol Solvents". *Fuel* 78 (1999), pp. 1363–1366.

[Moh06] D. Mohan. "Pyrolysis of Wood/Biomass for Bio-Oil: A Critical Review". *Energy Fuels* 20 (2006), pp. 848–889.

[MS1] D. Meier and W. Schweers. "Properties and decomposition of lignins isolated by means of an alcoholic water-mixtures .4. Production of monomeric phenols by catalytic hydrogenolysis". *Holzforschung* 35.2 (1981), 81–85.

[Nim+11a] T. Nimmanwudipong, R. Runnebaum, D. Block, and B. Gates. "Catalytic Conversion of Guaiacol Catalyzed by Platinum Supported on Alumina: Reaction Network Including Hydrodeoxygenation Reactions". *Energy Fuels* 25 (2011), pp. 3417–3427.

[Nim+11b] T. Nimmanwudipong, R. Runnebaum, D. Block, and B. Gates. "Catalytic Reactions of Guaiacol: Reaction Network and Evidence of Oxygen Removal in Reactions with Hydrogen". *Catalysis Letters* 141.6 (2011), pp. 779–783.

[Now+10] D. Nowakowski, A. Bridgwater, D. Elliott, D. Meier, and P. de Wild. "Lignin fast pyrolysis: Results from an international collaboration". *Journal of Analytical and Applied Pyrolysis* 88.1 (2010), pp. 53 –72.

[Nun+85] T. Nunn, J. Howard, J. Longwell, and W. Peters. "Product Compositions and Kinetics in the Rapid Pyrolysis of Milled Wood Lignin". *Industrial & Engineering Chemistry Process Design and Development* 24 (1985), pp. 844–852.

[OR11] S. J. Okullo and F. Reynès. "Can reserve additions in mature crude oil provinces attenuate peak oil?" *Energy* 36.9 (2011), pp. 5755 –5764.

[Pea67] I. Pearl. *The Chemistry of Lignin*. 1st ed. Marcel Dekker Inc., New York, USA, 1967. ISBN: 0824715454.

[Pfe04] A. Pfennig. "G^E-Modelle". *Thermodynamik der Gemische*. Ed. by A. Pfennig. 1st ed. Springer, 2004. Chap. 5.

[PK08] N. Prakash and T. Karunanithi. "Kinetic Modeling in Biomass Pyrolysis - A Review". *Journal of Applied Sciences Research* 4.12 (2008), pp. 1627–1636.

[PK84] F. Petrocelli and M. Klein. "Model Reaction Pathways in Kraft Lignin Pyrolysis". *Macromolecules* 17 (1984), pp. 161–169.

[PR76] D.-Y. Peng and D. B. Robinson. "A New Two-Constant Equation of State". *Industrial Engineering Chemistry Fundamentals* 15.1 (1976), pp. 59 –63.

[PT04] M. Peters and K. Timmerhaus. *Plant Design and Economics for Chemical Engineers*. Ed. by E. D. Glandt, M. T. Klein, and T. F. Edgar. 5th ed. McGraw-Hill, 2004. ISBN: 0072392665.

[Pul09] J. Puls. "Lignin - Verfügbarkeit, Markt und Verwendung: Perspektiven für schwefelfreie Lignine". *Gülzower Fachgespräche* 31.5 (2009), pp. 18–41.

[Ram70] M. Ramiah. "Thermogravimetric and differential thermal analysis of cellulose, hemicellulose, and lignin". *Journal of Applied Polymer Science* 14 (1970), pp. 1323–1337.

[RBS87] A. Roy, S. Bag, and S. Sen. “Studies on the Chemical Nature of Milled Wood Lignin of Jute Stick”. *Cellulose Chemistry & Technology* 21 (1987), pp. 343–348.

[Rob+1] V. M. Roberts, V. Stein, T. Reiner, A. Lemonidou, X. Li, and J. A. Lercher. “Towards Quantitative Catalytic Lignin Depolymerization”. *Chemistry-A European Journal* 17.21 (May 2011), 5939–5948.

[RS09] R. Rinaldi and F. Schuth. “Design of solid catalysts for the conversion of biomass”. *Energy & Environmental Science* 2.6 (2009), pp. 610–626.

[Run+12] R. C. Runnebaum, T. Nimmanwudipong, D. E. Block, and B. C. Gates. “Catalytic conversion of compounds representative of lignin-derived bio-oils: a reaction network for guaiacol, anisole, 4-methylanisole, and cyclohexanone conversion catalysed by $Pt/\gamma\text{-}Al_2O_3$”. *Catalysis Science & Technology* 2 (2012), pp. 113–118.

[RW12] R. Rinaldi and X. Wang. “Hydrogenolysis of Lignin to What You Want - The Role of Solvent”. *5^{th} TMFB International Workshop: Tailor-Made Fuels from Biomass*. Max-Planc-Insitut für Kohlenforschung. 2012.

[Sai+03] M. Saisu, T. Sato, M. Watanabe, T. Adschiri, and K. Arai. “Conversion of Lignin with Supercritical Water-Phenol Mixtures”. *Energy & Fuels* 17.4 (2003), pp. 922–928.

[Sch07] K. Schwarz. *Lignin-based Glue*. Patent WO2007048494. 2007.

[Sch12] C. Schröder. “Volvo Trucks: Erste Zwischenergebnisse beim Bio-DME-Projekt übertreffen die Erwartungen”. *Automobiltechnische Zeitschrift* (Mar. 2012).

[SH11] A. G. Sergeev and J. F. Hartwig. “Selective, Nickel-Catalyzed Hydrogenolysis of Aryl Ethers”. *Science* 6028.332 (Apr. 2011), pp. 439–443.

[SKR04] A. Sınağ, A. Kruse, and J. Rathert. “Influence of the Heating Rate and the Type of Catalyst on the Formation of Key Intermediates and on the Generation of Gases During Hydropyrolysis of Glucose in Supercritical Water in a Batch Reactor”. *Industrial & Engineering Chemistry Research* 43.2 (2004), pp. 502–508.

[SR11] W. Stinner and N. Rensberg. *Perspektive der Biogasgewinnung aus nachwachsenden Rohstoffen - Bewertung von Substratalternativen*. Study. Deutsches BiomasseForschungsZenrum (DBFZ), Apr. 2011.

[Tak+12] S. Takami, K. Okuda, X. Man, M. Umetsu, S. Ohara, and T. Adschiri. "Kinetic Study on the Selective Production of 2-(Hydroxybenzyl)-4-methylphenol from Organosolv Lignin in a Mixture of Supercritical Water and p-Cresol". *Industrial & Engineering Chemistry Research* 51.13 (2012), pp. 4804–4808.

[Tal81] A. Talwalkar. *Coal Conversion Systems Technical Data Book*. Tech. rep. Institute of Gas Technology, Chicago, IL (USA), Nov. 1981.

[Tow+07] M. Towers, T. Browne, R. Kerekes, J. Paris, and H. Tran. "Biorefinery opportunities for the Canadian pulp and paper industry". *Pulp Paper Canada* 6.6 (2007), pp. 109–112.

[TRR11] S. S. Toor, L. Rosendahl, and A. Rudolf. "Hydrothermal liquefaction of biomass: A review of subcritical water technologies". *Energy* 36.5 (2011), pp. 2328–2342.

[Var+97] G. Várhegyi, M. Antal, E. Jakab, and P. Szabó. "Kinetic Modeling of Biomass Pyrolysis". *Journal of Analytical and Applied Pyrolysis* 42.1 (1997), pp. 73–87.

[VCI11] VCI. *Chemiewirtschaft in Zahlen*. Tech. rep. Verband der Chemischen Industrie (VCI), 2011.

[VCI12] VCI. *Preisindex - Chemie Technik*. 2012.

[VDI06] VDI. *VDI-Wärmeatlas*. Ed. by Verein Deutscher Ingenieure (VDI) - Gesellschaft Verfahrenstechnik und Chemieingenieurwesen (GVC). Springer-Verlag, 2006. ISBN: 3540255044.

[Vuo86] A. Vuori. "Pyrolysis Studies of some Simple Coal Related Aromatic Methyl Esters". *Fuel* 65 (1986), pp. 1575–1583.

[Wag09] W. Wagner. *Wärmeaustauscher: Grundlagen, Aufbau und Funktion thermischer Apparate*. 4th ed. Vogel Business Media, 2009. ISBN: 3834331619.

[WGZ03] A. Wingren, M. Galbe, and G. Zacchi. "Techno-Economic Evaluation of Producing Ethanol from Softwood: Comparison of SSF and SHF and Identification of Bottlenecks". *Biotechnology Progress* 19.4 (2003), pp. 1109–1117.

[Wil+09] P. de Wild, R. Van der Laan, A. Kloekhorst, and E. Heeres. "Lignin valorisation for chemicals and (transportation) fuels via (catalytic) pyrolysis and hydrodeoxygenation". *Environmental Progress & Sustainable Energy* 28.3 (2009), pp. 461–469.

[WR12] X. Wang and R. Rinaldi. "Solvent Effects on the Hydrogenolysis of Diphenyl Ether with Raney Nickel and their Implications for the Conversion of Lignin". *ChemSusChem* 5.8 (2012), pp. 1455–1466.

[WSG08] Wahyudiono, M. Sasaki, and M. Goto. "Recovery of phenolic compounds through the decomposition of lignin in near and supercritical water". *Chemical Engineering and Processing: Process Intensification* 47.9-10 (2008), pp. 1609–1619.

[WSG09] Wahyudiono, M. Sasaki, and M. Goto. "Conversion of biomass model compound under hydrothermal conditions using batch reactor". *Fuel* 88.9 (2009), pp. 1656–1664.

[WSG11] Wahyudiono, M. Sasaki, and M. Goto. "Thermal Decomposition of Guaiacol in Sub- and Supercritical Water and its Kinetic Analysis". *Journal of Material Cycles and Waste Management* 13 (2011), pp. 68–79.

[Ye+12] Y. Ye, Y. Zhang, J. Fan, and J. Chang. "Novel Method for Production of Phenolics by Combining Lignin Extraction with Lignin Depolymerization in Aqueous Ethanol". *Industrial & Engineering Chemistry Research* 51.1 (2012), pp. 103–110.

[YM12] T. L.-K. Yong and Y. Matsumura. "Reaction Kinetics of the Lignin Conversion in Supercritical Water". *Industrial & Engineering Chemistry Research* 51.37 (2012), pp. 11975–11988.

[Yok+98] C. Yokoyama, K. Nishi, A. Nakajima, and K. Seino. "Thermolysis of organosolv lignin in supercritical water and supercritical methanol". *Sekiyu Gakkai* 41.4 (1998), pp. 243–250.

[YS98] J. Yu and P. Savage. "Decomposition of Formic Acid under Hydrothermal Conditions". *Industrial & Engineering Chemistry Research* 37.1 (1998), pp. 2–10.

[Yua+10] Z. Yuan, S. Cheng, M. Leitch, and C. Xu. "Hydrolytic Degradation of Alkaline Lignin in Hot-Compressed Water and Ethanol". *Bioresource Technology* 101.23 (2010), pp. 9308–9313.

[Zak+0] J. Zakzeski, P. C. A. Bruijnincx, A. L. Jongerius, and B. M. Weckhuysen. "The Catalytic Valorization of Lignin for the Production of Renewable Chemicals". *Chemical Reviews* 110.6 (June 2010), 3552–3599.

[Zha+1] C. Zhao, J. He, A. A. Lemonidou, X. Li, and J. A. Lercher. "Aqueous-phase hydrodeoxygenation of bio-derived phenols to cycloalkanes". *Journal of Catalysis* 280.1 (May 2011), 8–16.

[Zha+10a] C. Zhao, Y. Kou, A. A. Lemonidou, X. Li, and J. A. Lercher. "Hydrodeoxygenation of bio-derived phenols to hydrocarbons using RANEY-Ni and Nafion/SiO_2 catalysts". *Chemical Communications* 46 (2010), pp. 412–414.

[Zha+10b] W. Zhao, W.-J. Xu, X.-J. Lu, C. Sheng, S.-T. Zhong, S.-R. Tang, Z.-M. Zong, and X.-Y. Wei. "Preparation and Property Measurement of Liquid Fuel from Supercritical Ethanolysis of Wheat Stalk". *Energy & Fuels* 24.1 (2010), pp. 136–144.

[Zha+11] H. Zhao, D. Li, P. Bui, and S. Oyama. "Hydrodeoxygenation of guaiacol as model compound for pyrolysis oil on transition metal phosphide hydroprocessing catalysts". *Applied Catalysis A: General* 391.1-2 (2011), pp. 305–310.

[ZHR11] B. Zhang, H.-J. Huang, and S. Ramaswamy. "Reaction Kinetics of the Hydrothermal Treatment of Lignin". *Applied Biochemistry & Biotechnology* 147.1-3 (2011), pp. 119–131.

[ZL12] C. Zhao and J. A. Lercher. "Upgrading Pyrolysis Oil over Ni/HZSM-5 by Cascade Reactions". *Angewandte Chemie* 124.24 (2012), pp. 6037–6042.

[ZL2] C. Zhao and J. A. Lercher. "Selective Hydrodeoxygenation of Lignin-Derived Phenolic Monomers and Dimers to Cycloalkanes on Pd/C and HZSM-5 Catalysts". *ChemCatChem* 4.1 (Jan. 2012), 64–68.

List of Tables

1.1 BDE of the most predominant linkages (see Figure 1.1.) . . . 5

2.1 Characterisation of both lignin types from wheat straw and spruce. 14

3.1 Initial yields $y_{i,0}$ for the Aspen-calculation of thermodynamic equilibrium at 633 K, derived from the experimental results at 120 min in water (Exp. 90) and ethanol (Exp. 158, see Appendix E.1). 23

3.2 Equilibrium yields y_i of thermal lignin degradation in water and ethanol calculated with Unifac and Peng-Robinson-EoS at 633 K and 30 MPa, input concentrations are listed in Table 3.1. 24

4.1 Identified products with corresponding retention time in the GC-FID. 33

6.1 Characteristic FT-IR absorptions and observed changes between the biomass feed and the solid residue samples 51

6.2 Coefficient of determination R^2 for the model fit and standard deviation σ of calculated and experimental yields (see Appendix C.4). 57

6.3 Formal kinetic rate coefficients (k_j) of all 17 reactions defined within the developed model (see Figure 6.7) 59

6.4 Experimental conditions, estimated total reaction mass (m) and mass flow ($\dot{m}$) for batch and continuous reactor. 63

6.5 Coefficient of determination R^2 for the model fit and standard deviation σ of calculated and experimental yields of phenolic products (see Figure 6.12). 67

6.6 Formal kinetic rate coefficients k_j, apparent activation energies $E_{A,j}$ and Arrhenius factors A_j of the 17 reactions defined in the model (see Figure 6.7) at different temperatures for the CSTR-fit are compared with rate coefficients calculated for the batch-fit at 633 K. 68
6.7 Apparent activation energies $E_{A,j}$, Arrhenius factors A_j and rate coefficients k_j at different temperatures for the 15 reactions defined in the model (see Figure 6.17). 82
6.8 Comparison of different kinetic studies of thermal lignin degradation, all based on lump-models; values obtained from this work refer to a lump of the reactions represented by k_1+k_7 in the water model (Figure 6.17) and by $k_1+k_6+k_{10}$ in the ethanol model (Figure 6.7). 88
6.9 Comparison of different kinetic studies of thermal decomposition of methoxyphenols, lump of the reactions represented by k_2+k_3 in the water-model (Figure 6.17) and by k_2 in the ethanol-model (Figure 6.7), and catechols, lump of the reactions represented by $k_4+k_5+k_{12}$ in the water model. 91

7.1 Streams defined for the lignin liquefaction process (see Figure 7.1) for both, ethanol and water approach. 96
7.2 Parameters used for the estimation of the purchased costs of the pump. 97
7.3 Reaction conditions and resulting reactor volume V_R for both ethanol and water approach. 98
7.4 Data concerning heat exchanger (B and F) for both ethanol and water approach. 99
7.5 Estimated prices for reactants, products and utilities. 101
7.6 Total Capital Investment TCI calculated by various factors based on TBM. 103
7.7 Energy demands and utility costs (TUC). 104
7.8 Operating Labor Costs (OLC). 104
7.9 Total Manufacturing Costs COM. 106
7.10 Scenarios of the plant design and cost estimation for solvolytic lignin liquefaction and phenol production 109

A.1 Chemicals used 140
A.2 Catalysts 141
A.3 Construction materials 141

B.1 Applied values of $f_{d,i}$ for quantified phenolics i. 149

B.2 Distribution of phenolic products in a two phase system comprising water and ethyl acetate under different conditions. . . 150

C.1 Indices of reaction participant 155
C.2 Indices of reaction participant 157

D.1 Parameters describing the decomposition of catechol and phenol within hydrothermal catechol decomposition catalysed by Raney-Ni. 170

E.1 Experimental data: reaction conditions, input parameters, employed analytical methods. 175
E.2 Experimental data: Results of bulk components, gaseous compounds, H_2O and EtOH. 181
E.3 Experimental data: Results of phenolic and other compounds quantified via GC-FID. 187
E.4 Heating value and elemental composition of input and output components for solvolysis of wheat-straw lignin in ethanol and formic acid in a CSTR at 673 K, 25 MPa and 44 min mean residence time. 194
E.5 Mass and energy balance for experiment Exp. 66 scaled to 1 t/h lignin. 195

List of Figures

1.1 Example of lignin structure depicting some of the dominant linkages between the aromatic monomers [WR12]. 5

1.2 The three characteristic aromatic substances which constitute the characteristic monomeric units of lignin: A: *para*-coumaryl alcohol, B: sinapyl alcohol and C: coniferyl alcohol. 6

1.3 Monoaromatic products (phenolics) from lignin depolymerisation: A: phenol, B: catechol, C: guaiacol and D: syringol. . 7

3.1 Thermodynamic equilibrium calculated by Aspen with Unifac-method and Peng-Robinson-EoS compared with results from Exp. 148 a) mass fraction of of product phases and b) composition of the gas phase; $\tau = 1080$ min; spruce-lignin/water = 132 g/L; T = 633 K. 25

3.2 Thermodynamic equilibrium calculated by Aspen with Unifac-method and Peng-Robinson-EoS compared with results from Exp. 152 a) mass fraction of of product phases and b) composition of the gas phase; $\tau = 1080$ min; spruce-lignin/ethanol = 132 g/L; T = 633 K. 25

4.1 Results from thermal degradation of spruce lignin in ethanol (EtOH) or water (H_2O) at $T = 633$ K; spruce-lignin/solvent = 132 g/L; a) yield of gas and solid residue in EtOH (solid symbols, Exp. 153-161) and H_2O (open symbols, Exp. 85-93); b) Gas composition for $\tau = 480$ min 30

4.2 FT-IR-analysis of spruce-lignin and the solid residue after 15, 30, 60 and 480 min residence time in a 5mL MA2 with a) ethanol (Exp. 153, 154, 156, 161) and b) H_2O (Exp. 85, 86, 88, 93); lignin/solvent = 132 g/L; $T = 633$ K 31

4.3 GC-FID-chromatogram of liquid product (EtOH, Exp. 143) and organic phase after extraction of aqueous liquid product (H_2O, Exp. 142) after thermal treatment of spruce-lignin; lignin/solvent = 132 g/L; FA/solvent = 107g/L; T = 633 K, τ = 60 min 32

4.4 Yield of different phenolics from lignin solvolysis in ethanol (solid symbols, Exp 126-133) and H_2O (open symbols, Exp 134-141) at different temperatures; spruce-lignin/solvent = 80 g/L; 8 mg Pd-catalyst; 1 MPa H_2 initial pressure; τ = 60 min . . . 34

5.1 Effect of different heterogeneous catalysts on the yield of phenols, methoxyphenols and catechols from hydrothermal lignin degradation (Exp. 8-20 and 27-31), spruce-lignin/water = 133 g/L; T = 633 K; τ = 30 min; 0.10 g/g_{lignin} Raney-Ni, 0.08 g/g_{lignin} Rh on act. C, 0.08 g/g_{lignin} Pt on act. C, 0.07 g/g_{lignin} Co, 0.08 g/g_{lignin} $PdCl_2$, 0.13 g/g_{lignin} Al-Ni; reactor pressurised with a) N_2 (5 MPa initial pressure) and b) H_2 (5 MPa initial pressure). 38

5.2 Yield of PhOH, methoxyPhOH and catechols at different loadings of Raney-Ni (Exp 10-11 and 21-31); spruce-lignin/water = 133 g/L; T =633 K; τ =30 min. 40

5.3 Product composition after hydrogenation of 10 g/L catechol in water at different temperatures with 55 mg(dry matter) Raney-Ni (Exp 36-39); 1 MPa initial pressure H_2; τ = 60 min. 40

5.4 Selectivity of phenol over catechol conversion after hydrothermal catechol decomposition catalysed with Raney-Ni (Exp. 103-105, 114-118 and 122-125); input: 5 ml catechol/water-solution (5 g/L); different temperatures and residence times. 41

6.1 Liquid, gas and solid reaction products at varying residence times are compared with the input amounts of Lig, EtOH and FA at reaction time *zero* of the experimental series. All experiments (Exp. 44-53) were conducted at the same loading conditions: 0.33 g Lig, 0.27 g FA, and 2.5 g EtOH; T = 633 K. 47

6.2 Individual yield of the gaseous product components, quantified on GC-FID and GC-TCD. The values for CO and H_2 have been multiplied by a factor of 10, respectively 10000, to enable a better visibility on the given scale; T = 633 K. . . . 47

6.3 Gas and solid residue yields for experiments carried out at varying residence times. A transition zone, indicating the change from largely lignin characteristic solids to char is indicated, utilising the results from FT-IR analysis; $T = 633$ K. . 48

6.4 FT-IR spectra of unreacted lignin and of the collected solid residues at 90, 120 and 1180 min residence time. The largest alterations take place during the first 120 min and are documented in Table 6.1; $T = 633$ K. 49

6.5 Yields of key components for the different phenolic compound classes: a) methoxyphenols, b) catechols and c) phenols over residence time; $T = 633$ K. 52

6.6 Methoxyphenols, phenols, 4-ethylphenol and catechols in dependence from the conversion, a) first rank Delplot, b) second rank Delplot; $T = 633$ K 53

6.7 Scheme of main reaction participants and pathways of the depolymerisation of wheat straw lignin in ethanol and formic acid; gaseous products of ethanol and formic acid gasification take part in reactions 2-4, 7-9, 14 and 17. This is indicated by curved arrows; $T = 633$ K. 56

6.8 The experimental values are compared with the model fit functions for the quantified key phenolic compounds; $T = 633$ K. 58

6.9 Fits of the gas-lump and the solid residue compared with the experimental data. The differentiation between lignin and char in the solid residue was accomplished largely by FT-IR analysis, as illustrated in Figure 6.4; $T = 633$ K. 58

6.10 Comparison of calculated and experimental data for product yields of all phenolic (lump) components. Normalising factors (mg/g_{lignin}): MethoxyPhOH: 14.0, Catechols: 7.0, PhOH: 3.0, 4-EtPhe: 5.0, 2-EtPhe: 1.5. 60

6.11 Results of lignin degradation in MA1 and CSTR at 653 K and 60 min (mean) residence times (Exp. 58, 63); a) liquid, gas and solid reaction products compared on a wt% basis with the input amounts of lignin from wheat straw Lig, EtOH and FA, b) Composition of the product gas, c) yields of PhOH, methoxyPhOH and catechols. 64

6.12 Comparison between the CSTR-fit of phenolic lumps and their measured quantities for Exp. 64-66 conducted at a) 633 K, b) 653 K and c) 673 K; mean residence times are between 39 and 56 min (see Table 6.4). 66

6.13 Comparison of the fluxes of each reaction defined in the model (see Figure 6.7) calculated for both batch-fit and CSTR-fit at 60 min (mean) residence time τ (τ') and 633 K (see Appendix C.6). 69

6.14 Sensitivity on a scale from 0 to 100 % (see Appendix C.5) of the calculated yields at 633 K and 60 min (mean) residence time to a variation of rate coefficients by factor 2 for a) batch-fit and b) CSTR-fit. 71

6.15 Results from the CSTR-fit of the experimental yields at different temperatures and mean residence times (Exp. 64-66) of a) methoxyphenols and b) catechols. 72

6.16 Comparison of the normalised calculated and experimental data for product yields of all phenolic (lump) components. The following normalising factors (mg/g_{lignin}) were used for better comparability: MethoxyPhOH: 42.1; Catechols: 20.4; PhOH: 5.6; 4-EtPhe: 19.4; 2-EtPhe: 3.1. 74

6.17 Scheme of main reaction participants and pathways of the hydrothermal depolymerisation of spruce-lignin; gaseous components take part in reactions 2-6 and 13. This is indicated by curved arrows. 77

6.18 Comparison between the model-fit of solid and gaseous lump components and measured quantities of solid residue and stable gaseous compounds (CO_2 and CH_4) for experiments carried out at a) 593 K, b) 613 K, c) 633 K, d) 653 K. 80

6.19 Comparison between the model-fit of phenolic lumps and their measured quantities for experiments conducted at a) 593 K, b) 613 K, c) 633 K, d) 653 K; error bars show standard deviation σ obtained from similar reproduced experiments at the corresponding residence time and temperature. 81

6.20 Fluxes of main reactions comprised by the developed model of hydrothermal depolymerisation of spruce-lignin (see Figure 6.17), reactions r_1, r_2, r_4, r_5, r_6, r_7, r_9, r_{11} are compared with analogue reactions of lignin solvolysis in ethanol (see Section 6.1); τ = 131 min; T = 633 K; lignin/water=132 g/L. 84

6.21 Sensitivity matrices considering comparable reactions and intermediates or products of a) the model of hydrothermal degradation of spruce-lignin and b) the solvolysis in ethanol and formic acid of wheat-straw-lignin; τ = 131 min; T = 633 K; lignin/solvent=132 g/L. 85

7.1 Process scheme with main components (labelled with letters) an streams (labelled with numbers). 95

7.2 COM of phenol from lignin for the basic case and 2 different scenarios (see Table 7.10) for a) the water approach and b) the ethanol approach. 108

7.3 COM of phenol from lignin in dependence of the phenol yield for the basic case of both ethanol and water approach; scenario 3 (see Table 7.10) is displayed for the water approach. 108

A.1 Mechanical drawing of the MA1, simple version, 10 mL inner volume. 142

A.2 Mechanical drawing of the MA2, gas-input version for gas ventilation and loading, 5 mL inner volume. 143

A.3 Schematic of the CSTR including feeding, reactor and collection. 144

B.1 Sample workup scheme for product phases of experiments with ethanol. 146

B.2 sample workup scheme for product phases of experiments with water. 146

C.1 Mass balanced reactions for modelling thermal degradation of wheat-straw lignin in ethanol. 155

C.2 Mass balanced reactions for modelling the hydrothermal degradation of spruce-lignin. 158

D.1 Comparison of homogeneous basic catalysts with 0.12 mol/L input concentration in a spruce-lignin/water = 133 g/L suspension; T = 633 K (Exp. 1 and 7-9); τ = 30 min 164

D.2 Comparison of homogeneous acidic catalysts with varying input concentration in a spruce-lignin/water = 133 g/L suspension (Exp. 2-6 and 8-9); T = 633 K; τ = 30 min 164

D.3 Mass fractions of the input (residence time = 0) and output at 573 K and different residence times after hydrothermal decomposition of catechol in a 10 mL-MA2; 5 ml input of aqueous solution (catechol/water = 10 g/L); 2.2 mg Raney-Ni catalyst 166

D.4 Reaction scheme of the catalytic decomposition of catechol in water at temperatures between 523 K and 573 K based on delplot-analysis and literature research. 167

D.5 Concentration of catechol in the product after hydrothermal decomposition of catechol depending on the residence time at a) 573 K, b) 533 K, c) 523 K, d) 513 K; Data points represent experimental values, continuous line calculated according to Equation D.1; 5 ml input of catechol/water = 10 g/L; 2.2 mg Raney-Ni catalyst. 168
D.6 Concentration of phenol in the product after hydrothermal decomposition of catechol depending on the residence time at a) 513 K, b) 523 K, c) 533 K and d) 573 K; Data points from experiments, continuous line calculated according to Equation D.2; 5 ml input of catechol/water = 10 g/L; 2.2 mg Raney-Ni catalyst. 169
D.7 Arrhenius plot of pseudo-first order rate coefficients of the hydrothermal Raney-Ni catalysed decomposition of catechol (circular data points) and phenol (rectangular data points), $k' = 1\text{min}^{-1}$ 170

Appendix A

Materials

In this appendix the chemicals used for synthesis or analysis and their degree of purification are listed (see Table A.1). All chemicals were used as purchased. No further purification was required. The catalysts are listed separately in Table A.2 including the absorption surface according to Brunauer, Emmett, Teller (BET)-analysis. Furthermore, the composition of the alloys for the reactors are listed, a mechanical drawing of the MA and a flow scheme of the CSTR are provided.

Table A.1: Chemicals used

Chemical	Grade	Producer
Ethanol	$\geq$ 99.5%	Merck
FA	98-100%	Merck
acetic acid (AA)	96%	Merck
Ethyl acetate	$\geq$ 99.5%	Fluka
Water	$\geq$ 18.4 MΩ·cm	Millipore Direct Q3
KOH	acidimetric assay $\geq$ 85%	Merck
NaOH	$\geq$ 99%	Anala R
HCl	37%	Merck
H_2	$\geq$ 99.999%	Air Liquid
N_2	$\geq$ 99.9999%	Air Liquid
Pentacosane	$\geq$ 99%	Alfa Aesar
Pentadecane	$\geq$ 99%	Aldrich
KBr	$\geq$ 99%	Merck
Phenol	$\geq$ 99%	Merck
o-Cresol	$\geq$ 99%	Merck
p-Cresol	$\geq$ 98%	Merck
2-Ethylphenol	$\geq$ 98%	Merck
4-Ethylphenol	$\geq$ 98%	Merck
Guaiacol	$\geq$ 98%	Merck
4-Methylguaiacol	$\geq$ 98%	Merck
4-Ethylguaiacol	$\geq$ 98%	Alfa Aesar
Syringol	$\geq$ 99%	Aldrich
Catechol	$\geq$ 99%	Alfa Aesar
4-Methylcatechol	$\geq$ 96%	Alfa Aesar
4-Ethylcatechol	$\geq$ 98%	Alfa Aesar
Cyclohexanol	$\geq$ 99%	Merck
Cyclohexanone	$\geq$ 99%	Merck
$PdCl_2$	$\geq$ 99%	Merck

Table A.2: Catalysts

Catalyst	Carrier-Material	Grade	BET-surface	Producer
Raney-Ni	None	50 wt% in H_2O	53 m^2/g	Merck
Pd	Activated C	10 wt%	900 m^2/g	Fluka
Pt	Al_2O_3	5 wt%	12 m^2/g	Merck
Rh	Activated C	5 wt%	900 m^2/g	Merck
Al-Ni		50 wt% Ni, 50 wt% Al	4 m^2/g	Aldrich
Co	None	$\geq$ 99.6 wt%	23 m^2/g	Merck

Table A.3: Construction materials

Material	Composition max. (min) wt%
Inconel625	Ni (58) chromium (Cr) 20-30 Mo 8-10 niobium (Nb) & tantalum (Ta)3.15-4.15 iron (Fe) 5
1.4571	C 0.03 silicon (Si) 1.0 Mn 1.5 phosphor (P) 0.04 S 0.015 Cr10.5-12.5 Mo 2.0-2.5 Ni 10.0-13.5 titanium (Ti) 5xC-0.7

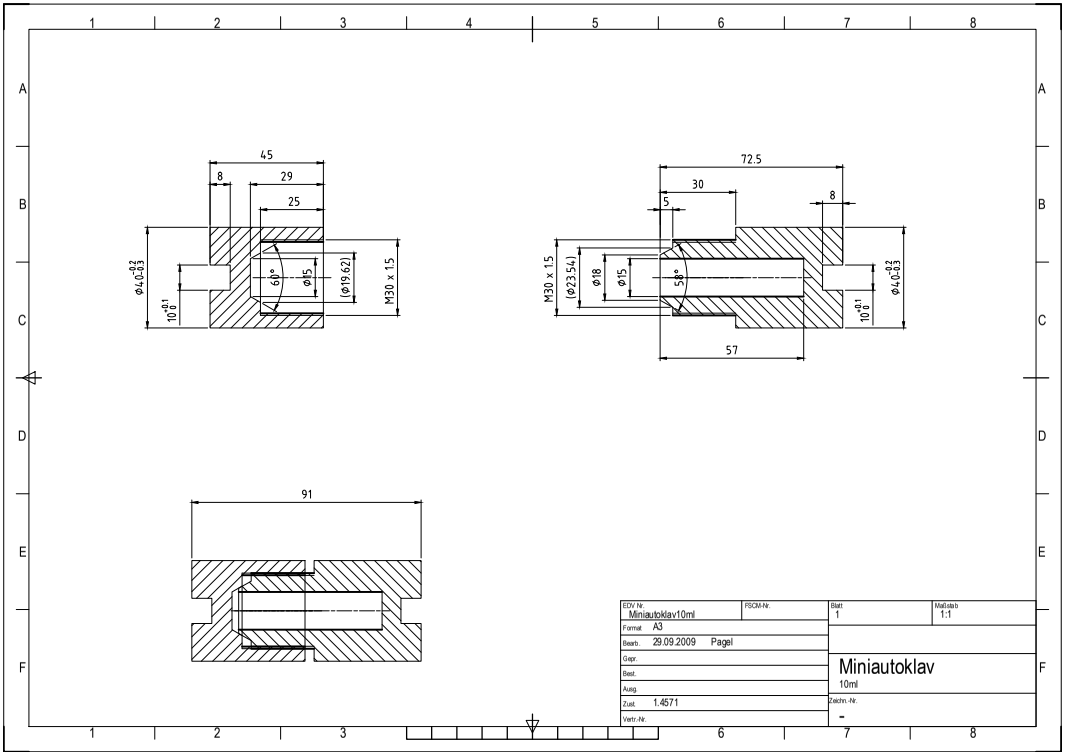

Figure A.1: Mechanical drawing of the MA1, simple version, 10 mL inner volume.

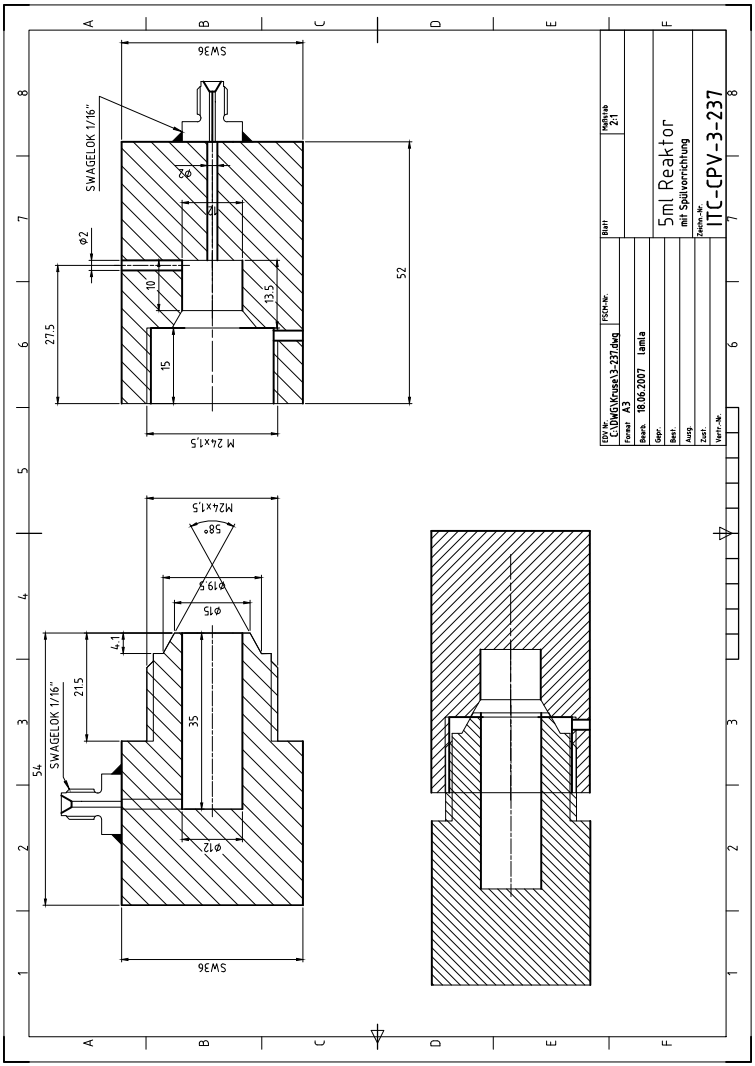

Figure A.2: Mechanical drawing of the MA2, gas-input version for gas ventilation and loading, 5 mL inner volume.

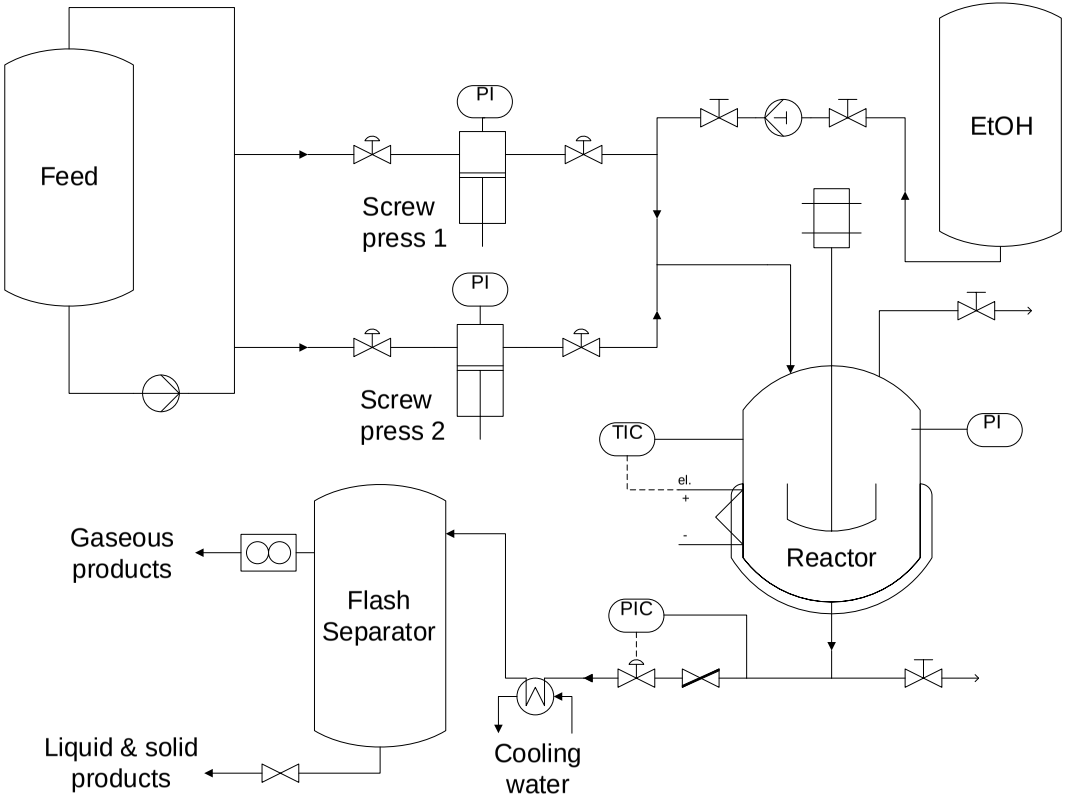

Figure A.3: Schematic of the CSTR including feeding, reactor and collection.

Appendix B

Sample workup

This appendix provides more detailed information about the workup of the solid, liquid and gaseous samples obtained from the experiments. The Section B.1 provides an overview for the separation of the different product phases and the analytical methods applied on them. In Section B.2 the extraction of the phenolic products from the aqueous liquid phase is explained in detail including the distribution coefficients of the phenolics which were quantified by GC-FID.

B.1 Analysis overview

After the separation of the gaseous phase which is different for either CSTR or MA, the gas was analysed on a GC equipped with both, a FID and a TCD. The mixture of liquid and solid residues was filtered with a filter purchased from Pall with 45 nm pore size for the separation of solid and liquid phase. The solid fraction was weighed, dried for 16 h at 378 K and weighed again after drying. On the dried solid FT-IR and elementary analysis is applied.

In the case water was used as solvent, the liquid products had to be extracted from the aqueous sample with ethyl acetate. After extraction the organic phase can be analysed with GC-FID or eventually GC-MS exactly like the liquid product from experiments with ethanol. For that purpose the organic sample, containing the liquid products diluted in ethyl acetate or ethanol, was mixed with an equal amount of ethyl acetate containing the internal standard pentacosane. Figure B.1 and B.2 show the schematic sample workup for experiments with ethanol and water, respectively.

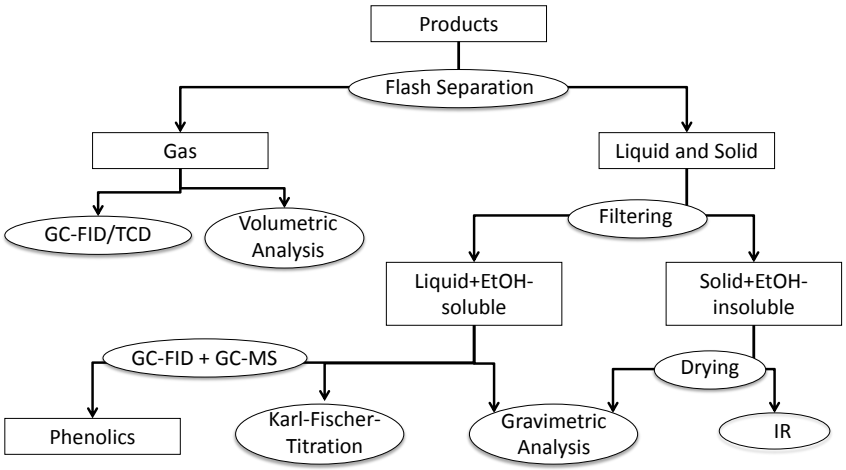

Figure B.1: Sample workup scheme for product phases of experiments with ethanol.

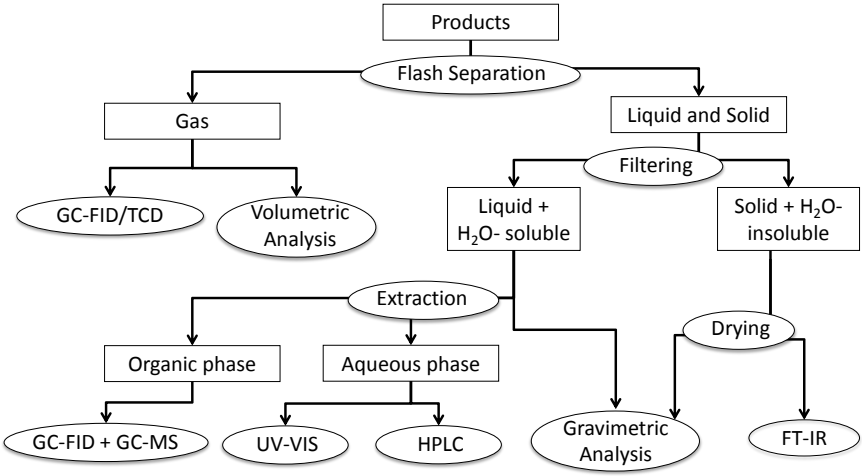

Figure B.2: sample workup scheme for product phases of experiments with water.

B.2 Extraction

For the analysis of phenolic products from the hydrothermal lignin degradation via GC, phenolics had to be extracted from the aqueous product phase. Ethyl acetate was selected as extractant. For a better performance of the extraction the pH of the aqueous phase was adjusted to a value between 3 and 5 by adding an adequate amount of HCl. 1.3 mL of the sample were thereafter mixed with 0.52 mL ethyl acetate. The phases were left to settle for one hour. A sample of the organic phase was analysed on a GC equipped with a FID, optionally on GC equipped with a MS. The concentration of the different compounds (solutes) in the original aqueous product phase can be calculated with the following Equation B.1

$$C_{i,aq,0} = C_{i,org} \cdot \frac{f_a \cdot f_b}{f_c \cdot f_{d,i}}, \qquad f_a = 2, \tag{B.1}$$

where $C_{i,org}$ is the measured concentration of the (solute) in the organic phase, $C_{i,aq,0}$ the concentration in the aqueous product phase before extraction and f_a, f_b, f_c and $f_{d,i}$ are factors considering the performance of the extraction. The factor f_a considers the dilution of the organic phase after the extraction with ethyl acetate including the internal standard pentacosane ($C_{25}H_{52}$) for the preparation of GC-analysis (ratio sample:standard = 1:1). The solvent (water) and extractant (ethyl acetate) are not completely insoluble. This fact was considered by the factor f_b which is proportional to the miscibility of ethyl acetate in water. The latter was found to be independent from the solute and its concentration. It was determined by adding the extraction standard pentadecane ($C_{15}H_{32}$) to the extractant which is practically insoluble in water. The concentration of pentadecane in the organic extractant was measured before ($C_{C_{15}H_{32},org,0}$) and after ($C_{C_{15}H_{32},org}$) the extraction. With the quotient of these values f_b can be calculated according to Equation B.2. The average value for f_b was 0.815 with a standard deviation of 0.024.

$$f_b = \frac{C_{C_{15}H_{32},org,0}}{C_{C_{15}H_{32},org}} = 0.815 \pm 0.024 \tag{B.2}$$

The factor f_c considers the alteration of the solute concentration due to the different input volumes of aqueous sample (V_{aq}) and extractant (V_{org}) and is calculated according to the following Equation B.3

$$f_c = \frac{V_{aq}}{V_{org}} = \frac{1.3\ mL}{0.52\ mL} = 2.5. \tag{B.3}$$

The factor $f_{d,i}$ considers the distribution ratio of the solutes i in both, the solvent and the extractant. It has to be clearly distinguished from the distribution coefficient. In fact, $f_{d,i}$ seems most convenient for the calculation of $C_{i,aq,0}$ as it relates the concentration of the solute in the extractant after the extraction $m_{i,org}$ with the initial concentration in the aqueous phase $m_{i,aq,0}$.

$$f_{d,i} = \frac{m_{i,org}}{m_{i,aq,0}} \tag{B.4}$$

The experimental evaluation of this factor $f_{d,i}$ and a list of the factors for each solute i are demonstrated in the following. For the evaluation of the factor $f_{d,i}$ several extraction experiments were carried out. A single solute (single experiments) or a mixture of various solutes (bulk experiments) were diluted in the solvent water with a determined concentration $C_{i,aq,0}$. Eventually NaCl was added in order to evaluate the influence of salts on the distribution between the two phases. The employed extractant was ethyl acetate containing 1000 mg/L pentadecane. The extraction was carried out as described above. The results are listed in Table B.2.

Extraction experiments with phenol, guaiacol, catechol, cyclopentanone, 2-methylcyclopentanone and cyclohexanol show good reproducibility even in the presence of other phenolics in the solvent. However, high amounts of salt (NaCl) and low solute concentrations give low values of $f_{d,i}$ and an increased standard deviation. Considering the ash content of the different types of lignin, a maximum salt concentration between 700 mg/L and 3000 mg/L is expected. However, increased salt concentrations in combination with low solute concentrations lead to lower values of $f_{d,i}$, that is an underestimation of the compound concentration in the aqueous phase and the compound yield. Thus, an assumption of a high value for $f_{d,i}$ must be legitimate. Extraction of all ethylated phenolics, namely 2-ethylphenol, 4-ethylphenol, 4-ethylguaiacol and 4-ethylcatechol, yield a $f_{d,i}$ between 80 % and 90 %. Although the standard deviation is relatively high (above 5 %), the assumption of 80 % $< f_{d,i} <$ 90 % seams reasonable. The increased uncertainty arising from the extraction of course has to be considered for all yields given within this work. High standard deviations and bad agreement for single and bulk experiments are obtained for cyclohexanone. Thus, $f_{d,i}$ for cyclohexanone is set to the highest measured value (80 %) with a standard deviation of 20 %. The distribution of methylcatechol, methylguaiacol, *p*-cresol and *o*-cresol can be determined with low standard deviation by UV-Vis. UV-Vis can however only be applied on the solvent after single experiments, that is, the obtained value does neither take into account the matrix in the aqueous phase, nor the analysis method which is usually

applied on the samples. In the case of methylcatechol, methylguaiacol and *o*-cresol the determination of $f_{d,i}$ via GC-analysis leads to varying values and high standard deviations. The value obtained from UV-Vis-analysis is employed for further calculation combined with the maximum standard deviation resulting from all GC-analysis-results. On the basis of the conducted experiments and the observations made above, the following values for $f_{d,i}$ are applied for the calculation of the concentration in the aqueous phase (see Table B.1).

Table B.1: Applied values of $f_{d,i}$ for quantified phenolics i.

Compound	$C_{i,aq,0}$	Standard deviation	Applied $f_{d,i}$
	mg/L	%	%
2-Ethylphenol	500-1000	6.6	89.0
2-Methylcyclopentanone	200-2000	3.6	77.4
4-Ethylcatechol	500-1000	4.6	88.7
4-Ethylguaiacol	500-1000	5.2	82.2
4-Ethylphenol	500-1000	6.7	85.0
4-Methylcatechol	500-1000	5.9	88.6
4-Methylguaiacol	250-1000	8.1	87.5
Catechol	200-2000	4.1	83.2
Cyclohexanol	100-1000	9.3	67.3
Cyclohexanone	200-2000	20.0	80.0
Cyclopentanone	200-2000	3.6	53.9
Guaiacol	100-1000	1.7	93.5
o-Cresol	500-2000	14.0	96.5
p-Cresol	200-1000	6.2	98.1
Phenol	200-1000	1.6	94.5

Table B.2: Distribution of phenolic products in a two phase system comprising water and ethyl acetate under different conditions.

Compound	Matrix	Analysis method	$C_{i,aq,0}$	NaCl	Exp. redundancy	Standard deviation	Average $f_{d,i}$
			mg/L	mg/L		%	%
2-Ethylphenol	bulk	GC	500-1000	0	8	6.6	89.0
	bulk	GC	100-1000	1000	8	5.3	86.0
2-Methylcyclopentanone	single	GC	500-2000	0	16	3.0	77.4
	single	GC	1000	10000	7	1.3	77.7
	bulk	GC	200-2000	0	14	3.6	76.5
	bulk	GC	100-2000	1000	8	6.9	71.0
4-Ethylcatechol	bulk	GC	500-1000	0	8	4.6	88.7
	bulk	GC	100-1000	1000	8	9.5	75.6
4-Ethylguaiacol	bulk	GC	500-1000	0	8	5.2	82.2
	bulk	GC	100-1000	1000	8	4.1	79.8
4-Ethylphenol	bulk	GC	500-1000	0	8	6.7	85.0
	bulk	GC	100-1000	1000	8	5.0	82.2
4-Methylcatechol	single	GC	500-2000	0	18	5.5	83.7
	single	GC	1000	10000	6	2.2	95.6
	single	UV-Vis	500-1000	0	12	1.2	88.6
	bulk	GC	100-1000	0	8	3.0	78.2
	bulk	GC	500-1000	1000	6	2.9	71.7
4-Methylguaiacol	single	GC	500-2000	0	18	7.1	111.3
	single	GC	1000	10000	6	2.7	99.8
	single	UV-Vis	250-1000	0	12	1.1	87.5
Catechol	single	GC	500-1500	0	10	2.0	83.5
	bulk	GC	200-2000	0	21	4.1	83.2
	bulk	GC	100-1000	1000	8	5.8	75.9
Cyclohexanol	single	GC	500-2000	0	18	2.7	69.0
	single	GC	1000	10000	6	2.5	63.8
	bulk	GC	100-1000	0	8	1.6	67.3
	bulk	GC	50-1000	1000	9	9.3	58.4
Cyclohexanone	single	GC	500-2000	0	18	4.4	57.5
	single	GC	1000	10000	6	2.3	61.1
	bulk	GC	200-2000	0	11	3.2	80.0
	bulk	GC	100-2000	1000	8	6.8	73.1
Cyclopentanone	single	GC	500-2000	0	18	2.3	52.8
	single	GC	1000	10000	6	1.2	56.9
	bulk	GC	200-2000	0	19	3.6	53.9
	bulk	GC	100-2000	1000	8	5.9	46.9
Guaiacol	bulk	GC	100-1000	0	8	1.7	93.5
	bulk	GC	50-1000	1000	9	12.1	82.3
	single	GC	500-2000	0	8	1.7	90.9
	single	GC	1000	1000	4	1.2	91.3
o-Cresol	bulk	GC	200-1000	0	6	15.9	102.3
	bulk	GC	100-1000	1000	11	10.1	88.7
	single	GC	500-2000	0	18	13.3	102.4
	single	GC	1000	10000	6	4.1	111.9
	single	UV-Vis	500-2000	0	12	0.9	96.5
p-Cresol	bulk	GC	200-1000	0	11	6.2	98.1
	bulk	GC	100-1000	1000	8	5.5	93.6
	single	GC	500-2000	0	18	3.4	85.5
	single	UV-Vis	500-2000	0	12	0.4	96.6
Phenol	bulk	GC	100-1000	0	8	1.6	94.5
	bulk	GC	50-1000	1000	9	5.8	88.1
	single	GC	1000	0	6	1.9	98.2
	single	GC	1000	1000	2	3.8	96.8

Appendix C

Modelling

This appendix contains detailed information about the equations and methods used for the modelling of the formal reaction kinetics of thermal lignin degradation in both solvents, ethanol and water. Information about the central optimisation function can be found in Section C.1. All mass balanced reactions and the resulting differential equations which were used for modelling, the thermal degradation of lignin originating from wheat straw in ethanol and formic acid are shown and explained in Section C.2. All mass balanced reactions and the resulting differential equations which were used for modelling the thermal degradation of lignin originating from spruce in water are shown and explained in Section C.3. In Section C.5 the formula for the calculation of the sensitivity analysis is displayed and explained. In Section C.6 the formula for the calculation of the flux analysis is displayed and explained.

C.1 Optimisation function

Modelling was performed in Matlab V 7.12.0, MathWorks using a set of differential equations, which were formulated according to the developed model of reaction participants and pathways which depends mainly on the employed type of solvent and the type of lignin. Every model comprises a number of l defined (lump) components and n reaction pathways. For each reaction pathway a formal kinetic rate coefficient is defined. The reaction order for all reactions is set to one. The unconstrained non-linear Matlab-function «fminsearch«, which uses the simplex search method by Lagarias et al. [Lag+98], was used for optimisation, because of its robustness and

because it does not need derivatives of the objection function. The function "fminsearch" finds the minimum of the scalar function given in Equation C.1, starting at $k_j = 0.001$:

$$f(\vec{k}) = \sum_{i=1}^{l} \sum_{\xi} exp(w_i[y_{i,\xi}^{meas} - y_i^{calc}(\vec{k})]) + exp\left[w_{l+1}\left(\sum_{i}^{l} y_i^{calc}(\vec{k}) - \sum_{i}^{l} y_{i,0}\right)\right], \tag{C.1}$$

where y_i is the yield defined by the following Equation C.2

$$y_i = \frac{m_i}{m_{Lig,0}}, \tag{C.2}$$

i indicates a reaction participant, ξ indicates an experiment, 0 indicates an input parameter, Lig indicates the reactant lignin, m is the mass, w is the weighing factor and $\vec{k} \in \mathbb{R}^n$ comprises the formal kinetic rate coefficients of all reactions k_j. The function f (see Equation C.1) consists of a term which considers the difference between calculated and experimental yields and an additional term which forces the calculation to respect the overall mass balance. If the temperature (T) dependence of k_j of each reaction j was considered, the following Arrhenius-Equation C.3 was employed

$$k_j(T) = A_j \cdot e^{-\frac{E_{A,j}}{RT}}, \; R = 8.314 \; J/(mol \cdot K^{-1}). \tag{C.3}$$

The target values for optimisation in this case were $E_{A,j}$ and A_j. The initial values were chosen to be $\mathrm{E}_{A,j=1,2,\ldots,n} = 100$ kJ/mol and $\mathrm{A}_{j=1,2,\ldots,n} = 10^7$ min^{-1}. If the temperature dependence of k_j was not considered, as for example in Section 6.1, the target value of optimisation was $\vec{k}$. The initial value was $\mathrm{k}_{j=1,2,\ldots,n} = 10^{-3}$ min^{-1}.

The term «apparent activation energy $E_{A,j}$» which expresses the temperature dependence of the formal kinetic rate coefficient k_j is used throughout this work. Since $E_{A,j}$ should fulfil Equation C.3, which comprises the ideal gas constant R, it necessarily has the unit J/mol. This is not correct from a strict scientific point of view, since most reactants are not ideal gases. However, the term «activation energy» is predominantly used in literature, even if only solid lignin is involved in the reaction. Thus for better comparison of the data obtained here with values obtained by other authors, the temperature dependence of the reactions was expressed by the term $E_{A,j}$. It should further be pointed out that a chemical reaction model would only then be

able to describe the experimental data correctly, if all the relevant reaction pathways are contained in the model. The ultimate number of reactions (and rate coefficients k_j) in a model are of minor significance.

C.2 Solvolysis in ethanol

The Equations (C.4) to (C.14) are the differential equations describing the formal kinetics of the developed model for thermal lignin degradation in ethanol and formic acid. They are based on the mass-balanced reactions shown in Figure C.1. The index j of the formal kinetic parameters k_j corresponds to the index of the reactions displayed in Figure C.1. Each index i of the yields y_i corresponds to one participating component. All components and their indices are listed in Table C.1.

The differential equations describe the consumption and formation of all components i through the reactions j considered by the model for solvolysis of wheat straw lignin in ethanol and formic acid (see Figure 6.7), where $y_{i,0}$ and y_i are, respectively, the entering and outgoing mass of the component i divided by the input mass of lignin $m_{Lig,0}$. If the model is applied for the simulation of thermal lignin degradation in a batch reactor Equations (C.4) to (C.14) were used without the term $\left[(y_{i,0} - y_i) \cdot \frac{\dot{m}}{m}\right]$. If it is used for the simulation of thermal lignin degradation in a CSTR they have to be employed with the mentioned term in rectangular brackets. The latter considers the continuous character of the process and the mixed flow inside the CSTR, assuming an ideal reactor. The following assumptions are to be considered only for CSTR: The quotient of the flow rate $\dot{m}$ divided by the reaction mass m is equivalent to the mean residence time τ'. The reaction mass is estimated by the volume of the reactor (200 mL) and the density of the solvent at given temperature and pressure displayed in Table 6.4. The experimental duration is defined as t, the set-point $t = 0$ is the start of the experiment when the suspension of ethanol, formic acid and lignin is pumped into the reactor.

$$\frac{dy_1}{dt} = -k_1 y_1 - k_6 y_1 - k_{10} y_1 + \left[(y_{1,0} - y_1) \cdot \frac{\dot{m}}{m}\right] \tag{C.4}$$

$$\frac{dy_2}{dt} = k_1 y_1 + k_{15} y_8 - k_2 y_2 + \left[(y_{2,0} - y_2) \cdot \frac{\dot{m}}{m}\right] \tag{C.5}$$

$$\frac{dy_3}{dt} = 0.89 \cdot k_2 y_2 - k_4 y_3 - k_3 y_3 + \left[(y_{3,0} - y_3) \cdot \frac{\dot{m}}{m}\right] \tag{C.6}$$

$$\begin{aligned}\frac{dy_4}{dt} =& 0.85 \cdot k_4 y_3 + 0.77 \cdot (k_7 y_6 - k_{14} y_4 + k_9 y_7 - k_8 y_4) + \\ & - k_5 y_4 - k_{17} y_4 + \left[(y_{4,0} - y_4) \cdot \frac{\dot{m}}{m}\right]\end{aligned} \tag{C.7}$$

$$\frac{dy_5}{dt} = 0.91 \cdot k_3 y_3 + 0.98 \cdot k_{17} y_4 + k_{16} y_8 + \left[(y_{5,0} - y_5) \cdot \frac{\dot{m}}{m}\right] \tag{C.8}$$

$$\frac{dy_6}{dt} = k_6 y_1 - k_7 y_6 + k_{14} y_4 + \left[(y_{6,0} - y_6) \cdot \frac{\dot{m}}{m}\right] \tag{C.9}$$

$$\frac{dy_7}{dt} = k_8 y_4 - k_9 y_7 + \left[(y_{7,0} - y_7) \cdot \frac{\dot{m}}{m}\right] \tag{C.10}$$

$$\frac{dy_8}{dt} = k_{10} y_1 - k_{11} y_8 - k_{15} y_8 - k_{16} y_8 + \left[(y_{8,0} - y_8) \cdot \frac{\dot{m}}{m}\right] \tag{C.11}$$

$$\begin{aligned}\frac{dy_9}{dt} =& 0.11 \cdot k_2 y_2 + 0.09 \cdot k_3 y_3 + 0.15 \cdot k_4 y_3 + k_5 y_4 + \\ & 0.23 \cdot (k_7 y_6 - k_{14} y_4 + k_9 y_7 - k_8 y_4 + k_{11} y_8) + k_{12} y_{11} + \\ & k_{13} y_{10} + 0.02 \cdot k_{17} y_4 + \left[(y_{9,0} - y_9) \cdot \frac{\dot{m}}{m}\right]\end{aligned} \tag{C.12}$$

$$\frac{dy_{10}}{dt} = -k_{13} y_{10} + \left[(y_{10,0} - y_{10}) \cdot \frac{\dot{m}}{m}\right] \tag{C.13}$$

$$\frac{dy_{11}}{dt} = -k_{12} y_{11} + \left[(y_{11,0} - y_{11}) \cdot \frac{\dot{m}}{m}\right] \tag{C.14}$$

For the kinetic modelling pseudo-elementary reactions were defined (see Figure C.1). In fact, the reactions r_2 - r_4 and r_{17} involve lumped components which can not be associated with a molecular structure as indicated in the reaction equation. However, the defined mass balanced reactions provide an orientation for the mass distribution throughout the reaction. The employed coefficients might be reconsidered in the future respecting the important condition that the right and the left side of each equation are equilibrated.

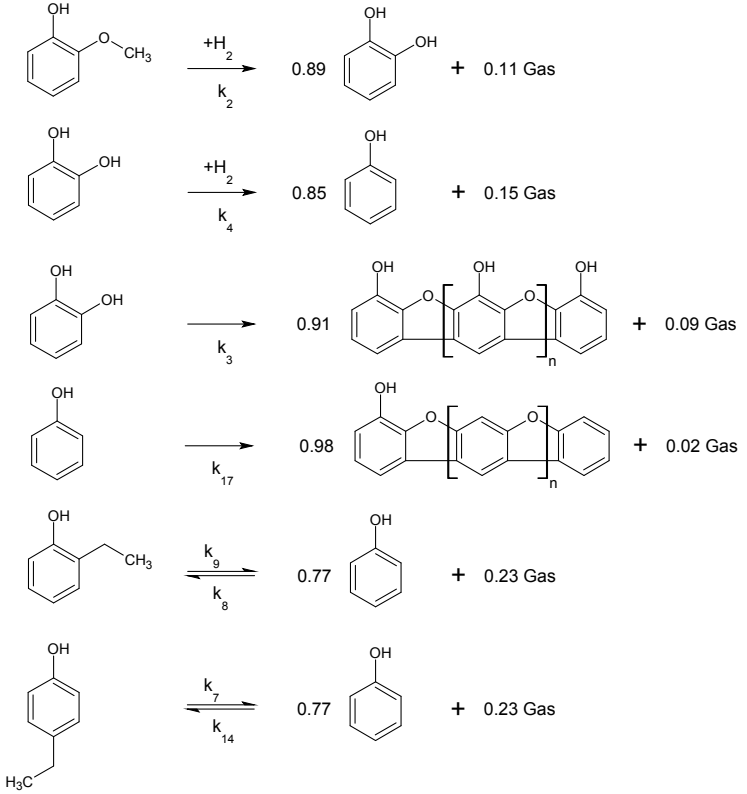

Figure C.1: Mass balanced reactions for modelling thermal degradation of wheat-straw lignin in ethanol.

Table C.1: Indices of reaction participant

Index	Participant	Index	Participant
1	Lignin	7	2-Ethylphenol
2	methoxyPhOH	8	L_D, EtOH-soluble residue
3	Catechols	9	Gas
4	PhOH	10	Formic Acid
5	Char, EtOH-insoluble residue[a]	11	Ethanol
6	4-Ethylphenol		

[a] except not reacted lignin.

C.3 Solvolysis in water

The Equations (C.15) to (C.24) are the differential equations describing the formal kinetics of the developed model for thermal lignin degradation in water. They are based on the mass-balanced reactions shown in Figure C.2. The index of the formal kinetic parameters corresponds to the index of the reactions displayed in Figure C.2. Each index i of the yields y_i or masses m_i corresponds to one participating component i. All components and indices are listed in Table C.1.

The differential equations describe the consumption and formation of all components i through the reactions j considered by the model for hydrothermal degradation of spruce lignin (see Figure 6.17), where $y_{i,0}$ and y_i are, respectively, before and after the reaction the mass of the component i divided by the input mass of lignin $m_{Lig,0}$. The optimisation function uses a numerical solution of Equations (C.15) to (C.24) for the calculation of y_i. For the kinetic modelling pseudo-elementary reactions were defined (see Figure C.1). In fact, the reactions r_2 - r_6 involve lumped components which can not be associated with a molecular structure as indicated by the reaction equation. However, the defined mass balanced reactions provide an orientation for the mass distribution throughout the reaction. The employed coefficients might be reconsidered in the future respecting the important condition that the right and the left side of each equation are equilibrated.

Table C.2: Indices of reaction participant

Index	Participant	Index	Participant
1	Lignin	6	L_{D2}, reactive intermediates, not detectable in GC
2	methoxyPhOH	7	CO_2 and CH_4
3	Catechols	8	Water
4	PhOH	9	L_{D2}, stable products, partially water-soluble
5	Char, Water-insoluble residue[a]	10	CO and H_2

[a] except not reacted lignin.

$$\frac{dy_1}{dt} = -k_1 y_1 - k_7 y_1 \tag{C.15}$$

$$\frac{dy_2}{dt} = k_1 y_1 - 0.98 \cdot k_2 y_2 - k_3 y_2 \tag{C.16}$$

$$\frac{dy_3}{dt} = 0.87 \cdot k_2 y_2 + k_{10} y_6 - 0.8 \cdot k_4 y_3 - k_5 y_3 - k_{12} y_3 \tag{C.17}$$

$$\frac{dy_4}{dt} = 0.68 \cdot k_4 y_3 + 0.76 \cdot k_3 y_2 - 0.62 \cdot k_6 y_4 \tag{C.18}$$

$$\frac{dy_5}{dt} = 0.82 \cdot k_5 y_3 + k_9 y_6 \tag{C.19}$$

$$\frac{dy_6}{dt} = k_7 y_1 - (k_8 + k_9 + k_{10} + k_{11} + k_{15}) y_6 \tag{C.20}$$

$$\frac{dy_7}{dt} = 0.13 \cdot k_2 y_2 + 0.24 \cdot k_3 y_2 + 0.32 \cdot k_4 y_3 + k_{11} y_6 + + 0.96 \cdot k_{13} y_{10} + k_{14} y_{10} + k_6 y_4 \tag{C.21}$$

$$\frac{dy_8}{dt} = 0.16 \cdot k_5 y_3 - 0.35 \cdot k_6 y_4 - 0.39 \cdot k_{13} y_{10} \tag{C.22}$$

$$\frac{dy_9}{dt} = k_8 y_6 + k_{12} y_3 \tag{C.23}$$

$$\frac{dy_{10}}{dt} = 0.02 \cdot k_5 y_3 + k_{15} y_6 - 0.02 \cdot k_2 y_2 - 0.2 \cdot k_4 y_3 - + 0.03 \cdot k_6 y_4 - 0.57 \cdot k_{13} y_{10} - k_{14} y_{10} \tag{C.24}$$

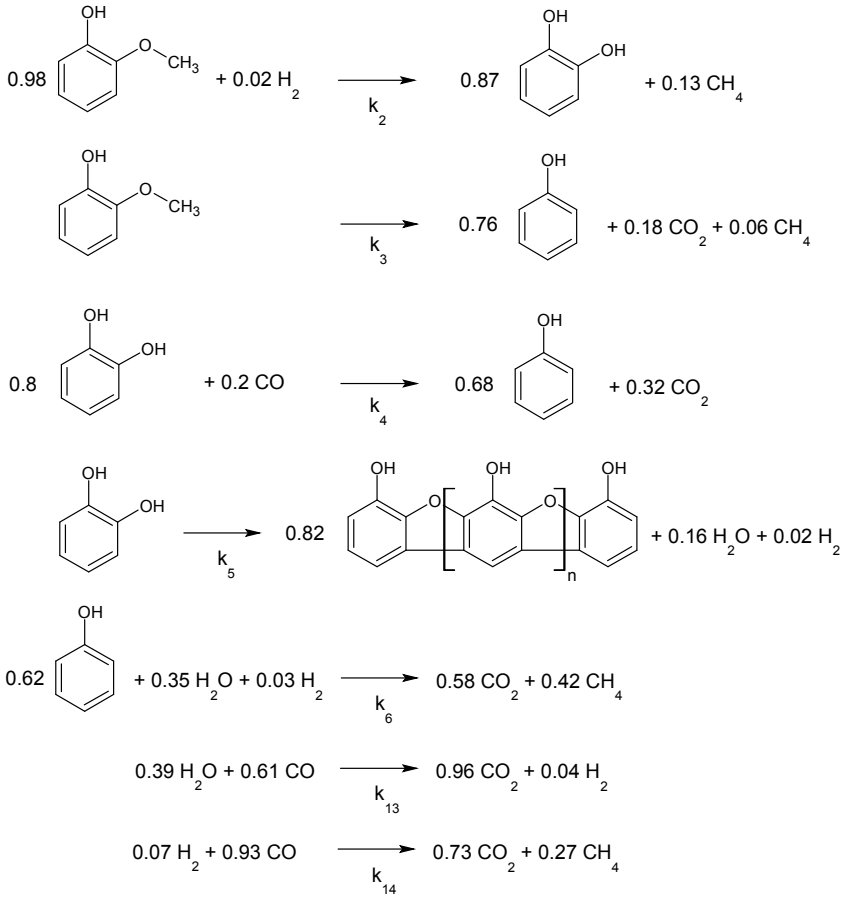

Figure C.2: Mass balanced reactions for modelling the hydrothermal degradation of spruce-lignin.

C.4 Analysis of error

For the analysis of the experimental error, multiple identical experiments were carried out. For the evaluation of the experimental error the standard deviation σ was employed. For the evaulation of the quality of kinetic modelling the coefficient of determination R^2 and the standard deviation σ were employed. R^2 was calculated (see Equation C.25) by comparing the difference of calculated yield y_i^{calc} or concentration and the measured yield $y_{i,\xi}^{meas}$ or concentration with the difference of measured yield $y_{i,\xi}^{meas}$ or concentration and the average yield $\overline{y}_i^{meas}$ or concentration.

$$R^2 = 1 - \frac{\sum_\xi (y_i^{calc} - y_{i,\xi}^{meas})^2}{\sum_\xi (\overline{y}_i^{meas} - y_{i,\xi}^{meas})^2} = 1 - \frac{\sum_\xi (C_i^{calc} - C_{i,\xi}^{meas})^2}{\sum_\xi (\overline{C}_i^{meas} - C_{i,\xi}^{meas})^2}, \qquad \text{(C.25)}$$

where $\overline{y}_i^{meas}$ is the average of the yield of the component i measured in the product of all experiments carried out at the same temperature. The standard deviation σ is given by Equation C.26

$$\sigma = \sqrt{(\Xi - 1)^{-1} \sum_{\xi=1}^{\Xi} \left(\frac{y_i^{calc} - y_{i,\xi}^{meas}}{y_{i,\xi}^{meas}} \right)^2}, \qquad \text{(C.26)}$$

where Ξ is the number of experiments which are considered. The difference between calculated yield y_i^{calc} and measured yield $y_{i,\xi}^{meas}$ is normed by dividing by $y_{i,\xi}^{meas}$ (see Equation C.26). If the standard deviation of the results of several identical experiments was calculated, glssymb:yicalc is to be replaced by the average of all considered identical experimental results $\overline{y}_i$. The denominator of the squared term is to be replaced by the average value $\overline{y}_i$ (see Equation C.27). The resulting value standard deviation is mostly displayed in %, thus multiplied by the factor 100.

$$\sigma = \sqrt{(\Xi - 1)^{-1} \sum_{\xi=1}^{\Xi} \left(\frac{\overline{y}_i - y_{i,\xi}^{meas}}{\overline{y}_i} \right)^2}, \qquad \text{(C.27)}$$

C.5 Sensitivity analysis

The sensitivity analysis shows the influence of the different reactions defined in a reaction model on the yield of the components. Single rate coefficients are altered by a factor of 2 and the resulting yields of the components are

compared with the original values. This difference is defined as the sensitivity. The sensitivity of a each component i to each reaction r_j is displayed in the sensitivity matrix (see Figure 6.14 and 6.21). In the case of the batch experiments the sensitivity $\Delta y_{i,Batch}$ is calculated by integration of the difference between the original yield y_i and the yield y_i' after modification of k_j. The lower limit of integration is the start of the reaction t_0 and the upper limit is the determined residence time τ (see Equation C.28). Contemplating Equation C.28 it becomes clear that the choice of the upper integration limit changes the resulting sensitivity. For comparison of the batch-fit and the CSTR-fit, the upper integration limit for $\Delta y_{i,Batch}$ is chosen to be equal to the mean residence time in the CSTR $\tau = \tau'$.

$$\Delta y_{i,Batch} = \frac{1}{\tau} \cdot \int_{t_0}^{\tau} \left| \frac{y_i' - y_i}{y_i} \right| dt, \tag{C.28}$$

In case of the CSTR the sensitivity is quantified by $\Delta y_{i,CSTR}$, which is the difference between the original yield y_i and the yield after modification of each rate coefficient y_i' in the stationary state ($t \to \infty$) at a set temperature and mean residence time τ'.

$$\Delta y_{i,CSTR} = \left| \frac{y_i' - y_i}{y_i} \right| \tag{C.29}$$

C.6 Flux analysis

The flux implies the mass of a component i that disappears via a certain reaction r_j during a certain time period in a determined reaction volume. In the case of the batch reactor, the flux from the start of the reaction until the residence time τ was calculated by integration, according to Equation C.30:

$$flux_{j,Batch} = C_{Lig,0} \cdot \int_{t_0}^{\tau} k_j y_{i,j}\, dt, \tag{C.30}$$

where $C_{Lig,0}$ is the initial concentration of lignin in the batch autoclave, k_j the formal kinetic rate coefficient of the first order reaction r_j and $y_{i,j}$ the time depending yield of the corresponding component i which is either a reactant or a product of this reaction. Since reactions are assumed to be first order reactions, the flux of each reaction depends on the yield $y_{i,j}$ of exactly one corresponding component. For comparison of the the fluxes in the two different types of reactor the integration limit τ was chosen to be identical to the mean residence time in the CSTR τ'. In the case of the CSTR the

flux in the steady state is calculated according to Equation C.31:

$$flux_{j,CSTR} = C_{Lig,0} \cdot \tau' \cdot k_j y_{i,j}, \tag{C.31}$$

where τ' is the mean residence time and $y_{i,j}$ is independent from the experimental duration since stationary state is assumed ($t \to \infty$).

Appendix D

Extended studies of catalysts

D.1 Homogeneous catalysts

Homogeneous catalysts in water were tested at a reaction temperature of 633 K and a residence time of 30 min. Basic catalysts, that are KOH and NaOH, as well as acidic catalysts, that are HCl, AA and FA, were used. Basic catalysts promote the formation of catechols. Their yield increases from approximately 5 to approximately 20 mg/g_{lignin}. The yield of methoxyphenols decreases slightly and the yield on phenols increases (see Figure D.1).

The use of acidic catalysts give very different results. If HCl is employed as catalyst for the hydrothermal degradation of spruce-lignin the yields of the main products are strongly dependent on the concentration of HCl. Lower concentrations (0.33 mol/L) yield relatively high amounts of catechols (16 mg/g_{lignin}) and CO (29 mg/g_{lignin}). Methoxyphenols could not be detected neither at low nor high concentrations (1.81 mol/L) of HCl. The yield of catechols and CO significantly decrease when the concentration of HCl is increased to 1.81 mol/L to approximately 10 mg/g_{lignin} and 12 mg/g_{lignin} respectively (see Figure D.2). In addition, at increasing concentrations of HCl an increase of the yield of CO_2 and hydrocarbon (HC)-gases is observed. The addition of AA into the reactor has no or a very small effect on the product distribution.

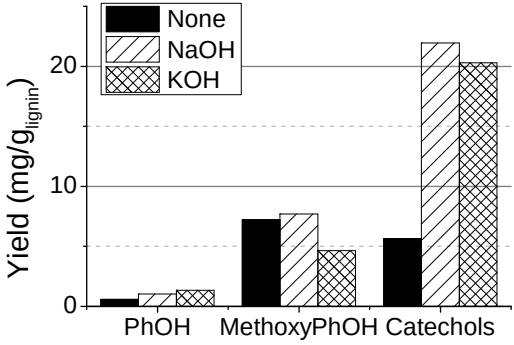

Figure D.1: Comparison of homogeneous basic catalysts with 0.12 mol/L input concentration in a spruce-lignin/water = 133 g/L suspension; $T = 633$ K (Exp. 1 and 7-9); $\tau = 30$ min

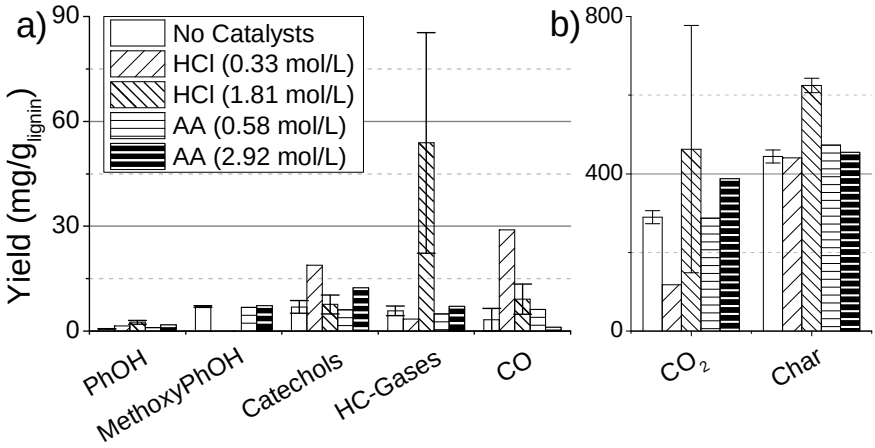

Figure D.2: Comparison of homogeneous acidic catalysts with varying input concentration in a spruce-lignin/water = 133 g/L suspension (Exp. 2-6 and 8-9); $T = 633$ K; $\tau = 30$ min

HCl obviously has a strong effect not only on the cleavage of the bonds between lignin monomers, as the increased yield of catechols shows, but also on the gasification and the char yield. Low concentrations yield high amounts of CO, probably coming from the lignin structure due to increased cleavage of ether bonds connected with the liberation of CO. Increased amounts of HCl lead to very high yields of CO_2 and Char. Water-gas shift reaction or oxidation of CO might be responsible for increased amounts of CO_2. The effects of formic acid on the phenolic products observed at the mentioned temperature are weaker than those of HCl. Obviously the input of acetic acid has to be increased significantly in order to obtain a similar effect as contemplated for experiments with HCl. A catalytic effect of both, acidic and basic media, on the hydrolysis of lignin in near critical water was observed like suggested by Toor, Rosendahl, and Rudolf [TRR11]. A more detailed investigation in order to optimise yield and selectivity of single phenolic products of the hydrothermal lignin depolymerisation is of high interest.

D.2 Catalytic hydrothermal decomposition of catechol

Catechols are produced within the hydrothermal lignin degradation. Among the phenolic products they are the most abundant compound class with yields above 3 wt% (see Section 6.3). However, for the chemical industry catechols are less interesting as platform chemicals. In addition, they have a high potential to repolymerise under pyrolytic conditions [McM+04]. Thus the transformation of catechols into higher value products such as phenol or benzene deserves a more detailed observation. In Chapter 5 the potential of the heterogeneous catalyst Raney-Ni for the conversion of catechol into phenol [For+12] was pointed out. This section shows a kinetic study of the hydrothermal conversion of catechol into phenol catalysed by Raney-Ni.

D.2.1 Results

For the purpose of a detailed investigation of the effects of Raney-Ni on the conversion of catechol into phenol a set of 23 experiments (Exp. 103-125, see Appendix E.1) was carried out at temperatures between 473 K and 573 K and residence times between 30 and 180 min. Catechol was therefore diluted in desalinated water and together with Raney-Ni and elemental H_2 treated in a 10 mL batch autoclave (MA2). In Figure D.3 the results of different experiments at 573 K and different residence times are demonstrated showing the mass fractions related to the input mass, that is the sum of the mass of

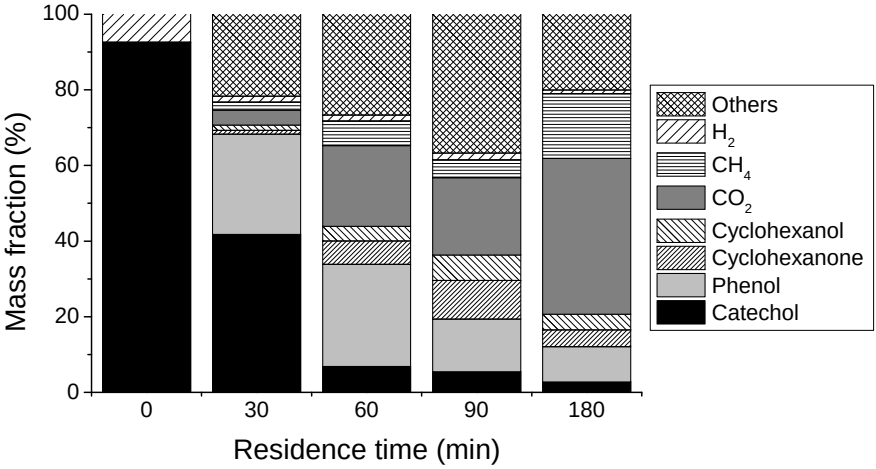

Figure D.3: Mass fractions of the input (residence time = 0) and output at 573 K and different residence times after hydrothermal decomposition of catechol in a 10 mL-MA2; 5 ml input of aqueous solution (catechol/water = 10 g/L); 2.2 mg Raney-Ni catalyst

catechol and H_2. Water was not considered to take part in any reaction. This is a simplification of the reaction system since water gas shift reaction and other reactions might occur and involve water. However, water is abundantly present throughout the reaction and thus changes of the water concentration may not influence the reaction kinetics. The results at 573 K show that phenol is produced in significant amounts as primary product. The amount of phenol decreases towards longer reaction times giving way to other phenol derivatives, such as cyclohexanol and cyclohexanone as well as to gaseous products such as CO_2 and CH_4. The elemental H_2 is partially consumed within the ongoing reactions.

In the following the reaction pathways of hydrothermal decomposition of catechol will be fathomed. Nimmanwudipong et al. showed that cyclohexanone is an important intermediate compound especially within the decomposition of methoxyphenols and is converted into cyclohexanol [Nim+11a; Nim+11b]. The rank of cyclohexanol and cyclohexanone could not be revealed by delplot-analysis for the present data. However, both compounds are produced in significant concentrations at high temperatures which indicates these substances to be secondary or tertiary products. The rank of the gaseous compounds as well stays unclear. Delplot analysis did not reveal any

illuminating hints. However, CO_2 and CH_4 appear at temperatures above 523 K and increased residence times. Hence, they are probably secondary or tertiary products formed within the decomposition of phenol and/or cyclohexanol and cyclohexanone. Gasification of catechol, that is the direct conversion of catechol into gaseous products, was not assumed. The focus of the kinetic studies lied on the formation and decomposition of phenol. Hence, phenol was assumed to be the only primary product derived from catechol.

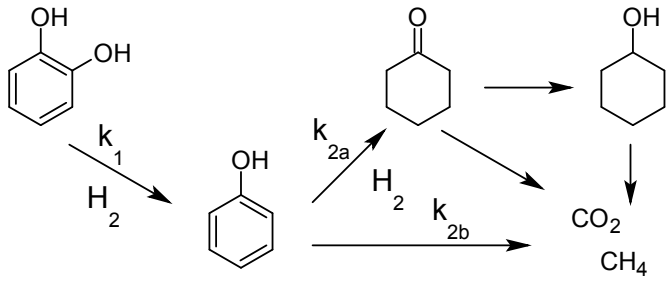

Figure D.4: Reaction scheme of the catalytic decomposition of catechol in water at temperatures between 523 K and 573 K based on delplot-analysis and literature research.

The hydrothermal decomposition of catechols can thus be modelled with the reaction pathways displayed in Figure D.4. The conversion of catechol into phenol (k_1) and the decomposition of phenol (k_{2a}+k_{2b}) as subsequent reaction is suggested to be sufficient to describe the concentration of phenol in the product mixture. The two reactions are treated like two first order reactions in series. The author is aware of the fact that the second reaction, that is the decomposition of phenol is not an intrinsic elementary reaction and might be a combination of two or more parallel reactions, *e.g.* reaction 2a and 2b. These assumptions lead to the following Equation D.1 for the calculation of the concentration of Catechol C_A in dependence on the residence time τ considering the initial concentration of catechol $C_{A,0}$ and the rate coefficient of the first order decomposition of catechol k_1.

$$C_A = C_{A0} \cdot e^{-k_1 \tau} \tag{D.1}$$

The concentration of phenol C_P can thus be calculated considering k_1

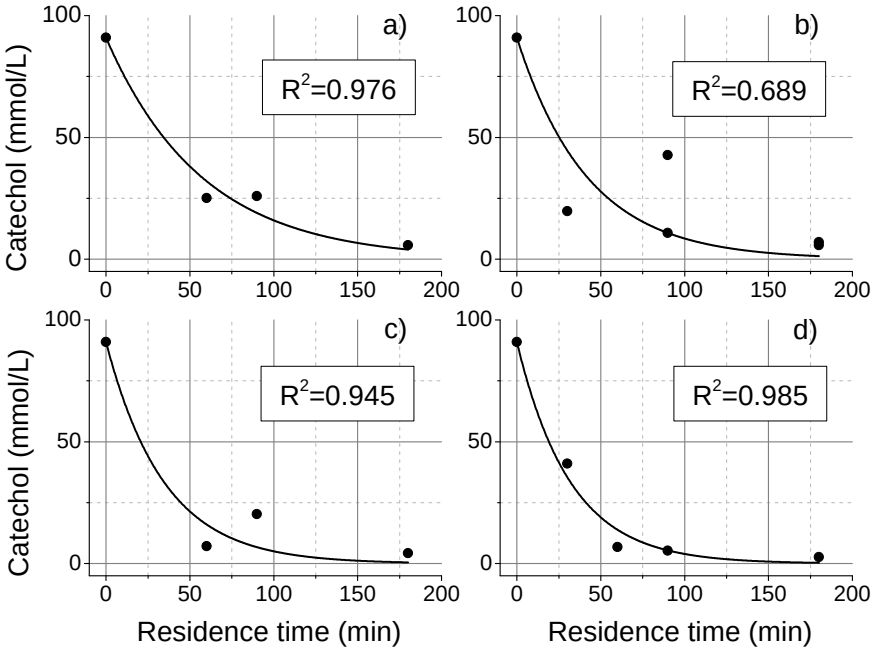

Figure D.5: Concentration of catechol in the product after hydrothermal decomposition of catechol depending on the residence time at a) 573 K, b) 533 K, c) 523 K, d) 513 K; Data points represent experimental values, continuous line calculated according to Equation D.1; 5 ml input of catechol/water = 10 g/L; 2.2 mg Raney-Ni catalyst.

and the rate coefficient of the phenol decomposition k_2.

$$C_P = C_{A0} \cdot \frac{k_1}{k_2 - k_1}(e^{-k_1\tau} - e^{-k_2\tau}), \quad k_2 = k_{2a} + k_{2b}. \tag{D.2}$$

The optimised rate coefficient of the decomposition of catechol k_1 is determined by minimising the difference between the concentration C_A calculated with Equation D.1 and the experimentally determined concentration C_A. The curves which are described by Equation D.1 providing the best fit to the experimentally determined C_A are plotted over the residence time at different temperatures (see Figure D.5). The resulting optimised rate coefficients k_1 an k_2 between 513 K and 573 K are plotted in an Arrhenius-diagram (see Figure D.7). Towards increasing temperatures the value of the

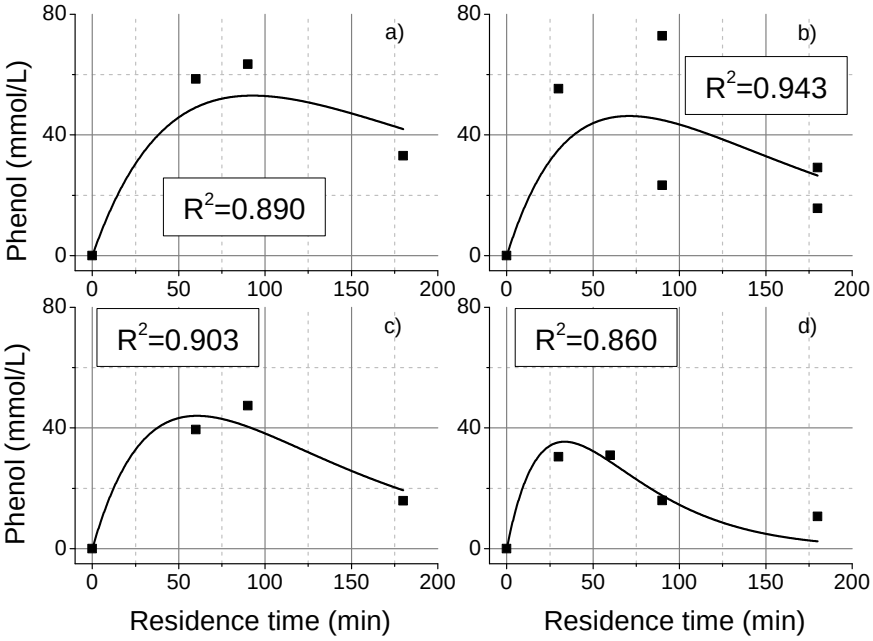

Figure D.6: Concentration of phenol in the product after hydrothermal decomposition of catechol depending on the residence time at a) 513 K, b) 523 K, c) 533 K and d) 573 K; Data points from experiments, continuous line calculated according to Equation D.2; 5 ml input of catechol/water = 10 g/L; 2.2 mg Raney-Ni catalyst.

optimised k_1 increases. The temperature dependence of a kinetic rate coefficient can be described by the Arrhenius-Equation C.3. Optimisation of the linear approach of k_1 in the Arrhenius-diagram yields the kinetic parameters $E_{A,j}$ and A_j, which are shown in Table D.1. The experimentally determined concentration of catechol is plotted over the residence time at different temperatures in Figure D.5. The curves resulting from the optimisation of k_1 are added. The regression of the catechol concentration was acceptable. For all temperatures except 523 K R^2 was above 0.9. The optimisation of the rate coefficient of the decomposition of phenol k_2 is carried out analogously. The difference between C_P calculated by Equation D.2 and the experimentally determined concentration C_P is minimised. The rate coefficient k_1 and the initial concentration of catechol were hereby fixed parameters in Equation D.2; k_1, E_{A1} and Arrhenius factor A_1 result from the prior optimisation.

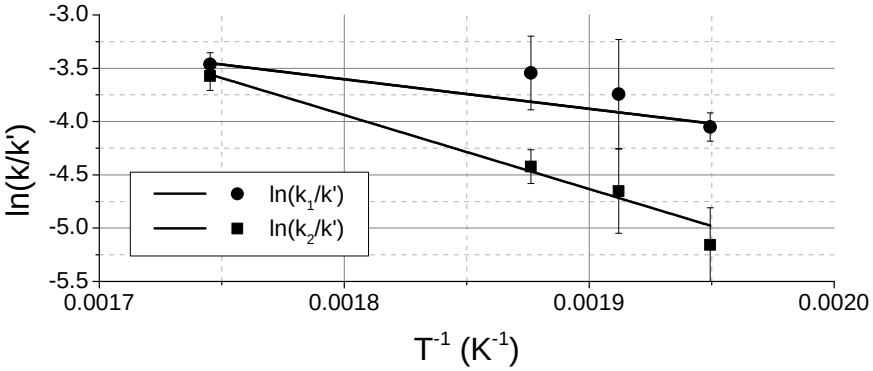

Figure D.7: Arrhenius plot of pseudo-first order rate coefficients of the hydrothermal Raney-Ni catalysed decomposition of catechol (circular data points) and phenol (rectangular data points), $k' = 1\text{min}^{-1}$

Table D.1: Parameters describing the decomposition of catechol and phenol within hydrothermal catechol decomposition catalysed by Raney-Ni.

r_j	k_j				$E_{A,j}$	A_j
	$T = 513$ K	$T = 523$ K	$T = 533$ K	$T = 573$ K		
	min^{-1}				kJ/mol	min^{-1}
r_1	0.017	0.024	0.029	0.031	23 ± 4	0.6 ± 0.4
r_2	0.006	0.010	0.012	0.028	58 ± 5	3.7 ± 0.4

Figure D.6 shows the concentration of phenols. The scattered data points represent the experimentally determined concentrations, the curves show the calculated concentration resulting from the optimisation of k_2. The rate coefficient of phenol decomposition k_2 in dependence of the temperature is plotted in Figure D.7. The coefficient of determination R^2 was above 0.85 for all temperatures.

D.2.2 Discussion

The experimental data shows that the concentration of catechol is declining with increasing temperature and residence time. The concentration of phenol increases at short residence times and decreases towards longer residence times in dependence on the temperature. The modelling of the experimental yields shows that a simple two step reaction pathway comprising the primary

conversion of catechol into phenol followed by the decomposition of phenol is able to describe the yields of catechol and phenol. The model fit is acceptable since in the temperature range from 513 to 573 K the coefficient of determination was above 0.65 and mostly above 0.85. The kinetics of the mentioned reaction series was analysed. The results show rather low apparent activation energies, about 23 kJ/mol for the decomposition catechol and 58 kJ/mol for the decomposition phenol. The activation energy calculated for the catechol decomposition within the hydrothermal lignin degradation (see Chapter 6.3) was 55 kJ/mol, the non-catalytic hydrothermal catechol decomposition studied by Wahyudiono, Sasaki, and Goto [WSG09] yielded an apparent activation energy of 51 kJ/mol, which is about two times higher than the apparent activation energy of the catalytic decomposition. This indicates that probably diffusion effects dominate the reaction rate of the catalytic catechol decomposition. These effects are especially important with increasing temperatures as the relatively low increase of reaction rate coefficient from 0.029 to 0.031 min^{-1} between 533 and 573 K shows (see Table D.1). However, it becomes clear that the reaction rate of hydrothermal catechol decomposition can be increased significantly by the application of Raney-Ni compared to experiments without catalyst. Wahyudiono et al. [WSG09] reported rate coefficients of about 0.0001 min^{-1} for non-catalytic catechol decomposition in supercritical water at 683 K, whereas catalytic catechol decomposition yields rate coefficients of about 0.03 min^{-1} at 533 K.

Appendix E

Experimental results

E.1 Tables of experimental results

The following tables contain the data of the experiments carried out. Listed are

- the type of reactor, MA meaning microbatch-autoclave, CSTR meaning continuous stirred tank reactor. Two types of MA were used that are MA1 which is the simple type and MA2 which is the gas-input version with the possibility of pressurising the reactor with any kind of gas,
- the reaction volume V_R which is equal to the volume of the reactor,
- the (mean) residence time τ (τ'),
- the reaction temperature T,
- type and initial input mass of the Biomass (Lignin),
- type and initial input mass of the solvent,
- type and initial input mass of the added gas or H_2-donor,
- type and initial input amount of the catalyst. The initial amount for homogeneous catalysts is given in mol/L, for heterogeneous catalysts in mg,
- the analysis methods applied on the product phases of each experiment, that are extraction (Ext), GC, KFT, UV-Vis, FT-IR,

- the mass of the liquid product phase which was gravimetrically determined,
- the output mass of gaseous and solid phase determined by the sum of the mass of each constituent and by gravimetric analysis respectively,
- the loss for each experiment which is the difference between the sum of the mass of all input materials and the sum of the mass of all output materials ($\sum m_{i,0} - \sum m_i$)
- the yield of the gaseous compounds that are methane, ethene, ethane, propene, propane, butane, carbon dioxide, hydrogen, carbon monoxide and other gases,
- the recovered amount of water and ethanol related to the input mass of lignin,
- the yield of all liquid products detected by GC-analysis, that are phenol (Phe), 2-methylphenol (MePhe), 4-MePhe, 2-EtPhe, 4-EtPhe, guaiacol (Gua), 4-methylguaiacol (MeGua), 4-ethylguaiacol (EtGua), syringol (Syr), catechol (CatOH), 4-methylcatechol (MeCatOH), 4-ethylcatechol (EtCatOH), cyclohexanol (CyclohexOH) and cyclohexanone (CyclohexO).

All yields are given in $mg/g_{Biomass}$. If the displayed value of the yield is zero, the detected yield was smaller than 0.5 $mg/g_{Biomass}$. If the compound was not detected even in small quantities, this is indicated by not detected (n.d.). If the compound was not quantified analytically this is indicated by not available (n.a.). For experiments in the CSTR the input and output amounts are given in g/h.

Table E.1: Experimental data: reaction conditions, input parameters, employed analytical methods.

Exp.	Reactor		τ (τ')	T	Biomass		Solvent		H-Donor/Gas		Catalyst		Analysis[c]
	Type	V_R			Type	$m_{i,0}$	Type	$m_{i,0}$	Type	$m_{i,0}$	Type	Amount[a]	
#		ml	min	K		g		g		mg			
1	MA2	5.5	30	633	spruce-Lig	0.40	H_2O	3.0	H2	14	KOH	0.12	Ext.GC
2	MA2	5.5	30	633	spruce-Lig	0.40	H_2O	3.0	N_2	3	HCl	1.81	Ext.GC
3	MA2	5.5	30	633	spruce-Lig	0.40	H_2O	3.0	N_2	4	HCl	0.33	Ext.GC
4	MA2	5.5	30	633	spruce-Lig	0.40	H_2O	3.0	N_2	155	HCl	1.81	Ext.GC
5	MA2	5.5	30	633	spruce-Lig	0.40	H_2O	3.0	N_2	155	Acetic Acid	2.92	Ext.GC
6	MA2	5.5	30	633	spruce-Lig	0.40	H_2O	3.0	N_2	188	Acetic Acid	0.58	Ext.GC
7	MA2	5.5	30	633	spruce-Lig	0.40	H_2O	3.0	N_2	188	NaOH	0.12	Ext.GC
8	MA2	5.5	30	633	spruce-Lig	0.40	H_2O	3.0	N_2	155	None	0	Ext.GC
9	MA2	5.5	30	633	spruce-Lig	0.40	H_2O	3.0	N_2	188	None	0	Ext.GC
10	MA2	5.5	30	633	spruce-Lig	0.40	H_2O	2.8	N_2	155	Raney-Ni	234	Ext.GC
11	MA2	5.5	30	633	spruce-Lig	0.40	H_2O	2.8	H_2	14	Raney-Ni	234	Ext.GC
12	MA2	5.5	30	633	spruce-Lig	0.40	H_2O	3.0	H_2	13	Rh(5 wt%)/C[b]	30	Ext.GC
13	MA2	5.5	30	633	spruce-Lig	0.40	H_2O	3.0	N_2	155	Co	27	Ext.GC
14	MA2	5.5	30	633	spruce-Lig	0.40	H_2O	3.0	H_2	14	Co	12	Ext.GC
15	MA2	5.5	30	633	spruce-Lig	0.40	H_2O	3.0	N_2	155	Pt(5 wt%)/Al_2O_3[b]	17	Ext.GC
16	MA2	5.5	30	633	spruce-Lig	0.40	H_2O	3.0	N_2	188	Pt(5 wt%)/Al_2O_3[b]	10	Ext.GC
17	MA2	5.5	30	633	spruce-Lig	0.40	H_2O	3.0	H_2	11	Pt(5 wt%)/Al_2O_3[b]	30	Ext.GC
18	MA2	5.5	30	633	spruce-Lig	0.40	H_2O	3.0	H_2	14	Pt(5 wt%)/Al_2O_3[b]	22	Ext.GC
19	MA2	5.5	30	633	spruce-Lig	0.40	H_2O	3.0	N_2	155	$PdCl_2$	32	Ext.GC
20	MA2	5.5	30	633	spruce-Lig	0.40	H_2O	3.0	H_2	14	$PdCl_2$	30	Ext.GC
21	MA2	5.5	30	633	spruce-Lig	0.40	H_2O	3.0	H_2	11	Raney-Ni	59	Ext.GC
22	MA2	5.5	30	633	spruce-Lig	0.40	H_2O	3.0	H_2	14	Raney-Ni	23	Ext.GC
23	MA2	5.5	30	633	spruce-Lig	0.40	H_2O	2.5	N_2	155	Raney-Ni	586	Ext.GC
24	MA2	5.5	30	633	spruce-Lig	0.40	H_2O	2.0	N_2	188	Raney-Ni	1172	Ext.GC
25	MA2	5.5	30	633	spruce-Lig	0.40	H_2O	2.9	N_2	155	Raney-Ni	117	Ext.GC
26	MA2	5.5	30	633	spruce-Lig	0.40	H_2O	2.7	N_2	188	Raney-Ni	352	Ext.GC
27	MA2	5.5	30	633	spruce-Lig	0.40	H_2O	2.8	N_2	155	Raney-Ni	234	Ext.GC
28	MA2	5.5	30	633	spruce-Lig	0.40	H_2O	2.8	N_2	3	Raney-Ni	234	Ext.GC
29	MA2	5.5	30	633	spruce-Lig	0.40	H_2O	2.8	N_2	38	Raney-Ni	234	Ext.GC
30	MA2	5.5	30	633	spruce-Lig	0.40	H_2O	2.8	N_2	62	Raney-Ni	234	Ext.GC

Exp.	Reactor Type	V_R	τ (τ')	T	Biomass Type	$m_{i,0}$	Solvent Type	$m_{i,0}$	H-Donor/Gas Type	$m_{i,0}$	Catalyst Type	Amount[a]	Analysis[c]
#		ml	min	K		g		g		mg			
31	MA2	5.5	30	633	spruce-Lig	0.40	H_2O	2.8	N_2	132	Raney-Ni	234	Ext.GC
32	MA2	5.5	30	633	spruce-Lig	0.40	H_2O	2.8	CO	56	Raney-Ni	234	Ext.GC
33	MA2	5.5	30	633	spruce-Lig	0.40	H_2O	3.0	CO	70	None	0	Ext.GC
34	MA2	5.5	30	633	spruce-Lig	0.40	H_2O	3.0	H_2	11	Al-Ni	57	Ext.GC
35	MA2	5.5	30	633	spruce-Lig	0.40	H_2O	3.0	N_2	191	Al-Ni	53	Ext.GC
36	MA2	10	60	523	Catechol	0.05	H_2O	5.0	H_2	2.0	Raney-Ni	67.2	Ext.GC
37	MA2	10	60	573	Catechol	0.05	H_2O	5.0	H_2	2.0	Raney-Ni	67.2	Ext.GC
38	MA2	10	60	603	Catechol	0.05	H_2O	5.0	H_2	2.0	Raney-Ni	67.2	Ext.GC
39	MA2	10	60	623	Catechol	0.05	H_2O	5.0	H_2	2.0	Raney-Ni	67.2	Ext.GC
40	MA2	10	60	523	Guaiacol	0.05	H_2O	5.0	H_2	2.0	Raney-Ni	67.2	Ext.GC
41	MA2	10	60	573	Guaiacol	0.05	H_2O	5.0	H_2	2.0	Raney-Ni	67.2	Ext.GC
42	MA2	10	60	603	Guaiacol	0.05	H_2O	5.0	H_2	2.0	Raney-Ni	67.2	Ext.GC
43	MA2	10	60	623	Guaiacol	0.05	H_2O	5.0	H_2	2.0	Raney-Ni	67.2	Ext.GC
44	MA2	5.5	15	633	wheat-Lig	0.33	EtOH	2.0	FA	268.4	None	0	GC.FT-IR
45	MA2	5.5	30	633	wheat-Lig	0.33	EtOH	2.0	FA	268.4	None	0	GC.FT-IR.KFT
46	MA2	5.5	45	633	wheat-Lig	0.33	EtOH	2.0	FA	268.4	None	0	GC.FT-IR
47	MA2	5.5	60	633	wheat-Lig	0.33	EtOH	2.0	FA	268.4	None	0	GC.FT-IR.KFT
48	MA2	5.5	90	633	wheat-Lig	0.33	EtOH	2.0	FA	268.4	None	0	GC.FT-IR
49	MA2	5.5	120	633	wheat-Lig	0.33	EtOH	2.0	FA	268.4	None	0	GC.FT-IR
50	MA2	5.5	240	633	wheat-Lig	0.33	EtOH	2.0	FA	268.4	None	0	GC.FT-IR.KFT
51	MA2	5.5	360	633	wheat-Lig	0.33	EtOH	2.0	FA	268.4	None	0	GC.FT-IR
52	MA2	5.5	480	633	wheat-Lig	0.33	EtOH	2.0	FA	268.4	None	0	GC.FT-IR.KFT
53	MA2	5.5	1180	633	wheat-Lig	0.33	EtOH	2.0	FA	268.4	None	0	GC.FT-IR.KFT
54	MA1	5.0	660	653	None	0.00	EtOH	1.6	None	0	None	0	GC
55	MA1	5.0	660	653	None	0.00	EtOH	1.6	FA	152.5	None	0	GC
56	MA1	10.0	150	653	wheat-Lig	0.35	EtOH	3.2	FA	390.4	None	0	GC.FT-IR.KFT
57	MA1	10.0	150	653	wheat-Lig	0.35	EtOH	3.2	FA	390.4	None	0	GC.FT-IR.KFT
58	MA1	10.0	60	653	wheat-Lig	0.35	EtOH	3.2	FA	390.4	None	0	GC.FT-IR.KFT
59	MA1	10.0	60	653	wheat-Lig	0.35	EtOH	3.2	FA	390.4	None	0	GC.FT-IR.KFT
60	MA1	10.0	140	653	wheat-Lig	0.35	EtOH	3.2	FA	390.4	None	0	GC.FT-IR.KFT
61	MA1	10.0	140	653	wheat-Lig	0.35	EtOH	3.2	FA	390.4	None	0	GC.FT-IR.KFT
62	CSTR	200	51	653	wheat-Lig	6.22	EtOH	59.0	FA	7.6	None	0	GC.FT-IR.KFT
63	CSTR	200	59	653	wheat-Lig	6.33	EtOH	60.0	FA	7.7	None	0	GC.FT-IR.KFT
64	CSTR	200	39	653	wheat-Lig	6.46	EtOH	61.3	FA	7.9	None	0	GC.FT-IR.KFT
65	CSTR	200	56	633	wheat-Lig	6.37	EtOH	60.4	FA	7.8	None	0	GC.FT-IR.KFT

Exp.	Reactor		τ (τ')	T	Biomass		Solvent		H-Donor/Gas		Catalyst		Analysis[c]
	Type	V_R			Type	$m_{i,0}$[d]	Type	$m_{i,0}$[d]	Type	$m_{i,0}$[d]	Type	Amount[a]	
#		ml	min	K		g		g		mg			
66	CSTR	200	44	673	wheat-Lig	6.52	EtOH	61.8	FA	8.0	None	0	GC.FT-IR.KFT
67	CSTR	200	37	653	wheat-Lig	8.77	EtOH	83.1	FA	10.6	None	0	GC.FT-IR.KFT
68	CSTR	200	21	653	wheat-Lig	15.43	EtOH	146.3	FA	18.7	None	0	GC.FT-IR.KFT
69	MA2	5.5	15	593	spruce-Lig	0.33	H_2O	2.5	None	0	None	0	Ext.GC.FT-IR
70	MA2	5.5	30	593	spruce-Lig	0.33	H_2O	2.5	None	0	None	0	Ext.GC.FT-IR
71	MA2	5.5	45	593	spruce-Lig	0.33	H_2O	2.5	None	0	None	0	Ext.GC.FT-IR
72	MA2	5.5	60	593	spruce-Lig	0.33	H_2O	2.5	None	0	None	0	Ext.GC.FT-IR
73	MA2	5.5	90	593	spruce-Lig	0.33	H_2O	2.5	None	0	None	0	Ext.GC.FT-IR
74	MA2	5.5	120	593	spruce-Lig	0.33	H_2O	2.5	None	0	None	0	Ext.GC.FT-IR
75	MA2	5.5	240	593	spruce-Lig	0.33	H_2O	2.5	None	0	None	0	Ext.GC.FT-IR
76	MA2	5.5	480	593	spruce-Lig	0.33	H_2O	2.5	None	0	None	0	Ext.GC.FT-IR
77	MA2	5.5	15	613	spruce-Lig	0.33	H_2O	2.5	None	0	None	0	Ext.GC.FT-IR
78	MA2	5.5	30	613	spruce-Lig	0.33	H_2O	2.5	None	0	None	0	Ext.GC.FT-IR
79	MA2	5.5	45	613	spruce-Lig	0.33	H_2O	2.5	None	0	None	0	Ext.GC.FT-IR
80	MA2	5.5	60	613	spruce-Lig	0.33	H_2O	2.5	None	0	None	0	Ext.GC.FT-IR
81	MA2	5.5	90	613	spruce-Lig	0.33	H_2O	2.5	None	0	None	0	Ext.GC.FT-IR
82	MA2	5.5	120	613	spruce-Lig	0.33	H_2O	2.5	None	0	None	0	Ext.GC.FT-IR
83	MA2	5.5	240	613	spruce-Lig	0.33	H_2O	2.5	None	0	None	0	Ext.GC.FT-IR
84	MA2	5.5	480	613	spruce-Lig	0.33	H_2O	2.5	None	0	None	0	Ext.GC.FT-IR
85	MA2	5.5	15	633	spruce-Lig	0.33	H_2O	2.5	None	0	None	0	Ext.GC.FT-IR
86	MA2	5.5	30	633	spruce-Lig	0.33	H_2O	2.5	None	0	None	0	Ext.GC.FT-IR
87	MA2	5.5	45	633	spruce-Lig	0.33	H_2O	2.5	None	0	None	0	Ext.GC.FT-IR
88	MA2	5.5	60	633	spruce-Lig	0.33	H_2O	2.5	None	0	None	0	Ext.GC.FT-IR
89	MA2	5.5	90	633	spruce-Lig	0.33	H_2O	2.5	None	0	None	0	Ext.GC.FT-IR
90	MA2	5.5	120	633	spruce-Lig	0.33	H_2O	2.5	None	0	None	0	Ext.GC.FT-IR

Exp.	Reactor		τ (τ')	T	Biomass		Solvent		H-Donor/Gas		Catalyst		Analysis[c]
	Type	V_R			Type	$m_{i,0}$	Type	$m_{i,0}$	Type	$m_{i,0}$	Type	Amount[a]	
#		ml	min	K		g		g		mg			
91	MA2	5.5	240	633	spruce-Lig	0.33	H_2O	2.5	None	0	None	0	Ext.GC.FT-IR
92	MA2	5.5	360	633	spruce-Lig	0.33	H_2O	2.5	None	0	None	0	Ext.GC.FT-IR
93	MA2	5.5	480	633	spruce-Lig	0.33	H_2O	2.5	None	0	None	0	Ext.GC.FT-IR
94	MA2	5.5	15	653	spruce-Lig	0.33	H_2O	2.5	None	0	None	0	Ext.GC.FT-IR
95	MA2	5.5	30	653	spruce-Lig	0.33	H_2O	2.5	None	0	None	0	Ext.GC.FT-IR
96	MA2	5.5	45	653	spruce-Lig	0.33	H_2O	2.5	None	0	None	0	Ext.GC.FT-IR
97	MA2	5.5	60	653	spruce-Lig	0.33	H_2O	2.5	None	0	None	0	Ext.GC.FT-IR
98	MA2	5.5	90	653	spruce-Lig	0.33	H_2O	2.5	None	0	None	0	Ext.GC.FT-IR
99	MA2	5.5	120	653	spruce-Lig	0.33	H_2O	2.5	None	0	None	0	Ext.GC.FT-IR
100	MA2	5.5	240	653	spruce-Lig	0.33	H_2O	2.5	None	0	None	0	Ext.GC.FT-IR
101	MA2	5.5	360	653	spruce-Lig	0.33	H_2O	2.5	None	0	None	0	Ext.GC.FT-IR
102	MA2	5.5	480	653	spruce-Lig	0.33	H_2O	2.5	None	0	None	0	Ext.GC.FT-IR
103	MA2	10	30	473	Catechol	0.05	H_2O	5.0	H_2	4	Raney-Ni	22	Ext.GC
104	MA2	10	90	473	Catechol	0.05	H_2O	5.0	H_2	4	Raney-Ni	22	Ext.GC
105	MA2	10	180	473	Catechol	0.05	H_2O	5.0	H_2	4	Raney-Ni	22	Ext.GC
106	MA2	10	60	493	Catechol	0.05	H_2O	5.0	H_2	4	Raney-Ni	22	Ext.GC
107	MA2	10	90	493	Catechol	0.05	H_2O	5.0	H_2	4	Raney-Ni	22	Ext.GC
108	MA2	10	60	503	Catechol	0.05	H_2O	5.0	H_2	4	Raney-Ni	22	Ext.GC
109	MA2	10	90	503	Catechol	0.05	H_2O	5.0	H_2	4	Raney-Ni	22	Ext.GC
110	MA2	10	180	503	Catechol	0.05	H_2O	5.0	H_2	4	Raney-Ni	22	Ext.GC
111	MA2	10	60	513	Catechol	0.05	H_2O	5.0	H_2	4	Raney-Ni	22	Ext.GC
112	MA2	10	90	513	Catechol	0.05	H_2O	5.0	H_2	4	Raney-Ni	22	Ext.GC
113	MA2	10	180	513	Catechol	0.05	H_2O	5.0	H_2	4	Raney-Ni	22	Ext.GC
114	MA2	10	30	523	Catechol	0.05	H_2O	5.0	H_2	4	Raney-Ni	22	Ext.GC
115	MA2	10	90	523	Catechol	0.05	H_2O	5.0	H_2	4	Raney-Ni	22	Ext.GC
116	MA2	10	90	523	Catechol	0.05	H_2O	5.0	H_2	4	Raney-Ni	22	Ext.GC
117	MA2	10	180	523	Catechol	0.05	H_2O	5.0	H_2	4	Raney-Ni	22	Ext.GC
118	MA2	10	180	523	Catechol	0.05	H_2O	5.0	H_2	4	Raney-Ni	22	Ext.GC
119	MA2	10	60	533	Catechol	0.05	H_2O	5.0	H_2	4	Raney-Ni	22	Ext.GC
120	MA2	10	90	533	Catechol	0.05	H_2O	5.0	H_2	4	Raney-Ni	22	Ext.GC

Exp.	Reactor		τ (τ')	T	Biomass		Solvent		H-Donor/Gas		Catalyst		Analysis[c]
	Type	V_R			Type	$m_{i,0}$	Type	$m_{i,0}$	Type	$m_{i,0}$	Type	Amount[a]	
#		ml	min	K		g		g		mg			
121	MA2	10	180	533	Catechol	0.05	H_2O	5.0	H_2	4	Raney-Ni	22	Ext.GC
122	MA2	10	30	573	Catechol	0.05	H_2O	5.0	H_2	4	Raney-Ni	22	Ext.GC
123	MA2	10	60	573	Catechol	0.05	H_2O	5.0	H_2	4	Raney-Ni	22	Ext.GC
124	MA2	10	90	573	Catechol	0.05	H_2O	5.0	H_2	4	Raney-Ni	22	Ext.GC
125	MA2	10	180	573	Catechol	0.05	H_2O	5.0	H_2	4	Raney-Ni	22	Ext.GC
126	MA2	5.5	60	573	spruce-Lig	0.16	EtOH	2.0	H_2	2.8	Pd(10 %wt)/C	9.0	GC
127	MA2	5.5	60	593	spruce-Lig	0.15	EtOH	2.0	H_2	2.8	Pd(10 %wt)/C	8.4	GC
128	MA2	5.5	60	613	spruce-Lig	0.16	EtOH	2.0	H_2	2.8	Pd(10 %wt)/C	8.0	GC
129	MA2	5.5	60	633	spruce-Lig	0.16	EtOH	2.0	H_2	2.8	Pd(10 %wt)/C	8.4	GC
130	MA2	5.5	60	653	spruce-Lig	0.16	EtOH	2.0	H_2	2.8	Pd(10 %wt)/C	8.6	GC
131	MA2	5.5	60	673	spruce-Lig	0.16	EtOH	2.0	H_2	2.8	Pd(10 %wt)/C	8.8	GC
132	MA2	5.5	60	693	spruce-Lig	0.16	EtOH	2.0	H_2	2.8	Pd(10 %wt)/C	8.2	GC
133	MA2	5.5	60	713	spruce-Lig	0.16	EtOH	2.0	H_2	2.8	Pd(10 %wt)/C	8.1	GC
134	MA2	5.5	60	573	spruce-Lig	0.16	H_2O	2.0	H_2	2.8	Pd(10 %wt)/C	8.2	Ext.GC
135	MA2	5.5	60	593	spruce-Lig	0.16	H_2O	2.0	H_2	2.8	Pd(10 %wt)/C	7.7	Ext.GC
136	MA2	5.5	60	613	spruce-Lig	0.17	H_2O	2.0	H_2	2.8	Pd(10 %wt)/C	7.9	Ext.GC
137	MA2	5.5	60	633	spruce-Lig	0.16	H_2O	2.0	H_2	2.8	Pd(10 %wt)/C	8.8	Ext.GC
138	MA2	5.5	60	653	spruce-Lig	0.16	H_2O	2.0	H_2	2.8	Pd(10 %wt)/C	8.5	Ext.GC
139	MA2	5.5	60	673	spruce-Lig	0.15	H_2O	2.0	H_2	2.8	Pd(10 %wt)/C	8.9	Ext.GC
140	MA2	5.5	60	693	spruce-Lig	0.16	H_2O	2.0	H_2	2.8	Pd(10 %wt)/C	8.1	Ext.GC
141	MA2	5.5	60	713	spruce-Lig	0.16	H_2O	2.0	H_2	2.8	Pd(10 %wt)/C	8.7	Ext.GC
142	MA2	5.5	60	633	spruce-Lig	0.33	H_2O	2.5	FA	268.4	None	0	Ext.GC.FT-IR
143	MA2	5.5	60	633	spruce-Lig	0.33	EtOH	2.0	FA	268.4	None	0	GC.FT-IR
144	MA2	5.5	240	633	spruce-Lig	0.33	H_2O	2.5	FA	268.4	None	0	Ext.GC.FT-IR
145	MA2	5.5	240	633	spruce-Lig	0.33	EtOH	2.0	FA	268.4	None	0	GC.FT-IR
146	MA2	5.5	1180	593	spruce-Lig	0.33	H_2O	2.5	None	0	None	0	Ext.GC.FT-IR
147	MA2	5.5	1180	613	spruce-Lig	0.33	H_2O	2.5	None	0	None	0	Ext.GC.FT-IR
148	MA2	5.5	1180	633	spruce-Lig	0.33	H_2O	2.5	None	0	None	0	Ext.GC.FT-IR
149	MA2	5.5	1180	653	spruce-Lig	0.33	H_2O	2.5	None	0	None	0	Ext.GC.FT-IR
150	MA2	5.5	1180	633	spruce-Lig	0.33	H_2O	2.5	FA	268.4	None	0	Ext.GC.FT-IR

Exp.	Reactor		τ (τ')	T	Biomass		Solvent		H-Donor/Gas		Catalyst		Analysis[c]
	Type	V_R			Type	$m_{i,0}$	Type	$m_{i,0}$	Type	$m_{i,0}$	Type	Amount	
#		ml	min	K		g		g		mg			
151	MA2	5.5	1180	633	spruce-Lig	0.33	EtOH	2.0	FA	268.4	None	0	GC.FT-IR
152	MA2	5.5	1180	633	spruce-Lig	0.33	EtOH	2.0	None	0	None	0	GC.FT-IR
153	MA2	5.5	15	633	spruce-Lig	0.33	EtOH	2.0	None	0	None	0	GC.FT-IR
154	MA2	5.5	30	633	spruce-Lig	0.33	EtOH	2.0	None	0	None	0	GC.FT-IR
155	MA2	5.5	45	633	spruce-Lig	0.33	EtOH	2.0	None	0	None	0	GC.FT-IR
156	MA2	5.5	60	633	spruce-Lig	0.33	EtOH	2.0	None	0	None	0	GC.FT-IR
157	MA2	5.5	90	633	spruce-Lig	0.33	EtOH	2.0	None	0	None	0	GC.FT-IR
158	MA2	5.5	120	633	spruce-Lig	0.33	EtOH	2.0	None	0	None	0	GC.FT-IR
159	MA2	5.5	240	633	spruce-Lig	0.33	EtOH	2.0	None	0	None	0	GC.FT-IR
160	MA2	5.5	360	633	spruce-Lig	0.33	EtOH	2.0	None	0	None	0	GC.FT-IR
161	MA2	5.5	480	633	spruce-Lig	0.33	EtOH	2.0	None	0	None	0	GC.FT-IR

[a] Unit of amount: mg in case of heterogeneous catalysts, mol/L in case of homogeneous catalysts.
[b] Catalyst/Carrier material
[c] GC=Gas Chromatography, FT-IR=Infra red spectroscopy, Ext=Extraction, KFT=Karl-Fischer-titration.
[d] Input unit of all input streams in case of CSTR is g/h.

Table E.2: Experimental data: Results of bulk components, gaseous compounds, H_2O and EtOH.

Exp. #	Liq. g	Char mg/$g_{Biomass}$	Gas	Loss[a] wt%	CH_4	C_2H_4	C_2H_6	C_3H_6	C_3H_8	C_4H_{10} mg/$g_{Biomass}$	CO_2	H_2	CO	Others	H_2O	EtOH
1	2.7	283	596	10	3	0	0	1	0	1	576	16	0	n.a.	n.a.	n.a.
2	2.3	638	295	23	25	0	0	0	0	6	240	12	12	n.a.	n.a.	n.a.
3	1.8	441	153	40	2	0	0	0	0	1	117	3	29	n.a.	n.a.	n.a.
4	2.5	612	782	16	51	0	3	0	2	19	685	15	6	n.a.	n.a.	n.a.
5	2.6	455	395	15	4	0	1	1	0	1	387	0	1	n.a.	n.a.	n.a.
6	2.5	473	298	18	3	0	0	1	0	0	287	0	6	n.a.	n.a.	n.a.
7	2.9	181	502	8	2	0	1	1	0	0	497	0	0	n.a.	n.a.	n.a.
8	2.4	432	309	21	4	0	1	1	0	1	302	0	1	n.a.	n.a.	n.a.
9	2.6	457	288	16	3	0	0	1	0	0	278	0	6	n.a.	n.a.	n.a.
10	2.4	0	726	18	37	0	4	0	3	2	680	0	0	n.a.	n.a.	n.a.
11	2.6	0	833	10	38	0	4	0	3	2	775	12	0	n.a.	n.a.	n.a.
12	2.6	344	323	17	3	0	1	0	1	1	288	24	4	n.a.	n.a.	n.a.
13	2.2	398	426	25	3	1	1	1	0	1	418	0	2	n.a.	n.a.	n.a.
14	2.5	347	363	17	2	1	0	1	0	1	325	28	5	n.a.	n.a.	n.a.
15	2.0	423	372	31	3	0	1	1	0	0	364	0	2	n.a.	n.a.	n.a.
16	1.9	411	212	36	3	0	1	1	0	0	202	0	5	n.a.	n.a.	n.a.
17	2.1	413	383	29	3	0	1	0	1	1	356	20	2	n.a.	n.a.	n.a.
18	2.4	436	313	21	3	0	1	0	1	1	273	32	3	n.a.	n.a.	n.a.
19	2.8	357	364	10	4	0	0	0	0	0	353	0	6	n.a.	n.a.	n.a.
20	2.8	258	248	11	2	0	1	0	0	0	200	32	13	n.a.	n.a.	n.a.
21	2.6	256	477	14	13	0	1	0	1	1	445	14	1	n.a.	n.a.	n.a.
22	2.6	212	377	17	7	0	1	1	1	1	334	27	5	n.a.	n.a.	n.a.
23	2.2	0	1015	19	47	0	4	0	2	1	961	0	0	n.a.	n.a.	n.a.
24	1.8	0	952	26	129	0	6	0	4	2	811	0	0	n.a.	n.a.	n.a.
25	2.4	101	605	19	21	0	2	0	2	1	579	0	0	n.a.	n.a.	n.a.
26	2.1	0	267	28	6	0	1	0	1	0	259	0	0	n.a.	n.a.	n.a.
27	2.2	0	742	23	41	0	4	0	3	2	692	0	0	n.a.	n.a.	n.a.
28	2.3	0	443	22	27	0	3	0	2	2	408	0	0	n.a.	n.a.	n.a.
29	2.8	0	464	10	18	0	2	0	1	1	441	0	1	n.a.	n.a.	n.a.
30	2.4	0	511	19	24	0	3	0	2	2	480	0	0	n.a.	n.a.	n.a.

Exp. #	Liq. g	Char mg/$g_{Biomass}$	Gas	Loss[a] wt%	CH_4	C_2H_4	C_2H_6	C_3H_6	C_3H_8	C_4H_{10} mg/$g_{Biomass}$	CO_2	H_2	CO	Others	H_2O	EtOH
31	2.5	0	591	18	30	0	3	0	2	1	554	0	0	n.a.	n.a.	n.a.
32	2.4	0	530	20	19	0	2	0	1	1	472	0	35	n.a.	n.a.	n.a.
33	2.4	403	308	23	2	0	0	0	0	0	125	0	180	n.a.	n.a.	n.a.
34	2.5	415	335	17	4	0	1	1	0	0	302	23	4	n.a.	n.a.	n.a.
35	2.1	411	310	29	4	0	1	1	0	0	297	0	7	n.a.	n.a.	n.a.
36	4.8	0	84	31	16	0	0	0	0	0	68	0	0	n.a.	n.a.	0
37	4.3	0	185	39	124	0	0	0	0	0	61	0	0	n.a.	n.a.	0
38	4.6	0	359	34	219	0	0	0	0	0	140	0	0	n.a.	n.a.	0
39	4.8	0	753	31	457	0	0	0	0	0	296	0	0	n.a.	n.a.	0
40	4.9	0	165	30	71	0	0	0	0	0	94	0	0	n.a.	n.a.	0
41	4.2	0	171	40	113	0	0	0	0	0	58	0	0	n.a.	n.a.	0
42	4.8	0	487	31	346	0	0	0	0	0	140	0	0	n.a.	n.a.	0
43	4.7	0	763	32	507	0	0	0	0	0	256	0	0	n.a.	n.a.	0
44	1.9	341	376	30	0	3	0	0	0	0	347	0	26	n.a.	n.a.	n.a.
45	1.9	138	876	27	1	19	6	0	8	0	795	0	46	n.a.	233	n.a.
46	1.9	188	1033	26	3	26	15	0	22	0	918	0	49	n.a.	n.a.	n.a.
47	2.0	157	1240	20	6	24	26	0	39	0	1104	0	42	n.a.	233	n.a.
48	2.0	95	1091	23	3	22	25	0	37	0	987	0	16	n.a.	n.a.	n.a.
49	1.8	154	1414	24	11	21	82	4	122	5	1164	0	5	n.a.	n.a.	n.a.
50	1.8	80	1985	19	8	20	134	12	199	16	1596	0	0	n.a.	377	n.a.
51	1.9	102	1725	21	9	20	151	20	224	29	1272	0	0	n.a.	n.a.	n.a.
52	1.6	147	1961	27	18	23	204	33	303	46	1328	0	5	n.a.	515	n.a.
53	1.6	149	3043	17	22	29	444	174	659	245	1470	0	0	n.a.	880	n.a.
54	0.9	n.d.	130[b]	18	7[b]	23[b]	4[b]	8[b]	4[b]	13[b]	6[b]	4[b]	15[b]	n.a.	n.a.	n.a.
55	1.1	n.d.	445[b]	-9	3[b]	37[b]	55[b]	10[b]	5[b]	51[b]	235[b]	3[b]	8[b]	n.a.	n.a.	n.a.
56	3.3	91	2310	-2	31	48	218	18	30	56	1445	0	65	400	0	0
57	3.1	122	2260	2	35	50	246	17	35	51	1311	0	81	434	0	0
58	3.0	159	1742	7	21	86	90	4	10	11	1140	0	159	221	483	6010
59	3.2	174	1757	3	21	96	91	3	9	9	1137	0	163	229	496	6330
60	3.2	208	2216	1	38	52	217	16	30	44	1319	0	103	397	503	5802

Exp. #	Liq. g	Char mg/g$_{Biomass}$	Gas	Loss[a] wt%	CH_4	C_2H_4	C_2H_6	C_3H_6	C_3H_8	C_4H_{10} mg/g$_{Biomass}$	CO_2	H_2	CO	Others	H_2O	EtOH
61	3.2	191	2271	3	39	54	222	16	31	46	1352	0	106	407	677	5925
62	73.0	79	1092	-10	24	36	76	0	0	0	512	10	241	193	559	9364
63	63.8	49	879	6	19	30	46	0	0	0	400	8	274	102	463	8116
64	68.6	18	828	2	18	33	41	0	0	0	436	7	265	28	431	8122
65	67.9	62	787	2	7	17	19	0	0	0	331	6	296	111	425	8374
66	66.7	17	1142	3	40	35	73	0	0	0	446	11	331	206	507	8129
67	93.7	9	998	0	15	22	28	0	0	0	441	10	329	153	416	8586
68	167.1	10	800	0	12	36	23	0	0	0	411	8	278	33	0	8755
69	2.4	497	40	16	0	0	0	0	0	0	38	0	2	n.a.	n.a.	n.a.
70	2.5	565	61	13	0	0	0	0	0	0	55	0	6	n.a.	n.a.	n.a.
71	2.5	486	84	15	1	0	0	0	0	0	78	0	6	n.a.	n.a.	n.a.
72	2.5	481	67	14	1	0	0	0	0	0	61	0	5	n.a.	n.a.	n.a.
73	2.5	328	90	17	1	0	0	0	0	0	83	0	6	n.a.	n.a.	n.a.
74	2.4	486	98	17	1	0	0	0	0	0	91	0	6	n.a.	n.a.	n.a.
75	2.3	471	105	19	2	0	0	0	0	0	101	0	2	n.a.	n.a.	n.a.
76	2.0	386	141	31	3	0	0	0	0	0	136	0	2	n.a.	n.a.	n.a.
77	2.3	554	75	18	0	0	0	0	0	0	69	0	5	n.a.	n.a.	n.a.
78	2.5	493	93	14	1	0	0	0	0	0	84	0	8	n.a.	n.a.	n.a.
79	2.4	444	95	18	1	0	0	0	0	0	86	0	7	n.a.	n.a.	n.a.
80	2.5	486	93	15	1	0	0	0	0	0	82	0	10	n.a.	n.a.	n.a.
81	2.2	444	113	25	2	0	0	0	0	0	105	0	6	n.a.	n.a.	n.a.
82	2.4	429	106	16	3	0	0	0	0	0	100	0	4	n.a.	n.a.	n.a.
83	2.1	375	152	26	5	0	0	0	0	0	145	0	2	n.a.	n.a.	n.a.
84	2.4	366	181	16	6	0	0	0	0	0	175	0	1	n.a.	n.a.	n.a.
85	2.3	498	67	19	1	0	0	0	0	0	58	0	8	n.a.	n.a.	n.a.
86	2.3	476	123	19	2	0	0	0	0	0	110	0	10	n.a.	n.a.	n.a.
87	2.4	408	122	18	4	0	0	0	0	0	109	0	9	n.a.	n.a.	n.a.
88	2.4	337	56	17	2	0	0	0	0	0	51	0	3	n.a.	n.a.	n.a.
89	2.2	322	151	24	5	0	0	0	0	0	141	0	5	n.a.	n.a.	n.a.
90	2.4	336	166	18	5	0	0	0	0	0	157	0	3	n.a.	n.a.	n.a.

Exp. #	Liq. g	Char mg/g$_{Biomass}$	Gas	Loss[a] wt%	CH_4	C_2H_4	C_2H_6	C_3H_6	C_3H_8	C_4H_{10} mg/g$_{Biomass}$	CO_2	H_2	CO	Others	H_2O	EtOH
91	2.3	357	160	21	7	0	0	0	0	0	148	0	6	n.a.	n.a.	n.a.
92	2.4	354	176	17	7	0	0	0	0	0	169	0	0	n.a.	n.a.	n.a.
93	2.4	361	165	17	6	0	0	0	0	0	159	0	0	n.a.	n.a.	n.a.
94	2.5	520	83	15	1	0	0	0	0	0	72	0	9	n.a.	n.a.	n.a.
95	2.2	345	161	24	6	0	0	0	0	0	141	0	15	n.a.	n.a.	n.a.
96	2.5	364	152	16	5	0	0	0	0	0	140	0	7	n.a.	n.a.	n.a.
97	1.9	339	165	33	7	0	0	0	0	0	154	0	4	n.a.	n.a.	n.a.
98	2.0	374	171	29	8	0	0	0	0	0	162	0	2	n.a.	n.a.	n.a.
99	2.3	344	180	21	8	0	0	0	0	0	171	0	1	n.a.	n.a.	n.a.
100	2.0	359	203	31	7	0	0	0	0	0	195	0	0	n.a.	n.a.	n.a.
101	2.3	362	207	20	12	0	0	0	0	0	196	0	0	n.a.	n.a.	n.a.
102	2.3	351	240	19	10	0	0	0	0	0	231	0	0	n.a.	n.a.	n.a.
103	n.a.	0	92	8	0	0	0	0	0	0	0	92	0	n.a.	n.a.	0
104	n.a.	0	28	8	0	0	0	0	0	0	7	21	0	n.a.	n.a.	0
105	n.a.	0	63	21	0	0	0	0	0	0	12	51	0	n.a.	n.a.	0
106	n.a.	0	0	38	0	0	0	0	0	0	0	0	0	n.a.	n.a.	0
107	n.a.	0	0	36	0	0	0	0	0	0	0	0	0	n.a.	n.a.	0
108	n.a.	0	0	50	0	0	0	0	0	0	0	0	0	n.a.	n.a.	0
109	n.a.	0	0	39	0	0	0	0	0	0	0	0	0	n.a.	n.a.	0
110	n.a.	0	0	32	0	0	0	0	0	0	0	0	0	n.a.	n.a.	0
111	n.a.	0	0	23	0	0	0	0	0	0	0	0	0	n.a.	n.a.	0
112	n.a.	0	72	11	1	0	0	0	0	0	22	49	0	n.a.	n.a.	0
113	n.a.	0	134	33	14	0	0	0	0	0	56	64	0	n.a.	n.a.	0
114	n.a.	0	0	8	0	0	0	0	0	0	0	0	0	n.a.	n.a.	0
115	n.a.	0	18	12	0	0	0	0	0	0	9	8	0	n.a.	n.a.	0
116	n.a.	0	0	35	0	0	0	0	0	0	0	0	0	n.a.	n.a.	0
117	n.a.	0	0	76	0	0	0	0	0	0	0	0	0	n.a.	n.a.	0
118	n.a.	0	120	11	14	0	0	0	0	0	35	72	0	n.a.	n.a.	0
119	n.a.	0	96	32	23	0	0	0	0	0	0	74	0	n.a.	n.a.	0
120	n.a.	0	47	32	0	0	0	0	0	0	5	41	0	n.a.	n.a.	0

Exp. #	Liq. g	Char mg/$g_{Biomass}$	Gas	Loss[a] wt%	CH_4	C_2H_4	C_2H_6	C_3H_6	C_3H_8	C_4H_{10} mg/$g_{Biomass}$	CO_2	H_2	CO	Others	H_2O	EtOH
121	n.a.	0	169	29	101	0	0	0	0	0	32	36	0	n.a.	n.a.	0
122	n.a.	0	76	22	22	0	0	0	0	0	39	15	0	n.a.	n.a.	0
123	n.a.	0	294	27	65	0	0	0	0	0	213	15	0	n.a.	n.a.	0
124	n.a.	0	270	37	47	0	0	0	0	0	204	18	0	n.a.	n.a.	0
125	n.a.	0	593	20	171	0	0	0	0	0	412	10	0	n.a.	n.a.	0
126	1.3	794	228	13	0	0	0	0	0	0	18	34	176	n.a.	0	6462
127	1.5	338	289	9	6	0	8	0	0	0	60	26	175	n.a.	0	8003
128	1.6	177	456	3	17	10	20	0	0	0	131	31	202	n.a.	0	7401
129	1.6	161	135	8	13	2	14	0	0	0	52	24	0	n.a.	0	7085
130	1.5	158	400	7	40	17	55	3	4	0	128	32	2	n.a.	0	6052
131	1.5	165	1198	3	120	46	216	22	31	20	260	26	0	n.a.	0	6053
132	1.5	137	1892	0	143	33	424	33	89	42	349	11	6	n.a.	0	6375
133	1.4	192	4678	-9	182	163	992	107	325	232	650	13	10	n.a.	0	8143
134	1.7	510	102	18	0	0	0	0	0	0	60	41	0	n.a.	0	0
135	1.7	506	97	15	1	0	0	0	0	0	68	28	0	n.a.	0	0
136	1.8	468	110	14	2	0	0	0	0	0	69	38	0	n.a.	0	0
137	2.0	468	106	5	4	0	1	0	0	0	84	13	0	n.a.	0	0
138	1.8	420	158	10	7	0	2	0	0	0	101	39	0	n.a.	0	0
139	1.8	194	133	12	12	0	0	0	0	0	98	12	0	n.a.	0	0
140	1.9	294	217	9	18	0	0	0	0	0	136	44	0	n.a.	0	0
141	1.9	232	264	10	23	0	7	0	5	5	164	20	0	n.a.	0	0
142	2.3	31	1391	24	0	0	0	0	0	21	1367	2	0	n.a.	n.a.	n.a.
143	2.0	27	1386	21	3	39	34	0	0	42	1265	0	3	n.a.	n.a.	n.a.
144	2.1	21	1259	31	3	0	0	0	0	17	1236	3	0	n.a.	n.a.	n.a.
145	1.8	23	1627	24	13	30	141	14	19	99	1302	0	8	n.a.	n.a.	n.a.
146	2.4	461	132	15	3	0	0	0	0	0	129	0	0	n.a.	n.a.	n.a.
147	2.4	420	170	18	5	0	0	0	0	0	165	0	0	n.a.	n.a.	n.a.
148	2.4	390	196	15	9	0	0	0	0	0	187	0	0	n.a.	n.a.	n.a.
149	2.3	333	248	21	11	0	0	0	0	0	237	0	0	n.a.	n.a.	n.a.
150	2.4	26	2407	11	5	0	0	0	0	83	2316	3	0	n.a.	n.a.	n.a.

Exp. #	Liq. g	Char mg/g$_{Biomass}$	Gas	Loss[a] wt%	CH_4	C_2H_4	C_2H_6	C_3H_6	C_3H_8	C_4H_{10} mg/g$_{Biomass}$	CO_2	H_2	CO	Others	H_2O	EtOH
151	1.6	18	2653	22	16	28	451	0	200	462	1496	0	0	n.a.	n.a.	n.a.
152	1.4	259	2081	13	47	0	14	0	7	55	1957	0	0	n.a.	n.a.	n.a.
153	1.8	519.9	28	21	4	1	3	0	0	19	0	0	0	n.a.	0	n.a.
154	1.9	335.8	93	19	3	3	4	0	0	3	52	0	28	n.a.	0	n.a.
155	1.9	339.0	129	20	6	7	8	0	0	2	77	0	29	n.a.	0	n.a.
156	1.8	318.7	86	24	8	4	5	0	0	3	33	0	31	n.a.	0	n.a.
157	1.6	285.2	149	30	17	13	22	0	2	9	84	0	0	n.a.	0	n.a.
158	1.3	279.4	206	41	15	21	30	1	0	2	137	0	0	n.a.	0	n.a.
159	1.9	253.8	502	16	29	31	37	0	0	17	388	0	0	n.a.	0	n.a.
160	1.7	324.1	676	21	33	41	185	16	26	58	306	0	11	n.a.	0	n.a.
161	1.7	241.6	660	21	31	30	201	14	38	44	288	0	13	n.a.	0	n.a.

[a] Percentage of total input. For Exp. 103-125 amount of converted catechol into not detectable substances
[b] For experiments Exp. 54 and 55 without input of biomass yields are given in *mg*.

Table E.3: Experimental data: Results of phenolic and other compounds quantified via GC-FID.

Exp. #	Phe [a]	2-Me-Phe	4-Me-Phe	2-Et-Phe	4-Et-Phe	Gua[a]	4-Me-Gua	4-Et-Gua	Syr[a]	CatOH[a]	4-Me-CatOH	4-Et-CatOH	Cyclo-hexOH[a]	Cyclo-hexO[a]
							mg/$g_{Biomass}$							
1	1	0	0	n.a.	n.a.	4	1	n.a.	n.a.	15	5	0	n.d.	n.d.
2	2	0	1	n.a.	n.a.	0	0	n.a.	n.a.	8	2	0	n.d.	n.d.
3	1	0	0	n.a.	n.a.	0	0	n.a.	n.a.	16	3	0	n.d.	n.d.
4	2	0	0	n.a.	n.a.	0	0	n.a.	n.a.	5	1	0	n.d.	n.d.
5	1	0	1	n.a.	n.a.	6	2	n.a.	n.a.	9	3	0	n.d.	n.d.
6	1	0	0	n.a.	n.a.	5	2	n.a.	n.a.	5	1	0	n.d.	n.d.
7	1	0	0	n.a.	n.a.	6	1	n.a.	n.a.	16	5	0	n.d.	n.d.
8	1	0	0	n.a.	n.a.	5	2	n.a.	n.a.	6	2	0	n.d.	n.d.
9	1	0	0	n.a.	n.a.	6	2	n.a.	n.a.	4	1	0	n.d.	n.d.
10	3	0	1	n.a.	n.a.	5	2	n.a.	n.a.	4	2	0	n.d.	n.d.
11	4	0	1	n.a.	n.a.	6	2	n.a.	n.a.	3	2	0	n.d.	n.d.
12	1	0	0	n.a.	n.a.	5	2	n.a.	n.a.	4	1	0	n.d.	n.d.
13	1	0	0	n.a.	n.a.	5	1	n.a.	n.a.	5	2	0	n.d.	n.d.
14	1	0	0	n.a.	n.a.	7	2	n.a.	n.a.	5	2	0	n.d.	n.d.
15	1	0	0	n.a.	n.a.	5	1	n.a.	n.a.	4	1	0	n.d.	n.d.
16	0	0	0	n.a.	n.a.	4	1	n.a.	n.a.	3	1	0	n.d.	n.d.
17	1	0	0	n.a.	n.a.	5	2	n.a.	n.a.	4	1	0	n.d.	n.d.
18	1	0	0	n.a.	n.a.	6	2	n.a.	n.a.	5	2	0	n.d.	n.d.
19	1	0	0	n.a.	n.a.	1	0	n.a.	n.a.	16	3	0	n.d.	n.d.
20	1	0	1	n.a.	n.a.	1	0	n.a.	n.a.	18	4	0	n.d.	n.d.
21	1	0	0	n.a.	n.a.	5	3	n.a.	n.a.	2	2	1	n.d.	n.d.
22	1	0	0	n.a.	n.a.	6	3	n.a.	n.a.	2	1	1	n.d.	n.d.
23	4	0	3	n.a.	n.a.	3	2	n.a.	n.a.	1	1	1	n.d.	n.d.
24	2	0	2	n.a.	n.a.	1	1	n.a.	n.a.	0	0	0	n.d.	n.d.
25	2	0	1	n.a.	n.a.	5	3	n.a.	n.a.	2	1	1	n.d.	n.d.
26	4	0	2	n.a.	n.a.	2	1	n.a.	n.a.	1	1	0	n.d.	n.d.
27	4	0	1	n.a.	n.a.	4	2	n.a.	n.a.	2	1	1	n.d.	n.d.
28	4	0	1	n.a.	n.a.	5	2	n.a.	n.a.	2	1	1	n.d.	n.d.
29	3	0	1	n.a.	n.a.	6	2	n.a.	n.a.	4	2	1	n.d.	n.d.
30	3	0	1	n.a.	n.a.	5	2	n.a.	n.a.	3	1	1	n.d.	n.d.

Exp. #	Phe [a]	2-Me-Phe	4-Me-Phe	2-Et-Phe	4-Et-Phe	Gua[a]	4-Me-Gua	4-Et-Gua	Syr[a]	CatOH[a]	4-Me-CatOH	4-Et-CatOH	Cyclo-hexOH[a]	Cyclo-hexO[a]
							mg/g$_{Biomass}$							
31	3	0	1	n.a.	n.a.	6	2	n.a.	n.a.	3	1	0	n.d.	n.d.
32	3	0	1	n.a.	n.a.	4	2	n.a.	n.a.	2	1	0	n.d.	n.d.
33	1	0	1	n.a.	n.a.	6	2	n.a.	n.a.	3	1	0	n.d.	n.d.
34	1	0	0	n.a.	n.a.	5	1	n.a.	n.a.	4	1	0	n.d.	n.d.
35	1	0	0	n.a.	n.a.	4	1	n.a.	n.a.	3	1	0	n.d.	n.d.
36	229	n.d.	n.d.	n.a.	n.a.	n.d.	n.d.	n.a.	n.a.	69	0	0	175	40
37	73	n.d.	n.d.	n.a.	n.a.	n.d.	n.d.	n.a.	n.a.	31	0	0	138	53
38	51	n.d.	n.d.	n.a.	n.a.	n.d.	n.d.	n.a.	n.a.	14	0	0	75	39
39	39	n.d.	n.d.	n.a.	n.a.	n.d.	n.d.	n.a.	n.a.	41	0	0	17	17
40	30	n.d.	n.d.	n.a.	n.a.	129	n.d.	n.a.	n.a.	0	0	0	602	123
41	29	n.d.	n.d.	n.a.	n.a.	65	n.d.	n.a.	n.a.	0	0	0	315	55
42	21	n.d.	n.d.	n.a.	n.a.	26	n.d.	n.a.	n.a.	0	0	0	82	47
43	40	n.d.	n.d.	n.a.	n.a.	40	n.d.	n.a.	n.a.	0	0	0	45	40
44	1	0	0	0	2	2	1	3	2	0	0	0	n.d.	n.d.
45	1	0	0	0	3	3	2	5	3	1	1	1	n.d.	n.d.
46	1	0	1	0	4	4	3	6	3	1	1	1	n.d.	n.d.
47	1	0	1	0	5	4	3	6	3	2	1	2	n.d.	n.d.
48	1	0	1	0	5	4	3	6	3	2	1	2	n.d.	n.d.
49	1	1	1	1	4	3	2	4	1	1	1	2	n.d.	n.d.
50	1	0	1	1	4	2	2	3	0	5	1	1	n.d.	n.d.
51	1	0	1	1	3	1	1	1	1	1	1	0	n.d.	n.d.
52	1	1	1	1	2	1	0	1	0	2	2	1	n.d.	n.d.
53	1	1	0	0	0	0	0	0	0	3	0	0	n.d.	n.d.
54	0	0	0	0	0	0	0	0	0	0	0	0	n.a.	n.a.
55	0	0	0	0	0	0	0	0	0	0	0	0	n.a.	n.a.
56	3	2	2	2	9	1	0	2	0	4	0	5	0	0
57	3	2	2	2	9	1	0	1	0	4	0	4	0	0
58	3	0	2	0	10	5	4	7	4	5	4	7	0	0
59	3	0	2	0	10	6	4	8	4	5	4	7	0	0
60	3	2	2	2	9	2	0	2	0	4	0	5	0	0

Exp. #	Phe [a]	2-Me-Phe	4-Me-Phe	2-Et-Phe	4-Et-Phe	Gua[a]	4-Me-Gua	4-Et-Gua	Syr[a]	CatOH[a]	4-Me-CatOH	4-Et-CatOH	Cyclo-hexOH[a]	Cyclo-hexO[a]
							mg/$g_{Biomass}$							
31	3	0	1	n.a.	n.a.	6	2	n.a.	n.a.	3	1	0	n.d.	n.d.
32	3	0	1	n.a.	n.a.	4	2	n.a.	n.a.	2	1	0	n.d.	n.d.
33	1	0	1	n.a.	n.a.	6	2	n.a.	n.a.	3	1	0	n.d.	n.d.
34	1	0	0	n.a.	n.a.	5	1	n.a.	n.a.	4	1	0	n.d.	n.d.
35	1	0	0	n.a.	n.a.	4	1	n.a.	n.a.	3	1	0	n.d.	n.d.
36	229	n.d.	n.d.	n.a.	n.a.	n.d.	n.d.	n.a.	n.a.	69	0	0	175	40
37	73	n.d.	n.d.	n.a.	n.a.	n.d.	n.d.	n.a.	n.a.	31	0	0	138	53
38	51	n.d.	n.d.	n.a.	n.a.	n.d.	n.d.	n.a.	n.a.	14	0	0	75	39
39	39	n.d.	n.d.	n.a.	n.a.	n.d.	n.d.	n.a.	n.a.	41	0	0	17	17
40	30	n.d.	n.d.	n.a.	n.a.	129	n.d.	n.a.	n.a.	0	0	0	602	123
41	29	n.d.	n.d.	n.a.	n.a.	65	n.d.	n.a.	n.a.	0	0	0	315	55
42	21	n.d.	n.d.	n.a.	n.a.	26	n.d.	n.a.	n.a.	0	0	0	82	47
43	40	n.d.	n.d.	n.a.	n.a.	40	n.d.	n.a.	n.a.	0	0	0	45	40
44	1	0	0	0	2	2	1	3	2	0	0	0	n.d.	n.d.
45	1	0	0	0	3	3	2	5	3	1	1	1	n.d.	n.d.
46	1	0	1	0	4	4	3	6	3	1	1	1	n.d.	n.d.
47	1	0	1	0	5	4	3	6	3	2	1	2	n.d.	n.d.
48	1	0	1	0	5	4	3	6	3	2	1	2	n.d.	n.d.
49	1	1	1	1	4	3	2	4	1	1	1	2	n.d.	n.d.
50	1	0	1	1	4	2	2	3	0	5	1	1	n.d.	n.d.
51	1	0	1	1	3	1	1	1	1	1	1	0	n.d.	n.d.
52	1	1	1	1	2	1	0	1	0	2	2	1	n.d.	n.d.
53	1	1	0	0	0	0	0	0	0	3	0	0	n.d.	n.d.
54	0	0	0	0	0	0	0	0	0	0	0	0	n.a.	n.a.
55	0	0	0	0	0	0	0	0	0	0	0	0	n.a.	n.a.
56	3	2	2	2	9	1	0	2	0	4	0	5	0	0
57	3	2	2	2	9	1	0	1	0	4	0	4	0	0
58	3	0	2	0	10	5	4	7	4	5	4	7	0	0
59	3	0	2	0	10	6	4	8	4	5	4	7	0	0
60	3	2	2	2	9	2	0	2	0	4	0	5	0	0

Exp. #	Phe [a]	2-Me-Phe	4-Me-Phe	2-Et-Phe	4-Et-Phe	Gua[a]	4-Me-Gua	4-Et-Gua	Syr[a]	CatOH[a]	4-Me-CatOH	4-Et-CatOH	Cyclo-hexOH[a]	Cyclo-hexO[a]
							mg/$g_{Biomass}$							
61	3	2	2	2	9	1	0	0	0	4	0	5	0	0
62	3	0	2	1	16	6	5	14	8	5	4	9	n.d.	n.d.
63	3	0	2	2	14	6	5	13	6	4	3	7	n.d.	n.d.
64	3	0	2	2	14	7	5	14	7	5	3	7	n.d.	n.d.
65	2	0	1	0	12	6	4	15	7	1	0	4	n.d.	n.d.
66	3	0	2	2	15	5	4	10	5	4	4	8	n.d.	n.d.
67	2	0	1	0	13	6	4	13	6	3	2	5	n.d.	n.d.
68	2	0	0	0	11	5	4	13	5	0	0	3	n.d.	n.d.
69	0	0	0	0	0	1	0	0	0	0	0	0	n.d.	n.d.
70	0	0	0	0	0	3	0	0	0	2	1	1	n.d.	n.d.
71	0	0	0	0	0	5	1	0	0	2	1	1	n.d.	n.d.
72	0	0	0	0	0	4	1	1	0	3	1	1	n.d.	n.d.
73	0	0	0	0	0	4	1	0	0	3	1	1	n.d.	n.d.
74	1	0	0	0	0	5	1	0	0	5	1	1	n.d.	n.d.
75	1	0	0	0	0	5	1	0	0	9	2	1	n.d.	n.d.
76	1	0	0	0	0	3	1	0	0	14	4	1	n.d.	n.d.
77	0	0	0	0	0	2	0	0	0	3	0	1	n.d.	n.d.
78	0	0	0	0	0	5	1	0	0	2	1	1	n.d.	n.d.
79	1	0	0	0	0	5	1	0	0	4	1	1	n.d.	n.d.
80	1	0	0	0	0	6	1	0	0	4	1	1	n.d.	n.d.
81	1	0	0	0	0	6	1	0	0	6	2	1	n.d.	n.d.
82	1	0	0	0	0	6	1	0	0	9	3	1	n.d.	n.d.
83	1	0	0	0	0	3	1	0	0	12	4	1	n.d.	n.d.
84	1	0	0	0	0	1	0	0	0	16	6	2	n.d.	n.d.
85	0	0	0	0	0	3	1	0	0	2	1	1	n.d.	n.d.
86	1	0	0	0	0	7	2	0	1	5	1	1	n.d.	n.d.
87	1	0	0	0	0	8	2	0	0	9	3	1	n.d.	n.d.
88	1	0	0	0	0	6	2	0	0	7	2	0	n.d.	n.d.
89	1	0	0	0	0	5	1	0	1	12	4	1	n.d.	n.d.
90	1	0	0	0	0	4	1	0	1	12	5	2	n.d.	n.d.

Exp. #	Phe [a]	2-Me-Phe	4-Me-Phe	2-Et-Phe	4-Et-Phe	Gua[a]	4-Me-Gua	4-Et-Gua	Syr[a]	CatOH[a]	4-Me-CatOH	4-Et-CatOH	Cyclo-hexOH[a]	Cyclo-hexO[a]
							mg/$g_{Biomass}$							
91	1	0	1	0	0	2	1	0	2	19	9	3	n.d.	n.d.
92	1	0	1	0	0	1	0	0	0	16	8	2	n.d.	n.d.
93	1	0	1	0	0	0	0	0	0	14	7	2	n.d.	n.d.
94	0	0	0	0	0	3	1	0	0	2	1	1	n.d.	n.d.
95	1	0	0	0	0	7	2	0	0	7	2	1	n.d.	n.d.
96	1	0	0	0	0	5	1	0	0	9	3	1	n.d.	n.d.
97	1	0	0	0	0	4	1	0	0	12	4	1	n.d.	n.d.
98	1	0	0	0	0	3	0	0	0	15	6	2	n.d.	n.d.
99	1	0	0	0	0	3	1	0	0	17	8	3	n.d.	n.d.
100	1	1	0	0	0	1	0	0	0	18	8	3	n.d.	n.d.
101	2	1	1	0	0	0	0	0	0	18	9	3	n.d.	n.d.
102	2	1	1	0	0	0	0	0	0	16	9	3	n.d.	n.d.
103	45	0	0	0	0	0	0	0	0	778	0	0	8	1
104	93	0	0	0	0	0	0	0	0	802	0	0	0	0
105	155	0	0	0	0	0	0	0	0	565	0	0	11	0
106	57	0	0	0	0	0	0	0	0	560	0	0	1	0
107	220	0	0	0	0	0	0	0	0	413	0	0	3	2
108	209	0	0	0	0	0	0	0	0	240	0	0	23	28
109	208	0	0	0	0	0	0	0	0	396	0	0	3	3
110	341	0	0	0	0	0	0	0	0	334	0	0	3	1
111	510	0	0	0	0	0	0	0	0	256	0	0	0	0
112	552	0	0	0	0	0	0	0	0	264	0	0	0	1
113	288	0	0	0	0	0	0	0	0	59	0	0	120	69
114	481	0	0	0	0	0	0	0	0	201	0	0	97	141
115	634	0	0	0	0	0	0	0	0	110	0	0	37	86
116	202	0	0	0	0	0	0	0	0	436	0	0	8	7
117	136	0	0	0	0	0	0	0	0	59	0	0	21	27
118	254	0	0	0	0	0	0	0	0	71	0	0	316	125
119	343	0	0	0	0	0	0	0	0	73	0	0	95	70
120	412	0	0	0	0	0	0	0	0	207	0	0	7	5

Exp. #	Phe [a]	2-Me-Phe	4-Me-Phe	2-Et-Phe	4-Et-Phe	Gua[a]	4-Me-Gua	4-Et-Gua	Syr[a]	CatOH[a]	4-Me-CatOH	4-Et-CatOH	Cyclo-hexOH[a]	Cyclo-hexO[a]
							mg/$g_{Biomass}$							
121	138	0	0	0	0	0	0	0	0	44	0	0	264	91
122	265	0	0	0	0	0	0	0	0	418	0	0	14	10
123	270	0	0	0	0	0	0	0	0	69	0	0	39	62
124	139	0	0	0	0	0	0	0	0	54	0	0	67	103
125	93	0	0	0	0	0	0	0	0	28	0	0	41	45
126	0	0	0	n.a.	n.a.	3	3	n.a.	n.a.	0	n.a.	n.a.	n.a.	n.a.
127	0	0	0	n.a.	n.a.	5	4	n.a.	n.a.	4	n.a.	n.a.	n.a.	n.a.
128	0	0	0	n.a.	n.a.	8	6	n.a.	n.a.	4	n.a.	n.a.	n.a.	n.a.
129	2	0	0	n.a.	n.a.	8	6	n.a.	n.a.	4	n.a.	n.a.	n.a.	n.a.
130	3	0	0	n.a.	n.a.	9	7	n.a.	n.a.	4	n.a.	n.a.	n.a.	n.a.
131	3	0	0	n.a.	n.a.	7	4	n.a.	n.a.	5	n.a.	n.a.	n.a.	n.a.
132	3	0	0	n.a.	n.a.	4	4	n.a.	n.a.	4	n.a.	n.a.	n.a.	n.a.
133	4	0	0	n.a.	n.a.	3	0	n.a.	n.a.	4	n.a.	n.a.	n.a.	n.a.
134	1	0	0	n.a.	n.a.	3	2	n.a.	n.a.	2	n.a.	n.a.	n.a.	n.a.
135	1	0	0	n.a.	n.a.	7	3	n.a.	n.a.	3	n.a.	n.a.	n.a.	n.a.
136	1	0	0	n.a.	n.a.	9	4	n.a.	n.a.	6	n.a.	n.a.	n.a.	n.a.
137	2	0	0	n.a.	n.a.	12	5	n.a.	n.a.	10	n.a.	n.a.	n.a.	n.a.
138	2	0	0	n.a.	n.a.	12	5	n.a.	n.a.	17	n.a.	n.a.	n.a.	n.a.
139	2	0	0	n.a.	n.a.	8	3	n.a.	n.a.	26	n.a.	n.a.	n.a.	n.a.
140	3	0	0	n.a.	n.a.	3	1	n.a.	n.a.	37	n.a.	n.a.	n.a.	n.a.
141	4	0	0	n.a.	n.a.	0	0	n.a.	n.a.	38	n.a.	n.a.	n.a.	n.a.
142	1	0	0	0	0	5	0	0	0	10	3	1	n.d.	n.d.
143	0	0	0	0	0	4	0	2	0	1	0	0	n.d.	n.d.
144	2	0	1	0	0	2	0	0	2	19	8	3	n.d.	n.d.
145	0	0	0	0	0	2	0	1	0	1	1	0	n.d.	n.d.
146	1	0	0	0	0	1	0	0	0	15	5	2	n.d.	n.d.
147	1	0	1	0	0	0	0	0	0	15	8	2	n.d.	n.d.
148	2	1	1	0	0	0	0	0	0	12	7	2	n.d.	n.d.
149	2	1	1	0	0	0	0	0	0	14	8	2	n.d.	n.d.
150	3	1	2	0	0	0	0	0	1	9	5	2	n.d.	n.d.

Exp. #	Phe [a]	2-Me-Phe	4-Me-Phe	2-Et-Phe	4-Et-Phe	Gua[a]	4-Me-Gua	4-Et-Gua	Syr[a]	CatOH[a]	4-Me-CatOH	4-Et-CatOH	Cyclo-hexOH[a]	Cyclo-hexO[a]
							mg/$g_{Biomass}$							
151	0	0	0	0	0	1	0	0	0	1	2	0	n.d.	n.d.
152	0	0	0	0	0	0	0	0	0	0	0	0	n.a.	n.a.
153	0	0	0	0	0	0	0	0	0	0	0	0	0	0
154	0	0	0	0	0	0	0	0	0	0	0	0	0	0
155	0	0	0	0	0	0	0	0	0	0	0	0	0	0
156	0	0	0	0	0	0	0	0	0	0	0	0	0	0
157	0	0	0	0	0	0	0	0	0	0	0	0	0	0
158	0	0	0	0	0	0	0	0	0	0	0	0	0	0
159	0	0	0	0	0	0	0	0	0	0	0	0	0	0
160	0	0	0	0	0	0	0	0	0	0	0	0	0	0
161	0	0	0	0	0	0	0	0	0	0	0	0	0	0

[a] Phe=phenol, Gua=guaiacol, Syr=syringol, CatOH=catechol, CyclohexOH=cyclohexanol, CyclohexO=cyclohexanone.

E.2 Energy and mass flow

In this section the energy content of the commonly applied biomass and of gaseous and solid products are presented (see Table E.4). The HHV was calculated consulting the results from CHNS analysis (see Section 2.3.4) employing the method by IGT [Tal81]. Additionally the mass and energy balance for experiment Exp. 66 is presented in Table E.5 scaled to 1 t/h lignin.

Table E.4: Heating value and elemental composition of input and output components for solvolysis of wheat-straw lignin in ethanol and formic acid in a CSTR at 673 K, 25 MPa and 44 min mean residence time.

Component	Results from elementary analysis						HHV
	C	H	N	S	O	Ash	
	%	%	%	%	%	%	kJ/kg
wheat-straw-lignin [a]	63.8	6	1.5	0.3	27	1.4	24955
Spruce-lignin[a]	60.5	6.7	0.6	0.1	30.1	2	24305
Ethanol	52.2	13	0	0	34.8	0	26865
Formic Acid	26.1	4.3	0	0	69.6	0	4561
H_2	0	100	0	0	0	0	120900
CO	42.9	0	0	0	57.1	0	10107
CH_4	75	25	0	0	0	0	50144
C_2H_4	85.7	14.3	0	0	0	0	47246
C_2H_6	80	20	0	0	0	0	47590
Others	52.2	13	0	0	34.8	0	26087
Char[a]	76.7	5.2	0	0	16.7	n.a.	29882
liquid product[b]	37.7	12.3	0	0	50	n.a.	20413

[a] heating values estimated from elemental analysis with the method by IGT [Tal81].
[b] Heating value from energy balance.

The enthalpy of each input and output stream $\dot{H}_i$ was calculated by multiplying the HHV with the mass flow $\dot{m}_i$. Exceptionally the HHV of the oil fraction, that is the liquid product without ethanol and phenolics, could not be measured. However, the enthalpy of the overall liquid fraction (ethanol, phenolics and oil) was determined. In addition, the enthalpy of the sum of all products $\dot{H}_{Sum}$ could be calculated by adding the enthalpy of all three product phases. The enthalpy of the oil fraction was thus determined

Table E.5: Mass and energy balance for experiment Exp. 66 scaled to 1 t/h lignin.

Input	$\dot{m}_i$ t/h	$\dot{H}_i$ MJ/h	Output	$\dot{m}_i$ t/h	$\dot{H}_i$ MJ/h
EtOH	9.48	254680	Ethanol	8.13	218395
Formic Acid	1.22	5564	Phenolics	0.07	1907
Lignin	1.00	24955	Gas	1.14	17119
			Char	0.02	518
			Oil[a]	2.34	12536
Sum	11.70	285200	Sum	11.70	250476
			ΔH_R		-34724

[a] not measured, see Equation E.1

by difference, according to Equation E.1

$$\dot{H}_{Oil} = \dot{H}_{Sum,Output} - \sum_{i \neq Oil} \dot{H}_i. \tag{E.1}$$

The reaction enthalpy ΔH_R was calculated according to Equation E.2.

$$\Delta H_R = \dot{H}_{Sum,Output} - \dot{H}_{Sum,Input}. \tag{E.2}$$

Lignin degradation in ethanol and formic acid has a reaction enthalpy of -34724 MJ/h and is thus exothermic. The results obtained from the energy balance were used for the feasibility study.

Appendix F

Cost offers

In this Appendix important cost offers are presented which were used for the calculations within the feasibility study. The first offer for a plunger pump was obtained from Schäfer & Urbach. The specifications of the pump are given in the offer-page. The second offer from ICIS is a cost information about the market prices of phenol in the first half of the year 2012. The market price of benzene is also included.

SCHÄFER & URBACH
System- und Hochdrucktechnik

Schäfer & Urbach GmbH & Co. KG, Postfach 10 17 05, D-40837 Ratingen

Hauptsitz:
Kaiserswerther Straße 74
40878 Ratingen - Germany
Telefon: (+49) 21 02 / 45 07 - 0
Telefax: (+49) 21 02 / 45 07 - 45

Niederlassung:
Breitenseer Weg 2-6
97633 Höchheim - Germany
Telefon: (+49) 97 64 / 91 91 - 0
Telefax: (+49) 97 64 / 91 91 - 40

KIT - Karlsruher Institut für
Technologie (ITC-CPV)
Herr Jonathan Jeras
Herrmann-von-Helmholtz-Platz 1

76344 Eggenstein-Leopoldshafen

Angebot **35212**

Anfragetext/Nr.:	Anfrage per E-Mail
Datum:	09.04.2010
Kunden-Nr.:	20471
Email:	franco.casola@schaefer-urbach.com
Sachbearbeiter:	Franco Casola
Durchwahl:	+49(2102)450727
Ihre Telefon-Nr.:	+49(7247)829133
Ihre Telefax-Nr.:	+49(7247)822244

Sehr geehrter Herr Jeras,

vielen Dank für Ihre Anfrage. Sie erhalten heute unser ausführliches Angebot.
Sollten Sie dazu noch Fragen haben, so setzen Sie sich bitte mit uns in Verbindung.

Pos.	Menge	Einheit	Artikelnummer/Artikelbezeichnung	Einzelpreis	Gesamtpreis
1	1,00	Stück	Triplexpumpe PPW 103 Liegende 3-Plungerpumpe Typ PPW 103 in folgender Ausführung Triebwerk mit Druckschmierung Tellerventile Plungerpanzerung Sicherheitsventil, angebaut am Pumpenkörper Satz Spezialwerkzeug 2 Satz Standard-Dokumentation Materialzertifikate für Flüssigkeitsseite DIN 50049/2.2	54.850,00 €	54.850,00 €
2	1,00	Stück	PPW 103 Antrieb bestehend aus: Grundrahmen für Pumpe, Getriebe und Motor	10.600,00 €	10.600,00 €
3	1,00	Stück	Elastische Kupplung zwischen Pumpe und Getriebe Schutzhaube Stirnradgetriebe Elastische Kupplung zwischen Getriebe und Motor	28.930,00 €	28.930,00 €
4	1,00	Stück	Antrieb: bestehend aus : E-Motor 200 kW, 1500 l/min, IP 55, 400 V, 50 Hz mit Kaltleiter.	13.380,00 €	13.380,00 €

Angebot 35212 vom: 09.04.2010

Pos.	Menge	Einheit	Artikelnummer/Artikelbezeichnung	Einzelpreis	Gesamtpreis

5 1,00 Stück Triplexpumpe PPW 103

A) BETRIEBSDATEN:

Fördermedium:	Ethanol mit Holzpartikel	
Arbeitstemperatur:	25 - 200	° C
Viskosität bei t:		(mm²/S)
Dichte bei t:		Kg/m³
Volumentstrom:	280	l/min
Saugdruck:	1 - 7	bar
Betriebsdruck:	300	bar
Leistungsbedarf a. d. Welle:	164	KW
Pumpendrehzahl:	230	1/min
Hub:	120	mm

B) WERKSTOFFE

Pumpenkörper:	C22.8	
Plunger:	CK45N/MD 63	1.1191
Saug- u. Druckventile:		1.4112
Triebwerksrahmen:	S355J2G3	1.0570
Kurbelwelle:	42 CrMo4v	1.7225
Pleuellager	Lagermetall	
Pleuelstangen:	42 Cr Mo 4 v	1.7225
Lagerung der Kurbelwelle:	Wälzlager	
Pumpenlänge:	1440mm	
Gewicht:	ca 1500 Kg	

Summe netto	107.760,00 €
Zzgl. 19% MwSt.	20.474,40 €
Summe brutto	128.234,40 €

Grundlage für dieses Angebot sind unsere Allgemeinen Verkaufs- und Lieferbedingungen.

Lieferzeit:	ca. 6 Monate nach in allen Punkten geklärten Bestellung
Preisgültigkeit:	90 Tage
Zahlungsbedingung:	nach Vereinbarung

SCHÄFER & URBACH
System- und Hochdrucktechnik

Angebot 35212 vom: 09.04.2010

Lieferbedingung: ab Werk ausschließlich Verpackung

Wir hoffen, dass Ihnen unser Angebot zusagt und würden uns freuen Ihren Auftrag zu erhalten.

Mit freundlichen Grüßen

Schäfer & Urbach GmbH & Co KG

29th June 2012

Phenol (Europe)

Editor Julia Meehan, julia.meehan@icis.com

CONTRACT PRICES					
Click for Price History			**Price Range**		**US CTS/LB**
FD NWE JUN	EUR/TONNE	+73.00	**1585.00-1625.00**	+73.00	91.10-93.40

SPOT PRICES						
Click for Price History			**Price Range**		**Four weeks ago**	**US CTS/LB**
FOB RDAM T2 EXP	USD/TONNE	+5	**1165-1190**	+20	1200-1210	52.84-53.98
FD NWE	EUR/TONNE	n/c	**1320-1350**	n/c	1250-1260	75.87-77.59
EX-WORKS RUSSIA	Rb/TONNE	-500	**49500-55500**	-500	53500-59000	

NOTE: for full details on the criteria ICIS pricing uses in making these price assessments visit www.icispricing.com and click on "methodology".

Phenol producers and consumers reduce operating rates

The majority of phenol producers and consumers have reduced operating rates because demand has slowed in Europe and for exports to Asia.

Reducing production ahead of the peak summer months of July and August is common and most sources said this week they would not be reducing output more than is normal for the time of year. However, some buyers said their own customers further downstream are considering extending outages for economic reasons.

In general, the phenol market in Europe is described as relatively balanced, but cutbacks in operating rates by producers and consumers of around 20%, has prevented an imbalance in the market.

Demand downstream has clearly slowed, more so for some derivatives than others. Those affected most are the epoxy resins and polycarbonates (PC) markets because of competitively prices imports.

In the nylon intermediate markets, the lack of European exports moving to Asia and margin pressure has meant that some makers of nylon and nylon intermediates are considering taking plants off line if market fundamentals do not improve in July.

July contract and benzene

The phenol market has been keeping a close eye on the spot benzene market this week in the hope that trading activity and the direction of the spot market might give some clue to the possible outcome of the July benzene contract price.

Even up until the close of business on Friday, downstream markets reliant on the benzene contract price were still in the dark about the direction of the market.

However, ahead of business close the benzene contract price for July settled at €953/tonne FOB NWE, down by €68/tonne.

Spot phenol

Spot phenol activity is very thin, since there is no demand. Producers and consumers are unable to suggest even a notional range because there is simply no interest for spot volumes. However, producers have said that there is no need to move spot prices below the benzene contract price plus €300/tonne.

The third-quarter adder over the benzene contract price

The third-quarter fee discussions are ongoing.

Consumers continue to push for reduction and in some cases a decrease of €5/tonne has been achieved.

Exports of phenol to Asia

As has been the case for many months now, outside long-term fixed contract volumes, exports to Asia have been non-existent and European spot prices have simply been tracking spot price developments in Asia.

This week in Asia, spot prices in Asia moved up by $5-20/tonne of the CFR China Main Port price range.

Russia

Phenol prices in Russia moved down because of increasing stocks and poor demand. Local phenol prices were expected to remain stable to soft in coming weeks. Russian domestic numbers include 18% VAT.

Feedstocks

The European propylene contract price for July settled at €935/tonne FD NWE, down by a record €170/tonne from June, because of weak upstream naphtha and ongoing soft supply-and-demand fundamentals. This is the lowest contract price since October 2010. The market viewed the settlement as a necessary adjustment given the challenges facing the European industry. Sources are hopeful that the new price will be the bottom of the market and will encourage some renewed interest for derivatives.

Production update

PKN Orlen started its planned maintenance on phenol and acetone production at its facility in Plock, Poland, on 22 June. The plant is due to restart on 1 August.

Domo will start a planned outage at its facility in Leuna, Germany, on 1 July for two weeks.

France's Novapex will undertake a regular summer shutdown during the first half of August.

Polimeri typically has a biennial shutdown in Mantova, Italy, and this is scheduled for next year.

($1 = €0.80)
(€1 = Rb41.22)

This week on ICIS www.icis.com
28/06/2012 18:28 Europe polyamide chain producers mull shuts if margins stay low
28/06/2012 16 PKN starts planned phenol/acetone maintenance shutdown
29/06/2012 08:1 6China's May cyclohexanone exports fall 74% month on month

FEEDSTOCK PRICES (CONTRACT)					
BENZENE					
Click for Price History			**Price**		**USD/GAL**
FOB NWE JUL	EUR/TONNE	-68.00	**953.00-953.00**	**-68.00**	4.02-4.02

Price history | Related reports | Full report list | Price Alert | Plant performance data Currency conversion (real time) | Glossary Methodology Latest product news Find a supplier